

510.5.4 Inelastic Material Modeling of Concrete

Solids, Beams, Plates, Walls and Shells

Details are given in Section 104.9, on page 363 in Jeremić et al. (1989-2025).

510.5.4.1 Calibration of Inelastic Material Model Parameters for Concrete

Details are given in Section 104.10, on page 368 in Jeremić et al. (1989-2025).

510.6 Modeling: Inelastic, Nonlinear Material Modeling for Contacts, Interfaces, and Joints

Recorded lectures, together with slides, about these topics are available at

http://sokocalo.engr.ucdavis.edu/~jeremic/Real_ESSI_Simulator/OnlineLectures

510.6.1 Material Modeling of Dry Contacts, Interfaces, and Joints (Concrete, Steel – Soil, Rock)

Details are given in Section [104.7](#), on page [306](#) in Jeremić et al. (1989-2025).

510.6.1.1 Calibration of Inelastic Material Model Parameters for Dry Contacts, Interfaces, and Joints (Concrete, Steel – Soil, Rock)

510.6.2 Material Modeling of Saturated Contacts, Interfaces, and Joints (Concrete, Steel – Soil, Rock)

Details are given in Section [104.7](#), on page [306](#) in Jeremić et al. (1989-2025).

510.6.2.1 Calibration of Inelastic Material Model Parameters for Saturated Contacts, Interfaces, and Joints (Concrete, Steel – Soil, Rock)

510.7 Modeling: Buoyancy

Details are given in Section [502.3.7](#), on page [2349](#) in Jeremić et al. (1989-2025).

510.8 Modeling: Base Isolator and Base Dissipator Systems

510.8.1 Base Isolator Systems

Details are given in Section [102.11](#), on page [136](#), in [Jeremić et al. \(1989-2025\)](#).

510.8.1.1 Calibration of Elastic/Inelastic Material Model Parameters for Base Isolator Systems

510.8.2 Base Dissipator Systems

Details are given in Section [102.11](#), on page [136](#), in [Jeremić et al. \(1989-2025\)](#).

510.8.2.1 Calibration of Elastic/Inelastic Material Model Parameters for Base Dissipator Systems

510.9 Modelling: Finite Element System

510.9.1 Mass Matrix

Details are given in Section 102.4, on page 114, Section 102.6, on page 126, Section 102.7, on page 126, Section 102.8, on page 129, Section 102.9, on page 135, Section 102.10, on page 135, Section 102.11, on page 136, and Section 102.12, on page 137, in Jeremić et al. (1989-2025).

510.9.1.1 Consistent Mass Matrix

510.9.1.2 Lumped Mass Matrix

510.9.2 Viscous Damping Matrix

Details are given in Section 108.4, on page 540, in Jeremić et al. (1989-2025).

510.9.2.1 Rayleigh Damping

510.9.2.2 Caughey Damping

510.9.3 Stiffness Matrix

Details are given in Section 102.4, on page 114, Section 102.6, on page 126, Section 102.7, on page 126, Section 102.8, on page 129, Section 102.9, on page 135, Section 102.10, on page 135, Section 102.11, on page 136, and Section 102.12, on page 137, in Jeremić et al. (1989-2025).

510.9.3.1 Tangent Stiffness Matrix

510.9.3.2 Consistent Stiffness Matrix

510.10 Modeling: Solid, Structure – Fluid Interaction Modeling

Details of OpenFOAM – Real-ESSI Simulator coupling are available starting with Section 111.2, on page 685, in [Jeremić et al. \(1989-2025\)](#).

510.11 Simulation: Nonlinear Finite Elements

Details are given in Section 102.2, on page 100 in Jeremić et al. (1989-2025).

510.11.1 Time Marching Algorithms for Solution of Nonlinear Equations of Motion

Details are given in Section 108.3, on page 538 in Jeremić et al. (1989-2025).

510.11.1.1 Newmark Algorithm

Details are given in Section 108.3.1, on page 538 in Jeremić et al. (1989-2025).

510.11.1.2 Hilber Hughes Taylor α Algorithm

Details are given in Section 108.3.2, on page 539 in Jeremić et al. (1989-2025).

510.11.2 Solution of Elastic-Plastic Constitutive Equations

Details are given in Section 104.2.2, on page 182 in Jeremić et al. (1989-2025).

510.11.2.1 Explicit Integration of Elastic-Plastic Constitutive Equations

Details are given in Section 104.3, on page 206 in Jeremić et al. (1989-2025).

Error accumulation.

510.11.2.2 Implicit Integration of Elastic-Plastic Constitutive Equations

Details are given in Section 104.4, on page 207 in Jeremić et al. (1989-2025).

Iterations and tolerance issues.

510.12 Modelling Guide for ESSI

Recorded lectures, together with slides, about these topics are available at

http://sokocalo.engr.ucdavis.edu/~jeremic/Real_ESSI_Simulator/OnlineLectures

More details about these topics are given in Section 502.3, on page 2332 in Jeremić et al. (1989-2025).

510.12.1 Buildings and NPPs on Shallow Foundations, Models

Details are given in Section 504.6, on page 2514 in Jeremić et al. (1989-2025).

510.12.2 Buildings and NPPs on Deeply Embedded Foundation (SMRs), Models

Details are given in Section 504.7, on page 2528 in Jeremić et al. (1989-2025).

510.12.3 Buildings and NPPs on Piles and Pile Group Foundations, Models

Details are given in Section 504.6, on page 2514 in Jeremić et al. (1989-2025).

510.12.4 Structure – Soil – Structure Interaction, Models

Details are given in Section 504.9, on page 2561 in Jeremić et al. (1989-2025).

510.13 Practical Steps for Inelastic ESSI Analysis

Recorded lectures, together with slides, about these topics are available at

http://sokocalo.engr.ucdavis.edu/~jeremic/Real_ESSI_Simulator/OnlineLectures

See Model Development section in Pecker et al. (2022).

510.13.1 Model Development for ESSI

Details are given in Section 502.4, on page 2354 in Jeremić et al. (1989-2025).

510.13.2 Earthquake Soil Structure Interaction: Model Analysis

510.13.3 Earthquake Soil Structure Interaction: Results Postprocessing

Details are given in Section 208.2, on page 1289 in Jeremić et al. (1989-2025).

510.14 Quality Assurance Procedures for ESSI Modeling and Simulation

Details of the quality assurance are given in Sections [314.3, on page 1893](#) and [314.4, on page 1896](#), in [Jeremić et al. \(1989-2025\)](#).

Moreover, verification procedures for ESSI modeling is given in part [300, on page 1436](#) in [Jeremić et al. \(1989-2025\)](#).

See also Verification and Validation section in [Pecker et al. \(2022\)](#).

510.14.1 Verification

510.14.2 Validation

510.15 Practical Examples, Nonlinear, Inelastic ESSI

Recorded lectures, together with slides, about these topics are available at

http://sokocalo.engr.ucdavis.edu/~jeremic/Real_ESSI_Simulator/OnlineLectures

- 510.15.1 Nuclear Power Plant, Inelastic Structure, Inelastic Soil, Inelastic Contact/Interface, 6C/3C/3×1C/1C Seismic Motions
- 510.15.2 Nuclear Power Plant on Piles, Inelastic Structure, Inelastic Soil, Inelastic Contact/Interface, 6C/3C/3×1C/1C Seismic Motions
- 510.15.3 Nuclear Power Plant, High Water Table, Inelastic Structure, Inelastic Soil, Cyclic Mobility and Liquefaction, Inelastic Saturated Contact/Interface, Buoyant Pressures, 6C/3C/3×1C/1C Seismic Motions
- 510.15.4 Small Modular Reactor, Deeply Embedded, Inelastic Structure, Inelastic Soil, Inelastic Contact/Interface, 6C/3C/3×1C/1C Seismic Motions
- 510.15.5 Small Modular Reactor, Deeply Embedded, High Water Table, Inelastic Structure, Inelastic Soil (Cyclic Mobility and Liquefaction), Inelastic Saturated Contact/Interface (Buoyant Pressures), 6C/3C/3×1C/1C Seismic Motions
- 510.15.6 Multiple Buildings and Nuclear Power Plants (Structure-Soil-Structure Interaction), Inelastic Structure, Inelastic Soil, Inelastic Contact/Interface, 6C/3C/3×1C/1C Seismic Motions
- 510.15.7 Multiple Small Modular Reactors (Structure-Soil-Structure Interaction), Deeply Embedded, High Water Table, Inelastic Structure, Inelastic Soil, Cyclic Mobility and Liquefaction, Inelastic Saturated Contact/Interface, Buoyant Pressures, 3C Seismic Motions

Chapter 511

ASCE-4, Chapter on Nonlinear ESSI analysis

(2016-2020-2021-)

511.1 Motivation: Modeling and Simulation of Earthquake Soil Structure Interaction

Main motivation of this write-up, chapter is to provide a clear, practical, up to date guide on how to perform nonlinear, inelastic Earthquake Soil Structure Interaction (ESSI) modeling and simulations for nuclear installations. This is particularly important at this time as a number of endeavors are underway to perform realistic ESSI analysis for a number of nuclear installations.

This write-up is further motivated by the modeling and simulation challenges that are part of any soil, rock – structure system. These challenges are illustrated in Figure 511.1 for a number of soil, rock and soil/rock-structure systems.

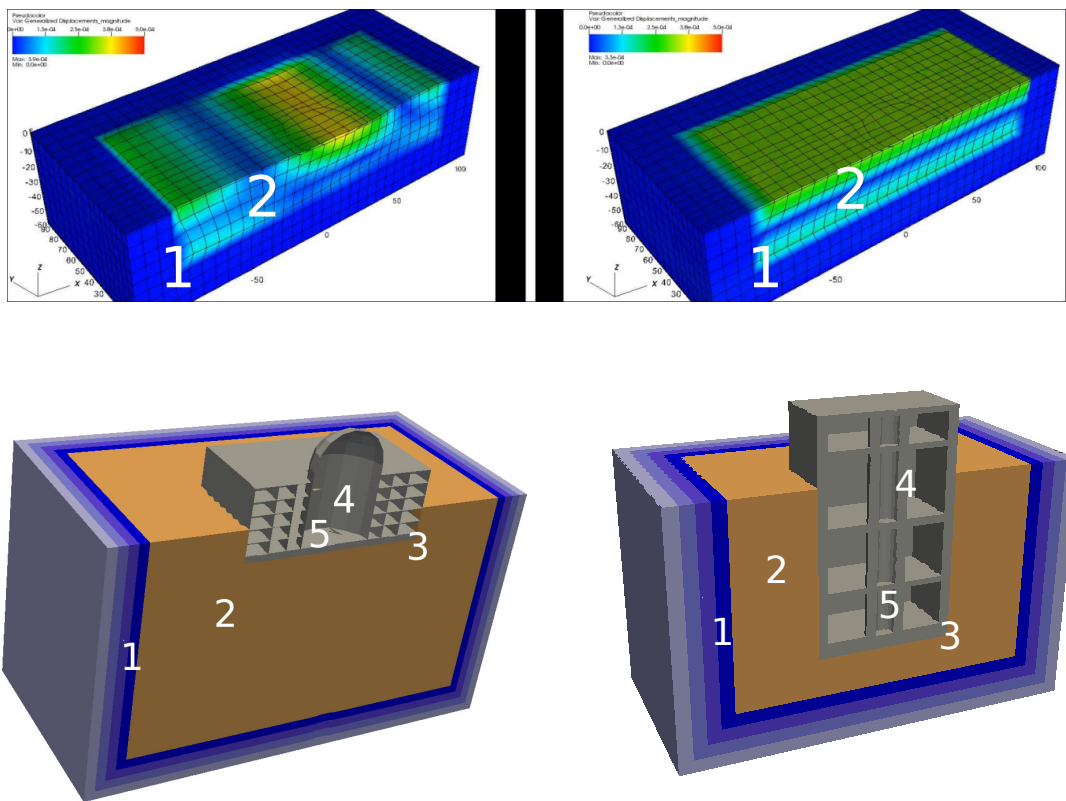


Figure 511.1: ESSI modeling and simulation challenges: Free field motions, 3C vs 3×1C; Nuclear Power Plant structure – soil/rock system, Small Modular Reactor structure – soil/rock system. Aspects of modeling: 1) Seismic motions, 2) Inelastic soil and rock, 3) Inelastic interface/contact/joints, foundation with soil/rock and interfaces/contacts/joints within structure, 4) Inelastic structure, systems and components, 5) Interaction with external (reservoirs, fluid pools...) and internal (saturated and un-saturated soil/rock and concrete).

Challenges for Modeling of Mechanics of Earthquake – Soil/Rock – Structure – Interaction. Presented are challenges related to the modeling of mechanics of ESSI problems.

- 1 Seismic motions: use of 1C, 3×1C and 3C motions, seismic motions input and radiation damping.
- 2 Inelastic, elastic plastic modeling of soil and rock, dry and/or partially or fully saturated, and energy dissipation in those soil/rock – structure components,
- 3 Inelastic, elastic plastic modeling of foundation concrete – soil/rock contacts/interfaces/joints that may be dry and/or partially or fully saturated, and energy dissipation in those parts of soil/rock – structure system,
- 4 Inelastic, elastic damage plastic modeling of structure, systems and components (SSCs). SSCs: beams, walls, plates, shell made of steel and reinforced concrete, base isolators and dissipators, systems and etc. and energy dissipation in those soil/rock – structure components,
- 5 Interaction of soil/rock – structure systems with internal, within structure or in pores of porous materials (soil, rock, concrete) and external fluids, reservoirs, pools, etc.

Challenges for Numerical Simulations of Earthquake – Soil/Rock – Structure – Interaction. Presented are challenges related to the numerical simulation of ESSI problems.

- A Inelastic simulations on constitutive level, stress-strain, constitutive problem solutions
- B Inelastic simulations on finite element level, nonlinear system of equations solutions
- C Time marching algorithms, numerical damping
- D High performance, parallel computing

511.2 Introduction

Focus is on modeling and simulation of linear elastic and nonlinear, inelastic, elastic-plastic behavior of soil/rock – structure systems during earthquakes.

It is assumed that earthquake motions, earthquake field is known. Earthquake motion or earthquake field, can be given as a simple 1C (1 Component) vertically propagating shear wave, that is obtained from a de-convolution of a given (1C) surface motion, using, for example SHAKE type analysis. Earthquake motion or earthquake field can also be given as a full 3C (3 Component) wave field that is obtained from analytic wave propagation solutions or from a regional geophysical model simulations, using, for example SW4 type analysis. In addition, earthquake motions can be defined in a probabilistic way...

[Pecker et al. \(2022\)](#).

511.3 Seismic Energy Input and Dissipation

511.3.1 Seismic Energy Input

Seismic energy input flux

511.3.2 Seismic Energy Dissipation

511.3.2.1 Seismic Energy Dissipation, Wave Reflection and Wave Radiation

Wave reflection and radiation damping

511.3.2.2 Seismic Energy Dissipation, Viscous Coupling

velocity proportional, viscous damping

511.3.2.3 Seismic Energy Dissipation, Material Inelasticity

Elastic-plastic energy dissipation of material, Displacement proportional

511.3.2.4 Seismic Energy Dissipation, Numerical, Algorithmic Positive and Negative Damping

511.4 Modeling: Seismic Motions

511.4.1 Seismic Motions: Available Data

511.4.2 Seismic Motion Development

511.4.2.1 Seismic Motions from Empirical Models

511.4.2.2 Seismic Motions from Geophysical Models

Small Scale Geophysical Models.

Large Scale Regional Geophysical Models

511.4.2.3 Seismic Motions from 3D/3C Analytic Models

511.4.3 6C vs 3C vs $3 \times 1C$ vs 1C Seismic Motions

511.4.4 Incoherent Seismic Motions

511.4.5 Seismic Motion Input into FEM Models

511.5 Modeling: Inelastic, Nonlinear Material Modeling for Solids and Structures

511.5.1 Inelastic Material Modeling of Rock

511.5.1.1 Calibration of Inelastic Material Model Parameters for Rock

511.5.2 Inelastic Material Modeling of Soil

511.5.2.1 Dry Soil

511.5.2.2 Fully Saturated Soil

511.5.2.3 Partially Saturated, Unsaturated Soil

511.5.2.4 Calibration of Inelastic Material Model Parameters for Soil

511.5.3 Inelastic Material Modeling of Steel

511.5.3.1 Calibration of Inelastic Material Model Parameters for Steel

511.5.4 Inelastic Material Modeling of Concrete

Solids, Beams, Plates, Walls and Shells

511.5.4.1 Calibration of Inelastic Material Model Parameters for Concrete

511.6 Modeling: Inelastic, Nonlinear Material Modeling for Contacts, Interfaces, and Joints

511.6.1 Material Modeling of Dry Contacts, Interfaces, and Joints (Concrete, Steel – Soil, Rock)

511.6.1.1 Calibration of Inelastic Material Model Parameters for Dry Contacts, Interfaces, and Joints (Concrete, Steel – Soil, Rock)

511.6.2 Material Modeling of Saturated Contacts, Interfaces, and Joints (Concrete, Steel – Soil, Rock)

511.6.2.1 Calibration of Inelastic Material Model Parameters for Saturated Contacts, Interfaces, and Joints (Concrete, Steel – Soil, Rock)

511.7 Modeling: Base Isolator and Base Dissipator Systems

511.7.1 Base Isolator Systems

511.7.1.1 Calibration of Elastic/Inelastic Material Model Parameters for Base Isolator Systems

511.7.2 Base Dissipator Systems

511.7.2.1 Calibration of Elastic/Inelastic Material Model Parameters for Base Dissipator Systems

511.8 Modeling: Buried Pipes and Conduits

511.9 Modeling: Buoyancy

511.10 Modelling: Finite Element System

511.10.1 Mass Matrix

511.10.1.1 Consistent Mass Matrix

511.10.1.2 Lumped Mass Matrix

511.10.2 Viscous Damping Matrix

511.10.2.1 Rayleigh Damping

511.10.2.2 Caughey Damping

511.10.3 Stiffness Matrix

511.10.3.1 Tangent Stiffness Matrix

511.10.3.2 Consistent Stiffness Matrix

511.11 Modeling: Solid, Structure – Fluid Interaction Modeling

511.12 Simulation: Nonlinear Finite Elements

511.12.1 Time Marching Algorithms for Solution of Nonlinear Equations of Motion

511.12.1.1 Newmark Algorithm

511.12.1.2 Hilber Hughes Taylor α Algorithm

511.12.2 Solution of Elastic-Plastic Constitutive Equations

511.12.2.1 Explicit Integration of Elastic-Plastic Constitutive Equations

511.12.2.2 Implicit Integration of Elastic-Plastic Constitutive Equations

511.13 Modelling Guide for ESSI

511.13.1 Buildings and NPPs on Shallow Foundations, Models

511.13.2 Buildings and NPPs on Deeply Embedded Foundation (SMRs), Models

511.13.3 Buildings and NPPs on Piles and Pile Group Foundations, Models

511.13.4 Structure – Soil – Structure Interaction, Models

511.14 Practical Steps for Inelastic ESSI Analysis

511.14.1 Model Development for ESSI

511.14.2 Earthquake Soil Structure Interaction: Model Analysis

511.14.3 Earthquake Soil Structure Interaction: Results Postprocessing

511.15 Quality Assurance Procedures for ESSI Modeling and Simulation

511.15.1 Verification

511.15.2 Validation

511.16 Standard for Nonlinear/Inelastic Earthquake-Soil-Structure Analysis

511.16.1 Standard for Solids Analysis

511.16.2 Standard for Structure Analysis

511.16.3 Standard for Elastic-Plastic Analysis

511.17 Practical Examples, Nonlinear, Inelastic ESSI

511.17.1 Nuclear Power Plant, Inelastic Structure, Inelastic Soil, Inelastic Contact/Interface, 6C/3C/3×1C/1C Seismic Motions

511.17.2 Nuclear Power Plant on Piles, Inelastic Structure, Inelastic Soil, Inelastic Contact/Interface, 6C/3C/3×1C/1C Seismic Motions

511.17.3 Nuclear Power Plant, High Water Table, Inelastic Structure, Inelastic Soil, Cyclic Mobility and Liquefaction, Inelastic Saturated Contact/Interface, Buoyant Pressures, 6C/3C/3×1C/1C Seismic Motions

511.17.4 Small Modular Reactor, Deeply Embedded, Inelastic Structure, Inelastic Soil, Inelastic Contact/Interface, 6C/3C/3×1C/1C Seismic Motions

511.17.5 Small Modular Reactor, Deeply Embedded, High Water Table, Inelastic Structure, Inelastic Soil (Cyclic Mobility and Liquefaction), Inelastic Saturated Contact/Interface (Buoyant Pressures), 6C/3C/3×1C/1C Seismic Motions

511.17.6 Multiple Buildings and Nuclear Power Plants (Structure-Soil-Structure Interaction), Inelastic Structure, Inelastic Soil, Inelastic Contact/Interface, 6C/3C/3×1C/1C Seismic Motions

511.17.7 Multiple Small Modular Reactors (Structure-Soil-Structure Interaction), Deeply Embedded, High Water Table, Inelastic Structure, Inelastic Soil, Cyclic Mobility and Liquefaction, Inelastic Saturated Contact/Interface, Buoyant Pressures, 3C Seismic Motions

Chapter 512

Earthquake-Soil-Structure Interaction, Core Functionality

(2017-2018-2019-2021-)

(In collaboration with Dr. Yuan Feng, Prof. Han Yang and Dr. Hexiang Wang)

512.1 Core Functionality for ESSI Analysis of Nuclear Installations

Presented here are models that represent core functionality for elastic and inelastic analysis of infrastructure objects, including nuclear installations. There exist a number of other models, with different sophistication levels, that can be used, depending on the amount of data available, about the soil, rock, concrete, contacts/interfaces and seismic motions ([Jeremić et al., 1989-2025](#)). However, in order to begin to use of inelastic/nonlinear analysis, and assess inelastic/nonlinear effects on a dynamic response of soil structure systems, a set of initial models and analysis parameters are needed. Provided below is a set of models and materials parameters that are recommended for initial use of inelastic/nonlinear analysis of soil structure systems, using the Real-ESSI Simulator system. (<http://real-essi.info/>). It is noted that a detailed description of examples, commands and the Real-ESSI Simulator system is provided by [Jeremić et al. \(1989-2025, 1988-2025\)](#) and is also available at the Real-ESSI Simulator web site <http://real-essi.info/>. In addition, preprocessing, model development and postprocessing, results visualization for the Real-ESSI Simulator system is also described in detail pre and post processing documents that are available at <http://real-essi.info/>.

512.2 Model Setup

Each model has to be named:

```
model name "model_name_string";
```

In addition to that, there are a number of other considerations to be aware of:

- Each command line has to end with a semicolon ";"
- Comment on a line begins with either "/" or "!" and last until the end of current line.
- Units are required (see more below) for all quantities and variables.
- Include statements allow splitting source into several files
- All variables are double precision (i.e. floats) with a unit attached.
- All standard arithmetic operations are implemented, and are unit sensitive.
- Internally, all units are represented in the base SI units ($m - s - kg$).
- The syntax ignores extra white spaces, tabulations and newlines. Wherever they appear, they are there for code readability only. (This is why all commands need to end with a semicolon).

512.3 Linear Elastic Modeling

for single stage linear elastic modeling, one stage of loading has to be defined

```
1 new loading stage "self weight loading stage";
```

512.4 Nonlinear/Inelastic Modeling

For inelastic modeling, stages of loading have to be defined in proper sequence.

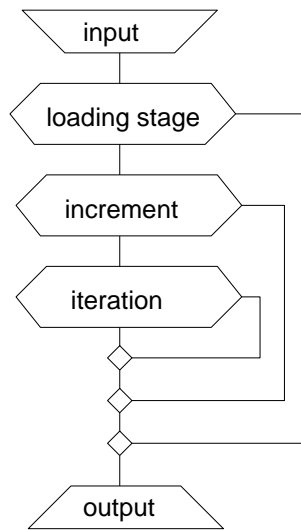


Figure 512.1:

```
1 new loading stage "self weight loading stage";
```

...

```
1 new loading stage "Seismic Loading";
```

...

512.5 Model Domain

Finite element model is developed by defining the finite element mesh which is made of nodes, finite elements, the material, and the loads.

512.5.1 Nodes

For example:

```
1 add node No 1 at (1.0*m, 2.5*m, 3.33*m) with 3 dofs;
```

adds a node number 1 at coordinates $x = 1.0m$, $y = 2.5m$ and $z = 3.33m$ with 3 dofs. The nodes can be of 3dofs $[u_x, u_y, u_z]$, 4dofs $[u_x, u_y, u_z, p]$ (u-p elements), 6dofs $[u_x, u_y, u_z, r_x, r_y, r_z]$ (beams and shells) and 7 ddfs $[u_x, u_y, u_z, p, U_x, U_y, U_z]$ (upU element) types.

512.5.2 Boundary Conditions

Example fix translation x and y for node #3 fix node # 3 dofs ux uy;

Example fix all appropriate DOFs for node #7. fix node # 7 dofs all;

512.5.3 Static Acceleration Field

Example adding acceleration induced loading field for (some) elements

```
1 add acceleration field # 1
2 ax = 0*m/s^2
3 ay = 0*m/s^2
4 az = -9.81*m/s^2;
```

512.5.4 Dynamic Acceleration Field, Earthquake

One Example of add DRM load from wave fields:

```
1 add load # 1 type DRM from wave field
2   # 1 in direction ux
3   # 2 in direction uy
4   soil_surface at z = 60.0*m
5   hdf5_file = "input.hdf5" ;
```

512.5.5 Super Element

Super element is defined by providing mass and stiffness matrix, together with nodes and DOF numbering. It is assumed that the Super Element is a linear elastic element that is made up of a number of other finite elements. Super Element represents a part of model (structure, solid) that is linear elastic, and that has stiffness and mass matrix already defined using other finite element programs. Other finite element programs export stiffness and mass matrix. In addition, information about Super Element node numbers and degrees of freedom (DOFs) needs to be supplied as well.

512.6 Structural Modeling

Presented in this section are models that are used for modeling and simulation of structural behavior. Following the usually made assumption that structural components will remain linear elastic, only linear elastic material is used for structural modeling. It is noted, that fully nonlinear (inelastic, elastic-damage-plastic) models are also available for modeling of structural components ([Jeremić et al., 1989-2025, 1988-2025](#)). However, for the purpose of presenting core functionality features, those models are not covered here.

It is noted that a complete structural model can be replaced with one linear elastic super element, as described in section [512.5.5 on page 2769](#).

512.6.1 Truss

Truss element represents a 3D two node linear geometry truss member. Real-ESSI command for truss element is given in detail in section ??.

```

1 add element # 1 type truss
2   with nodes (1,2)
3   use material # 1
4   cross_section = 1*m^2
5   mass_density = 2000*kg/m^3;
```

512.6.2 Beam

Beam finite element represents a 3D linear geometry, two node Bernoulli beam member, with 6 DOFs per node. Real-ESSI command for beam element is given in detail in section ??.

```

1 add element # 1 type beam_elastic
2   with nodes (1, 2)
3   cross_section = 1*m^2
4   elastic_modulus = 2e8*Pa
5   shear_modulus = 1e8*Pa
6   torsion_Jx = 0.33*m^4
7   bending_Iy = 1.0/12*m^4
8   bending_Iz = 1.0/12*m^4
9   mass_density = 2000*kg/m^3
10  xz_plane_vector = (1, 0, 1 )
11  joint_1_offset = (0*m, 0*m, 0*m )
12  joint_2_offset = (0*m, 0*m, 0*m );
```

512.6.3 Shell

Shell finite element represents a 3D linear elastic geometry, 4 node ANDES shell member with 6DOFs per node, including drilling DOFs (in plane twist). Real-ESSI command for shell element is given in detail in section ??.

```

1 add element # 1 type 4NodeShell_ANDES
2   with nodes (1,2,3,4)
3   use material # 1
4   thickness = 1*m ;

```

512.7 Solid Modeling

Presented in this section are models that are used for modeling and simulation of soils, using solid and contact/interface elements for interface of foundations and soil. Models for soil can be linear elastic, while they can also be nonlinear/inelastic, mimicking simple G/G_{max} behavior. Models for contact/interface can represent bonded contact, where no slip or gapping is allowed, and also a frictional slip and gapping contact/interface.

It is noted, that a number of more or less sophisticated material models for soil and for contact/interface are also available ([Jeremić et al., 1989-2025, 1988-2025](#)). However, for the purpose of presenting core functionality features, those models are not covered here.

512.7.1 Solid Brick

Solid brick finite element with 8 nodes, linear interpolation of displacements between nodes, and three DOFs per node is available. This element is very good for modeling soil volume close to and far away from the structural. Real-ESSI command for 8 node solid brick is given in detail in section ??.

```

1 add element # 1 type 8NodeBrick
2   using 2 Gauss points each direction
3   with nodes (1, 2, 3, 4, 5, 6, 7, 8)
4   use material # 1;

```

512.7.2 Contact, Interfaces, Joints

```

1 add element # 1 type StressBasedSoftContact_NonLinHardShear
2   with nodes (1, 2)
3   initial_axial_stiffness = 5*MPa
4   stiffening_rate = 100
5   max_axial_stiffness = 800*MPa

```

```

6 initial_shear_stiffness = 800*kPa
7 axial_viscous_damping = 50*Pa*s
8 shear_viscous_damping = 50*Pa*s
9 residual_friction_coefficient = 0.68
10 shear_zone_thickness = 5e-3*m
11 contact_plane_vector = (0, 0, 1 );

```

512.8 Core Material Modeling Parameters for Soil, Rock, Concrete, and Steel

512.8.1 Linear and Nonlinear Elastic Soil, Rock, Concrete, and Steel Modeling

512.8.2 Inelastic/Nonlinear Soil Modeling

Simple modeling of soil can be done using the so called stiffness degradation curves, or G/G_{max} curves, and damping curves, as developed by [Seed and Idriss \(1970a\)](#).

As an example, an elastic plastic material model based on von Mises yield surface with isotropic hardening or softening and Armstrong Frederick nonlinear kinematic hardening can be used to develop such curves. Model parameters are given below:

```

1 add material # 1 type vonMisesArmstrongFrederick
2 mass_density = 2500*kg/m^3
3 elastic_modulus = 30 * MPa
4 poisson_ratio = 0.3
5 von_mises_radius = 300 * Pa
6 armstrong_frederick_ha = 150 * MPa
7 armstrong_frederick_cr = 25000
8 isotropic_hardening_rate = 0*Pa;

```

while the corresponding G/G_{max} and damping curves are given in Figure [512.2](#).

It is noted that von Mises Armstrong-Frederick Nonlinear Kinematic Hardening material model is a full 3D elastic plastic material model, that is capable of modeling G/G_{max} and damping behavior, defined in 1D shear testing, fairly well in full 3D.

The command is

```

1 add material # <.> type vonMisesArmstrongFrederick
2 mass_density = <M/L^3>
3 elastic_modulus = <F/L^2>
4 poisson_ratio = <.>
5 von_mises_radius = <.>
6 armstrong_frederick_ha = <F/L^2>
7 armstrong_frederick_cr = <.>
8 isotropic_hardening_rate = <F/L^2> ;

```

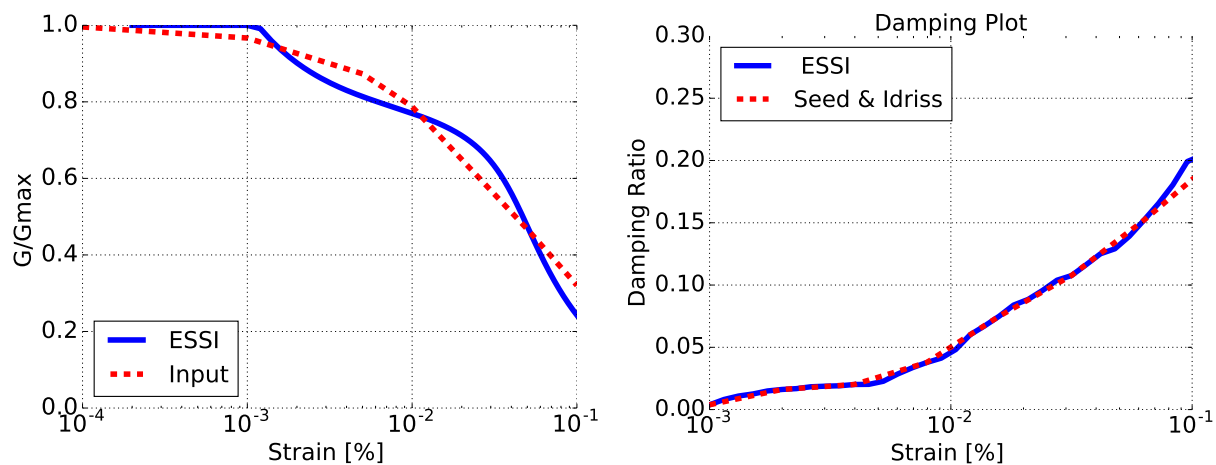


Figure 512.2: Stiffness degradation (G/G_{max}) and damping curves developed using von Mises Armstrong-Frederick Nonlinear Kinematic Hardening material model.

512.8.3 Inelastic/Nonlinear Rock Modeling

512.8.4 Inelastic/Nonlinear Concrete Modeling

512.8.5 Inelastic/Nonlinear Steel Modeling

512.9 Core Material Modeling Parameters for Contacts, Interfaces and Joints

The command for stress based dry soft nonlinear hardening is:

```

1 add element # 1 type StressBasedSoftContact_NonLinHardShear
2   with nodes (1, 2)
3   initial_axial_stiffness = 5*MPa
4   stiffening_rate = 100
5   max_axial_stiffness = 800*MPa
6   initial_shear_stiffness = 800*kPa
7   axial_viscous_damping = 50*Pa*s
8   shear_viscous_damping = 50*Pa*s
9   residual_friction_coefficient = 0.68
10  shear_zone_thickness = 5e-3*m
11  contact_plane_vector = (0, 0, 1 );

```

512.9.1 Mass Concrete Against Silt, Sand, Gravel and Clay

A set of initial recommended material parameters for frictional contact/interface are given in Tables 512.1 for contact between mass concrete and sand/gravel. Frictional properties given below are recommended by NAVFAC (1986).

Table 512.1: Friction coefficients for contact/interface of dissimilar materials, mass concrete against soil.

Mass concrete on soil	Friction coefficient ($\tan \phi$)	Friction angle (ϕ)
Clean sound rock	0.70	35°
Clean gravel, gravel sand mixture, coarse sand	0.55 – 0.60	$29^\circ – 31^\circ$
Clean fine to medium sand, silty medium to coarse sand	0.45 – 0.55	$24^\circ – 29^\circ$
Fine sandy silt, nonplastic silt	0.35 – 0.45	$19^\circ – 24^\circ$
Very stiff clay	0.40 – 0.50	$22^\circ – 27^\circ$

Example command for a contact/interface element for mass concrete against clean sand, silty sand-gravel mix, single size rock fill (friction coefficient 0.30) is given below:

```

1 add element # 1 type StressBasedSoftContact_NonLinHardShear
2   with nodes ( 1, 2)
3   initial_axial_stiffness = 10 * MPa
4   stiffening_rate = 100
5   max_axial_stiffness = 50 * MPa
6   initial_shear_stiffness = 40 * kPa
7   axial_viscous_damping = 100 * Pa * s
8   shear_viscous_damping = 100 * Pa * s
9   residual_friction_coefficient = 0.30
10  shear_zone_thickness = 5e-3*m

```

```
11 contact_plane_vector = (0, 0, 1);
```

Another example, for contact/interface element for mass concrete against clean gravel, gravel sand mixture, coarse sand (friction coefficient 0.55-0.60) is given below:

```
1 add element # 1 type StressBasedSoftContact_NonLinHardShear
2   with nodes ( 1, 2)
3     initial_axial_stiffness = 20 * MPa
4     stiffening_rate = 100
5     max_axial_stiffness = 100 * MPa
6     initial_shear_stiffness = 80 * kPa
7     axial_viscous_damping = 200 * Pa * s
8     shear_viscous_damping = 200 * Pa * s
9     residual_friction_coefficient = 0.55
10    shear_zone_tkness = 1e-2*m
11    contact_plane_vector = (0, 0, 1);
```

512.9.2 Steel Sheet Against Sand, Gravel and Rockfill

Recommended material parameters for frictional contact/interface of steel sheets against sand and gravel are given in Tables 512.2. Frictional properties given below are recommended by NAVFAC (1986).

Table 512.2: Friction coefficients for contact/interface of dissimilar materials, steel sheet piles against soil.

Steel sheets against soil	Friction coefficient ($\tan \phi$)	Friction angle (ϕ)
Clean gravel, sand-gravel mix, well graded rock fill	0.40	22°
Clean sand, silty sand-gravel mix, single size rock fill	0.30	17°
Fine sandy silt, nonplastic silt	0.20	11°

Example commands for contact/interface element for steel sheets against clean sand, silty sand-gravel mix, single size rock fill (friction coefficient 0.30) is given below:

```
1 add element # 1 type StressBasedSoftContact_NonLinHardShear
2   with nodes ( 1, 2)
3     initial_axial_stiffness = 1000 * MPa
4     stiffening_rate = 100
5     max_axial_stiffness = 5 * GPa
6     initial_shear_stiffness = 4 * MPa
7     axial_viscous_damping = 100 * Pa * s
8     shear_viscous_damping = 100 * Pa * s
9     residual_friction_coefficient = 0.30
```

```

10    shear_zone_thickness = 5e-3*m
11    contact_plane_vector = (0, 0, 1);

```

and for steel sheets against clean gravel, sand-gravel mix, well graded rock fill, with friction coefficient 0.40, command is:

```

1 add element # 1 type StressBasedSoftContact_NonLinHardShear
2   with nodes ( 1, 2)
3     initial_axial_stiffness = 2000 * MPa
4     stiffening_rate = 100
5     max_axial_stiffness = 10 * GPa
6     initial_shear_stiffness = 8 * MPa
7     axial_viscous_damping = 100 * Pa * s
8     shear_viscous_damping = 100 * Pa * s
9     residual_friction_coefficient = 0.40
10    shear_zone_thickness = 5e-3*m
11    contact_plane_vector = (0, 0, 1);

```

512.9.3 Formed Concrete Against Sand, Gravel and Rockfill

Recommended material parameters for frictional contact/interface of formed concrete against sand and gravel are given in Tables 512.3. Frictional properties given below are recommended by NAVFAC (1986).

Table 512.3: Friction coefficients for contact/interface of dissimilar materials, formed concrete against soil.

Formed concrete against soil	Friction coefficient ($\tan \phi$)	Friction angle (ϕ)
Clean gravel, sand-gravel mix, well graded rock fill	0.40 – 0.50	22° – 27°
Clean sand, silty sand-gravel mix, single size rock fill	0.30 – 0.40	17° – 22°
Silty sand, gravel or sand mixed with silt and clay	0.30	17°
Fine sandy silt, nonplastic silt	0.25	14°

Example command for contact/interface element for formed concrete against clean gravel, sand-gravel mix, well graded rock fill (friction coefficient 0.40-0.50) is given below:

```

1 add element # 1 type StressBasedSoftContact_NonLinHardShear
2   with nodes ( 1, 2)
3     initial_axial_stiffness = 30 * MPa
4     stiffening_rate = 100
5     max_axial_stiffness = 150 * MPa
6     initial_shear_stiffness = 120 * kPa
7     axial_viscous_damping = 100 * Pa * s

```

```

8   shear_viscous_damping = 100 * Pa * s
9   residual_friction_coefficient = 0.40
10  shear_zone_thickness = 5e-3*m
11  contact_plane_vector = (0, 0, 1);

```

512.9.4 Rock or Concrete on Rock or Concrete

More recently, [Lei and Barton \(2022\)](#) presented a very nice set of experiments with data for proper choice of interface parameters for rock on rock interface, that can also be used for concrete as well.

512.10 Earthquake Motion Modeling

512.10.1 One Component (1C) Seismic Motions Defined at Surface or at Depth

DRM...

One can add DRM loading directly, where `input.hdf5` specifies the DRM motions to all DRM nodes.

```

1 add load # 1 type DRM
2   hdf5_file = "input.hdf5"
3   scale_factor = 1.0 ;

```

Since the direct specification of DRM motions to all DRM nodes is complicated, alternatively, user is able to specify DRM motion using a surface motion. Internally, wave deconvolution is conducted to specify the DRM motions to all DRM nodes.

```

1 add wave field # 1 with
2   acceleration_filename = "acceleration.txt"
3   unit_of_acceleration = 1 * m/s^2
4   displacement_filename = "displacement.txt"
5   unit_of_displacement = 1 * m
6   add_compensation_time = 0.0 * s
7   motion_depth = 0 * m
8   monitoring_location = within_soil_layer
9   soil_profile_filename = "soil_profile.txt"
10  unit_of_Vs = 1 * m/s
11  unit_of_rho = 1 * kg/m^3
12  unit_of_damping = absolute
13  unit_of_thickness = 1*m
14  ;

```

```

1 add load # 1 type DRM from wave field # 1 in direction ux
2   soil_surface at z = 0.0*m
3   hdf5_file = "input.hdf5" ;

```

where `input.hdf5` specifies the HDF5 file which contain the information about the DRM elements and DRM nodes.

512.10.2 $3 \times 1C$ Seismic Motions Defined at Surface or at Depth

One Example of add DRM load from wave fields:

```

1 add load # 1 type DRM from wave field
2   # 1 in direction ux
3   # 2 in direction uy
4   # 3 in direction uz
5   soil_surface at z = 0.0*m
6   hdf5_file = "input.hdf5" ;

```

512.10.3 Seismic Motions Imposed at Model Base

```

1 add load # 1 type imposed motion to node # 1 dof ux
2   time_step = 0.01*s
3   displacement_scale_unit = 1*m
4   displacement_file = "displacement.txt"
5   velocity_scale_unit = 1*m/s
6   velocity_file = "velocity.txt"
7   acceleration_scale_unit = 1*m/s^2
8   acceleration_file = "acceleration.txt";

```

512.10.4 Eigen Analysis

For structural model alone.

```

1 simulate using eigen algorithm
2   number_of_modes = 3;

```

512.11 Core Modeling and Simulation Commands: Simulation Parameters

Developed model, using core functionality, as described above, numerically simulated using core functionality simulation controls.

Finite element system of equations can be solved in sequential processing mode, for smaller models, on sequential, single CPU computers (laptops, desktops, single CPU Amazon Web Services computers, etc.):

```

1 define solver sequential umfpack;

```

For larger models, parallel processing mode, on parallel computers ((multi CPU laptops, multi CPU desktops, clusters of PCs, Amazon Web Services parallel computers, Supercomputers, etc.):

Command Example for a direct solver:

```
1 define solver parallel petsc "-pc_type lu -pc_factor_mat_solver_package mumps" ;
```

For selfweight phase of loading, static solution algorithm is used:

```
1 simulate 100 steps using static algorithm;
```

For static loading, for example self weight as described above, load application and the simulation process is controlled through load control:

```
1 define load factor increment 0.01;
```

For dynamic loads, simulation process is controlled using Newmark time integration method:

```
1 define dynamic integrator Newmark with gamma = 0.6000 beta = 0.3025;
```

The dynamic simulation process is performed in a number of steps:

```
1 simulate 2000 steps using transient algorithm time_step = 0.01*s;
```

For proper integration of constitutive equations on the integration point (Gauss point) level, within each finite element, constitutive algorithm needs to be defined:

```
1 define NDMaterial constitutive integration algorithm Forward_Euler;
```

For the finite element level, analysis of nonlinear systems require definition of nonlinear iteration algorithm:

```
1 define algorithm With_no_convergence_check;
```

Part 600

References

Bibliography

- A. Angabini. Anisotropy of rock elasticity behavior and of gas migration in a Variscan Carboniferous rock mass in the South Limburg, The Netherlands. *Engineering Geology*, 67(3-4):353–372, 2003.
- T. Abdoun, R. Dobry, and T. D. O'Rourke. Centrifuge and numerical modeling of soil–pile interaction during earthquake induced soil liquefaction and lateral spreading. In *Geotechnical Special Publications* 64, pages 76–90. ASCE, 1997.
- J. A. Abell, N. Orbović, D. B. McCallen, and B. Jeremić. Earthquake soil structure interaction of nuclear power plants, differences in response to 3-D, 3×1-D, and 1-D excitations. *Earthquake Engineering and Structural Dynamics*, 47(6):1478–1495, May 2018. doi: 10.1002/eqe.3026. URL <https://onlinelibrary.wiley.com/doi/abs/10.1002/eqe.3026>.
- R. Abraham, J. Marsden, and T. Ratiu. *Manifolds, Tensor Analysis, and Applications*, volume 75 of *Applied Mathematical Sciences*. Springer Verlag, second edition, 1988.
- N. Abrahamson. Spatial variation of earthquake ground motion for application to soil-structure interaction. *EPRI Report No. TR-100463*, March., 1992a.
- N. Abrahamson. Generation of spatially incoherent strong motion time histories. In A. Bernal, editor, *Earthquake Engineering, Tenth World Conference*, pages 845–850. Balkema, Rotterdam, 1992b. ISBN 90 5410 060 5.
- N. Abrahamson. Updated coherency model. *Report Prepared for Bechtel Corporation*, April, 2005.
- N. A. Abrahamson, J. F. Schneider, and J. C. Stepp. Empirical spatial coherency functions for applications to soil–structure interaction analysis. *Earthquake Spectra*, 7(1):1–27, 1991.
- A. N. Afanasenkov, V. M. Bogomolov, and I. M. Voskoboinikov. Generalized shock Hugoniot of condensed substances. *Journal of Applied Mechanics and Technical Physics*, 10(4):660–664, July 1969.
- S. AG. Verification, ve56 interface element. Technical report, SOFISTIK AG, 2020.

- G. Agha. Actors: A Model of Concurrent Computation in Distributed Systems. MIT Press, 1984.
- K. Aki and P. G. Richards. Quantitative Seismology. University Science Books, 2nd edition, 2002.
- M. A. AL-Shudeifat. Highly efficient nonlinear energy sink. Nonlinear Dynamics, 76:1905–1920, January 2014. URL <https://link.springer.com/article/10.1007/s11071-014-1256-x#citeas>.
- M. A. AL-Shudeifat, N. Wierschem, D. D. Quinn, A. F. Vakakis, L. A. Bergman, and B. F. Spencer. Numerical and experimental investigation of a highly effective single-sided vibro-impact non-linear energy sink for shock mitigation. International Journal of Non-Linear Mechanics, 52:96–109, 2013. ISSN 0020-7462. doi: <https://doi.org/10.1016/j.ijnonlinmec.2013.02.004>. URL <https://www.sciencedirect.com/science/article/pii/S0020746213000322>.
- K. Alvin, H. M. de la Fuente, B. Haugen, and C. A. Felippa. Membrane triangles with corner drilling freedoms – I. the EFF element. Finite Elements in Analysis and Design, 12:163–187, 1992.
- B. Amadei. Rock anisotropy and the theory of stress measurements. Lecture notes in engineering. Springer-Verlag, 1983.
- B. Amadei and R. E. Goodman. The influence of rock anisotropy on stress measurements by overcoring techniques. Rock Mechanics, 15:167–180, December 1982. 10.1007/BF01240588.
- T. v. Andel. New Views on an Old Planet. Cambridge University Press, Cambridge, 2 edition, 2008.
- M. Anders and M. Hori. Stochastic finite element method for elasto-plastic body. International Journal for Numerical Methods in Engineering, 46:1897–1916, 1999.
- M. Anders and M. Hori. Three-dimensional stochastic finite element method for elasto-plastic bodies. International Journal for Numerical Methods in Engineering, 51:449–478, 2000.
- Working Paper for Draft Proposed International Standard for Information Systems–Programming Language C++. ANSI/ISO, Washington DC, April 1995. Doc. No. ANSI X3J16/95-0087 ISO WG21/N0687.
- I. Antoniadis, E. Chatzi, D. Chronopoulos, A. Paradeisiotis, I. Sapountzakis, and S. Konstantopoulos. Low-frequency wide band-gap elastic/acoustic meta-materials using the k-damping concept, 2017.
- T. H. Antoun, I. N. Lomov, and L. A. Glenn. Simulation of the penetration of a sequence of bombs into granitic rock. International Journal of Impact Engineering, 29(1-10):81–94, December 2003.
- R. J. Apsel and J. E. Luco. Impedance functions for foundations embedded in a layered medium: An integral equation approach. Earthquake Engineering & Structural Dynamics, 15(2):213–231, 1987.

- Y. Araki, T. Asai, and T. Masui. Vertical vibration isolator having piecewise-constant restoring force. *Earthquake Engineering & Structural Dynamics*, 38(13):1505–1523, 2009.
- G. C. Archer. *Object Oriented Finite Analysis*. PhD thesis, University of California, Berkeley, 1996.
- G. C. Archer, G. Fenves, and C. Thewalt. A new object-oriented finite element analysis program architecture. *Computers and Structures*, 70(1):63–75, 1999.
- Architectural Institute of Japan. *Recommendation for design of building foundations*, 1988.
- G. B. Arfken and H. J. Weber. *Mathematical methods for physicists*. AAPT, 1999.
- J. Argyris and H.-P. Mlejnek. *Dynamics of Structures*. North Holland in USA Elsevier, 1991.
- P. Armstrong and C. Frederick. A mathematical representation of the multiaxial Bauschinger effect. Technical Report RD/B/N/ 731,, C.E.G.B., 1966.
- K. Arulanandan and R. F. Scott, editors. *Verification of Numerical Procedures for the Analysis of Soil Liquefaction Problems*. A. A. Balkema, 1993.
- C. Ashcraft. Ordering sparse matrices and transforming front trees. Technical report, Boeing Shared Service Group, 1999.
- C. Ashcraft, D. Pierce, D. K. Wah, and J. Wu. *The Reference Manual for SPOOLES, Release 2.2: An Object Oriented Software Library for Solving Sparse Linear Systems of Equations*. Boeing Shared Services Group, Seattle, Washington, 1999.
- ASME-VV-10. Standard for verification and validation in computational solid mechanics, V&V 10 - 2019. Technical report, American Society of Mechanical Engineers, 2019. ISBN: 9780791873168.
- ASME-VV-20. Standard for verification and validation in computational fluid dynamics and heat transfer V&V 20 - 2009(r2016). Technical report, American Society of Mechanical Engineers, 2009. ISBN: 9780791832097.
- ASME-VV-40. Assessing credibility of computational modeling through verification and validation: Application to medical devices V&V 40 - 2018. Technical report, American Society of Mechanical Engineers, 2018. ISBN: 9780791872048.
- D. Aubry, A. Modaressi, and H. Modaressi. A constitutive model for cyclic behaviour of interfaces with variable dilatancy. *Computers and Geotechnics*, 9(1-2):47–58, 1990.

- U. Ayachit. The ParaView Guide: A Parallel Visualization Application. Kitware, Inc., USA, 2015. ISBN 1930934300, 9781930934306.
- I. Babuska and P. Chatzipantelidis. On solving elliptic stochastic partial differential equations. Computer Methods in Applied Mechanics and Engineering, 191:4093–4122, 2002.
- I. Babuška and J. T. Oden. Verification and validation in computational engineering and science: basic concepts. Computer Methods in Applied Mechanics and Engineering, 193(36-38):4057–4066, Sept 2004.
- I. Babuska, F. Nobile, J. Oden, and R. Tempone. Reliability, uncertainty estimates, validation and verification. Technical Report 04-05, ICES, 2004.
- D. Baffet, J. Bielak, D. Givoli, T. Hagstrom, and D. Rabinovich. Long-time stable high-order absorbing boundary conditions for elastodynamics. Computer Methods in Applied Mechanics and Engineering, 241-244(0):20 – 37, 2012. ISSN 0045-7825. doi: <http://dx.doi.org/10.1016/j.cma.2012.05.007>. URL <http://www.sciencedirect.com/science/article/pii/S0045782512001557>.
- Z. Bai. Class notes on large scale scientific computing. ECS 231, Department of Computer Science, UC Davis, 2007.
- S. Balay, W. D. Gropp, L. C. McInnes, and B. F. Smith. Efficient management of parallelism in object oriented numerical software libraries. In E. Arge, A. M. Bruaset, and H. P. Langtangen, editors, Modern Software Tools in Scientific Computing, pages 163–202. Birkhäuser Press, 1997.
- S. Balay, K. Buschelman, W. D. Gropp, D. Kaushik, M. G. Knepley, L. C. McInnes, B. F. Smith, and H. Zhang. PETSc Web page, 2001. <http://www.mcs.anl.gov/petsc>.
- S. Balay, K. Buschelman, V. Eijkhout, W. D. Gropp, D. Kaushik, M. G. Knepley, L. C. McInnes, B. F. Smith, and H. Zhang. PETSc users manual. Technical Report ANL-95/11 - Revision 2.1.5, Argonne National Laboratory, 2004.
- A. Baltov and A. Sawczuk. A rule of anisotropic hardening. Acta Mechanica, 1(2):81–92, 1965.
- S. Bandis, A. Lumsden, and N. Barton". Fundamentals of rock joint deformation. International Journal of Rock Mechanics and Mining Sciences & Geomechanics Abstracts, 20(6):249 – 268, 1983.
- A. Banerjee, E. Calius, and R. Das. Impact based wideband nonlinear resonating metamaterial chain. International Journal of Non-Linear Mechanics, 103:138–144, 2018. ISSN 0020-7462. doi: <https://doi.org/10.1016/j.ijnonlinmec.2018.04.011>. URL <https://www.sciencedirect.com/science/article/pii/S0020746218300775>.

- J. P. Bardet, K. Ichii, and C. H. Lin. Eera, a computer program for equivalent-linear earthquake site response analyses of layered soil deposits. Technical report, University of Southern California, 2000.
- M. Bart, J. F. Shao, and D. Lydzba. Poroelastic behaviour of saturated brittle rock with anisotropic damage. *International Journal for Numerical and Analytical Methods in Geomechanics*, 24(15):1139–1154, 2000.
- F. Basone, M. Wenzel, O. S. Bursi, and M. Fossetti. Finite locally resonant metafoundations for the seismic protection of fuel storage tanks. *Earthquake Engineering & Structural Dynamics*, 48(2):232–252, 2019. doi: <https://doi.org/10.1002/eqe.3134>. URL <https://onlinelibrary.wiley.com/doi/abs/10.1002/eqe.3134>.
- U. Basu. Explicit finite element perfectly matched layer for transient three-dimensional elastic waves. *International Journal for Numerical Methods in Engineering*, 77(2):151–176, 2009.
- K.-J. Bathe. *Finite Element Procedures in Engineering Analysis*. Prentice Hall Inc., 1982.
- K.-J. Bathe. *Finite Element Procedures in Engineering Analysis*. Prentice Hall Inc., 1996. ISBN 0-13-301458-4.
- K.-J. Bathe and E. Dvorkin. On the automatic solution of nonlinear finite element equations. *Computers & Structures*, 17(5-6):871–879, 1983.
- K.-J. Bathe and L. Wilson, Edward. *Numerical Methods in Finite Element Analysis*. Prentice Hall Inc., 1976.
- J. Batoz and G. Dhatt. Incremental displacement algorithms for nonlinear problems. *International Journal for Numerical Methods in Engineering*, 14:1262–1267, 1979. Short Communications.
- H. Bavestrello, P. Avery, and C. Farhat. Incorporation of linear multipoint constraints in domain-decomposition-based iterative solvers - Part II: Blending FETI-DP and mortar methods and assembling floating substructures. *Computer Methods in Applied Mechanics and Engineering*, 196(8):1347–1368, January 2007.
- K. Been and M. Jefferies. A state parameter for sands. *Geotechnique*, 35(2):99–112, 1985.
- T. Belytschko, B. Moran, and M. Kulkarni. On the crucial role of imperfections in quasi-static viscoplastic solutions. *Journal of Applied Mechanics*, 58:658–665, 1991.
- T. Belytschko, W. K. Liu, and B. Moran. *Nonlinear finite elements for continua and structures*. John Wiley & Sons, 2000.

- T. Belytschko, W. K. Liu, and B. Moran, editors. Nonlinear Finite Element for Continua and Structures. John Wiley & Sons Ltd., New York, 2001.
- Y. Ben-Haim and I. Elishakoff. Convex Models of Uncertainty in Applied Mechanics. Elsevier, Amsterdam, 1990.
- T. Benz and R. Schwabb. A quantitative comparison of six rock failure criteria. International Journal of Rock Mechanics and Mining Sciences, 45(7):1176–1186, October 2008.
- M. Benzi. Preconditioning techniques for large linear systems: A survey. Journal of Computational Physics, 182:418–477, 2002.
- M. Benzi and M. Tůma. A robust incomplete factorization preconditioner for positive definite matrices. Numerical Linear Algebra with Applications, 10:385–400, 2003.
- M. Benzi, C. D. Meyer, and M. Tůma. A sparse approximate inverse preconditioner for the conjugate gradient method. SIAM Journal on Scientific Computing, 17(5):1135–1149, 1996.
- M. Benzi, J. K. Cullum, and M. Tůma. Robust approximate inverse preconditioning for the conjugate gradient method. SIAM Journal on Scientific Computing, 22(4):1318–1332, 2000.
- P. G. Bergan and C. A. Felippa. A triangular membrane element with rotational degrees of freedom. Computer Methods in Applied Mechanics and Engineering, 50:25–69, 1985.
- J. B. Berril, S. A. Christensen, R. J. Keenan, W. Okada, and J. K. Pettinga. Lateral-spreading loads on a piled bridge foundations. In S. E. Pinto, editor, Seismic Behavior of Ground and Geotechnical Structures, pages 173–183, 1997.
- J. F. Besseling and E. Van Der Giessen. Mathematical modeling of inelastic deformation, volume 5. CRC Press, 1994.
- P. N. Bičanić. Exact evaluation of contact stress state in computational elasto plasticity. Engineering Computations, 6:67–73, 1989.
- J. Bielak. Dynamic response of non-linear building-foundation systems. Earthquake Engineering & Structural Dynamics, 6(1):17–30, 1978.
- J. Bielak, K. Loukakis, Y. Hisada, and C. Yoshimura. Domain reduction method for three-dimensional earthquake modeling in localized regions. part I: Theory. Bulletin of the Seismological Society of America, 93(2):817–824, 2003a.

- J. Bielak, K. Loukakis, Y. Hisada, and C. Yoshimura. Domain reduction method for three dimensional earthquake modeling in localized regions. part i: Theory. *Bulletin of the Seismological Society of America*, 93(2):817–824, 2003b.
- A. Bilbao, R. Aviles, J. Agirrebeitia, and G. Ajuria. Proportional damping approximation for structures with added viscoelastic dampers. *Finite Elements in Analysis and Design*, 42:492–502, 2006.
- B. A. Bilby, L. R. T. Gardner, and A. N. Stroh. Continuous distributions of dislocations and the theory of plasticity. In *IX^e Congrès International de Mécanique Appliquée*, volume VIII, pages 35–44, Université de Bruxelles, 50. Avènue Franklin Roosevelt, 1957.
- M. Biot. Mechanics of deformation and acoustic propagation in porous media. *Journal of Applied Physics*, 33(4):1482–1498, April 1962.
- M. A. Biot. Theory of finite deformations of porous solids. *Indiana University Mathematical Journal*, 21(7):597–620, January 1972.
- J. Bishop and R. Hill. A theory of the plastic distortion of a polycrystalline aggregate under combined stresses. *The London, Edinburgh, and Dublin Philosophical Magazine and Journal of Science*, 42(327):414–427, 1951.
- F. Black and M. Scholes. The pricing of options and corporate liabilities. *Journal of Political Economy*, 81(3):637–654, 1973.
- J. Bloch. How to design a good api and why it matters. In D. Musser, editor, *Library-Centric Software Design LCSD'05. Object-Oriented Programming, Systems, Languages and Applications*, October 2005. Presentation Slides.
- W. Boggs and M. Boggs. *Mastering UML with Rational Rose 2002*. Sybex, Alameda CA 94501, 2002.
- M. Bollhöfer and Y. Saad. On the relations between ILUs and factored approximate inverses. Technical Report UMSI-2001-67, Department of Computer Science and Engineering, University of Minnesota, 2001.
- M. Bolton. The strength and dilatancy of sands. *Geotechnique*, 36(1):65–78, 1986.
- G. Booch. *Object Oriented Analysis and Design with Applications*. Series in Object–Oriented Software Engineering. Benjamin Cummings, second edition, 1994.
- R. Borja and A. Amies. Multiaxial cyclic plasticity model for clays. *Journal of Geotechnical Engineering*, 120(6):1051–1070, 1994.

- R. Borja, C. Lin, K. Sama, and G. Masada. Modelling non-linear ground response of non-liquefiable soils. *Earthquake Engineering and Structural Dynamics*, 29:63–83, 2000.
- R. I. Borja. Conditions for instabilities in collapsible solids including volume implosion and compaction banding. *Acta Geotechnica*, 1:107–122, 2006.
- R. I. Borja, H. Yih Chao, F. J. Montána, and C. Hua Lin. Nonlinear ground response at Lotung LSST site. *ASCE Journal of Geotechnical and Geoenvironmental Engineering*, 125(3):187–197, March 1999.
- R. W. Boulanger and K. Tokimatsu, editors. *Seismic Performance and Simulation of Pile Foundations in Liquefied and Laterally Spreading Ground*. Geotechnical Special Publication No 145. ASCE Press, Reston, VA, 2006. 321 pp.
- M. Boulon. Basic features of soil structure interface behaviour. *Computers and Geotechnics*, 7(1-2):115–131, 1989.
- M. Boulon and R. Nova. Modelling of soil-structure interface behaviour a comparison between elasto-plastic and rate type laws. *Computers and Geotechnics*, 9(1-2):21–46, 1990.
- M. Boutea and Y. Gueguen. Mechanical properties of rocks: Pore pressure and scale effects. *Oil & Gas Science and Technology*, 54(6):703–714, 1999. URL [RockPapers/R12.pdf](#).
- B. L. Boyce, S. L. B. Kramer, H. E. Fang, T. E. Cordova, M. K. Neilsen, K. Dion, A. K. Kaczmarowski, E. Karasz, L. Xue, A. J. Gross, A. Ghahremaninezhad, K. Ravi-Chandar, S.-P. Lin, S.-W. Chi, J. S. Chen, E. Yreux, M. Rüter, D. Qian, Z. Zhou, S. Bhamare, D. T. O'Connor, S. Tang, K. I. Elkhodary, J. Zhao, J. D. Hochhalter, A. R. Cerrone, A. R. Ingraffea, P. A. Wawrzynek, B. J. Carter, J. M. Emery, M. G. Veilleux, P. Yang, Y. Gan, X. Zhang, Z. Chen, E. Madenci, B. Kilic, T. Zhang, E. Fang, P. Liu, J. Lua, K. Nahshon, M. Miraglia, J. Cruce, R. DeFrese, E. T. Moyer, S. Brinckmann, L. Quinkert, K. Pack, M. Luo, and T. Wierzbicki. The Sandia fracture challenge: blind round robin predictions of ductile tearing. *International Journal of Fracture*, 186:5–68, January 2014. doi: 10.1007/s10704-013-9904-6. URL <https://doi.org/10.1007/s10704-013-9904-6>.
- M. Bragg. In Our Time, Seismology. BBC Podcast, March 2022. <https://www.bbc.co.uk/sounds/play/m00154gh>.
- S. J. Brandenberg, R. W. Boulanger, B. L. Kutter, and D. Chang. Static pushover analyses of pile groups in liquefied and laterally spreading ground in centrifuge tests. *Journal of Geotechnical and Geoenvironmental Engineering*, 133(9):1055–1066, 2007.

- H. J. Braudel, M. Abouaf, and J. L. Chenot. An implicit and incremental formulation for the solution of elastoplastic problems , by the finite element method. *Computers Structures*, 22(5):801–814, 1986.
- L. Brillouin. *Wave Propagation in Periodic Structures*. McGraw-Hill Book Company, Inc, (1946) and Dover Publications, Inc. (1953), 1953.
- D. A. Brown and C.-F. Shie. Three dimensional finite element model of laterally loaded piles. *Computers and Geotechnics*, 10:59–79, 1990a.
- D. A. Brown and C.-F. Shie. Numerical experiments into group effects on the response of piles to lateral loading. *Computers and Geotechnics*, 10:211–230, 1990b.
- D. A. Brown and C.-F. Shie. Some numerical experiments with a three dimensional finite element model of a laterally loaded pile. *Computers and Geotechnics*, 12:149–162, 1991.
- D. A. Brown, C. Morrison, and L. C. Reese. Lateral loaded behavior of pile group in sand. *Journal of Geotechnical Engineering*, 114(11):1261–1277, November 1988.
- S. Brûlé, E. H. Javelaud, S. Enoch, and S. Guenneau. Experiments on seismic metamaterials: Molding surface waves. *Phys. Rev. Lett.*, 112:133901, Mar 2014. doi: 10.1103/PhysRevLett.112.133901. URL <https://link.aps.org/doi/10.1103/PhysRevLett.112.133901>.
- W. Brumund and G. Leonards. Experimental study of static and dynamic friction between sand and typical constuction materials. *Journal of Testing and Evaluation*, 1(2):162–165, 1973.
- A. Burnol, A. A. L. Landes, D. Raucoules, M. Foumelis, C. Allanic, F. Paquet, J. Maury, H. Aochi, T. Guillou, M. Delatre, P. Dominique, A. Bitri, S. Lopez, P. P. Pébay, and B. Bazargan-Sabet. Impacts of Water and Stress Transfers from Ground Surface on the Shallow Earthquake of 11 November 2019 at Le Teil (France). *Remote Sens.*, 2023. doi: 10.3390/rs15092270.
- P. Cacciola, A. Tombari, and A. Giaralis. An inerter-equipped vibrating barrier for noninvasive motion control of seismically excited structures. *Structural Control and Health Monitoring*, 27(3):e2474, 2020. doi: <https://doi.org/10.1002/stc.2474>. URL <https://onlinelibrary.wiley.com/doi/abs/10.1002/stc.2474>. e2474 STC-18-0444.R2.
- C. Cai, J. Zhou, L. Wu, K. Wang, D. Xu, and H. Ouyang. Design and numerical validation of quasi-zero-stiffness metamaterials for very low-frequency band gaps. *Composite Structures*, 236:111862, 2020. ISSN 0263-8223. doi: <https://doi.org/10.1016/j.compstruct.2020.111862>. URL <https://www.sciencedirect.com/science/article/pii/S0263822319331459>.

- B. Capra and A. Sellier. Orthotropic modelling of alkali-aggregate reaction in concrete structures: numerical simulations. *Mechanics of materials*, 35(8):817–830, 2003.
- A. Cardona, I. Klapka, and M. Geradin. Design of a new finite element programming environment. *Engineering Computations*, 11:365–381, 1994.
- I. Carol, E. Rizzi, and K. Willam. Current issues in elastic degradation and damage. In S. Sture, editor, *Proceedings of 10th Conference*, pages 521–524. Engineering Mechanics Division of the American Society of Civil Engineers, May 1995.
- I. Carol, E. Rizzi, and K. William. On the formulation of anisotropic elastic degradadation. I. theory based on a pseudo–logarithmic damage tensor rate. *International Journal of Solids and Structures*, 38:491–518, 2001a.
- I. Carol, E. Rizzi, and K. William. On the formulation of anisotropic elastic degradadation. II. generalized pseudo–Rankine model for tensile damage. *International Journal of Solids and Structures*, 38:519–546, 2001b.
- G. Carta, G. Giacu, and M. Brun. A phononic band gap model for long bridges. the 2018brabau2019 bridge case. *Engineering Structures*, 140:66–76, 2017. ISSN 0141-0296. doi: <https://doi.org/10.1016/j.engstruct.2017.01.064>. URL <https://www.sciencedirect.com/science/article/pii/S0141029617303103>.
- W. T. Carter, T. L. Sham, and K. H. Law. A Parallel Finite Element Method and It's Prototype Implementation on a Hypercube. *Computers and Structures*, 31(6):921–934, 1989.
- O. Casablanca, G. Ventura, F. Garescì, B. Azzerboni, B. Chiaia, M. Chiappini, and G. Finocchio. Seismic isolation of buildings using composite foundations based on metamaterials. *Journal of Applied Physics*, 123(17):174903, 2018. doi: 10.1063/1.5018005. URL <https://doi.org/10.1063/1.5018005>.
- A. Casagrande and F. Rendon. Gyratory shear apparatus; design, testing procedures. Technical Report S-78-15, U.S. Army Corps of Engineers, Waterways Experiment Station, Vicksburg, Miss., 1978.
- A. H.-C. Chan. *A Unified Finite Element Solution to Static and Dynamic Problems in Geomecahnics*. PhD thesis, Department of Civil Engineering, University College of Swansea, February 1988.
- G. Chang and J. B. Mander. *Seismic energy based fatigue damage analysis of bridge columns: Part I-Evaluation of seismic capacity*. National Center for Earthquake Engineering Research Buffalo, NY, 1994.

- R. G. Charlwood, S. V. Solymar, and D. D. Curtis. A review of alkali aggregate reactions in hydroelectric plants and dams. In Proceedings of the International Conference of Alkali-Aggregate Reactions in Hydroelectric Plants and Dams, Fredericton, Canada, pages 129–135, 1992.
- L. Chen, J. Shao, and H. Huang. Coupled elastoplastic damage modeling of anisotropic rocks. Computer and Geotechnics, 37:187–194, 2010.
- L. Chen, J. Zang, A. Hillis, G. Morgan, and A. Plummer. Numerical investigation of wave–structure interaction using openfoam. Ocean Engineering, 88:91–109, 2014.
- S. Chen, B. Wang, S. Zhu, X. Tan, J. Hu, X. Lian, L. Wang, and L. Wu. A novel composite negative stiffness structure for recoverable trapping energy. Composites Part A: Applied Science and Manufacturing, 129:105697, 2020. ISSN 1359-835X. doi: <https://doi.org/10.1016/j.compositesa.2019.105697>. URL <https://www.sciencedirect.com/science/article/pii/S1359835X19304464>.
- W. F. Chen and D. J. Han. Plasticity for Structural Engineers. Springer Verlag, 1988a.
- W. F. Chen and D. J. Han. Plasticity for Structural Engineers. Springer-Verlag, 1988b.
- X. Chen and K. Phoon. Some numerical experiences on convergence criteria for iterative finite element solvers. Computers and Geotechnics, 36(8):1272–1284, October 2009.
- Z. Cheng and B. Jeremić. Numerical modeling and simulation of soil lateral spreading against piles. In In proceedings of the GeoOrlando, Geo Institute Annual Conference, Orlando, Florida, March 2009a.
- Z. Cheng and B. Jeremić. Numerical modeling and simulations of piles in liquefiable soil. Soil Dynamics and Earthquake Engineering, 29:1405–1416, 2009b.
- Z. Cheng and Z. Shi. Composite periodic foundation and its application for seismic isolation. Earthquake Engineering & Structural Dynamics, 47(4):925–944, 2018. doi: <https://doi.org/10.1002/eqe.2999>. URL <https://onlinelibrary.wiley.com/doi/abs/10.1002/eqe.2999>.
- Z. Cheng, M. Taiebat, B. Jeremić, and Y. Dafalias. Modeling and simulation of saturated geomaterials. In In proceedings of the GeoDenver conference, 2007.
- S. Chiriță, C. Galeș, and I. Ghiba. On spatial behavior of the harmonic vibrations in kelvin-voigt materials. Journal of Elasticity, 93(1):81–92, 2008.
- C. H. Choi. Physical and Mathematical Modeling of Coarse-Grained Soils. PhD thesis, Department of Civil and Environmental Engineering, University of Washington, Seattle, Washington, 2004.

- K. A. Chondrogiannis, V. Dertimanis, B. Jeremić, and E. Chatzi. On the vibration attenuation properties of metamaterial design using negative stiffness elements. In W. Lacarbonara, B. Balachandran, M. J. Leamy, J. Ma, J. T. Machado, and G. Stepan, editors, *Advances in Nonlinear Dynamics - Proceedings of the Second International Nonlinear Dynamics Conference (NODYCON 2021)*, volume 3, Sapienza, Università di Roma, 16-19 February 2021. Springer Nature.
- K. A. I. Chondrogiannis, V. K. Dertimanis, S. F. Masri, and E. N. Chatzi. Vibration absorption performance of metamaterial lattices consisting of impact dampers. In M. Papadrakakis, M. Fragiadakis, and C. Papadimitriou, editors, *EURODYN 2020, XI International Conference on Structural Dynamics*, Athens, Greece, 23-26 November 2020 2020. URL <https://doi.org/10.3929/ethz-b-000451611>.
- A. K. Chopra. *Dynamics of Structures, Theory and Application to Earthquake Engineering*. Prentice Hall, second edition, 2000. ISBN 0-13-086973-2.
- A. K. Chopra and J. A. Gutierrez. Earthquake response analysis of multistorey buildings including foundation interaction. *Earthquake Engineering & Structural Dynamics*, 3(1):65–77, 1974.
- R. Chudoba and Z. Bittnar. Explicit Finite Element Computation: An Object-Oriented Approach. In *Computing in Civil and Building Engineering: Proceedings of the Sixth International Conference on Computing in Civil and Building Engineering*, Berlin, Germany, July 12-15 1995.
- R. Clifton, J. Duffy, K. Hartley, and T. Shawki. On critical conditions for shear band formation at high strain rates. *Scripta Metallurgica*, 18(5):443–448, 1984.
- I. Collins. Associated and non-associated aspects of the constitutive laws for coupled elastic/plastic materials. *International Journal of Geomechanics*, 2(2):259–267, 2002.
- I. Collins. A systematic procedure for constructing critical state models in three dimensions. *International Journal of Solids and Structures*, 40(17):4379–4397, 2003.
- I. Collins and P. Kelly. A thermomechanical analysis of a family of soil models. *Geotechnique*, 52(7):507–518, 2002.
- I. F. Collins and G. T. Housby. Application of thermomechanical principles to the modelling of geotechnical materials. *Proceedings of Royal Society London*, 453:1975–2001, 1997.
- A. Colombi, D. Colquitt, P. Roux, S. Guenneau, and R. V. Craster. A seismic metamaterial: The resonant metawedge. *Scientific Reports*, 6(27717):1–6, June 2016a. URL <https://www.nature.com/articles/srep27717#citeas>.

- A. Colombi, D. Colquitt, P. Roux, S. Guenneau, and R. V. Craster. Forests as a natural seismic metamaterial: Rayleigh wave bandgaps induced by local resonances. *Scientific Reports*, 6(19238):1–7, January 2016b. URL <https://www.nature.com/articles/srep19238>.
- A. Colombi, R. Zaccherini, G. Aguzzi, A. Palermo, and E. Chatzi. Mitigation of seismic waves: Metabarriers and metafoundations bench tested. *Journal of Sound and Vibration*, 485:115537, 2020. ISSN 0022-460X. doi: <https://doi.org/10.1016/j.jsv.2020.115537>. URL <https://www.sciencedirect.com/science/article/pii/S0022460X20303692>.
- R. D. Cook, D. S. Malkus, M. E. Plesha, and R. J. Witt. *Concepts and Applications of Finite Element Analysis*. John Wiley & Sons, 2002.
- J. O. Coplien. *Advanced C++, Programming Styles and Idioms*. Addison – Wesley Publishing Company, 1992.
- M. Corigliano, L. Scandella, C. G. Lai, and R. Paolucci. Seismic analysis of deep tunnels in near fault conditions: a case study in southern Italy. *Bulletin of Earthquake Engineering*, 9(4):975–995, 2011.
- E. Cosenza, G. Manfredi, and R. Ramasco. The use of damage functionals in earthquake engineering: a comparison between different methods. *Earthquake engineering & structural dynamics*, 22(10):855–868, 1993.
- E. Cosserat. *Théorie des Corps Déformables*. Éditions Jacques Gabay (2008), 151 bis rue Saint-Jacques, 75005 Paris, France, 1909. ISBN 978-2-87647-301-0. (originally published in 1909, by Librairie Scientifique A. Herman et Fils, 6, rue de la Sorbonne, 6, Paris).
- R. Courant and D. Hilbert. *Methods of Mathematical Physics*. Wiley, 1989. ISBN 979-0-471-50447-4.
- O. Coussy. *Mechanics of Porous Continua*. John Wiley and Sons, 1995. ISBN 471 95267 2.
- O. Coussy. *Poromechanics*. John Wiley & Sons, 2004.
- M. A. Crisfield. Consistent schemes for plasticity computation with the Newton Raphson method. *Computational Plasticity Models, Software, and Applications*, 1:136–160, 1987.
- M. A. Crisfield. A consistent co-rotational formulation for non-linear, three-dimensional, beam-elements. *Computer methods in applied mechanics and engineering*, 81(2):131–150, 1990.
- M. A. Crisfield. *Non-Linear Finite Element Analysis of Solids and Structures Volume 1: Essentials*. John Wiley and Sons, Inc. New York, 605 Third Avenue, New York, NY 10158–0012, USA, 1991.

- M. A. Crisfield. Non-Linear Finite Element Analysis of Solids and Structures Volume 2: Advanced Topics. John Wiley and Sons, Inc. New York, 605 Third Avenue, New York, NY 10158–0012, USA, 1997a.
- M. A. Crisfield. Non-linear Finite Element Analysis of Solids and Structures. John Wiley & Sons, 1997b.
- L. Crivelli and C. Farhat. Implicit transient finite element structural computations on mimm systems: Feti v.s. direct solvers. In 34th AIAA/ASME/ASCE/AHS/ASC Structures, Structural Dynamics, and Materials Conference, La Jolla, CA, USA, April 19-22 1993.
- M. Čubrinovski. Private communications. ..., 2007 –.
- M. Čubrinovski and K. Ishihara. Assessment of pile group response to lateral spreading by single pile analysis. In Seismic Performance and Simulation of Pile Foundations in Liquefied and Laterally Spreading Ground, Geotechnical Special Publication No. 145, pages 242–254. ASCE, 2006.
- M. Čubrinovski, R. Uzuoka, H. Sugita, K. Tokimatsu, M. Sato, K. Ishihara, Y. Tsukamoto, and T. Kamata. Prediction of pile response to lateral spreading by 3-d soil-coupled dynamic analysis: Shaking in the direction of ground flow. Soil Dynamics and Earthquake Engineering, 28(6):421–435, June 2008.
- D. Curran. A pressure-induced strength transition in water-saturated geologic materials. In International Conference on Mechanical and Behaviour of Materials under Dynamic Loading / Congrès international sur le comportement mécanique et physique des matériaux sous sollicitations dynamiques, volume J. Phys. IV France 04 (1994) C8-243-C8-247, 1994. URL <http://hal.archives-ouvertes.fr/docs/00/25/33/91/PDF/ajp-jp4199404C836.pdf>. DOI: 10.1051/jp4:1994836.
- W. J. N. D. Erskine and S. T. Weir. Shock wave profile study of tuff from the nevada test site. Journal of Geophysical Research, 99(B8):15,529–15,537, 1994.
- Y. Dafalias. A model for soil behavior under monotonic and cyclic loading conditions. In Proceedings of the 5th international conference on SMiRT, volume K 1/8, 1979.
- Y. Dafalias and E. Popov. A model of nonlinearly hardening materials for complex loading. Acta mechanica, 21(3):173–192, 1975.
- Y. Dafalias and E. Popov. Cyclic loading for materials with a vanishing elastic region. Nuclear Engineering and Design, 41(2):293–302, 1977.
- Y. Dafalias, D. Schick, C. Tsakmakis, K. Hutter, and H. Baaser. A simple model for describing yield surface evolution. In Lecture notes in applied and computational mechanics, pages 169–201. Springer, 2002.

- Y. F. Dafalias. Il'iushin's postulate and resulting thermodynamic conditions on elastic–plastic coupling. *International Journal of Solids and Structures*, 13:239–251, 1977.
- Y. F. Dafalias. Bounding surface plasticity. I: Mathematical foundations and hypoplasticity. *ASCE Journal of Engineering Mechanics*, 112(9):966–987, September 1986.
- Y. F. Dafalias and M. T. Manzari. Simple plasticity sand model accounting for fabric change effects. *Journal of Engineering Mechanics*, 130(6):622–634, 2004a.
- Y. F. Dafalias and M. T. Manzari. Simple plasticity sand model accounting for fabric change effects. *ASCE Journal of Engineering Mechanics*, 130(6):622–634, June 2004b.
- Y. F. Dafalias, M. T. Manzari, and A. G. Papadimitriou. SANICLAY: simple anisotropic clay plasticity model. *International Journal for Numerical and Analytical Methods in Geomechanics*, 30(12):1231–1257, 2006.
- J. D'Alembert. *Traité de Dynamique*. Éditions Jacques Gabay, 151 bis rue Saint-Jacques, 75005 Paris, France, 1758. ISBN 2-87647-064-0. (originally published in 1758), This edition published in 1990.
- S. K. Das and P. K. Basudhar. Comparison of intact rock failure criteria using various statistical methods. *Acta Geotechnica*, 4(3):223–231, September 2009.
- M. T. Davisson and H. L. Gill. Laterally loaded piles in a layered soil system. *Journal of the Soil Mechanics and Foundations Division*, 89(SM3):63–94, May 1963. Paper 3509.
- S. M. Day. *Finite Element Analysis of Seismic Scattering Problems*. PhD thesis, University of California at San Diego, 1977.
- R. de Boer, W. Ehlers, and Z. Liu. One-dimensional transient wave propagation in fluid-saturated incompressible porous media. *Archive of Applied Mechanics*, 63(1):59–72, January 1993.
- R. de Borst. Computation of post-bifurcation and post-failure behavior of strain-softening solids. *Computers & Structures*, 25(2):211–224, 1987.
- R. de Borst. Smeared cracking, plasticity, creep, and thermal loading - a unified approach. *Computer Methods in Applied Mechanics and Engineering*, 62:89–110, 1987.
- R. de Borst. Simulation of strain localization: a reappraisal of the Cosserat continuum. *Engineering Computations*, 8(4):317–332, 1991. doi: 10.1108/eb023842.

- R. de Borst. A generalisation of J2-flow theory for polar continua. *Computer Methods in Applied Mechanics and Engineering*, 103(3):347–362, 1993. ISSN 00457825. doi: 10.1016/0045-7825(93)90127-J.
- R. de Borst and P. H. Feenstra. Studies in anisotropic plasticity with reference to the hill criterion. *International Journal for Numerical Methods in Engineering*, 29:315–336, 1990.
- B. S. L. P. De Lima, E. C. Teixeira, and N. F. F. Ebecken. Probabilistic and possibilistic methods for the elastoplastic analysis of soils. *Advances in Engineering Software*, 132:569–585, 2001.
- M. K. Deb, I. M. Babuska, and J. T. Oden. Solution of stochastic partial differential equations using Galerkin finite element techniques. *Computer Methods in Applied Mechanics and Engineering*, 190: 6359–6372, 2001.
- B. J. Debusschere, H. N. Najm, A. Matta, O. M. Knio, and R. G. Ghanem. Protein labeling reactions in electrochemical microchannel flow: Numerical simulation and uncertainty propagation. *Physics of Fluids*, 15:2238–2250, 2003.
- D. J. DeGroot and G. B. Baecher. Estimating autocovariance of in-situ soil properties. *Journal of Geotechnical Engineering*, 119(1):147–166, January 1993.
- A. R. Dehkordi. *3D Finite Element Cosserat Continuum Simulation of Layered Geomaterials*. PhD thesis, University of Toronto, 2008.
- J. T. DeJong and Z. J. Westgate. Role of initial state, material properties, and confinement condition on local and global soil-structure interface behavior. *ASCE Journal of Geotechnical and Geoenvironmental Engineering*, 135(11):1646–1660, November 2009.
- J. T. Dejong, D. J. White, and M. F. Randolph. Microscale observation and modeling of soil-structure interface behavior using particle image velocimetry. *Soils and Foundations*, 46(1):15–28, 2006.
- I. Demirdžić and M. Perić. Space conservation law in finite volume calculations of fluid flow. *International journal for numerical methods in fluids*, 8(9):1037–1050, 1988.
- J. W. Demmel. *Applied Numerical Linear Algebra*. SIAM, Philadelphia, 1997.
- J. W. Demmel, M. T. Heath, and H. A. van der Vorst. Parallel numerical linear algebra. Technical report, LAPACK Working Note 60, UT CS-93-192, 1993.
- J. W. Demmel, S. C. Eisenstat, J. R. Gilbert, X. S. Li, and J. W. H. Liu. A supernodal approach to sparse partial pivoting. *SIAM J. Matrix Analysis and Applications*, 20(3):720–755, 1999a.

- J. W. Demmel, J. R. Gilbert, and X. S. Li. An asynchronous parallel supernodal algorithm for sparse gaussian elimination. *SIAM J. Matrix Analysis and Applications*, 20(4):915–952, 1999b.
- J. W. Demmel, J. R. Gilbert, and X. S. Li. *SuperLU Users' Guide*, 2003.
- D. Deniz, J. Song, and J. F. Hajjar. Energy-based seismic collapse criterion for ductile planar structural frames. *Engineering Structures*, 141:1–13, 2017.
- J. E. Dennis, Jr. and R. B. Schnabel. *Numerical Methods for Unconstrained Optimization and Nonlinear Equations*. Prentice Hall , Engelwood Cliffs, New Jersey 07632., 1983.
- A. Der Kiureghian and B. J. Ke. The stochastic finite element method in structural reliability. *Journal of Probabilistic Engineering Mechanics*, 3(2):83–91, 1988.
- V. K. Dertimanis, I. A. Antoniadis, and E. N. Chatzi. Feasibility analysis on the attenuation of strong ground motions using finite periodic lattices of mass-in-mass barriers. *Journal of Engineering Mechanics*, 142(9):04016060, 2016. doi: 10.1061/(ASCE)EM.1943-7889.0001120. URL <https://ascelibrary.org/doi/abs/10.1061/%28ASCE%29EM.1943-7889.0001120>.
- C. Desai. Behavior of interfaces between structural and geologic media. Technical report, University of Missouri–Rolla, 1981.
- C. Desai and B. Nagaraj. Modeling for cyclic normal and shear behavior of interfaces. *Journal of engineering mechanics*, 114(7):1198–1217, 1988.
- S. S. Deshpande, L. Anumolu, and M. F. Trujillo. Evaluating the performance of the two-phase flow solver interfoam. *Computational Science & Discovery*, 5(1):014016, 2012.
- C. di Prisco and F. Pisanò. An exercise on slope stability and perfect elasto-plasticity. *Géotechnique*, 61(11):923–934, 2011.
- C. di Prisco and D. Wood. *Mechanical Behaviour of Soils Under Environmentally-Induced Cyclic Loads*. Springer, 2012.
- C. di Prisco, M. Pastor, and F. Pisanò. Shear wave propagation along infinite slopes: A theoretically based numerical study. *International Journal for Numerical and Analytical Methods in Geomechanics*, 36(5):619–642, 2012. ISSN 1096-9853. doi: 10.1002/nag.1020. URL <http://dx.doi.org/10.1002/nag.1020>.
- S. E. Dickenson. *Dynamic response of soft and deep cohesive soils during the Loma Prieta earthquake of October 17, 1989*. PhD thesis, University of California, Berkeley, 1994.

- S. Dmitriev. Language oriented programming: The next programming paradigm. published online <http://www.onboard.jetbrains.com/is1/articles/04/10/lop/>, November 2004.
- R. Dobry and T. Abdoun. Recent studies on seismic centrifuge modeling of liquefaction and its effects on deep foundations. In S. Prakash, editor, Proceedings of Fourth International Conference on Recent Advances in Geotechnical Earthquake Engineering and Soil Dynamics, San Diego, March 26-31 2001.
- R. Dobry, T. Abdoun, T. D. O'Rourke, and S. H. Goh. Single piles in lateral spreads: Field bending moment evaluation. Journal of Geotechnical and Geoenvironmental Engineering, 129(10):879–889, 2003.
- C. R. Dohrmann. A preconditioner for substructuring based on constrained energy minimization. SIAM Journal of Scientific Computing, 25(1):246–258, September/October 2003.
- M. Dolinski, D. Rittel, and A. Dorogoy. Modeling adiabatic shear failure from energy considerations. Journal of the Mechanics and Physics of Solids, 58(11):1759–1775, 2010.
- J. Donea, S. Giuliani, and J.-P. Halleux. An arbitrary lagrangian-eulerian finite element method for transient dynamic fluid-structure interactions. Computer methods in applied mechanics and engineering, 33(1-3):689–723, 1982.
- P. Donescu and T. A. Laursen. A generalized object-oriented approach to solving ordinary and partial differential equations using finite elements. Finite Elements in Analysis and Design, 22:93–107, 1996.
- J. Dongarra, I. Foster, G. Fox, W. Gropp, K. Kennedy, L. Torczon, and A. White. Source Book of Parallel Computing. Morgan Kaufmann Publishers, 2003.
- J. J. Dongarra, I. S. Duff, D. C. Sorensen, and H. A. van der Vorst. Numerical Linear Algebra for High Performance Computers. Prentice Hall, New Jersey, 1996.
- D. C. Drucker. On uniqueness in the theory of plasticity. Quarterly of Applied Mathematics, pages 35–42, 1956.
- D. C. Drucker. A definition of stable inelastic material. Technical report, DTIC Document, 1957.
- M. Dryden. Nees sfsi demonstration project. In NEES Project Meeting, Austin, TX, August 2005.
- Y. Dubois-Pèlerein and T. Zimmermann. Object-oriented finite element programing: iii. an efficient implementation in c++. Computer Methods in Applied Mechanics and Engineering, 108:165–183, 1993.

- Y. Dubois-Pélerin and P. Pegon. Object-oriented programming in nonlinear finite element analysis. *Computers & Structures*, 67(4):225–241, 1998.
- Y. Dubois-Pélerin and T. Zimmermann. *Object Oriented Finite Element Programming: Theory and C++ Implementation for FEM_Objects C++ 01*. Elmepress International, P.O.Box 2 CH 1015 Lausanne 15, Switzerland, 1992.
- Y. Dubois-Pelerin and T. Zimmermann. Object-Oriented Finite Element Programming: III. An Efficient Implementation in C++. *Computer Methods in Applied Mechanics and Engineering*, 108(1-2):165–183, 1993.
- Y. Dubois-Pelerin, T. Zimmermann, and P. Bomme. Object-Oriented Finite Element Programming: II. A Prototype Program in Smalltalk. *Computer Methods in Applied Mechanics and Engineering*, 98(3):361–397, 1992.
- Y.-D. Dubois-Pelerin. *Object Oriented Finite Elements: Programming Concepts and Implementation*. PhD thesis, Ecole Polytechnique Federale de Lausanne, 1992.
- J. M. Duncan. State of the art: Limit equilibrium and finite-element analysis of slopes. *ASCE Journal of Geotechnical and Geoenvironmental Engineering*, 122(7):577–596, July 1996.
- J. M. Duncan. Factors of safety and reliability in geotechnical engineering. *ASCE Journal of Geotechnical and Geoenvironmental Engineering*, 126(4):307–316, April 2000a.
- J. M. Duncan. Factors of safety and reliability in geotechnical engineering. *ASCE Journal of Geotechnical and Geoenvironmental Engineering*, 126(4):307–316, April 2000b.
- J. M. Duncan and C.-Y. Chang. Nonlinear analysis of stress and strain in soils. *Journal of Soil Mechanics and Foundations Division*, 96:1629–1653, 1970.
- Š. Dunica and B. Kolundžija. *Nelinarna Analiza Konstrukcija*. Gradjevinski fakultet Univerziteta u Beogradu, Bulevar revolucije 73 i IRO "Naučna knjiga", Beograd, Uzun–Mirkova 5, 1986. Nonlinear Analysis of Structures, In Serbian.
- B. Eckel. *Using C++*. Osborne McGraw – Hill, 1989.
- H. El Ganainy and M. El Naggar. Seismic performance of three-dimensional frame structures with underground stories. *Soil Dynamics and Earthquake Engineering*, 29(9):1249–1261, 2009.
- A. Elgamal, Z. Yang, and E. Parra. Computational modeling of cyclic mobility and post-liquefaction site response. *Soil Dynamics and Earthquake Engineering*, 22:259–271, 2002.

- A. Elgamal, Z. Yang, E. Parra, and A. Ragheb. Modeling of cyclic mobility in saturated cohesionless soils. *International Journal of Plasticity*, 19(6):883–905, 2003.
- A. Elgamal, L. Yan, Z. Yang, and J. P. Conte. Three-dimensional seismic response of humboldt bay bridge-foundation-ground system. *ASCE Journal of Structural Engineering*, 134(7):1165–1176, July 2008.
- M. A. Ellis and B. Stroustrup. *The Annotated C++ Reference Manual*. AT&T Bell Laboratories, Murray Hill, New Jersey and Addison - Wesley Publishing Company, 1990.
- A. C. Eringen. *Microcontinuum field theories: I. Foundations and solids*. Springer Science & Business Media, 2012.
- E. Evgin and K. Fakharian. Effect of stress paths on the behaviour of sand steel interfaces. *Canadian geotechnical journal*, 33(6):853–865, 1997.
- D. Eyheramendy. *Object–Oriented Finite Element Programming: symbolic Derivations and Automatic Programming*. PhD thesis, Ecole Polytechniques Fédéral de Lausanne, 1997.
- D. Eyheramendy and T. Zimmermann. Object–oriented finite elements II. a symbolic environment for automatic programming. *Computer Methods in Applied Mechanics and Engineering*, 132:277–304, 1996.
- D. Eyheramendy and T. Zimmermann. Object-oriented finite elements. iv. symbolic derivations and automatic programming of nonlinear formulations. *Computer Methods in Applied Mechanics and Engineering*, 190(22-23):2729–2751, 2001.
- F. Fadi and M. C. Constantinou. Evaluation of simplified methods of analysis for structures with triple friction pendulum isolators. *Earthquake Engineering & Structural Dynamics*, 39(1):5–22, January 2010.
- C. Fairhurst. Stress estimation in rock: a brief history and review. *International Journal of Rock Mechanics and Mining Sciences*, 40(7-8):957–973, October – December 2003.
- K. Fakharian. *Three-dimensional monotonic and cyclic behaviour of sand-steel interfaces: Testing and modelling*. University of Ottawa (Canada), 1996.
- K. Fakharian and E. Evgin. Simple shear versus direct shear tests on interfaces during cyclic loading. In *Proceedings of International Conference on Recent Advances in geotechnical Earthquake Engineering and Soil Dynamics*, volume 1. University of Missouri–Rolla, 1995.

- K. Fakharian and E. Evgin. An automated apparatus for three-dimensional monotonic and cyclic testing of interfaces. *Geotechnical Testing Journal*, 19(1):22–31, 1996.
- K. Fakharian and E. Evgin. Cyclic simple-shear behavior of sand-steel interfaces under constant normal stiffness condition. *Journal of Geotechnical and Geoenvironmental Engineering*, 123(12):1096–1105, 1997.
- K. Fakharian, E. Evgin, et al. A comprehensive experimental study of sand-steel interfaces subjected to various monotonic and cyclic stress paths. In *The Twelfth International Offshore and Polar Engineering Conference*. International Society of Offshore and Polar Engineers, 2002.
- C. Farhat. *Multiprocessors in Computational Mechanics*. PhD thesis, University of California, Berkeley, 1987.
- C. Farhat. Saddle-point principle domain decomposition method for the solution of solid mechanics problems. In *Fifth International Symposium on Domain Decomposition Methods for Partial Differential Equations*, Norfolk, VA, USA, May 6–8 1991.
- C. Farhat and L. Crivelli. A transient FETI methodology for large-scale parallel implicit computations in structural mechanics. *International Journal for Numerical Methods in Engineering*, 37:1945–1975, 1994.
- C. Farhat and M. Geradin. Using a reduced number of lagrange multipliers for assembling parallel incomplete field finite element approximations. *Computer Methods in Applied Mechanics and Engineering*, 97(3):333–354, June 1992.
- C. Farhat and F. Roux. Method of finite element tearing and interconnecting and its parallel solution algorithm. *International Journal for Numerical Methods in Engineering*, 32(6):1205–1227, October 1991a.
- C. Farhat and F. X. Roux. A method of finite element tearing and interconnecting and its parallel solution algorithm. *International Journal for Numerical Methods in Engineering*, 32(6):1205–1227, 1991b.
- C. Farhat, M. Lesoinne, and K. Pierson. A scalable dual-primal domain decomposition method. *Numerical Linear Algebra with Applications*, 7(7–8):687–714, 2000.
- C. Farhat, M. Lesoinne, P. LeTallec, K. Pierson, and D. Rixen. FETI-DP: a dual-primal unified FETI method - Part I: a faster alternative to the two-level FETI method. *International Journal for Numerical Methods in Engineering*, 50(7):1523–1544, 2001.

- R. Faria, J. Oliver, and M. Cervera. A strain-based plastic viscous-damage model for massive concrete structures. *International Journal for Solids and Structures*, 35(14):1533–1558, 1998.
- W. Farren and G. Taylor. The heat developed during plastic extension of metals. *Proceedings of the royal society of London A: mathematical, physical and engineering sciences*, 107(743):422–451, 1925.
- M. Fasan. ADVANCED SEISMOLOGICAL AND ENGINEERING ANALYSIS FOR STRUCTURAL SEISMIC DESIGN. PhD thesis, UNIVERSITÀ DEGLI STUDI DI TRIESTE, 2016.
- M. Fasan, A. Magrin, C. Amadio, F. Romanelli, F. Vaccari, and G. F. Panza. A seismological and engineering perspective on the 2016 Central Italy earthquakes. *Int. J. Earthquake and Impact Engineering*, 1(4):395–420, 2016. doi: 10.1504/IJEIE.2016.10004076.
- B. Fatahi and S. H. R. Tabatabaiefar. Fully nonlinear versus equivalent linear computation method for seismic analysis of midrise buildings on soft soils. *International Journal of Geomechanics*, 14(4):04014016, 2013.
- Federal Highway Administration. Geotechnical engineering circular No 5. U.S. Department of Transportation, Publication No. FHWA-IF-02-034, April 2002.
- H. P. Feigenbaum and Y. F. Dafalias. Directional distortional hardening in metal plasticity within thermodynamics. *International Journal of Solids and Structures*, 44(22-23):7526–7542, 2007.
- C. A. Felippa. Dynamic relaxation under general incremental control. In W. K. Liu, T. Belytschko, and K. C. Park, editors, Innovative Methods for Nonlinear Problems, pages 103–133. Pineridge Press, Swansea U.K., 1984.
- C. A. Felippa. Introduction to linear finite element methods, lecture notes, i and ii. Technical report, University of Colorado at Boulder, 1989. Report No. CU-CSSC-89-19 Septembar 1989.
- C. A. Felippa. Object oriented finite element programing. Lecture Notes at CU Boulder, august - decembar 1992a.
- C. A. Felippa. Object oriented finite element programing. Lecture Notes at CU Boulder, august - decembar 1992b.
- C. A. Felippa. Nonlinear finite element methods. Lecture Notes at CU Boulder, 1993.
- C. A. Felippa and S. Alexander. Membrane triangles with corner drilling freedoms – III. implementation and performance evaluation. *Finite Elements in Analysis and Design*, 12:203–239, 1992.

- C. A. Felippa and C. Militello. Membrane triangles with corner drilling freedoms – II. the ANDES element. *Finite Elements in Analysis and Design*, 12:189–201, 1992.
- C. A. Felippa and K. Park. Advanced finite element methods. Lecture Notes at CU Boulder, January-May 1995.
- Y. Feng, H. Wang, H. Yang, and B. Jeremić. Hardware aware plastic domain decomposition for nonlinear finite element simulation. *Advances in Engineering Software*, to be submitted, 2024.
- G. A. Fenton. Estimation of stochastic soil models. *Journal of Geotechnical and Geoenvironmental Engineering*, 125(6):470–485, June 1999a.
- G. A. Fenton. Random field modeling of CPT data. *Journal of Geotechnical and Geoenvironmental Engineering*, 125(6):486–498, June 1999b.
- G. A. Fenton and D. V. Griffiths. Probabilistic foundation settlement on spatially random soil. *Journal of Geotechnical and Geoenvironmental Engineering*, 128(5):381–390, May 2002.
- G. A. Fenton and D. V. Griffiths. Bearing capacity prediction of spatially random $c - \phi$ soil. *Canadian Geotechnical Journal*, 40:54–65, 2003.
- G. A. Fenton and D. V. Griffiths. Three-dimensional probabilistic foundation settlement. *Journal of Geotechnical and Geoenvironmental Engineering*, 131(2):232–239, February 2005.
- G. L. Fenves. Object –oriented programming for engineering software development. *Engineering with Computers*, 6:1–15, 1990.
- P. A. Ferrer. Elastoplastic characterization of granular materials. Master's thesis, University of Puerto Rico, 1992.
- G. Festa and S. Nielsen. Pml absorbing boundaries. *Bulletin of the Seismological Society of America*, 93(2):891–903, 2003.
- F. C. Filippou, V. V. Bertero, and E. P. Popov. Effects of bond deterioration on hysteretic behavior of reinforced concrete joints. Technical report, Earthquake Engineering Research Center, University of California, Berkeley, 1983.
- S. Fiore, G. Finocchio, R. Zivieri, M. Chiappini, and Garesc?F. Wave amplitude decay driven by anharmonic potential in nonlinear mass-in-mass systems. *Applied Physics Letters*, 117(12):124101, 2020. doi: 10.1063/5.0020486. URL <https://doi.org/10.1063/5.0020486>.

- B. W. R. Forde, R. O. Foschi, and S. F. Steimer. Object – oriented finite element analysis. *Computers and Structures*, 34(3):355–374, 1990.
- L. Fox, H. D. Huskey, and J. H. Wilkinson. Notes on the solution of algebraic linear simultaneous equations. *Quarterly Journal of Mechanics and Applied Mathematics*, 1:149–173, 1948.
- N. Fox. On the continuum theories of dislocations and plasticity. *Quarterly Journal of Mechanics and Applied Mathematics*, XXI(1):67–75, 1968.
- R. E. Fulton and P. S. Su. Parallel substructure approach for massively parallel computers. *Computers in Engineering*, 2:75–82, 1992.
- H. H. G. W. Ma and Y. X. Zhou. Modeling of wave propagation induced by underground explosion. *Computers and Geotechnics*, 22(3/4):283–303, 1998.
- S. Gajan and D. S. Saravanathiiban. Modeling of energy dissipation in structural devices and foundation soil during seismic loading. *Soil Dynamics and Earthquake Engineering*, 31(8):1106 – 1122, 2011. ISSN 0267-7261. doi: 10.1016/j.soildyn.2011.02.006. URL <http://www.sciencedirect.com/science/article/pii/S0267726111000923>.
- A. Gajo. Influence of viscous coupling in propagation of elastic waves in saturated soil. *ASCE Journal of Geotechnical Engineering*, 121(9):636–644, September 1995.
- A. Gajo and L. Mongiovi. An analytical solution for the transient response of saturated linear elastic porous media. *International Journal for Numerical and Analytical Methods in Geomechanics*, 19(6): 399–413, 1995.
- A. Gajo, A. Saetta, and R. Vitaliani. Evaluation of three- and two-field finite element methods for the dynamic response of saturated soil. *International Journal for Numerical Methods in Engineering*, 37: 1231–1247, 1994.
- E. Gamma, R. Helm, R. Johnson, and J. Vlissides. *Design Patterns. Elements of Reusable Object-Oriented Software*. Professional Computing Series. Addison-Wesley, 1995. ISBN 0-201-63361-2.
- C. W. Gardiner. *Handbook of Stochastic Methods for Physics, Chemistry and the Natural Science*. Springer:Complexity. Springer-Verlag, Berlin Heidelberg, third edition, 2004.
- S. K. Garg, H. Nayfeh, and A. J. Good. Compressional waves in fluid-saturated elastic porous media. *Journal of Applied Physics*, 45(5):1968–1974, 1974.

- G. C. Gazetas and J. M. Roesset. Vertical vibration of machine foundations. *Journal of Geotechnical Engineering*, 105(12):1435–1454, 1979.
- A. Gens, I. Carol, and E. Alonso. A constitutive model for rock joints formulation and numerical implementation. *Computers and Geotechnics*, 9(1-2):3–20, 1990.
- M. Georgiadis. Development of p-y curves for layered soils. In *Geotechnical Practice in Offshore Engineering*, pages 536–545. Americal Society of Civil Engineers, April 1983.
- C. Geuzaine and J.-F. Remacle. Gmsh: A 3-D finite element mesh generator with built-in pre- and post-processing facilities. *International Journal for Numerical Methods in Engineering*, 79(11):1309–1331, 2009.
- R. Ghanem and R. M. Kruger. Numerical solution of spectral stochastic finite element systems. *Computer Methods in Applied Mechanics and Engineering*, 129(3):289 – 303, 1996. doi: [http://dx.doi.org/10.1016/0045-7825\(95\)00909-4](http://dx.doi.org/10.1016/0045-7825(95)00909-4).
- R. G. Ghanem and P. D. Spanos. *Stochastic Finite Elements, A Spectral Approach*. Dover Publications Inc., revised edition edition, 1991.
- P. A. Gilbert. Investigation of density variation in triaxial test specimens of cohesionless soil subjected to cyclic and monotonic loadin. Technical Report GL-84-10, U.S. Army Corps of Engineers, Waterways Experiment Station, Vicksburg, Miss., 1984.
- D. Givoli. Non-reflecting boundary conditions. *Journal of computational physics*, 94:1–29, 1991.
- L. A. Glenn. The influence of rock material models on seismic discrimination of underground nuclear explosions. In *1995 APS Topical Conference on Shock Compression of Condensed Matter*, Seattle, WA, August 13-18 1995. Lawrence Livermore National Laboratory. URL <http://www.osti.gov/bridge/servlets/purl/93963-W1J2gq/webviewable/93963.pdf>. UCRL-JC-120689.
- P. Goldstein and A. Snoke. Sac availability for the iris community. *Incorporated Institutions for Seismology Data Management Center Electronic Newsletter*, 7, 2005.
- P. Grammenoudis and C. Tsakmakis. Finite element implementation of large deformation micropolar plasticity exhibiting isotropic and kinematic hardening effects. *International Journal for Numerical Methods in Engineering*, 62(12):1691 – 1720, 2005.
- G. Green. On the laws of the reflexion and refraction of light at the common surface of two non-crystallized media. *Transactions of the Cambridge Philosophical Society*, 7:1, 1848.

- D. Griffiths and P. Lane. Slope stability analysis by finite elements. *Geotechnique*, 49(3):387–403, 1999.
- D. V. Griffiths, G. A. Fenton, and N. Manoharan. Bearing capacity of rough rigid strip footing on cohesive soil: Probabilistic study. *Journal of Geotechnical and Geoenvironmental Engineering*, 128(9):743–755, 2002.
- T. H. Group. HDF5. <https://www.hdfgroup.org/HDF5/>, 2020.
- B. Guidio and C. Jeong. Full-waveform inversion of incoherent dynamic traction in a bounded 2D domain of scalar wave motions. *ASCE Journal of Engineering Mechanics*, 147(4):04021010, 2021.
- B. Guidio, B. Jeremić, L. Guidio, and C. Jeong. Passive-seismic inversion of sh-wave input motions in a domain truncated by wave-absorbing boundary conditions. *Soil Dynamics and Earthquake Engineering*, 2022a. In Print.
- B. Guidio, B. Jeremić, L. Guidio, and C. Jeong. Full-waveform inversion of sh-wave input motions in a domain truncated by wave-absorbing boundary conditions. *Structural Dynamics and Earthquake Engineering*, 2022b. in print.
- B. P. Guidio. *Full-waveform Inversion of Seismic Input Motions in a Near-surface Domain*. PhD thesis, The Catholic University of America, 2020.
- M. A. Gutierrez and R. De Borst. Numerical analysis of localization using a viscoplastic: Influence of stochastic material defects. *International Journal for Numerical Methods in Engineering*, 44:1823–1841, 1999.
- D. Hadley and H. Kanamori. Seismic structure of the transverse ranges, California. *Geological Society of America Bulletin*, 88(10):1469–1478, 1977.
- J. F. Hajjar and J. F. Abel. Parallel processing for transient nonlinear structural dynamics of three-dimensional framed structures using domain decomposition. *Computers & Structures*, 30(6):1237–1254, 1988.
- J. F. Hall. Problems encountered from the use (or misuse) of Rayleigh damping. *Earthquake Engineering & Structural Dynamics*, 35(5):525–545, 2006.
- M. Hamada. Large ground deformations and their effects on lifelines: 1964 Niigata earthquake. In Hamada and O'Rourke, editors, *Case Studies of Liquefaction and Lifeline Performance During Past Earthquakes*, Vol 1: Japanese Case Studies, Chapter 3, pages 3:1 – 3:123, 1992.

- Y. Hamiel, V. Lyakhovsky, and A. Agnon. Rock dilation, nonlinear deformation, and pore pressure change under shear. *Earth and Planetary Science Letters*, 237:577–589, 2005.
- B. O. Hardin. The nature of stress-strain behavior of soils. In *Proceedings of the Specialty Conference on Earthquake Engineering and Soil Dynamics*, volume 1, pages 3–90, Pasadena, 1978.
- H. G. Harris and G. M. Sabnis. *Structural Modeling and Experimental Techniques*. CRC Press, 1999. ISBN 0849324696.
- J. P. D. Hartog. *Advanced Strength of Materials*. Dover Publications, Inc., 1952.
- Y. Hashash and D. Park. Non-linear one-dimensional wave propagation in the Mississippi embayment. *Engineering Geology*, 62(1–3):185–206, 2001.
- Y. Hashash and D. Park. Viscous damping formulation and high frequency motion in non-linear site response analysis. *Soil Dynamics and Earthquake Engineering*, 22:611–624, 2002.
- Y. M. Hashash, J. J. Hook, B. Schmidt, I. John, and C. Yao. Seismic design and analysis of underground structures. *Tunnelling and underground space technology*, 16(4):247–293, 2001.
- Z. Hashin. Analysis of composite materials. *Journal of Applied Mechanics*, 50:481–505, 1983.
- N. Haskell. Radiation pattern of surface waves from point sources in a multi-layered medium. *Bulletin of the Seismological Society of America*, 54(1):377–393, 1964.
- N. A. Haskell. The dispersion of surface waves on multilayered media. *Bulletin of the Seismological Society of America*, 43(1):17–34, 1953.
- H. M. Hassan, M. Fasan, M. A. Sayed, F. Romanelli, M. N. ElGabry, F. Vaccari, and A. Hamed. Site-specific ground motion modeling for a historical Cairo site as a step towards computation of seismic input at cultural heritage sites. *Engineering Geology*, 2020. doi: 10.1016/j.enggeo.2020.105524.
- L. Hatton. The T experiments: Errors in scientific software. *IEEE Computational Science and Engineering*, 4(2):27–38, April–June 1997.
- S. Helgason. *Differential Geometry, Lie Groups, and Symmetric Spaces*. Pure and Applied Mathematics. Academic Press, 1978.
- B. Hendrickson and R. Leland. A multilevel algorithm for partitioning graphs. *Proceedings Supercomputing '95*, 1995.

- M. R. Hestenes and E. Stiefel. Methods of conjugate gradients for solving linear systems. *Journal of Research of the National Bureau of Standards*, 49:409–436, 1952.
- C. Hewitt, P. Bishop, and R. Steiger. A Universal Modular ACTOR Formalism for Artificial Intelligence. In *Proceedings of the 3rd International Joint Conference on Artificial Intelligence*, Stanford, CA, August 1973.
- K. Hijikata, M. Takahashi, T. Aoyagi, and M. Mashimo. Behavior of a base-isolated building at fukushima dai-ichi nuclear power plant during the great east japan earthquake. In *Proceedings of the International Symposium on Engineering Lessons Learned from the 2011 Great East Japan Earthquake*, Tokyo, Japan, March 1-4 2012.
- H. M. Hilber, T. J. R. Hughes, and R. L. Taylor. Improved numerical dissipation for time integration algorithms in structural dynamics. *Earthquake Engineering and Structure Dynamics*, 5(3):283–292, 1977.
- R. Hill. *The Mathematical Theory of Plasticity*. The Oxford Engineering Science Series. Oxford at the Clarendon Press, 1st. edition, 1950.
- R. Hill. A general theory of uniqueness and stability in elastic-plastic solids. *Journal of the Mechanics and Physics of Solids*, 6(3):236–249, 1958.
- R. Hill. Aspects of invariance in solid mechanics. In C.-S. Yih, editor, *Advances in Applied Mechanics*, volume 18, pages 1–72. Academic Press, 1978.
- M. Hiltl, C. R. Hagelberg, W. J. Nellis, T. C. Carney, and R. P. Swift. Dynamic response of berea sandstone shock-loaded under dry, wet and water-pressurized conditions. In *Proceedings of International Conference on High Pressure Science and Technology*, Honolulu, HI (USA), 1999. Preprint: UCRL-JC-135647.
- A. C. Hindmarsh, P. N. Brown, K. E. Grant, S. L. Lee, R. Serban, D. E. Shumaker, and C. S. Woodward. SUNDIALS: SUite of Nonlinear and DIfferential/ALgebraic equation Solvers. *ACM Transactions on Mathematical Software*, 31(3):363–396, 2005.
- C. Hird and D. Russell. A benchmark for soil-structure interface elements. *Computers and Geotechnics*, 10(2):139 – 147, 1990. ISSN 0266-352X. doi: [https://doi.org/10.1016/0266-352X\(90\)90003-E](https://doi.org/10.1016/0266-352X(90)90003-E). URL <http://www.sciencedirect.com/science/article/pii/0266352X9090003E>.

- M. S. Hiremath, R. S. Sandhu, L. W. Morland, and W. E. Wolfe. Analysis of one-dimensional wave propagation in a fluid-saturated finite soil column. *International Journal for Numerical and Analytical Methods in Geomechanics*, 12:121–139, 1988.
- C. Hirt, A. A. Amsden, and J. Cook. An arbitrary lagrangian-eulerian computing method for all flow speeds. *Journal of computational physics*, 14(3):227–253, 1974.
- C. W. Hirt and B. D. Nichols. Volume of fluid (vof) method for the dynamics of free boundaries. *Journal of computational physics*, 39(1):201–225, 1981.
- Y. Hisada. Broadband strong motion simulation in layered half-space using stochastic green's function technique. *Journal of Seismology*, 12(2):265–279, 2008.
- K. Hjelmstad. *Fundamentals of Structural Mechanics*. Prentice-Hall, 1997. ISBN 0-13-485236-2.
- J. Hodowany, G. Ravichandran, A. Rosakis, and P. Rosakis. Partition of plastic work into heat and stored energy in metals. *Experimental mechanics*, 40(2):113–123, 2000.
- E. Hoek, C. Carranza-Torres, and B. Corkum. Hoek-Brown failure criterion: 2002 edition. In *5th North American Rock Mechanics Symposium and 17th Tunneling Association of Canada Conference: NARMS-TAC*, pages 267–271, 2002.
- C. Holyoke and T. Rushmer. An experimental study of grain scale melt segregation mechanisms in two common crustal rock types. *Journal of Metamorphic Geology*, 20(5):493–512, 2002.
- E. Hopf. Statistical hydromechanics and functional calculus. *Journal of rational Mechanics and Analysis*, 1:87–123, June 1952.
- M. Hori. *Introduction to Computational Earthquake Engineering*. Imperial College Press, 2006. ISBN ISBN-10: 1848163983; ISBN-13: 978-1848163980.
- K. Horikoshi, A. Tateishi, and T. Fujiwara. Centrifuge modeling of single pile subjected to liquefaction-induced lateral spreading. *Soils and Foundations, Special Issue*(2):193–208, 1998.
- G. Houlsby and A. Puzrin. A thermomechanical framework for constitutive models for rate-independent dissipative materials. *International Journal of Plasticity*, 16(9):1017–1047, 2000.
- G. W. Housner. Interaction of building and ground during an earthquake. *Bulletin of the Seismological Society of America*, 47(3):179–186, 1957.
- <http://graal.ens-lyon.fr/MUMPS/>. *MULTifrontal Massively Parallel Solver (MUMPS Version 4.6.2) Users' Guide*, 2006.

- http://www.sdsc.edu/user_services/datastar/. Ibm datastar user guide. San Diego Supercomputer Center at UCSD, 2020.
- L. Hu and J. Pu. Testing and modeling of soil-structure interface. Journal of Geotechnical and Geoenvironmental Engineering, 130(8):851–860, 2004.
- C. Hua. An inverse transformation for quadrilateral isoparametric elements: analysis and application. Finite elements in analysis and design, 7(2):159–166, 1990.
- Y.-N. Huang, A. S. Whittaker, and N. Luco. Seismic performance assessment of base-isolated safety-related nuclear structures. Earthquake Engineering and Structures Dynamics, Early View: 20 SEP 2010 — DOI: 10.1002/eqe.1038:1–22, 2010.
- T. Hughes. The Finite Element Method ; Linear Static and Dynamic Finite Element Analysis. Prentice Hall Inc., 1987.
- T. Hughes and K. Pister. Consistent linearization in mechanics of solids and structures. Computers and Structures, 8:391–397, 1978.
- T. J. R. Hughes and W. K. Liu. Implicit-explicit finite elements in transient analaysis: implementation and numerical examples. Journal of Applied Mechanics, pages 375–378, 1978a.
- T. J. R. Hughes and W. K. Liu. Implicit-explicit finite elements in transient analaysis: stability theory. Journal of Applied Mechanics, pages 371–374, 1978b.
- F.-N. Hwang and X.-C. Cai. A class of parallel two-level nonlinear Schwarz preconditioned inexact Newton algorithms . Computer Methods in Applied Mechanics and Engineering, 196(8):1603–1611, January 2007.
- I. M. Idriss and J. I. Sun. SHAKE91: A Computer Program for Equivalent Linear Seismic Response Analyses of Horizontally Layered Soil Deposits. Center for Geotechnical Modeling Department of Civil & Environmental Engineering University of California Davis, California, 1992.
- M. Iguchi and J. E. Luco. Dynamic response of flexible rectangular foundations on an elastic half-space. Earthquake Engineering and Structural Dynamics, 9(3):239–249, 1 1981.
- M. Iida. Three-dimensional finite-element method for soil-building interaction based on an input wave field. International Journal of Geomechanics, 13(4):430–440, 2012.
- A. Il'lushin. On the postulate of plasticity. Journal of Applied Mathematics and Mechanics, 25(3):746–752, 1961.

- Y. Inada, T. Okawa, H. Mashimo, and Y. Kokudo. Failure characteristics of rock under compression at high and low temperatures. In J. Hudson, editor, Rock Characterization, pages 63–68. Thomas Telford Ltd., 1992.
- K. Ishihara. Soil behaviour in earthquake geotechnics. Clarendon Press, Oxford University Press, 1996.
- ISO-90003. ISO/IEC/IEEE 90003, software engineering – guidelines for the application of ISO 9001:2015 to computer software. Technical Report ISO/IEC/IEEE 90003:2018(E), ISO, 2018.
- ISO/IEC/IEEE 90003 Developers, International Organization for Standardization (ISO), International Electrotechnical Commission (IEC), and Institute of Electrical and Electronics Engineers (IEEE). International Standard ISO/IES/IEEE 90003, Software Engineering - Guidelines for applicaiton of ISO 9001:2015 to computer software. ISO/IEC/IEEE, first edition 2018-11 edition, November 2018.
- K. A. Issen and J. W. Rudnicki. Theory of compaction bands in porous rock. Physics and Chemistry of the Earth, Part A: Solid Earth and Geodesy, 26(1–2):95–100, 2001.
- J. Jaeger, N. Cook, and R. Zimmerman. Fundamentals of rock mechanics. Blackwell Pub., 2007. ISBN 9780632057597.
- N. Janbu. Soil compressibility as determined by odometer and triaxial tests. In Proceedings of European Conference on Soil Mechanics and Foundation Engineering, pages 19–25, 1963.
- Japanese Road Association. Specification for highway bridges, 1980.
- Japanese Society of Civil Engineers. The report of damage investigation in the 1964 Niigata Earthquake. Japanese Soc. of Civil Engineers, Tokyo, 1966. in Japanese.
- H. Jasak. Error analysis and estimation for finite volume method with applications to fluid flow. PhD thesis, Imperial College of Science, Technology and Medicine, 1996.
- H. Jasak and Z. Tukovic. Automatic mesh motion for the unstructured finite volume method. Transactions of FAMENA, 30(2):1–20, 2006.
- S. Y. Je, Y.-S. Chang, and S.-S. Kang. Dynamic characteristics assessment of reactor vessel internals with fluid-structure interaction. Nuclear Engineering and Technology, 2017.
- B. Jeremić. Dynamic analysis of axisymmetric solids subjected to non-symmetric loading by the finite element method. Diploma thesis,, Faculty of Civil Engineering, Belgrade University, july 1989. in Serbian. (Борис Јеремић Динамичка Анализа Ротационо Симетричних Тела оптерећених

- Несиметричним Оптерећењима Методом Коначних Елемената, *Дипломски Рад* Грађевински Факултет Универзитета у Београду.
- B. Jeremić. nDarray programming tool. Object Oriented Approach to Numerical Computations in Elastoplasticity, Reference Manual University of Colorado at Boulder, December 1993.
- B. Jeremić. Implicit integration rules in plasticity: Theory and implementation. Master's thesis, University of Colorado at Boulder, May 1994.
- B. Jeremić. Finite Deformation Hyperelasto–Plasticity of Geomaterials. PhD thesis, University of Colorado at Boulder, July 1997.
- B. Jeremić. Line search techniques in elastic–plastic finite element computations in geomechanics. Communications in Numerical Methods in Engineering, 17(2):115–125, January 2001.
- B. Jeremić. Lectures notes on computational geomechanics: Inelastic finite elements for pressure sensitive materials. –, April 2004.
- B. Jeremić. High fidelity modeling and simulation of sfs interaction: energy dissipation by design. In R. P. Orense, N. Chouw, and M. Pender, editors, Soil-Foundation-Structure Interaction, pages 125–132. CRC Press, Taylor & Francis Group, 2010. ISBN 978-0-415-60040-8 (Hbk); 978-0-203-83820-4 (eBook).
- B. Jeremić and Z. Cheng. Numerical modeling and simulations of piles in liquefied soils. Soil Dynamics and Earthquake Engineering, in Print, 2009.
- B. Jeremić and M. Preisig. Seismic soil – foundation – structure interaction: Numerical modeling issues. In SEI Structures Congress, 2005.
- B. Jeremić and K. Sett. The influence of uncertain material parameters on stress-strain response. In P. V. Lade and T. Nakai, editors, Geomechanics II: Testing, Modeling, and Simulation (Proceedings of the Second-U.S. Workshop on Testing, Modeling, and Simulation in Geomechanics, held in Kyoto, Japan from September 8-10, 2005), Geotechnical Special Publication No. 156, pages 132–147. American Society for Civil Engineers, August 2006.
- B. Jeremić and K. Sett. Uncertain soil properties and elastic-plastic simulations in geomechanics. In GeoDenver, 2007.
- B. Jeremić and K. Sett. On probabilistic yielding of materials. Communications in Numerical Methods in Engineering, 25(3):291–300, 2009a.

- B. Jeremić and K. Sett. On probabilistic yielding of materials. *Communications in Numerical Methods in Engineering*, 25(3):291–300, 2009b.
- B. Jeremić and K. Sett. Uncertain seismic wave propagation in 1D. *Soil Dynamics and Earthquake Engineering*, 2010. in Review.
- B. Jeremić and S. Sture. Implicit integrations in elasto–plastic geotechnics. *International Journal of Mechanics of Cohesive–Frictional Materials*, 2:165–183, 1997.
- B. Jeremić and S. Sture. Implicit integrations in elastoplastic geotechnics. *Mechanics of Cohesive–Frictional Materials*, 2(2):165–183, 1997.
- B. Jeremić and S. Sture. Tensor data objects in finite element programming. *International Journal for Numerical Methods in Engineering*, 41(1):113–126, 1998.
- B. Jeremić and C. Xenophontos. Application of the p -version of the finite element method to elasto-plasticity with localization of deformation. *Communications in Numerical Methods in Engineering*, 15(12):867–876, December 1999.
- B. Jeremić and Z. Yang. Template elastic–plastic computations in geomechanics. *International Journal for Numerical and Analytical Methods in Geomechanics*, 26(14):1407–1427, 2002.
- B. Jeremić and Z. Yang. Template elastic-plastic computations in geomechanics. *International Journal for Numerical and Analytical Methods in Geomechanics*, 26(14):1407–1427, December 2002.
- B. Jeremić, G. Jie, Z. Cheng, N. Tafazzoli, P. Tasiopoulos, F. Pisanò, J. A. Abell, K. Watanabe, Y. Feng, S. K. Sinha, F. Behbehani, H. Yang, H. Wang, and K. D. Staszewska. *The Real-ESSI Simulator System*. University of California, Davis, 1988-2025. <http://real-essi.us/>.
- B. Jeremić, Z. Yang, Z. Cheng, G. Jie, N. Tafazzoli, M. Preisig, P. Tasiopoulos, F. Pisanò, J. Abell, K. Watanabe, Y. Feng, S. K. Sinha, F. Behbehani, H. Yang, H. Wang, and K. D. Staszewska. *Nonlinear Finite Elements: Modeling and Simulation of Earthquakes, Soils, Structures and their Interaction*. Self-Published-Online, University of California, Davis, CA, USA, 1989-2025. ISBN 978-0-692-19875-9. URL: <http://sokocalo.engr.ucdavis.edu/~jeremic/LectureNotes/>.
- B. Jeremić, K. Runesson, and S. Sture. Large deformation constitutive integration algorithm. In Mukrakami and Luco, editors, *Proceedings of the 12th Conference*, pages 1029–1032, La Jolla, California, May 1998. Engineering Mechanics Division of the American Society of Civil Engineers.

- B. Jeremić, N. Straz, M. Akers, and K. Makles. Beowulf class parallel computer “NorthCountry”: Design, construction and testing. Report CEE-98-01, Clarkson University, Department of Civil and Environmental Engineering, May 1998. <http://sokocalo.sc.clarkson.edu/>
- B. Jeremić, K. Runesson, and S. Sture. A model for elastic–plastic pressure sensitive materials subjected to large deformations. *International Journal of Solids and Structures*, 36(31/32):4901–4918, 1999.
- B. Jeremić, Z. Yang, and M. Olton. Beowulf class parallel computer “GeoWulf”: Design, construction and testing. Progress report, University of California, Davis, Department of Civil and Environmental Engineering, 1999. <http://sokocalo.engr.ucdavis.edu/~jeremic/GeoWulf>
- B. Jeremić, S. Kunnath, and F. Xiong. Influence of soil–foundation–structure interaction on seismic response of the i-880 viaduct. *Engineering Structures*, 26(3):391–402, 2004.
- B. Jeremić, K. Sett, and M. L. Kavvas. Probabilistic elasto-plasticity: formulation in 1D. *Acta Geotechnica*, 2(3):197–210, October 2007a.
- B. Jeremić, K. Sett, and M. L. Kavvas. Probabilistic elasto-plasticity: Formulation in 1-D. *Acta Geotechnica*, 2(3):197–210, September 2007b.
- B. Jeremić, Z. Cheng, M. Taiebat, and Y. F. Dafalias. Numerical simulation of fully saturated porous materials. *International Journal for Numerical and Analytical Methods in Geomechanics*, 32(13):1635–1660, 2008.
- B. Jeremić, G. Jie, M. Preisig, and N. Tafazzoli. Time domain simulation of soil–foundation–structure interaction in non-uniform soils. *Earthquake Engineering and Structural Dynamics*, 38(5):699–718, 2009.
- P. Jetteur. Implicit integration algorithm for elastoplasticity in plane stress analysis. *Engineering Computations*, 3:251–253, 1986.
- H. Jin, Y. Liu, and H.-J. Li. Experimental study on sloshing in a tank with an inner horizontal perforated plate. *Ocean Engineering*, 82:75–84, 2014.
- S. Johnson. Objecting the objects. WTEC'94 Proceedings of the USENIX Winter 1994 Technical Conference, USENIX Winter 1994 Technical Conference, september 1994.
- S. C. Johnson. Yacc: Yet another compiler-compiler. Technical report, AT&T Bell Laboratories, Murray Hill, New Jersey 07974, 1975. URL <http://dinosaur.compiletools.net/>.

- S. Kacin, M. Ozturk, U. K. Sevim, B. A. Mert, Z. Ozer, O. Akgol, E. Unal, and M. Karaaslan. Seismic metamaterials for low-frequency mechanical wave attenuation. *Natural Hazards*, 107:213–229, May 2021.
- E. Kalkan and S. Kunnath. Effective cyclic energy as a measure of seismic demand. *Journal of Earthquake Engineering*, 11(5):725–751, 2007.
- E. Kalkan and S. Kunnath. Relevance of absolute and relative energy content in seismic evaluation of structures. *Advances in Structural Engineering*, 11(1):17–34, 2008.
- L. F. Kallivokas, J. Bielak, and R. C. MacCamy. A simple impedance–infinite element for the finite element solution of the three-dimensional wave equation in unbound domains. *Computer Methods in Applied Mechanics and Engineering*, 147:235–262, 1997.
- C. Kanellopoulos, N. Psycharis, H. Yang, B. Jeremić, I. Anastasopoulos, and B. Stojadinović. Seismic resonant metamaterials for the protection of an elastic-plastic sdof system against vertically propagating seismic shear waves (SH) in nonlinear soil. *Soil Dynamics and Earthquake Engineering*, 162:107366, 2022. ISSN 0267-7261. doi: <https://doi.org/10.1016/j.soildyn.2022.107366>. URL <https://www.sciencedirect.com/science/article/pii/S0267726122002159>.
- K. Karhunen. Über lineare methoden in der wahrscheinlichkeitsrechnung. *Ann. Acad. Sci. Fenniae. Ser. A. I. Math.-Phys.*, 37:1–79, 1947.
- W. Karush. Minima of functions of several variables with inequalities as side constraints. Master's thesis, University of Chicago, Chicago, IL., 1939.
- G. Karypis and V. Kumar. Multilevel k -way partitioning scheme for irregular graphs. *Journal of Parallel and Distributed Computing*, 48(1), 1998a.
- G. Karypis and V. Kumar. A fast and highly quality multilevel scheme for partitioning irregular graphs. *SIAM Journal on Scientific Computing*, 1998b. A short version appears in Intl. Conf. on Parallel Processing 1995.
- G. Karypis and V. Kumar. *METIS A Software Package for Partitioning Unstructured Graphs, Partitioning Meshes, and Computing Fill-Reducing Orderings of Sparse Matrices Version 4.0*. Army HPC Research Center, Department of Computer Science and Engineering, University of Minnesota, Minneapolis, MN 55455, September 1998c.
- G. Karypis and V. Kumar. *METIS: A Software Package for Partitioning Unstructured Graphs, Partitioning Meshes, and Computing Fill-Reducing Orderings of Sparse Matrices, Version 4.0*. Army HPC Research

- Center, Department of Computer Science and Engineering, University of Minnesota, Minneapolis, MN 55455, September 1998d.
- G. Karypis, K. Schloegel, and V. Kumar. PARMETIS Parallel Graph Partitioning and Sparse Matrix Ordering Library Version 3.1. Army HPC Research Center, Department of Computer Science and Engineering, University of Minnesota, Minneapolis, MN 55455, August 2003.
- E. Kausel. Fundamental Solutions in Elastodynamics, A Compendium. Cambridge University Press, The Edinburgh Building, Cambridge CB2 2RU, UK, 2006. ISBN ISBN-10: 0521855705; ISBN-13: 978-0521855709.
- E. Kausel and J. M. Roessel. Dynamic stiffness of circular foundations. Journal of the Engineering Mechanics Division , ASCE, 101(6):771–785, 1975.
- M. L. Kavvas. Nonlinear hydrologic processes: Conservation equations for determining their means and probability distributions. Journal of Hydrologic Engineering, 8(2):44–53, March 2003.
- M. L. Kavvas and A. Karakas. On the stochastic theory of solute transport by unsteady and steady groundwater flow in heterogeneous aquifers. Journal of Hydrology, 179:321–351, 1996.
- G. Karypis and V. Kumar. Multilevel k -way partitioning scheme for irregular graphs. Journal of Parallel and Distributed Computing, 48(1):96–129, 1998.
- A. Keese. A review of recent developments in the numerical solution of stochastic partial differential equations (stochastic finite elements). Scientific Computing 2003-06, Deapartment of Mathematics and Computer Science, Technical University of Braunschweig, Brunswick, Germany, 2003.
- A. Keese and H. G. Matthies. Efficient solvers for nonlinear stochastic problem. In H. A. Mang, F. G. Rammerstorfer, and J. Eberhardsteiner, editors, Proceedings of the Fifth World Congress on Computational Mechanics, July 7-12, 2002, Vienna, Austria, <http://wccm.tuwien.ac.at/publications/Papers/fp81007.pdf>, 2002.
- J. Kelly and S. Hodder. Experimental study of lead and elastomeric dampers for base isolation systems in laminated neoprene bearings. Bulletin of the New Zealand National Society for Earthquake Engineering, 15(2):53–67, 1982.
- J. M. Kelly. A long-period isolation system using low-damping isolators for nuclear facilities at soft soil sites. Technical Report UCB/EERC-91/03, Earthquake Engineering Research Center, University of California at Berkeley, March 1991a.

- J. M. Kelly. Dynamic and failure characteristics of Bridgestone isolation bearings. Technical Report UCB/EERC-91/04, Earthquake Engineering Research Center, University of California at Berkeley, March 1991b.
- D. Kent and R. Park. Flexural members with confined concrete. ASCE Journal of Structural Division, 97:1969–1990, 1971.
- M. Kimura, T. Adachi, H. Kamei, and F. Zhang. 3-D finite element analyses of the ultimate behavior of laterally loaded cast-in-place concrete piles. In G. N. Pande and S. Pietruszczak, editors, Proceedings of the Fifth International Symposium on Numerical Models in Geomechanics, NUMOG V, pages 589–594. A. A. Balkema, September 1995.
- H. Kishida and M. Uesugi. Tests of the interface between sand and steel in the simple shear apparatus. Geotechnique, 37(1):45–52, 1987.
- O. Klaas, M. Kreienmeyer, and E. Stein. Elastoplastic finite element analysis on a MIMD parallel-computer. Engineering Computations, 11:347–355, 1994.
- M. Kleiber and T. D. Hien. The Stochastic Finite Element Method: Basic Perturbation Technique and Computer Implementation. John Wiley & Sons, Baffins Lane, Chichester, West Sussex PO19 1UD , England, 1992.
- C. Knott. Reflection and refraction of elastic waves with seismological applications. Philosophical Magazine, 48:64–97, 1899.
- D. E. Knuth. Literate programming. Computer Journal (British Computer Society), 27(2):97–111, 1984.
- A. Koenig. C++ columns. Journal of Object Oriented Programming, 1989 - 1993.
- W. T. Koiter. Stress - strain relations, uniqueness and variational theorems for elastic - plastic materials with singular yield surface. Quarterly of Applied Mathematics, 2:350–354, 1953.
- W. T. Koiter. General theorems for elastic-plastic solids. In I. N. Sneddon and R. Hill, editors, Progress in Solid Mechanics, pages 165–221. North Holland, 1960.
- M. Kojić. Computational Procedures in Inelastic Analysis of Solids and Structures. Center for Scientific Research of Serbian Academy of Sciences and Arts and University of Kragujevac and Faculty of Mechanical Engineering University of Kragujevac, 1997. ISBN 86-82607-02-6.

- Милош. Којић. . М. Којић. Општи концепт имплицитне интеграције конститутивних релација при нееластичном деформирању материјала. Монографија Центра за научна истраживања Српске академије наука и уметности и Универзитета у Крагујевцу , 1993. (Miloš Kojić, A General Concept of Implicit Integration of Constitutive Relations for Inelastic Material Deformation, in Serbian).
- K. Kolozvari, K. Orakcal, and J. Wallace. Shear-flexure interaction modeling for reinforced concrete structural walls and columns under reversed cyclic loading. Technical Report PEER Report No. 2015/12, Pacific Earthquake Engineering Research Center, Pacific Earthquake Engineering Research Center, Richmod, CA, December 2015.
- S. Koutsourelakis, J. H. Prevost, and G. Deodatis. Risk assesment of an interacting structure-soil system due to liquefaction. Earthquake Engineering and Structural Dynamics, 31:851–879, 2002.
- S. L. Kramer. Geotechnical Earthquake Engineering. Prentice Hall, Inc, Upper Saddle River, New Jersey, 1996a.
- S. L. Kramer. Geotechnical Earthquake Engineering. Prentice Hall, New Jersey, 1996b.
- S. Krödel, N. Thomé, and C. Daraio. Wide band-gap seismic metastructures. Extreme Mechanics Letters, 4:111–117, 2015. ISSN 2352-4316. doi: <https://doi.org/10.1016/j.eml.2015.05.004>. URL <https://www.sciencedirect.com/science/article/pii/S2352431615000772>.
- E. Kröner. Algemeine kontinuumstheorie der versetzungen und eignspannungen. Archive for Rational Mechanics and Analysis, 4(4):273–334, 1960.
- P. Krysl and Z. Bittnar. Parallel explicit finite element solid dynamics with domain decomposition and message passing: dual partitioning scalability. Computers and Structures, 79:345–360, 2001.
- R. Kubo. Stochastic Liouville equations. J. Math. Phys., 4(2):174–183, 1963.
- H. W. Kuhn and A. W. Tucker. Nonlinear programming. In J. Neyman, editor, Proceedings of the Second Berkeley Symposium on Mathematical Statistics and Probability, pages 481 – 492. University of California Press, July 31 – August 12 1950 1951.
- M. Kumar, A. S. Whittaker, and M. C. Constantinou. An advanced numerical model of elastomeric seismic isolation bearings. Earthquake Engineering & Structural Dynamics, 43(13):1955–1974, 2014. ISSN 1096-9845. doi: 10.1002/eqe.2431. URL <http://dx.doi.org/10.1002/eqe.2431>.
- H. Kupfer, H. K. Hilsdorf, and H. Rusch. Behavior of concrete under biaxial stresses. In Journal Proceedings, volume 66/8, pages 656–666, 1969.

- A. Kurtulus, J. J. Lee, and K. H. Stokoe. Summary report — site characterization of capital aggregates test site. Technical report, Department of Civil Engineering, University of Texas at Austin, 2005.
- W.-P. Kwan and S. Billington. Simulation of structural concrete under cyclic load. *Journal of Structural Engineering*, 127(12):1391–1401, 2001.
- J. Labuz and L. Biolzi. Experiments with rock: Remarks on strength and stability issues. *International Journal of Rock Mechanics and Mining Sciences*, 44(4):525–537, June 2007.
- S. Lacasse and F. Nadim. Uncertainties in characterizing soil properties. In C. D. Shackelford and P. P. Nelson, editors, *Uncertainty in Geologic Environment: From Theory to Practice, Proceedings of Uncertainty 1996, July 31-August 3, 1996, Madison, Wisconsin*, volume 1 of *Geotechnical Special Publication No. 58*, pages 49–75. ASCE, New York, 1996.
- P. V. Lade. Elastoplastic stress strain theory for cohesionless soil with curved yield surfaces. *International Journal of Solids and Structures*, 13:1019–1035, 1977.
- P. V. Lade. Model and parameters for the elastic behavior of soils. In Swoboda, editor, *Numerical Methods in Geomechanics*, pages 359–364, Innsbruck, 1988a. Balkema, Rotterdam.
- P. V. Lade. Effects of voids and volume changes on the behavior of frictional materials. *International Journal for Numerical and Analytical Methods in Geomechanics*, 12:351–370, 1988b.
- P. V. Lade. Instability, shear banding, and failure in granular materials. *International Journal of Solids and Structures*, 39(13):3337–3357, 2002.
- P. V. Lade and R. B. Nelson. Modeling the elastic behavior of granular materials. *International Journal for Numerical and Analytical Methods in Geomechanics*, 4, 1987.
- I. P. Lam and H. K. Law. Soil–foundation–structure-interaction analytical considerations by empirical p – y methods. In *The fourth Caltrans Seismic Research Workshop*, Sacramento, CA, July 1996. California Dept. of Transportation, Engineering Service Center.
- H. Lamb. *Hydrodynamics*. Cambridge university press, 1932.
- W. T. Lambe and R. V. Whitman. *Soil Mechanics, SI Version*. John Wiley and Sons, 1979.
- H. Langtangen. A general numerical solution method for Fokker-Planck equations with application to structural reliability. *Probabilistic Engineering Mechanics*, 6(1):33–48, 1991.
- D. B. Larson and G. D. Anderson. Plane shock wave studies of porous geologic media. *Journal of Geophysical Research*, 84(B9):357–363, 1979.

- D. B. Larson and G. D. Anderson. Plane shock wave studies of westerly granite and nugget sandstone. *International Journal of Rock Mechanics and Mining Sciences & Geomechanics Abstracts*, 17(6):357–363, 1980.
- P. Le Tallec and J. Mouro. Fluid structure interaction with large structural displacements. *Computer methods in applied mechanics and engineering*, 190(24):3039–3067, 2001.
- R. Lebrun and A. Dutfoy. An innovating analysis of the Nataf transformation from the copula viewpoint. *Probabilistic Engineering Mechanics*, 24(3):312–320, 2009.
- E. H. Lee. Elastic–plastic deformation at finite strains. *Journal of Applied Mechanics*, 36(1):1–6, 1969.
- E. H. Lee and D. T. Liu. Finite–strain elastic–plastic theory with application to plane–wave analysis. *Journal of Applied Physics*, 38(1):19–27, January 1967.
- J. Lee and G. L. Fenves. Plastic-damage model for cyclic loading of concrete structures. *Journal of engineering mechanics*, 124(8):892–900, 1998.
- L. C. Lee. Wave propagation in a random medium: A complete set of the moment equations with different wavenumbers. *Journal of Mathematical physics*, 15(9):1431–1435, September 1974.
- S. L. Lee and G. P. Karunaratne. Laterally loaded piles in layered soil. *Soils and Foundations*, 27(4):1–10, Dec. 1987.
- P. Léger and S. Dussault. Seismic-energy dissipation in mdof structures. *Journal of Structural Engineering*, 118(5):1251–1269, 1992.
- F. Lehmann, F. Gatti, M. Bertin, and D. Clouteau. FOURIER NEURAL OPERATOR SURROGATE MODEL TO PREDICT 3D SEISMIC WAVES PROPAGATION. *arXiv - PHYS - Geophysics*, 2023. doi: 10.48550/arXiv.2304.10242.
- Q. Lei and N. Barton. On the selection of joint constitutive models for geomechanics simulation of fractured rocks. *Computers and Geotechnics*, 145:104707, 2022. ISSN 0266-352X. doi: <https://doi.org/10.1016/j.compgeo.2022.104707>. URL <https://www.sciencedirect.com/science/article/pii/S0266352X22000714>.
- J. Lemaitre and J. Chaboche. *Mechanics of Solid Materials*. Cambridge University Press, 1990. ISBN 0 521 47758 1 ; TA405.L3813 1990.

- M. Lesk and E. Schmidt. Lex - a lexical analyzer generator. Technical Report UNIX TIME-SHARING SYSTEM:UNIX PROGRAMMER'S MANUAL, Seventh Edition, Volume 2B, AT&T Bell Laboratories, Murray Hill, New Jersey 07974, 1975. URL <http://dinosaur.compilertools.net/>.
- J. Li and J. Bing Chen. Dynamic response and reliability analysis of structures with uncertain parameters. *International Journal for Numerical Methods in Engineering*, 62(2):289–315, 2005.
- J. Li and O. B. Widlund. On the use of inexact subdomain solvers for BDDC algorithms . *Computer Methods in Applied Mechanics and Engineering*, 196(8):1415–1428, January 2007.
- X. S. Li and J. W. Demmel. Making sparse Gaussian elimination scalable by static pivoting. In *Proceedings of SC98: High Performance Networking and Computing Conference*, Orlando, Florida, November 7–13 1998.
- X. S. Li and J. W. Demmel. SuperLU_DIST: A scalable distributed-memory sparse direct solver for unsymmetric linear systems. *ACM Trans. Mathematical Software*, 29(2):110–140, June 2003.
- X. S. Li and Y. Wang. Linear representation of steady-state line for sand. *Journal of Geotechnical and Geoenvironmental Engineering*, 124(12):1215–1217, 1998.
- S. Liao and A. Zerva. Physically compliant, conditionally simulated spatially variable seismic ground motions for performance-based design. *Earthquake Engineering & Structural Dynamics*, 35:891–919, 2006.
- C. M. Linton and P. McIver. *Handbook of mathematical techniques for wave/structure interactions*. CRC Press, 2001.
- I. Littleton. An experimental study of the adhesion between clay and steel. *Journal of terramechanics*, 13(3):141–152, 1976.
- J. W. H. Liu. Modification of the minimum degree algorithm by multiple elimination. *ACM Transactions on Mathematical Software*, 11(2):141–153, June 1985.
- L. Liu and R. Dobry. Effect of liquefaction on lateral response of piles by centrifuge model tests. In *NCEER Bulletin*, volume 9:1, pages 7–11. National Center for Earthquake Engineering Research, January 1995.
- P. L. Liu and A. Der Kiureghian. A finite element reliability of geometrically nonlinear uncertain structures. *Journal of Engineering Mechanics*, 117(8):1806–1825, 1991.

- D. S. Liyanapathirana and H. G. Poulos. Pseudostatic approach for seismic analysis of piles in liquefying soil. *Journal of Geotechnical and Geoenvironmental Engineering*, 131(12):1480–1487, 2005.
- K. Lo, T. Yung, and B. Lukajic. A field method for the determination of rock-mass modulus. *Canadian Geotechnical Journal*, 24:406–413, 1987.
- D. A. Lockner and S. A. Stanchits. Undrained poroelastic response of sandstones to deviatoric stress change. *JOURNAL OF GEOPHYSICAL RESEARCH*, 107(B12):ETG 13–1 – ETG 13–14, 2002. doi:10.1029/2001JB001460.
- M. Loève. Fonctions aleatoires du second ordre. Supplement to P. Levy, Processus Stochastic et Mouvement Brownien, Gauthier-Villars, Paris, 1948.
- I. N. Lomov, M. Hiltl, O. Y. Vorobiev, and L. A. Glenn. Dynamic behavior of berea sandstone for dry and water-saturated conditions. *International Journal of Impact Engineering*, 26(1-10):465–474, December 2001.
- B. Loret and E. Rizzi. Anisotropic stiffness degradation triggers onset of strain localization. *International Journal of Plasticity*, 13(5):447–459, 1997.
- M. Lou, H. Wang, X. Chen, and Y. Zhai. Structure-soil-structure interaction: literature review. *Soil Dynamics and Earthquake Engineering*, 31(12):1724–1731, 2011.
- A. Love. Some problems of geodynamics. *Some Problems of Geodynamics* Publisher: Cambridge University Press, Cambridge, 1911, 1, 1911.
- X. Lu, J. P. Bardet, and M. Huang. Numerical solutions of strain localization with nonlocal softening plasticity. *Computer Methods Applied Mechanics and Engineering*, 198:3702–3711, 2009.
- J. Lubliner. On the thermodynamic foundations of non-linear solid mechanics. *International Journal of Non-Linear Mechanics*, 7:237–254, 1972.
- J. Lubliner. *Plasticity Theory*. Macmillan Publishing Company, New York., 1990.
- J. E. Luco. Impedance functions for a rigid foundation on a layered medium. *Nuclear Engineering and Design*, 31:204–217, 1974.
- J. E. Luco, H. L. Wong, and F. C. P. D. Barros. Three-dimensional response of a cylindrical canyon in a layered half-space. *Earthquake Engineering & Structural Dynamics*, 19(6):799–817, 1990.
- P. Lumb. The variability of natural soils. *Canadian Geotechnical Journal*, 3:74–97, 1966.

- J. Lysmer. SASSI: A computer program for dynamic soil structure interaction analysis. Report UBC/GT81-02. University of California, Berkeley, CA, USA., 1988.
- J. Lysmer and R. L. Kuhlemeyer. Finite dynamic model for infinite media. Journal of Engineering Mechanics Division, ASCE, 95(EM4):859–877, 1969.
- P. C. Lysne. A comparison of calculated and measured low-stress Hugoniots and release adiabats of dry and water-saturated tuff. Journal of Geophysical Research, 75(23):4375–4386, 1970.
- M.A.Biot. Theory of propagation of elastic waves in a fluid-saturated porous solid. low-frequency range. The journal of acoustical society of America, 28(2):168–178, March 1956.
- R. I. Mackie. Object-Oriented Methods - Finite Element Programming and Engineering Software Design. In Computing in Civil and Building Engineering: Proceedings of the Sixth International Conference on Computing in Civil and Building Engineering, Berlin, Germany, July 12-15 1995.
- A. Magrin. MULTI-SCALE SEISMIC HAZARD SCENARIOS. PhD thesis, UNIVERSITÀ DEGLI STUDI DI TRIESTE, 2012.
- A. Magrin, A. A. Gusev, F. Romanelli, F. Vaccari, and G. F. Panza. Broadband NDSHA computations and earthquake ground motion observations for the Italian territory. Int. J. Earthquake and Impact Engineering, 1(1/2):131–158, 2016.
- L. E. Malvern. Introduction to the Mechanics of a Continuous Medium. In Engineering of the Physical Sciences. Prentice Hall Inc., 1969.
- E. J. Malwick, B. L. Kutter, R. W. Boulanger, and R. Kulasingam. Shear localization due to liquefaction-induced void redistribution in a layered infinite slope. ASCE Journal of Geotechnical and Geoenvironmental Engineering, 132(10):1293–1303, 2006.
- J. Mandel and C. R. Dohrmann. Convergence of a balancing domain decomposition by constraints and energy minimization. Numerical Linear Algebra with Applications, 10(7):639–659, 2003.
- J. B. Mander, M. J. Priestley, and R. Park. Theoretical stress-strain model for confined concrete. Journal of structural engineering, 114(8):1804–1826, 1988.
- T. Manteuffel. An incomplete factorization technique for positive definite linear systems. Mathematics of Computation, 34:473–497, 1980.
- M. T. Manzari and Y. F. Dafalias. A critical state two-surface plasticity model for sands. Géotechnique, 47(2):255–272, 1997.

- M. T. Manzari and R. Prachathananukit. On integartion of a cyclic soil plasticity model. *International Journal for Numerical and Analytical Methods in Geomechanics*, 25:525–549, 2001.
- L. Marconato, P. Leloup, C. Lasserre, R. Jolivet, S. Carigt, R. Grandin, M. Métois, O. Cavalié, and L. Audin. Insights on fault reactivation during the 2019 November 11, Mw 4.9 Le Teil earthquake in southeastern France, from a joint 3-D geological model and InSAR time-series analysis. *Geophys. J. Int.*, 229:758–775, 2022. doi: 10.1093/gji/ggab498.
- K. T. Marosi and D. R. Hiltunen. Characterization of spectral analysis of surface waves shear wave velocity measurement uncertainty. *Journal of Geotechnical and Geoenvironmental Engineering*, 130(10):1034–1041, October 2004.
- J. M. M. C. Marques. Stress computations in elastoplasticity. *Engineering Computations*, 1:42–51, 1984.
- J. E. Marsden and T. J. R. Hughes. *Mathematical Foundations of Elasticity*. Prentice Hall Inc., 1983. local CM65; 4QA 931.M42 ; ISBN 0-13-561076-1.
- G. R. Martin, M. L. March, D. G. Anderson, R. L. Mayes, and M. S. Power. Recommended design approach for liquefaction induced lateral spreads. In *Proceedings of the 3rd National Seismic Conf and Workshop on Bridges and highways*, MCEER-02-SP04, Buffalo, NY, 2002.
- J. Martin and W. Moyce. An experimental study of the collapse of liquid columns on a rigid horizontal plane. *Philosophical Transactions of the Royal Society of London. Series A, Mathematical and Physical Sciences*, pages 312–324, 1952.
- A. Martinez, J. D. Frost, and G. L. Hebeler. Experimental study of shear zones formed at sand/steel interfaces in axial and torsional axisymmetric tests. *Geotechnical Testing Journal*, 38(4):409–426, 2015.
- J. Mason, A. Rosakis, and G. Ravichandran. On the strain and strain rate dependence of the fraction of plastic work converted to heat: an experimental study using high speed infrared detectors and the kolsky bar. *Mechanics of Materials*, 17(2-3):135–145, 1994.
- A. Masud and L. A. Bergman. Application of multi-scale finite element methods to the solution of the Fokker-Planck equation. *Computer Methods in Applied Mechanics and Engineering*, 194(1):1513–1526, April 2005.
- H. Matsuoka and T. Nakai. Stress, deformation and strength characteristics under three different principal stresses. *Proceedings of Japanese Society of Civil Engineers*, 232:59–70, 1974.

- H. G. Matthies, C. E. Brenner, C. G. Bucher, and C. G. Soares. Uncertainties in probabilistic numerical analysis of structures and soils - stochastic finite elements. *Structural Safety*, 19(3):283–336, 1997.
- G. P. Mavroeidis and A. S. Papageorgiou. A mathematical representation of near-fault ground motions. *Bulletin of the Seismological Society of America*, 93(3):1099–1131, June 2003.
- D. Mayer-Rosa and B. Cadot. A review of the 1356 Basel earthquake: Basic data,. *Tectonophysics*, 53(3):325–333, 1979. doi: [https://doi.org/10.1016/0040-1951\(79\)90077-5](https://doi.org/10.1016/0040-1951(79)90077-5). URL <https://www.sciencedirect.com/science/article/pii/0040195179900775>. Proceedings of the 16th General Assemble of the European Seismological Commission.
- G. G. Mayerhoff. Development of geotechnical limit state design. In *Proceedingd of International Symposium on Limit State Design in Geotechnical Engineering, Cpenhagen*, pages 1–12. ASCE, ASCE, New York, 1993.
- I. Mazzieri, M. Stupazzini, R. Guidotti, and C. Smerzini. SPEED: SPectral Elements in Elastodynamics with Discontinuous Galerkin: a non-conforming approach for 3D multi-scale problems. *Int. J. Numer. Meth. Engng*, 2013. doi: 10.1002/nme.4532.
- S. Mazzoni, F. McKenna, M. H. Scott, G. L. Fenves, and B. Jeremić. *Open System for Earthquake Engineers Simulation (OpenSees) : User Manual*. Pacific Earthquake Engineering Research Center, Richmond, December 2002.
- F. T. McKenna. *Object Oriented Finite Element Programming: Framework for Analysis, Algorithms and Parallel Computing*. PhD thesis, University of California, Berkeley, 1997.
- F. T. McKenna. *Object-Oriented Finite Element Programming: Frameworks for Analysis, Algorithms and Parallel Computing*. PhD thesis, University of California, Berkeley, 1997.
- M. McVay, R. Casper, , and T.-I. Shang. Lateral response of three-row groups in loose to dense sands at 3D and 5D pile spacing. *Journal of Geotechnical Engineering*, 121(5):436–441, May 1995.
- M. McVay, L. Zhang, T. Molnit, and P. Lai. Centrifuge testing of large laterally loaded pile groups in sands. *Journal of Geotechnical and Geoenvironmental Engineering*, 124(10):1016–1026, October 1998.
- J. A. Meijerink and H. A. van der Vorst. An iterative solution method for linear systems of which the coefficient matrix is a symmetric M -matrix. *Mathematics of Computation*, 31:148–162, 1977.
- L. Mejia and E. Dawson. Earthquake deconvolution for flac. In *4th International FLAC Symposium on Numerical Modeling in Geomechanics*, pages 04–10, 2006.

- R. Mellah, G. Auvinet, and F. Masrouri. Stochastic finite element method applied to non-linear analysis of embankments. *Probabilistic Engineering Mechanics*, 15:251–259, 2000.
- M. Menegotto and P. E. Pinto. Method of analysis for cyclically loaded reinforced concrete plane frames including changes in geometry and non-elastic behaviour of elements under combined normal force and bending. In *Proceedings of IABSE Symposium*, pages 15–22, 1973.
- P. Menétrey and T. Zimmermann. Object-oriented non-linear finite element analysis: Application to J2 plasticity. *Computers and Structures*, 49(5):767–77, 1993.
- M. Mernik, J. Heering, and A. M. Sloane. When and how to develop domain-specific languages. *ACM Computing Surveys*, 37(4):316–344, December 2005. <http://doi.acm.org/10.1145/1118890.1118892>.
- M. G. Mezgebo and E. M. Lui. A new methodology for energy-based seismic design of steel moment frames. *Earthquake Engineering and Engineering Vibration*, 16(1):131–152, 2017.
- C. Militello and C. A. Felippa. The first ANDES elements: 9-dof plate bending triangles. *Computer Methods in Applied Mechanics and Engineering*, 93:217–246, 1991.
- G. R. Miller. An object – oriented approach to structural analysis and design. *Computers and Structures*, 40(1):75–82, 1991.
- G. R. Miller and M. D. Rucki. A Program Architecture for Interactive Nonlinear Dynamic Analysis of Structures. In *Computing in Civil and Building Engineering: Proceedings of the Fifth International Conference V_ICCCBE*, Anaheim, CA, June 7–9 1993.
- R. D. Mindlin and H. Deresiewicz. Elastic spheres in contact under varying oblique forces. *ASME Journal of Applied Mechanics*, 53(APM-14):327–344, September 1953.
- M. Miniaci, A. Krushynska, F. Bosia, and N. Pugno. Large scale mechanical metamaterials as seismic shields. *New Journal of Physics*, 18:083041, 08 2016. doi: 10.1088/1367-2630/18/8/083041.
- G. P. Mitchell and D. R. J. Owen. Numerical solution for elasto - plastic problems. *Engineering Computations*, 5:274–284, 1988.
- F. Miura, H. E. Stewart, and T. D. O'Rourke. Nolinear analysis of piles subjected to liquefaction induced large ground deformation. In *Proceedings of the Second U.S.–Japan Workshop on Liquefaction , Large Ground Deformations and Their Effect on Lifelines*, number 0032 in NCEER-89, Sept. 26-29 1989.
- K. Mogi. *Experimental Rock Mechanics*. Taylo and Francis, 2006. ISBN ISBN-10: 0415394430.

- B. Monien, R. Preis, and R. Diekmann. Quality matching and local improvement for multilevel graph-partitioning. Technical report, University of Paderborn, 1999.
- D. C. Montgomery and G. C. Runger. *Applied Statistics and Probability for Engineers*. John Wiley & Sons, 605 Third Avenue, New York, NY 10158, third edition, 2003.
- R. Moore. *Methods and Applications of Interval Analysis*. SIAM, Philadelphia, 1979.
- K. N. Morman. The generalized strain measures with application to nonhomogeneous deformation in rubber-like solids. *Journal of Applied Mechanics*, 53:726–728, 1986.
- G. Mortara, A. Mangiola, and V. N. Ghionna. Cyclic shear stress degradation and post-cyclic behaviour from sand–steel interface direct shear tests. *Canadian Geotechnical Journal*, 44(7):739–752, 2007.
- Y. E. Mostafa and M. H. El Naggar. Dynamic analysis of laterally loaded pile groups in sand and clay. *Canadian Geotechnical Journal*, 39(6):1358–1383, 2002.
- F. Moukalled, L. Mangani, M. Darwish, et al. *The finite volume method in computational fluid dynamics*. Springer, 2016.
- A. Moustafa. Damage-based design earthquake loads for single-degree-of-freedom inelastic structures. *Journal of Structural Engineering*, 137(3):456–467, 2011.
- A. Moustafa and S. Mahmoud. Damage assessment of adjacent buildings under earthquake loads. *Engineering Structures*, 61:153–165, 2014.
- Z. Mróz, V. A. Norris, and O. C. Zienkiewicz. An anisotropic hardening model for soils and its application to cyclic loading. *International Journal for Numerical and Analytical Methods in Geomechanics*, 2: 203–221, 1978.
- D. Mu, H. Shu, L. Zhao, and S. An. A review of research on seismic metamaterials. *Advanced Engineering Materials*, 22(4):1901148, 2020. doi: <https://doi.org/10.1002/adem.201901148>. URL <https://onlinelibrary.wiley.com/doi/abs/10.1002/adem.201901148>.
- D. Muir Wood. *Soil Behaviour and Critical State Soil Mechanics*. Cambridge University Press, 1990.
- A. Muqtadir and C. S. Desai. Three dimensional analysis of a pile-group foundation. *International journal for numerical and analysis methods in geomechanics*, 10:41–58, 1986.
- C. M. Murea and S. Sy. Updated lagrangian/arbitrary lagrangian–eulerian framework for interaction between a compressible neo-hookean structure and an incompressible fluid. *International Journal for Numerical Methods in Engineering*, 109(8):1067–1084, 2017.

NASA. Standard for models and simulations, NASA-STD-7009, July 2008. URL <https://standards.nasa.gov/standard/nasa/nasa-std-7009>.

NASA. Standard for models and simulations, NASA-STD-7009A-Change-1, December 2016. URL <https://standards.nasa.gov/standard/nasa/nasa-std-7009>.

National Research Council. Liquefaction of soils during earthquakes. National Academy Press, Washington, D.C., 1985.

NAVFAC. Foundations & Earth Structures, DESIGN MANUAL 7.02. Naval Facilities Engineering Command, 200 Stovall Street, Alexandria, Virginia 22332-2300, USA, revalidated by change 1 september 1986 edition, 1986.

G. C. Nayak and O. C. Zienkiewicz. Elasto - plastic stress analysis a generalization for various constitutive relations including strain softening. International Journal for Numerical Methods in Engineering, 5: 113–135, 1972.

M. Nehdi, M. S. Alam, and M. Youssef. Development of corrosion-free concrete beam–column joint with adequate seismic energy dissipation. Engineering Structures, 32(9):2518–2528, 2010.

S. Nemat-Nasser. On finite plastic flow of crystalline solids and geomaterials. Journal of Applied Mechanics, 50:1114–1126, 1983.

M. Nenning and M. Schanz. Infinite elements in a poroelastodynamic fem. INTERNATIONAL JOURNAL FOR NUMERICAL AND ANALYTICAL METHODS IN GEOMECHANICS, Early View DOI: 10.1002/nag.980, 2010.

N. M. Newmark. A method of computation for structural dynamics. ASCE Journal of the Engineering Mechanics Division, 85:67–94, July 1959.

C. W. W. Ng, L. Zhang, and D. C. N. Nip. Response of laterally loaded large-diameter bored pile groups. Journal of Geotechnical and Geoenvironmental Engineering, 127(8):658–669, Aug. 2001.

E. Ng and B. Peyton. Block sparse cholesky algorithms on advanced uniprocessor computers. SIAM Journal on Scientific and Statistical Computing, 14(5):1034–1056, September 1993.

E. Niebler. xpressive: Dual-mode dsel library design. In D. Musser, editor, Library-Centric Software Design LCSD'05. Object-Oriented Programming, Systems, Languages and Applications, October 2005.

A. Niemunis. Private correspondence, 2015 –.

- E. Nikbakht, K. Rashid, F. Hejazi, and S. A. Osman. A numerical study on seismic response of self-centring precast segmental columns at different post-tensioning forces. *Latin American Journal of solids and structures*, 11(5):864–883, 2014.
- V. N. Nikolaevskiy, S. M. Kapustynskiy, M. Thiercelin, and A. G. Zhilenkov. Explosion dynamics in saturated rocks and solids. *Transport in Porous Media*, 65:485–504, 2006. URL <http://www.springerlink.com/index/R221288861444442.pdf>. DOI 10.1007/s11242-006-6752-0.
- A. Nobahar. *Effects of Soil Spatial Variability on Soil-Structure Interaction*. Doctoral dissertation, Memorial University, St. John's, NL, 2003.
- A. K. Noor, A. Kamel, and R. E. Fulton. Substructuring techniques – status and projections. *Computers & Structures*, 8:628–632, 1978.
- R. Nova and D. M. Wood. A constitutive model for sand in triaxial compression. *International Journal for Numerical and Analytical Methods in Geomechanics*, 3:255–278, 1979.
- V. D. Novellis, V. Convertito, S. Valkaniotis, F. Casu, R. Lanari, M. F. M. Tobar, and N. A. Pino. Coincident locations of rupture nucleation during the 2019 Le Teil earthquake, France and maximum stress change from local cement quarrying. *Communications Earth & Environment*, 1(20), 2020. doi: <https://doi.org/10.1038/s43247-020-00021-6>.
- W. Nowacki. *Baudynamik*. Ingenieurbauten. Springer, Vienna, 1974.
- W. Oberkampf. Material from the short course on verification and validation in computational mechanics. Albuquerque, New Mexico, July 2003.
- W. L. Oberkampf and M. Pilch. *Simulation Verification and Validation for Managers*. NAFEMS, 2017. ISBN 978-1-910643-33-4.
- W. L. Oberkampf and C. J. Roy. *Verification and Validation in Scientific Computing*. Cambridge University Press, 2010. ISBN 978-0-521-11360-1.
- W. L. Oberkampf and T. G. Trucano. Verification and validation benchmarks. *Nuclear engineering and Design*, 238(3):716–743, 2008. URL <http://www.sciencedirect.com/science/article/pii/S0029549307003548>.
- W. L. Oberkampf, T. G. Trucano, and C. Hirsch. Verification, validation and predictive capability in computational engineering and physics. In *Proceedings of the Foundations for Verification and Validation on the 21st Century Workshop*, pages 1–74, Laurel, Maryland, October 22-23 2002. Johns Hopkins University / Applied Physics Laboratory.

- W. L. Oberkampf, M. M. Pilch, and T. G. Trucano. Predictive capability maturity model for computational modeling and simulation. [OSTI](#), (SAND2007-5948, TRN: US20100910 2007. doi: 10.2172/976951. URL <https://www.osti.gov/biblio/976951>.
- J. T. Oden, I. Babuška, F. Nobile, Y. Feng, and R. Tempone. Theory and methodology for estimation and control of errors due to modeling, approximation, and uncertainty. [Computer Methods in Applied Mechanics and Engineering](#), 194(2-5):195–204, February 2005.
- T. Oden, R. Moser, and O. Ghattas. Computer predictions with quantified uncertainty, part i. [SIAM News](#), 43(9), November 2010a.
- T. Oden, R. Moser, and O. Ghattas. Computer predictions with quantified uncertainty, part ii. [SIAM News](#), 43(10), December 2010b.
- R. W. Ogden. [Non-Linear Elastic Deformations](#). Series in mathematics and its applications. Ellis Horwood Limited, Market Cross House, Cooper Street, Chichester, West Sussex, PO19 1EB, England, 1984.
- W. A. Olsson. Theoretical and experimental investigation compaction of bands in porous rock. [JOURNAL OF GEOPHYSICAL RESEARCH](#), 104(B4):7219–7228, April 1999.
- W. A. Olsson. Quasistatic propagation of compaction fronts in porous rock. [Mechanics of Materials](#), 33(11):659–668, 2001.
- OpenCFD Ltd. [OpenFOAM User Guide](#), v1906 edition, 2019.
- OpenSees Development Team (Open Source Project). OpenSees: open system for earthquake engineering simulations. <http://opensees.berkeley.edu/>, 2000-2006.
- I. Oprsal and D. Fäh. 1D vs 3D strong ground motion hybrid modelling of site, and pronounced topography effects at augusta raurica, switzerland-earthquakes or battles. In [Proceedings of 4th International Conference on Earthquake Geotechnical Engineering June 25–28, 2007, Greece](#), 2007.
- F. M. T. D. O'Rourke. Lateral spreading effects on pile foundations. In [Proceedings of the Third U.S.–Japan Workshop on Earthquake Resistant Design of Lifeline Facilities and Countermeasures for Soil Liquefaction](#), number 0001 in NCEER-91, Feb. 1 1991.
- M. Ortiz and E. P. Popov. Accuracy and stability of integration algorithms for elastoplastic constitutive relations. [International Journal for Numerical Methods in Engineering](#), 21:1561–1576, 1985.
- S. Osovski, D. Rittel, and A. Venkert. The respective influence of microstructural and thermal softening on adiabatic shear localization. [Mechanics of Materials](#), 56:11–22, 2013.

- F. Ostdan. Sassi2000 a system for analysis of soil-structure interaction, version 3, user's manual. Program Manual, April 2007.
- W. Ostermann, W. Wunderlich, and H. Cramer. Object-Oriented Tools for the Development of User Interface for Interactive Teachware. In Computing in Civil and Building Engineering: Proceedings of the Sixth International Conference on Computing in Civil and Building Engineering, Berlin, Germany, July 12-15 1995.
- J. Padovan. Applications of 3-d finite element procedures to static and dynamic problems in micropolar elasticity. Computers & Structures, 8(2):231–236, 1978. ISSN 00457949. doi: 10.1016/0045-7949(78)90027-5.
- G. M. Paice, D. V. Griffiths, and G. A. Fenton. Finite element modeling of settlement on spatially random soil. Journal of Geotechnical Engineering, 122(9):777–779, 1996.
- A. L. Pais and E. Kausel. On rigid foundations subjected to seismic waves. Earthquake Engineering & Structural Dynamics, 18(4):475–489, 1989.
- A. Palermo and A. Marzani. Control of love waves by resonant metasurfaces. Scientific Reports, 8, 05 2018. doi: 10.1038/s41598-018-25503-8.
- A. Palermo, S. Krödel, A. Marzani, and C. Daraio. Engineered metabarrier as shield from seismic surface waves. Scientific Reports, 6:39356, 12 2016. doi: 10.1038/srep39356.
- A. Palermo, S. Krödel, K. H. Matlack, R. Zaccherini, V. K. Dertimanis, E. N. Chatzi, A. Marzani, and C. Daraio. Hybridization of guided surface acoustic modes in unconsolidated granular media by a resonant metasurface. Phys. Rev. Applied, 9:054026, May 2018. doi: 10.1103/PhysRevApplied.9.054026. URL <https://link.aps.org/doi/10.1103/PhysRevApplied.9.054026>.
- J. L. Pan, A. T. C. Goh, K. S. Wong, and A. R. Selby. Three-dimensional analysis of single pile response to lateral soil movements. International Journal for Numerical and Analytical Methods in Geomechanics, 26:747–758, 2002.
- G. F. Panza, C. L. Mura, A. Peresan, F. Romanelli, and F. Vaccari. Advances in Geophysics, volume 53, chapter Seismic Hazard Scenarios as Preventive Tools for a Disaster Resilient Society, pages 93–165. Elsevier Inc., 2012. ISSN 0065-2687.
- R. Paolucci, M. Shirato, and M. T. Yilmaz. Seismic behaviour of shallow foundations: Shaking table experiments vs numerical modelling. Earthquake Engineering & Structural Dynamics, 37(4):577–595, 2008.

- R. Paolucci, I. Mazzieri, G. Piunno, C. Smerzini, M. Vanini, and A. Özcebe. Earthquake ground motion modeling of induced seismicity in the Groningen gas field. *Earthquake Engineering & Structural Dynamics*, n/a(n/a):20, 2020. doi: 10.1002/eqe.3367. URL <https://onlinelibrary.wiley.com/doi/abs/10.1002/eqe.3367>.
- R. Paolucci, C. Smerzini, and M. Vanini. BB-SPEEDset: A Validated Dataset of Broadband Near-Source Earthquake Ground Motions from 3D Physics-Based Numerical Simulations. *Bulletin of the Seismological Society of America*, 111(5):2527–2545, October 2021. doi: 10.1785/0120210089.
- A. G. Papadimitriou and G. D. Bouckovalas. Plasticity model for sand under small and large cyclic strains: A multiaxial formulation. *Soil Dynamics and Earthquake Engineering*, 22(3):191–204, 2002.
- A. S. Papageorgiou and D. Pei. A discrete wavenumber boundary element method for study of the 3-d response 2-d scatterers. *Earthquake Engineering & Structural Dynamics*, 27(6):619–638, 1998.
- E. Papamichos, I. Vardoulakis, and H.-B. Mühlhaus. Buckling of layered elastic media: A Cosserat-continuum approach and its validation. *International Journal for Numerical and Analytical Methods in Geomechanics*, 14:473–498, 1990.
- W. G. Pariseau. *Design Analysis in Rock Mechanics*. Taylor & Francis, 1st edition, October 2006. ISBN 978-0415413817.
- J. Park. A brief review of tensor operations for students of continuum mechanics. *Journal of Applied Engineering Mathematics*, 5:1–4, December 2018.
- J.-B. Park, Y. Choi, S.-J. Lee, N.-C. Park, K.-S. Park, Y.-P. Park, and C.-I. Park. Modal characteristic analysis of the apr1400 nuclear reactor internals for seismic analysis. *Nuclear Engineering and Technology*, 46(5):689–698, 2014.
- S. Park and P. Byrne. Practical constitutive model for soil liquefaction. In *Proc., 9th Int. Symp. on Numerical Models in Geomechanics (NUMOG IX)*, pages 181–186. CRC Press, Boca Raton, FL, 2004.
- M. Pastor, O. C. Zienkiewicz, and A. H. C. Chan. Generalized plasticity and the modeling of soil behaviour. *International Journal for Numerical and Analytical Methods in Geomechanics*, 14:151–190, 1990.
- L. F. Pavarino. BDDC and FETI-DP preconditioners for spectral element discretizations. *Computer Methods in Applied Mechanics and Engineering*, 196(8):1380–1388, January 2007.
- C. E. Pearson, editor. *Handbook of Applied Mathematics*. Van Nostrand Reinhold Company, 1974.

- A. Pecker, J. J. Johnson, and B. Jeremić. Methodologies for Seismic Soil-Structure Interaction Analysis in the Design and Assessment of Nuclear Installations. Number IAEA-TECDOC-1990. United Nations, International Atomic Energy Agency, UN-IAEA, External Events Safety Section, IAEA, VIC, PO Box 100, 1400 Vienna, Austria, February 2022. ISBN 978-92-0-143021-2. IAEAL 21-01471.
- A. Pérez-Foguet and A. Huerta. Plastic flow potential for the cone region of the MRS–Lade model, 1997.
- A. Pérez-Foguet, A. Rodríguez-Ferran, and A. Huerta. Numerical differentiation for non-trivial consistent tangent matrices: an application to the mrs-lade model. International Journal for Numerical Methods in Engineering, 48:159–184, 2000.
- A. Pérez-Foguet, A. Rodríguez-Ferran, and A. Huerta. Consistent tangent matrices for substepping schemes. Computer Methods in Applied Mechanics and Engineering, 190(35-36):4627 – 4647, 2001. ISSN 0045-7825. doi: [http://dx.doi.org/10.1016/S0045-7825\(00\)00336-4](http://dx.doi.org/10.1016/S0045-7825(00)00336-4). URL <http://www.sciencedirect.com/science/article/pii/S0045782500003364>.
- D. Perić. Localized Deformation and Failure Analysis of Pressure Sensitive Granular Material. PhD thesis, University of Colorado at Boulder, 1991.
- N. A. Petersson and B. Sjögreen. High order accurate finite difference modeling of seismo-acoustic wave propagation in a moving atmosphere and a heterogeneous earth model coupled across a realistic topography. Journal of Scientific Computing, -(14):290–323, 2018.
- K.-K. Phoon and F. H. Kulhawy. Characterization of geotechnical variability. Canadian Geotechnical Journal, 36:612–624, 1999a.
- K.-K. Phoon and F. H. Kulhawy. Evaluation of geotechnical property variability. Canadian Geotechnical Journal, 36:625–639, 1999b.
- R. M. V. Pidaparti and A. V. Hudli. Dynamic analysis of structures using object-oriented techniques. Computers and Structures, 49(1):149–156, 1993.
- F. Pisanò and B. Jeremić. Simulating stiffness degradation and damping in soils via a simple viscoelastic-plastic model. Soil Dynamics and Geotechnical Earthquake Engineering, 63:98–109, 2014.
- R. Popescu. Stochastic variability of soil properties: data analysis, digital simulation, effects on system behavior. Doctoral dissertation, Princeton University, Princeton, NJ, 1995.
- R. Popescu, J. H. Prevost, and G. Deodatis. Effects of spatial variability on soil liquefaction: Some design recommendations. Geotechnique, 47(5):1019–1036, 1997.

- R. Popescu, J. H. Prevost, and G. Deodatis. Spatial variability of soil properties: Two case studies. In P. Dakoulas and M. Yegian, editors, Geotechnical Earthquake Engineering and Soil Dynamics III: Proceedings of a Speciality Conference held in Seattle, Washington, August 3-6, 1998, Geotechnical Special Publication No. 75, pages 568–579. Geo-Institute of ASCE, ASCE, Reston, VA, 1998.
- S. Popovics. A numerical approach to the complete stress-strain curve of concrete. Cement and concrete research, 3(5):583–599, 1973.
- D. Post. The coming crisis in computational science. Technical Report LA-UR-04-0388, 2004. Submitted to: Keynote Address, Proceedings of the IEEE International Conference on High Performance Computer Architecture: Workshop on Productivity and Performance in High-End Computing, Madrid, Spain, February 14, 2004.
- A. Pothier and J. Rencis. Three-dimensional finite element formulation for microelastic solids. Computers & Structures, 51(1):1–21, 1994. ISSN 00457949. doi: 10.1016/0045-7949(94)90031-0.
- J. G. Potyondy. Skin friction between various soils and construction materials. Geotechnique, 11(4):339–353, 1961.
- M. Preisig. Nonlinear finite element analysis of dynamic Soil - Foundation - Structure interaction. Master's thesis, University of California, Davis, 2005.
- W. H. Press, B. P. Flannery, S. A. teukolsky, and W. T. Vetterling. Numerical Recipes in C. Cambridge University Press, Cambridge, 1988a.
- W. H. Press, B. P. Flannery, S. A. Teukolovsky, and W. T. Vetterling. Numerical Recipes in C, The Art of Scientific Computing. Cambridge University Press, 1988b.
- J. S. Pressley and H. G. Poulos. Finite element analysis of mechanisms of pile group behavior. International Journal for Numerical and Analytical Methods in Geomechanics, 10:213–221, 1986.
- J. H. Prevost. A simple plasticity theory for frictional cohesionless soils. International Journal of Soil Dynamics and Earthquake Engineering, 4(1):9 – 17, 1985a. ISSN 0261-7277. doi: [http://dx.doi.org/10.1016/0261-7277\(85\)90030-0](http://dx.doi.org/10.1016/0261-7277(85)90030-0). URL <http://www.sciencedirect.com/science/article/pii/0261727785900300>.
- J. H. Prevost. Wave propagation in fluid-saturated porous media: an efficient finite element procedure. Soil Dynamics and Earthquake Engineering, 4(4):183 –202, 1985b.

- J. H. Prevost. DYNA1D: A computer program for nonlinear site response analysis, technical documentation. technical report no. nceer-89-0025. Technical report, National Center for Earthquake Engineering Research, State University of New York at Buffalo, 1989.
- J. H. Prevost and R. Popescu. Constitutive relations for soil materials. *Electronic Journal of Geotechnical Engineering*, October 1996. available at <http://139.78.66.61/ejge/>.
- J. S. Przemieniecki. *Theory of Matrix Structural Analysis*. McGraw Hill, New York, 1985.
- R. Rackwitz. Reviewing probabilistic soil modelling. *Computers and Geotechnics*, 26:199–223, 2000.
- R. Ramey. Making a boost library. In D. Musser, editor, *Library-Centric Software Design LCSD'05. Object-Oriented Programming, Systems, Languages and Applications*, October 2005.
- E. Ramm. Strategies for tracing the nonlinear response near limit points. In W. Wunderlich, E. Stein, and K.-J. Bathe, editors, *Nonlinear Finite Element Analysis in Structural Mechanics*, pages 63–89. Springer-Werlag Berlini Heidelberg New York, 1981.
- E. Ramm. The Riks/Wempner approach – an extension of the displacement control method in nonlinear analysis. In E. Hinton, D. Owen, and C. Taylor, editors, *Recent Advances in Non-Linear Computational Mechanics*, chapter 3, pages 63–86. Pineridge Press, Swansea U.K., 1982.
- E. Ramm and A. Matzenmiller. Consistent linearization in elasto - plastic shell analysis. *Engineering Computations*, 5:289–299, 1988.
- B. Raphael and C. S. Krishnamoorthy. Automating finite element development using object oriented techniques. *Engineering Computations*, 10:267–278, 1993.
- G. Ravichandran, A. J. Rosakis, J. Hodowany, P. Rosakis, M. D. Furnish, N. N. Thadhani, and Y. Horie. On the conversion of plastic work into heat during high-strain-rate deformation. In *AIP conference proceedings*, volume 620/1, pages 557–562. AIP, 2002.
- L. Rayleigh. On waves propagated along the plane surface of an elastic solid. *Proceedings of the London Mathematical Society*, 1(1):4, 1885.
- L. C. Reese, J. D. Allen, and J. Q. Hargrove. Laterally loaded piles in layered soils. In P. C. of X IC-SMFE, editor, *Proceedings of the Tenth International Conference on Soil Mechanics and Foundations Engineering*, volume 2, pages 819–822, Stockholm, June 1981. A. A. Balkema.
- L. C. Reese, S. T. Wang, W. M. Isenhower, and J. A. Arrellaga. *LPILE plus 4.0 Technical Manual*. ENSOFT, INC., Austin, TX, version 4.0 edition, Oct. 2000a.

- L. C. Reese, S. T. Wang, I. W. M., A. J. A., and H. J. LPILE plus 4.0 User Guide. ENSOFT, INC., Austin, TX, version 4.0 edition, Oct. 2000b.
- B. Ren and S. Li. Meshfree simulations of plugging failures in high-speed impacts. Computers & structures, 88(15):909–923, 2010.
- P. L. Renault, N. A. Abrahamson, K. J. Coppersmith, M. Koller, P. Roth, and A. Höller. Probabilistic Seismic Hazard Analysis for Swiss Nuclear Power Plant Sites - PEGASOS Refinement Project. Final Report, Vol. 1-5 . Technical report, Swissnuclear, 2013.
- C. Reschke, T. Sterling, D. Ridge, D. Savarese, D. J. Becker, and P. Merkey. A design study of alternative network topologies for the Beowulf parallel workstation. In Proceedings, High Performance and Distributed Computing, 1996. <http://cesdis.gsfc.nasa.gov/beowulf/papers.html>
- A. Riahi and J. H. Curran. Full 3D finite element Cosserat formulation with application in layered structures. Applied Mathematical Modelling, 33(8):3450–3464, 2009. ISSN 0307904X. doi: 10.1016/j.apm.2008.11.022.
- F. E. Richart, J. J. R. Hall, and R. D. Woods. Vibration of Soils and Foundations, International Series in Theoretical and Applied Mechanics. Prentice-Hall, Englewood Cliffs, N.J., 1970.
- D. Ridge, D. J. Becker, P. Merkey, and T. Sterling. BEOWULF: Harnessing the power of parallelism in a Pile-of-PCs. In Proceedings, IEEE Aerospace, 1997. <http://cesdis.gsfc.nasa.gov/beowulf/papers.html>
- E. Riks. The application of Newton's method to the problems of elastic stability. Journal of Applied Mechanics, 39:1060–1066, December 1972.
- E. Riks. An incremental approach to the solution of snapping and buckling problems. International Journal for Solids and Structures, 15:529–551, 1979.
- H. Risken. The Fokker-Planck Equation: Methods of Solutions and Applications. Springer Series in Synergetics. Springer-Verlag, Berlin Heidelberg, second edition, 1989.
- D. Rittel. An investigation of the heat generated during cyclic loading of two glassy polymers. part i: Experimental. Mechanics of Materials, 32(3):131–147, 2000.
- D. Rittel and Y. Rabin. An investigation of the heat generated during cyclic loading of two glassy polymers. part ii: Thermal analysis. Mechanics of Materials, 32(3):149–159, 2000.

- D. Rittel, N. Eliash, and J. Halary. Hysteretic heating of modified poly (methylmethacrylate). *Polymer*, 44(9):2817–2822, 2003.
- J.-F. Ritz, S. Baize, M. Ferry, C. Larroqu, L. Audin, B. Delouis, and E. Mathot. Surface rupture and shallow fault reactivation during the 2019 Mw 4.9 Le Teil earthquake, France. *COMMUNICATIONS EARTH & ENVIRONMENT*, 1(10), 2020. doi: 10.1038/s43247-020-0012-z.
- D. Rixena and F. Magoulès. Domain decomposition methods: Recent advances and new challenges in engineering. *Computer Methods in Applied Mechanics and Engineering*, 196(8):1345–1346, January 2007.
- E. Rizzi. Localization analysis of damaged materials. Master's thesis, University of Colorado at Boulder, 1993.
- P. J. Roache. *Verification and Validation in Computational Science and Engineering*. Hermosa Publishers, Albuquerque, New Mexico, 1998. ISBN 0-913478-08-3.
- Y. Robert. Regular incomplete factorizations of real positive definite matrices. *Linear Algebra and Its Applications*, 48:105–117, 1982.
- A. D. Robison. C++ gets faster for scientific computing. *Computers in Physics*, 10(5):458–462, Sept/Oct 1996.
- C. Roblee, W. Silva, G. Toro, and N. Abrahamson. Variability in site-specific seismic ground-motion predictions. In *Proceedings: Uncertainty in the Geologic Environment*, page 21p, Madison WI., August 1-2 1996. American Society of Civil Engineers.
- A. Rodgers. Private communications. SW4 – Real-ESSI connection, 2017.
- K. M. Rollins, K. T. Peterson, and T. J. Weaver. Lateral load behavior of full scale pile group in clay. *Journal of geotechnical and geoenvironmental engineering*, 124(6):468–478, June 1997.
- K. M. Rollins, T. M. Gerber, J. D. Lane, and S. A. Ashford. Lateral resistance of a full-scale pile group in liquefied sand. *Journal of Geotechnical and Geoenvironmental Engineering*, 131(1):115–125, 2005.
- A. Romero, P. Galvín, and J. Domínguez. 3D non-linear time domain fem–bem approach to soil–structure interaction problems. *Engineering Analysis with Boundary Elements*, 37(3):501–512, 2013.
- P. Rosakis, A. Rosakis, G. Ravichandran, and J. Hodowany. A thermodynamic internal variable model for the partition of plastic work into heat and stored energy in metals. *Journal of the Mechanics and Physics of Solids*, 48(3):581–607, 2000.

- K. H. Roscoe and J. B. Burland. On the generalized stress-strain behaviour of "wet" clay. In Engineering plasticity, pages 553–609. Cambridge University Press, 1968.
- K. H. Roscoe, A. N. Schofield, and C. P. Wroth. On the yielding of soils. Geotechnique, 8(1):22–53, 1958.
- K. H. Roscoe, A. N. Schofield, and A. Thurairajah. Yielding of clays in states wetter than critical. Géotechnique, 13(3):211–240, 1963.
- C. Rose and M. D. Smith. Mathematical Statistics with Mathematica. Springer Texts in Statistics. Springer-Verlag, New York, 2002.
- T. J. Ross, L. R. Wagner, and G. F. Luger. Object-Oriented Programming for Scientific Codes. II: Examples in C++. Journal of Computing in Civil Engineering, 6(4):497–514, 1992.
- P. W. Rowe. The stress–dilatancy relation for static equilibrium of an assembly of particles in contact. Proceedings of the Royal Society, 269(1339):500–527, 9 October 1962. Series A Mathematical and Physical Sciences.
- C. Roy, A. J. Roffel, S. Bolourchi, L. Todorovski, and M. Khoncarly. Study of seismic structure-soil-structure interaction between two heavy structures. In Transactions, SMiRT-22, pages 1–7, San Francisco, August 2013. IASMiRT.
- C. J. Roy and W. L. Oberkampf. A comprehensive framework for verification, validation, and uncertainty quantification in scientific computing. Computer Methods in Applied Mechanics and Engineering, 200 (25-28):2131 – 2144, 2011. ISSN 0045-7825. doi: 10.1016/j.cma.2011.03.016. URL <http://www.sciencedirect.com/science/article/pii/S0045782511001290>.
- M. D. Rucki and G. R. Miller. An Algorithmic Framework for Flexible Finite Element-Based Structural Modeling. Computer Methods in Applied Mechanics and Engineering, 136(3–4):363–384, 1996.
- J. W. Rudnicki and J. R. Rice. Conditions for the localization of deformation in pressure-sensitive dilatant materials. Journal of the Mechanics and Physics of Solids, 23:371 to 394, 1975.
- P. F. Ruesta and F. C. Townsend. Evaluation of laterally loaded pile group at Roosevelt bridge. Journal of Geotechnical and Geoenvironmental Engineering, 123(12):1153–1161, December 1997.
- J. Rumbaugh, M. Blaha, W. Premerhani, F. Eddy, and W. Lorenzen. Object-Oriented Modeling and Design. Prentice Hall, Englewood Cliffs, New Jersey, 1991.

- K. Runesson. Implicit integration of elastoplastic relations with reference to soils. *International Journal for Numerical and Analytical Methods in Geomechanics*, 11:315–321, 1987.
- K. Runesson. Constitutive theory and computational technique for dissipative materials with emphasis on plasticity, viscoplasticity and damage: Part III. Lecture Notes, Chalmers Technical University, Göteborg, Sweden, September 1996.
- K. Runesson and Z. Mróz. A note on nonassociated plastic flow rules. *International Journal of Plasticity*, 5:639–658, 1989.
- K. Runesson and A. Samuelsson. Aspects on numerical techniques in small deformation plasticity. In G. N. P. J. Middleton, editor, *NUMETA 85 Numerical Methods in Engineering, Theory and Applications*, pages 337–347. AA.Balkema., 1985.
- H. Ryan. Ricker, Ormsby, Klander, Butterworth - a choice of wavelets. *Canadian Society of Exploration Geophysicists Recorder*, 19(7):8–9, September 1994. URL <http://www.cseg.ca/publications/recorder/1994/09sep/sep94-choice-of-wavelets.pdf>.
- Y. Saad. *Iterative Methods for Sparse Linear Systems*. SIAM, Philadelphia, second edition, 2003.
- S. Sakamoto and R. Ghanem. Polynomial chaos decomposition for the simulation of non-gaussian nonstationary stochastic processes. *Journal of Engineering Mechanics*, 128(2):190–201, February 2002.
- T. Sakemi, M. Tanaka, Y. Higuchi, K. Kawasaki, and K. Nagura. Permeability of pore fluids in the centrifugal fields. In *10th Asian Regional Conference on Soil Mechanics and Foundation Engineering (10ARC)*, Beijing, China, August 29 - Sept 2 1995.
- M. D. Salas. The curious events leading to the theory of shock waves. In *17th Shock Interaction Symposium*, Rome, Italy, 4–8 September 2006. URL http://ntrs.nasa.gov/archive/nasa/casi.ntrs.nasa.gov/20060047586_2006228914.pdf.
- V. Saouma and L. Perotti. Constitutive model for alkali-aggregate reactions. *Materials Journal*, 103(3):194–202, 2006.
- V. E. Saouma. Prof. Saouma's lecture notes, manuals, &c. (available through his web page: <http://civil.colorado.edu/~saouma/>), 1992–2013.
- R. Z. Sarica and M. S. Rahman. A wavelet analysis of ground motion characteristics. In *U.S.-Taiwan Workshop on Soil Liquefaction*, 2003.

- M. Sarkis and D. B. Szyld. Optimal left and right additive Schwarz preconditioning for minimal residual methods with Euclidean and energy norms. *Computer Methods in Applied Mechanics and Engineering*, 196(8):1612–1621, January 2007.
- R. Sause and J. Song. Object-Oriented Structural Analysis with Substructures. In *Computing in Civil Engineering: Proceedings of the First Conference held in Conjunction with A/E/C Systems' 94*, Washington, D.C., June 20–22 1994.
- J. C. J. Schellekens and H. Parisch. On finite deformation elasticity. Technical Report ISD Nr. 94/3, Institute for Statics and Dynamics of Aerospace Structures, Pfaffenwaldring 27, 70550 Stuttgart, 1994.
- K. Schloegel, G. Karypis, and V. Kumar. Graph partitioning for high performance scientific simulations. Technical report, Army HPC Research Center, Department of Computer Science and Engineering, University of Minnesota, 1999.
- K. Schloegel, G. Karypis, and V. Kumar. A unified algorithm for load-balancing adaptive scientific simulations. Technical report, Army HPC Research Center, Department of Computer Science and Engineering, University of Minnesota, 2000.
- P. Schnabel, J. Lysmer, and H. B. Seed. Shake – a computer program for equation response analysis of horizontally layered sites. report eerc 72-12. Technical report, University of California Berkeley, 1972.
- A. Schofield and C. Wroth. *Critical state soil mechanics*. McGraw-Hill, London, 1968.
- S.-P. Scholz. Elements of an object – oriented FEM++ program in C++. *Computers and Structures*, 43(3):517–529, 1992.
- G. I. Schüeller. A state-of-the-art report on computational stochastic mechanics. *Probabilistic Engineering Mechanics*, 12(4):197–321, 1997.
- B. Scott, R. Park, and M. Priestley. Fiber element modeling for seismic performance of bridge columns made of concrete-filled frp tubes. *Journal of the American Concrete Institute*, 79(1):13–27, 1982.
- H. B. Seed and I. M. Idriss. Soil moduli and damping factors for dynamic response analyses. report eerc 70-10. Technical report, University of California Berkeley, 1970a.
- H. B. Seed and I. M. Idriss. Soil moduli and damping factors for dynamic response analyses. report eerc 70-10. Technical report, University of California Berkeley, 1970b.
- J. F. Semblat. Rheological interpretation of rayleigh damping. *Journal of Sound and Vibration*, 206(5):741–744, 1997.

- J.-F. Semblat and A. Pecker. Waves and Vibrations in Soils: Earthquakes, Traffic, Shocks, Construction works. IUSS Press, first edition, 2009. ISBN ISBN-10: 8861980309; ISBN-13: 978-8861980303.
- J.-F. Semblat, L. Lenti, and A. Gandomzadeh. A simple multi-directional absorbing layer method to simulate elastic wave propagation in unbounded domains. International Journal for Numerical Methods in Engineering, doi: 10.1002/nme.3035, 2010. URL <http://dx.doi.org/10.1002/nme.3035>.
- S. J. Semnani, J. A. White, and R. I. Borja. Thermoplasticity and strain localization in transversely isotropic materials based on anisotropic critical state plasticity. International Journal for Numerical and Analytical Methods in Geomechanics, 40(18):2423–2449, 2016.
- K. Sett. Probabilistic elasto-plasticity and its application in finite element simulations of stochastic elastic-plastic boundary value problems. Doctoral Dissertation, University of California, Davis, CA, September 2007.
- K. Sett and B. Jeremić. Uncertain soil properties and elastic-plastic simulations in geomechanics. In K. K. Phoon, G. A. Fenton, E. F. Glynn, C. H. Juang, T. F. Griffiths, T. F. Wolff, and L. Zhang, editors, Probabilistic Applications in Geotechnical Engineering (Proceedings of Geo-Denver 2007: New Peaks in Geotechnics, held in Denver, CO from February 18-21, 2007), Geotechnical Special Publication No. 170, pages 1–11. American Society for Civil Engineers, 2007.
- K. Sett and B. Jeremić. Forward and backward probabilistic simulations in geotechnical engineering. In M. Iskander, D. F. Laefer, and M. H. Hussein, editors, Contemporary Topics in Insitu Testing, Analysis, and Reliability of Foundations (Selected Papers from the 2009 International Foundation Congress and Equipment Expo, held in Orlando, FL, from March 15-19, 2009), volume 186 of Geotechnical Special Publications No. 186, pages 1–11. American Society for Civil Engineers, 2009.
- K. Sett and B. Jeremić. Probabilistic yielding and cyclic behavior of geomaterials. International Journal for Numerical and Analytical Methods in Geomechanics, 34(15):1541–1559, 2010. 10.1002/nag.870 (first published online March 11, 2010).
- K. Sett, B. Jeremić, and M. L. Kavvas. Probabilistic elasto-plasticity: Solution and verification in 1D. Acta Geotechnica, 2(3):211–220, October 2007a.
- K. Sett, B. Jeremić, and M. L. Kavvas. The role of nonlinear hardening in probabilistic elasto-plasticity. International Journal for Numerical and Analytical Methods in Geomechanics, 31(7):953–975, June 2007b.

- K. Sett, B. Jeremić, and M. L. Kavvas. Probabilistic elasto-plasticity: Solution and verification in 1-D. *Acta Geotechnica*, 2(3):211–220, September 2007c.
- K. Sett, B. Jeremić, and M. L. Kavvas. The role of nonlinear hardening/softening in probabilistic elasto-plasticity. *International Journal for Numerical and Analytical Methods in Geomechanics*, 31(7):953–975, June 2007d.
- K. Sett, B. Unutmaz, K. O. Çetin, S. Koprivica, and B. Jeremić. Soil uncertainty and its influence on simulated G/G_{max} and damping behaviors. *Journal of Geotechnical and Geoenvironmental Engineering*, 2008. In review.
- K. Sett, B. Jeremić, and M. L. Kavvas. Stochastic elastic-plastic finite elements. *Computer Methods in Applied Mechanics and Engineering*, 200(9-12):997–1007, February 2011a. ISSN 0045-7825. doi: DOI:10.1016/j.cma.2010.11.021.
- K. Sett, B. Unutmaz, K. Önder Çetin, S. Koprivica, and B. Jeremić. Soil uncertainty and its influence on simulated G/G_{max} and damping behavior. *ASCE Journal of Geotechnical and Geoenvironmental Engineering*, 137(3):218–226, 2011b. 10.1061/(ASCE)GT.1943-5606.0000420 (July 29, 2010).
- I. Shahrou and F. Rezaie. An elastoplastic constitutive relation for the soil-structure interface under cyclic loading. *Computers and Geotechnics*, 21(1):21–39, 1997.
- I. Shahrou, F. Khoshnoudian, M. Sadek, and H. Mroueh. Elastoplastic analysis of the seismic response of tunnels in soft soils. *Tunnelling and underground space technology*, 25(4):478–482, 2010.
- N. Sharma, K. Dasgupta, and A. Dey. Optimum lateral extent of soil domain for dynamic ssi analysis of rc framed buildings on pile foundations. *Frontiers of Structural and Civil Engineering*, 14(1):62–81, 2020.
- B. Shen, W. Xu, J. Wang, Y. Chen, W. Yan, J. Huang, and Z. Tang. Seismic control of super high-rise structures with double-layer tuned particle damper. *Earthquake Engineering & Structural Dynamics*, 50(3):791–810, 2021. doi: <https://doi.org/10.1002/eqe.3372>. URL <https://onlinelibrary.wiley.com/doi/abs/10.1002/eqe.3372>.
- F. Shipman, V. Gregson, and A. Jones. A shock wave study of coconino sandstone. Technical Report NASA CR-1842, NASA, May 1971.
- T. Sigaki, K. Kiyohara, Y. Sono, D. Kinoshita, T. Masao, R. Tamura, C. Yoshimura, and T. Ugata. Estimation of earthquake motion incident angle at rock site. In *Proceedings of 12th world conference on earthquake engineering*, pages 1–8, 2000.

- J.-F. Sigrist, D. Broc, and C. Lainé. Dynamic analysis of a nuclear reactor with fluid–structure interaction: Part i: Seismic loading, fluid added mass and added stiffness effects. *Nuclear engineering and design*, 236(23):2431–2443, 2006.
- W. Silva. Body waves in a layered anelastic solid. *Bulletin of the Seismological Society of America*, 66(5):1539–1554, 1976.
- J. Simo and J. Ju. Strain- and stress-based continuum damage models: Formulation. *International Journal of Solids and Structures*, 23(7):821 – 840, 1987. ISSN 0020-7683. doi: [https://doi.org/10.1016/0020-7683\(87\)90083-7](https://doi.org/10.1016/0020-7683(87)90083-7). URL <http://www.sciencedirect.com/science/article/pii/0020768387900837>.
- J. C. Simo. A framework for finite strain elastoplasticity based on maximum plastic dissipation and the multiplicative decomposition: Part i. continuum formulation. *Computer Methods in Applied Mechanics and Engineering*, 66:199–219, 1988. TA345. C6425.
- J. C. Simo. Algorithms for static and dynamic multiplicative plasticity that preserve the classical return mapping schemes of the infinitesimal theory. *Computer Methods in Applied Mechanics and Engineering*, 99:61–112, 1992.
- J. C. Simo and R. L. Taylor. Quasi-incompressible finite elasticity in principal stretches. continuum basis and numerical algorithms. *Computer Methods in Applied Mechanics and Engineering*, 85:273–310, 1991.
- J. C. Simo and S. Govindjee. Exact closed - form solution of the return mapping algorith in plane stress elasto - viscoplasticity. *Engineering Computations*, 5:254–258, 1988.
- J. C. Simo and T. J. R. Hughes, editors. *Computational Inelasticity*. Springer-verlag, New York, 1998.
- J. C. Simo and C. Miehe. Associative coupled thermoplasticity at finite strains: Formulation, numerical analysis and implementation. *Computer Methods in Applied Mechanics and Engineering*, 98:41–104, 1992.
- J. C. Simo and K. S. Pister. Remarks on rate constitutive equations for finite deformations problems: Computational implications. *Computer Methods in Applied Mechanics and Engineering*, 46:201–215, 1984.
- J. C. Simo and R. L. Taylor. Consistent tangent operators for rate-independent elastoplasticity. *Computer Methods in Applied Mechanics and Engineering*, 48:101–118, 1985.

- J. C. Simo and R. L. Taylor. A returning mapping algorithm for plane stress elastoplasticity. *International Journal for Numerical Methods in Engineering*, 22:649–670, 1986.
- S. K. Sinha and B. Jeremić. Modeling of dry and saturated soil-foundation contact. Technical Report UCD-CompGeoMech-01–2017, University of California, Davis, August 2017.
- S. K. Sinha, Y. Feng, H. Yang, H. Wang, N. Orbović, D. B. McCallen, and B. Jeremić. 3-D non-linear modeling and its effects in earthquake soil-structure interaction. In *Proceedings of the 24th International Conference on Structural Mechanics in Reactor Technology (SMiRT 24)*, Busan, South Korea, August 20-25 2017.
- B. Sjögren and N. A. Petersson. A Fourth Order Accurate Finite Difference Scheme for the Elastic Wave Equation in Second Order Formulation. *J. Sci. Comput.*, 52(1):17–48, 2011. ISSN 0885-7474. doi: 10.1007/s10915-011-9531-1. URL [http://link.springer.com/10.1007/s10915-011-9531-1\\$\\backslash\\$https://computation-rnd.llnl.gov/serpentine/pubs/wpp4th2011.pdf\\$\\backslash\\$https://computation-rnd.llnl.gov/serpentine/publications.html](http://link.springer.com/10.1007/s10915-011-9531-1$\\backslash$https://computation-rnd.llnl.gov/serpentine/pubs/wpp4th2011.pdf$\\backslash$https://computation-rnd.llnl.gov/serpentine/publications.html).
- A. Skempton. The pore-pressure coefficients a and b . *Geotechnique*, 4:143–147, 1954.
- C. Smerzini, M. Vanini, R. Paolucci, and P. Traversa. Regional physics-based simulation of ground motion within the Rhône Valley, France, during the Mw 4.9 2019 Le Teil earthquake. *Bulletin of Earthquake Engineering*, 21:1747–1774, 2023. doi: 10.1007/s10518-022-01591-w.
- I. Sobol. Global sensitivity indices for nonlinear mathematical models and their Monte Carlo estimates. *Mathematics and Computers in Simulation*, 55(1):271 – 280, 2001. ISSN 0378-4754. doi: [https://doi.org/10.1016/S0378-4754\(00\)00270-6](https://doi.org/10.1016/S0378-4754(00)00270-6). URL <http://www.sciencedirect.com/science/article/pii/S0378475400002706>. The Second IMACS Seminar on Monte Carlo Methods.
- C. Soize. *The Fokker-Planck Equation for stochastic dynamical systems and its explicit steady state solutions*. World Scientific, Singapore, 1994.
- T. Soong and B. Spencer. Supplemental energy dissipation: state-of-the-art and state-of-the-practice. *Engineering Structures*, 24(3):243–259, 2002.
- M. Souli and J. Zolesio. Arbitrary lagrangian-eulerian and free surface methods in fluid mechanics. *Computer Methods in Applied Mechanics and Engineering*, 191(3):451–466, 2001.
- E. Spacone, F. C. Filippou, and F. F. Taucer. Fibre beam-column model for non-linear analysis of r/c frames: Part i. formulation. *Earthquake Engineering & Structural Dynamics*, 25(7):711–725, July 1996a.

- E. Spacone, F. C. Filippou, and F. F. Taucer. Fibre beam-column model for non-linear analysis of r/c frames: Part ii. applications. *Earthquake Engineering & Structural Dynamics*, 25(7):727–742, July 1996b.
- A. Spencer. *Continuum Mechanics*. Longman Mathematical Texts. Longman Group Limited, 1980.
- C. Spyros, P. Patel, and F. Kokkinos. Assessment of computational practices in dynamic soil-structure interaction. *Journal of computing in civil engineering*, 3(2):143–157, 1989.
- A. Stavrogin, B. Tarasov, and e. C. Fairhurst. *Experimental physics and rock mechanics*. A.A. Balkema, Lisse ; Exton PA, 2001. ISBN 9058092135.
- A. N. Stavrogin and E. D. Pevzner. Critical states for rocks at changing deformation rates. *Journal of Mining Science*, 19(5):359–366, 1983.
- A. N. Stavrogin and A. G. Protosenya. Rock plasticity in conditions of variable deformation rates. *Journal of Mining Science*, 19(4):245–255, 1983.
- T. Sterling, D. J. Becker, D. Savarese, J. E. Dorband, U. A. Ranawake, and C. V. Parker. BEOWULF: A parallel workstation for scientific computations. In *Proceedings of the International Conference on Parallel on Parallel Processing*, 1995. <http://cesdis.gsfc.nasa.gov/beowulf/papers.html>
- T. Sterling, T. Cwik, D. Becker, J. Salmon, M. Warren, and B. Nitzberg. An assessment of Beowulf-class computing for NASA requirements: Initial findings from the first NASA workshop on beowulf-class clustered computing. In *Proceedings, IEEE Aerospace*, 1998. <http://www.beowulf.org/papers/index.html>.
- T. L. Sterling, J. Salmon, D. J. Becker, and D. F. Savarese. *How to Build a Beowulf: A Guide to the Implementation and Application of PC Clusters*. Scientific and Engineering Computations Series. The MIT Press, 1999. ISBN 0-262-69218-X ; QA 76.58.S854 1998.
- J. B. Stevens and J. M. E. Audibert. Re-examination of p-y curve formulations. In *Eleventh Annual Offshore Technology Conference*, volume I, pages 397–403, Dallas, TX, April 1979. Americal Society of Civil Engineers.
- S.Timoshenko and D.H.Young. *Engineering Mechanics*. McGraw-Hill Book Company, London, 1940.
- K. H. Stokoe II, R. B. Darendeli, R. B. Gilbert, F.-Y. Menq, and W. K. Choi. Development of a new family of normalized modulus reduction and material damping curves. In *International Workshop on Uncertainties in Nonlinear Soil Properties and their Impact on Modeling Dynamic Soil Response*, PEER Headquarters, UC Berkeley, March 18-19, 2004, Plenary Paper, http://peer.berkeley.edu/lifelines/Workshop304/pdf/Stokoe_PlenaryPaper.pdf, 2004. PEER.

- O. O. Storaasli and P. Bergan. Nonlinear substructuring method for concurrent processing computers. *AIAA Journal*, 25(6):871–876, 1987.
- S. Stošić. Private communications, 1984-2022.
- B. Stroustrup. *The C++ Programming Language*. Series in Computer Sciences. Addison – Wesley, reprint 1987 edition, 1986.
- B. Stroustrup. *The Design and Evolution of C++*. Addison-Wesley Publishing Company, 1994.
- B. Stroustrup. A rationale for semantically enhanced library languages. In D. Musser, editor, *Library-Centric Software Design LCSD'05*. Object-Oriented Programming, Systems, Languages and Applications, October 2005.
- S. Sture. Engineering properties of soils. Lecture Notes at CU Boulder, January - May 1993.
- H. H. Stutz. *Hypoplastic Models for Soil-Structure Interfaces-Modelling and Implementation*. PhD thesis, Christian-Albrechts Universität Kiel, 2016.
- B. Sudret. Global sensitivity analysis using polynomial chaos expansions. *Reliability engineering & system safety*, 93(7):964–979, 2008.
- B. Sudret and A. Der Kiureghian. Stochastic finite element methods and reliability: A state of the art report. Technical Report UCB/SEMM-2000/08, University of California, Berkeley, 2000.
- M. Symans and M. Constantinou. Passive fluid viscous damping systems for seismic energy dissipation. *ISET Journal of Earthquake Technology*, 35(4):185–206, 1998.
- M. Symans, F. Charney, A. Whittaker, M. Constantinou, C. Kircher, M. Johnson, and R. McNamara. Energy dissipation systems for seismic applications: current practice and recent developments. *Journal of structural engineering*, 134(1):3–21, 2008.
- B. Szabó and R. Actis. Simulation governance: Technical requirements for mechanical design. *Computer Methods in Applied Mechanics and Engineering*, 249-252:158–168, 2012. doi: 10.1016/j.cma.2012.02.008.
- B. A. Szabó and R. L. Actis. Simulation governance: New technical requirements for software tools in computational solid mechanics. Presentation at the: International Workshop on Verification and Validation in Computational Science University of Notre Dame, 17-19 October 2011.
- M. Tabatabaei, N. Abrahamson, and J. Singh. Effect of seismic wave inclination on structural response. In *Dynamic Response of Structures*, pages 613–620. ASCE, 1986.

- N. Tafazzoli. Methods, Computational Platform, Verification, and Application of Earthquake-Soil-Structure-Interaction Modeling and Simulation. PhD thesis, University of California at Davis, 2012.
- M. Taiebat and Y. F. Dafalias. SANISAND: Simple anisotropic sand plasticity model. International Journal for Numerical and Analytical Methods in Geomechanics, 2008. (in print, available in earlyview).
- F. Taucer, E. Spacone, and F. C. Filippou. A fiber beam-column element for seismic response analysis of reinforced concrete structures. Technical Report Report No. UCB/EERC-91/17, Earthquake Engineering Research Center, College of Engineering, University of California, Berkeley, December 1991.
- G. I. Taylor and H. Quinney. The latent energy remaining in a metal after cold working. Proceedings of the Royal Society of London. Series A, Containing Papers of a Mathematical and Physical Character, 143(849):307–326, 1934.
- R. Taylor, J. Simo, O. Zienkiewicz, and A. Chen. The patch test – a condition for assessing FEM convergence. International Journal for Numerical Methods in Engineering, 22:39–62, 1986.
- R. Teisseire, T. Minoru, and E. Majewski. Earthquake source asymmetry, structural media and rotation effects. Springer, 2006.
- J. Tejchman and W. Wu. Experimental and numerical study of sand–steel interfaces. International journal for numerical and analytical methods in geomechanics, 19(8):513–536, 1995.
- R. Temam. Mathematical Problems in Plasticity. Gauthier–Villars, 1985.
- W. T. Thomson. Transmission of elastic waves through a stratified solid medium. Journal of Applied Physics, 21(2):89–93, 1950.
- S. S. Timoshenko. History of Strength of Materials. McGraw–Hill, Book Company, Inc., 1953.
- T. C. T. Ting. Determination of $C^{1/2}$, $C^{-1/2}$ and more general isotropic tensor functions of C . Journal of Elasticity, 15:319–323, 1985.
- K. Tokida, H. Matsumoto, and H. Iwasaki. Experimental study of drag action of piles in ground flowing by liquefaction. In Proceedings of Fourth Japan–U.S. Workshop on Earthquake Resistant Design of Lifeline Facilities and Countermeasures for Soil Liquefaction, volume 1 of NCEER92-0019, SUNY Buffalo, N. Y., 1992.

- K. Tokimatsu and Y. Asaka. Effects of liquefaction-induced ground displacements on pile performance in the 1995 hyogoken-nambu earthquake. *Special Issue of Soils and Foundations, Japanese Geotechnical Society*, pages 163–177, 1998.
- H. Toopchi-Nezhad, M. J. Tait, and R. G. Drysdale. Lateral response evaluation of fiber-reinforced neoprene seismic isolators utilized in an unbonded application. *ASCE Journal of Structural Engineering*, 134(10):1627–1637, October 2008.
- M. Trifunac. A note on rotational components of earthquake motions on ground surface for incident body waves. *International Journal of Soil Dynamics and Earthquake Engineering*, 1(1):11–19, 1982.
- A. M. Trochanis, J. Bielak, and P. Christiano. Three-dimensional nonlinear study of piles. *Journal of Geotechnical Engineering*, 117(3):429–447, March 1991.
- W. Tseng, K. Lilhanand, F. Ostdan, and S. Tuann. Post-earthquake analysis and data correlation for the 1/4-scale containment model of the Lotung experiment. Technical Report NP-7305-SL, EPRI, Electric Power Research Institute, 3412 Hillview Avenue, Palo Alto, California, 94304, 1991.
- A. Tyapin. The frequency-dependent elements in the code SASSI: A bridge between civil engineers and the soil–structure interaction specialists. *Nuclear Engineering and Design*, 237:1300–1306, 2007.
- C.-M. Uang and V. V. Bertero. Evaluation of seismic energy in structures. *Earthquake Engineering & Structural Dynamics*, 19(1):77–90, 1990.
- M. Uesugi and H. Kishida. Influential factors of friction between steel and dry sands. *Soils and foundations*, 26(2):33–46, 1986a.
- M. Uesugi and H. Kishida. Frictional resistance at yield between dry sand and mild steel. *Soils and foundations*, 26(4):139–149, 1986b.
- M. Uesugi, H. Kishida, and Y. Tsubakihara. Friction between sand and steel under repeated loading. *Soils and foundations*, 29(3):127–137, 1989.
- M. Uesugi, H. Kishida, and Y. Uchikawa. Friction between dry sand and concrete under monotonic and repeated loading. *Soils and Foundations*, 30(1):115–128, 1990.
- S. Utku, R. Melosh, M. Islam, and M. Salama. On nonlinear finite element analysis in single– multi– and parallel processors. *Computers & Structures*, 15(1):39–47, 1982.
- R. Uzuoka, M. Čubrinovski, H. Sugita, M. Sato, K. Tokimatsu, N. Sento, M. Kazama, F. Zhang, A. Yashima, and F. Oka. Prediction of pile response to lateral spreading by 3-d soil–coupled dynamic

- analysis: Shaking in the direction perpendicular to ground flow. *Soil Dynamics and Earthquake Engineering*, 28(6):436–452, June 2008.
- N. G. Van Kampen. Stochastic differential equations. *Phys. Rep.*, 24:171–228, 1976.
- R. Van Loon, P. Anderson, F. Van de Vosse, and S. Sherwin. Comparison of various fluid–structure interaction methods for deformable bodies. *Computers & structures*, 85(11):833–843, 2007.
- E. Vanmarcke. *Random Fields: Analysis and Synthesis*. The MIT Press, Cambridge, Massachusetts, 1983.
- E. H. Vanmarcke. Probabilistic modeling of soil profiles. *Journal of Geotechnical Engineering Division*, 103(11):1227–1246, 1977.
- I. Vardoulakis. Shear-banding and liquefaction in granular materials on the basis of a Cosserat continuum theory. *Ingenieur Archiv*, 59:106–113, 1989.
- I. Vardoulakis and J. Sulem. *Bifurcation Analysis in Geomechanics*. Blackie Academic & Professional, 1995. ISBN 0-7514-0214-1.
- R. S. Varga, E. B. Saff, and V. Mehrmann. Incomplete factorizations of matrices and connections with H -matrices. *SIAM Journal on Numerical Analysis*, 17:787–793, 1980.
- Various Authors. The C++ report: Columns on C++, 1991-.
- A. V. Vasilev, E. E. Lovetskii, and V. I. Selyakov. Injection effect in a contained explosion in a liquid-saturated medium. *translated from Zhurnal Prikladnoi Mekhaniki i Tekhnicheskoi Fiziki*, 4:107–112, July – August 1980. URL <http://www.springerlink.com/index/N24126788T374535.pdf>.
- M. F. Vassiliou, A. Tsavos, and B. Stojadinović. Dynamics of inelastic base-isolated structures subjected to analytical pulse ground motions. *EARTHQUAKE ENGINEERING & STRUCTURAL DYNAMICS*, 42:2043–2060, 2013.
- T. Veldhuizen. Using C++ template metaprograms. *C++ Report*, 7(4):36–43, May 1995a.
- T. Veldhuizen. Expression templates. *C++ Report*, 7(5):26–31, June 1995b.
- T. Veldhuizen. Rapid linear algebra in C++. *Dr. Dobb's Journal*, August 1996.
- T. Veldhuizen. Software libraries and their reuse: Entropy, kolmogorov complexity, and zipf's law. In D. Musser, editor, *Library-Centric Software Design LCSD'05. Object-Oriented Programming, Systems, Languages and Applications*, October 2005.

- T. L. Veldhuizen and M. E. Jernigan. Will C++ be faster than FORTRAN. In J. Hull, editor, Proceedings of the first Internationa conference Scientific Computing in Object-Oriented Parallel Environments (ISCOPE) Conference. Springer Verlag, 1997.
- C. M. Venier, C. I. Pairetti, S. M. Damian, and N. M. Nigro. On the stability analysis of the piso algorithm on collocated grids. Computers & Fluids, 147:25–40, 2017.
- R. Verdugo and K. Ishihara. The steady state of sandy soils. Soils and foundations, 36(2):81–91, 1996.
- A. Verruijt. Soil Mechanics. Verruijt Self Published, 2012. URL <http://geo.verruijt.net/>.
- E. Veveakis, I. Vardoulakis, and G. Di Toro. Thermoporomechanics of creeping landslides: The 1963 vajont slide, northern Italy. Journal of Geophysical Research: Earth Surface, 112(F3), 2007.
- E. Veveakis, J. Sulem, and I. Stefanou. Modeling of fault gouges with Cosserat continuum mechanics: Influence of thermal pressurization and chemical decomposition as coseismic weakening mechanisms. Journal of Structural Geology, 38:254–264, 2012.
- E. Viallet, J. Berger, P. Traversa, E. E. Haber, E. Hervé-Secourgeon, G. Hervé-Secourgeon, L. Zuchowski, and G. Dupuy. 2019-11-11 Le Teil earthquake - the ultimate missing piece of experience feedback related to a nuclear power plant built on seismic base isolation: A real earthquake. In Transactions, SMiRT-26. SMiRT, July 2022.
- M. Vucetic and R. Dobry. Degradation of marine clays under cyclic loading. Journal of Geotechnical Engineering, 114(2):133–149, February 1988.
- M. Vucetic and R. Dobry. Effect of soil plasticity on cyclic response. Journal of Geotechnical Engineering, 117(1):89–107, January 1991.
- B. R. Wair, J. T. de Jong, and T. Shantz. Guidelines for estimation of shear wave velocity profiles. Technical Report 8, PEER, 2012. 95 pages.
- A. Wakai, S. Gose, and K. Ugai. 3-d elasto-plastic finite element analysis of pile foundations subjected to lateral loading. Soil and Foundations, 39(1):97–111, Feb. 1999.
- D. Wald, T. Heaton, and K. Hudnut. The slip history of the 1994 northridge, california, earthquake determined from strong-motion, teleseismic, gps, and leveling data. Bulletin of the Seismological Society of America, 86(1B):S49–S70, 1996.

- M. A. Walling. Non-Ergodic Probabilistic Seismic Hazard Analysis and Spatial Simulation of Variation in Ground Motion. PhD thesis, University of California at Berkeley, Spring 2009. Under guidance of Professor Norman Abrahamson.
- C. Walshaw and M. Cross. Parallel optimisation algorithms for multilevel mesh partitioning. Technical Report 99/IM/44, University of Greenwich, London, UK, 1999.
- C. Wang and R. Herrmann. A numerical study of p-, sv-, and sh-wave generation in a plane layered medium. Bulletin of the Seismological Society of America, 70(4):1015–1036, 1980.
- H. Wang, H. Yang, S. K. Sinha, Y. Feng, C. Luo, D. B. McCallen, and B. Jeremić. 3-D non-linear earthquake soil-structure interaction modeling of embedded small modular reactor (SMR). In Proceedings of the 24th International Conference on Structural Mechanics in Reactor Technology (SMiRT 24), Busan, South Korea, August 20-25 2017.
- H. Wang, H. Yang, Y. Feng, F. Wang, and B. Jeremić. Wave potential-domain reduction method for 3D earthquake soil structure interaction. Soil Dynamics and Earthquake Engineering, 2020a. In review.
- H. Wang, H. Yang, Y. Feng, and B. Jeremić. Modeling and simulation of earthquake soil structure interaction excited by inclined seismic waves. Soil Dynamics and Earthquake Engineering, 146:106720, 2021. ISSN 0267-7261. doi: <https://doi.org/10.1016/j.soildyn.2021.106720>. URL <https://www.sciencedirect.com/science/article/pii/S0267726121001421>.
- M. Wang, S. Nagarajaiah, and F.-F. Sun. Dynamic characteristics and responses of damped outrigger tall buildings using negative stiffness. Journal of Structural Engineering, 146(12):04020273, 2020b. doi: 10.1061/(ASCE)ST.1943-541X.0002846. URL <https://ascelibrary.org/doi/abs/10.1061/%28ASCE%29ST.1943-541X.0002846>.
- Y. Wang, Z. Y. Bu, and L. Hu. Seismic behavior of precast segmental bridge columns with carbon fibre reinforcement as energy dissipation bars. In Applied Mechanics and Materials, volume 157, pages 1148–1152. Trans Tech Publ, 2012.
- M. P. Ward. Language oriented programming. Computer Science Department, Science Labs, South Rd, Durham, DH1 3LE, <http://www.cse.dmu.ac.uk/~mward/martin/papers/middle-out-t.pdf>, January 17 2003.
- M. S. Warren, T. C. Germann, P. S. Lomdahl, D. M. Beazley, and J. K. Salmon. Avalon: an Alpha/Linux cluster achieves 10 Gflops for \$ 150K. Gordon Bell Price/Performance Prize Entry, 1998.
- C. Warshaw. Parallel JOSTLE User Guide. University of Greenwich, London, 1998.

- K. Watanabe, F. Pisanò, and B. Jeremić. Discretization effects in the finite element simulation of seismic waves in elastic and elastic-plastic media. *Engineering with Computers*, 33(3):519–545, Jul 2017. ISSN 1435-5663. doi: 10.1007/s00366-016-0488-4. URL <http://dx.doi.org/10.1007/s00366-016-0488-4>.
- J. D. Waugh. *Nonlinear analysis of T-shaped concrete walls subjected to multi-directional displacements*. Iowa State University, 2009.
- S. Wehmeyer, F. W. Zok, C. Eberl, P. Gumbsch, N. Cohen, R. M. McMeeking, and M. R. Begley. Post-buckling and dynamic response of angled struts in elastic lattices. *Journal of the Mechanics and Physics of Solids*, 133:103693, 2019. ISSN 0022-5096. doi: <https://doi.org/10.1016/j.jmps.2019.103693>. URL <https://www.sciencedirect.com/science/article/pii/S0022509619303758>.
- X. Wei, Z. Zhao, and J. Gu. Numerical simulations of rock mass damage induced by underground explosion. *International Journal of Rock Mechanics and Mining Sciences*, 46(7):1206–1213, October 2009.
- G. A. Wempner. Discrete approximations related to nonlinear theories of solids. *International Journal for Solids and Structures*, 7:1581–1599, 1971.
- M. Wenzel, O. S. Bursi, and I. Antoniadis. Optimal finite locally resonant metafoundations enhanced with nonlinear negative stiffness elements for seismic protection of large storage tanks. *Journal of Sound and Vibration*, 483:115488, 2020. ISSN 0022-460X. doi: <https://doi.org/10.1016/j.jsv.2020.115488>. URL <https://www.sciencedirect.com/science/article/pii/S0022460X20303205>.
- R. V. Whitman. On liquefaction. In *Proceedings of the 11th Int. Conf. on Soil Mechanics and Foundation Engineering*, pages 1923–1926, San Francisco, 1985. Balkema, Rotterdam, The Netherlands.
- E. Wiechert and K. Zoeppritz. *Über Erdbebenwellen*, volume 1. Nachrichten der K. Gesellschaft der Wissenschaften zu Göttingen, 1907.
- N. Wiener. The homogeneous chaos. *American Journal of Mathematics*, 60:897–936, 1938.
- M. L. Wilkins. *Computer Simulation of Dynamic Phenomena*. Scientific Computation. Springer, 1999. ISBN ISBN-10: 3540630708 ; ISBN-13: 978-3540630708.
- K. Willam. Plasticity and elastic degradation. Lecture Notes at CU Boulder, august - decembar 1993.
- K. J. Willam and E. P. Warnke. Constitutive model for the triaxial behaviour of concrete. In *Proceedings IABSE Seminar on Concrete Bergamo*. ISMES, 1974.

- W. Wittke. Rock mechanics based on an Anisotropic Jointed Rock Model AJRM. Ernst & Sohn, Berlin, 2014.
- J. P. Wolf. Dynamic Soil-Structure-Interaction. Prentice-Hall, Englewood Cliffs (NJ), 1985.
- J. P. Wolf. Soil-Structure-Interaction Analysis in Time Domain. Prentice-Hall, Englewood Cliffs (NJ), 1988.
- J. P. Wolf. Foundation Vibration Analysis Using Simple Physical Models. Prentice-Hall, Englewood Cliffs (NJ), 1994.
- J. P. Wolf and M. Preisig. Dynamic stiffness of foundation embedded in layered halfspace based on wave propagation in cones. Earthquake Engineering and Structural Dynamics, 32(7):1075–1098, JUN 2003.
- J. P. Wolf and C. M. Song. Some cornerstones of dynamic soil-structure interaction. Engineering Structures, 24(1):13–28, 2002.
- K. Wong. Seismic energy dissipation of inelastic structures with tuned mass dampers. Journal of engineering mechanics, 134(2):163–172, 2008.
- L. H. Wong and J. E. Luco. Tables of impedance functions and input motions for rectangular foundations. Technical report, Department of Civil Engineering, University of Southern California, Los Angeles, California, Report CE-78-15, 1978.
- L. H. Wong and J. E. Luco. Tables of impedance functions for square foundations on layered media. International Journal of Soil Dynamics and Earthquake Engineering, 4(2):64–81, 1985.
- D. Wood, K. Belkheir, and D. Liu. Strain softening and state parameter for sand modelling. Geotechnique, 44(3):335–339, 1994.
- D. M. Wood. Geotechnical Modeling. Spoon Press, 2004. ISBN 0-415-34304.
- P. Wriggers. Computational Contact Mechanics. John Wiley & Sons, 2002.
- T. Wu Tai. The effect of inclusion shape on the elastic moduli of a two - phase material. International Journal of Solids and Structures, 2:1–8, 1966.
- D. Xiu. Numerical Methods for Stochastic Computations. Princeton University Press, 2010.
- D. Xiu and G. E. Karniadakis. The wiener–askey polynomial chaos for stochastic differential equations. SIAM Journal on Scientific Computing, 24(2):619–644, 2002. doi: 10.1137/S1064827501387826.

- D. Xiu and G. E. Karniadakis. A new stochastic approach to transient heat conduction modeling with uncertainty. *International Journal of Heat and Mass Transfer*, 46:4681–4693, 2003.
- H. Yang, S. K. Sinha, Y. Feng, D. B. McCallen, and B. Jeremić. Energy dissipation analysis of elastic-plastic materials. *Computer Methods in Applied Mechanics and Engineering*, 331:309–326, 2018.
- H. Yang, Y. Feng, H. Wang, and B. Jeremić. Energy dissipation analysis for inelastic reinforced concrete and steel beam-columns. *Engineering Structures*, 197:109431, 2019a. ISSN 0141-0296. doi: <https://doi.org/10.1016/j.engstruct.2019.109431>. URL <http://www.sciencedirect.com/science/article/pii/S0141029618323459>.
- H. Yang, H. Wang, Y. Feng, F. Wang, and B. Jeremić. Energy dissipation in solids due to material inelasticity, viscous coupling, and algorithmic damping. *ASCE Journal of Engineering Mechanics*, 145(9), 2019b.
- H. Yang, H. Wang, B. Jeremić, and J. Salamon. Earthquake soil structure interaction analysis of a gravity dam. In G. MAZZA, editor, *Proceedings of the 15th International Benchmark Workshop on Numerical Analysis of Dams*. ICOLD, PoLiMi, September 2019c.
- Z. Yang. *Three Dimensional Nonlinear Finite Element Analysis of Soil–Foundation–Structure Interaction*. PhD thesis, University of California at Davis, Davis, California, September 2002.
- Z. Yang and B. Jeremić. Numerical analysis of pile behaviour under lateral loads in layered elastic-plastic soils. *International Journal for Numerical and Analytical Methods in Geomechanics*, 26(14):1385–1406, 2002.
- Z. Yang and B. Jeremić. Numerical study of the effective stiffness for pile groups. *International Journal for Numerical and Analytical Methods in Geomechanics*, 27(15):1255–1276, Dec 2003.
- Z. Yang and B. Jeremić. Soil layering effects on lateral pile behavior. *ASCE Journal of Geotechnical and Geoenvironmental Engineering*, 131(6):762–770, June 2005.
- Z. Yang, A. Elgamal, and E. Parra. Computational model for cyclic mobility and associated shear deformation. *Journal of Geotechnical and Geoenvironmental Engineering*, 129(12):1119–1127, 2003.
- M. H. M. Yassin. *Nonlinear analysis of prestressed concrete structures under monotonic and cyclic loads*. PhD thesis, University of California, Berkeley, 1994.
- K. Yokoyama, K. Tamura, and O. Matsuo. Design methods of bridge foundations against soil liquefaction and liquefaction induced ground flow. In *2nd Italy–Japan Workshop on Seismic Design and Retrofit of Bridges*, page 23 pages, Rome, Italy, 27–28 Feb. 1997.

- Y. Yoshimi and T. Kishida. A ring torsion apparatus for evaluating friction between soil and metal surfaces. *Geotechnical Testing Journal*, 4(4):145–152, 1981.
- C. Yoshimura, J. Bielak, and Y. Hisada. Domain reduction method for three-dimensional earthquake modeling in localized regions. part II: Verification and examples. *Bulletin of the Seismological Society of America*, 93(2):825–840, 2003a.
- C. Yoshimura, J. Bielak, and Y. Hisada. Domain reduction method for three dimensional earthquake modeling in localized regions. part ii: Verification and examples. *Bulletin of the Seismological Society of America*, 93(2):825–840, 2003b.
- T. L. Youd and S. F. Bartlett. Case histories of lateral spreads from the 1964 Alaskan earthquake. In *Proceedings of the Third Japan–U.S. Workshop on Earth Resistant Design of Lifeline Facilities and Countermeasures for Soils Liquefaction*, number 91-0001 in NCEER, Feb 1. 1989.
- O. Yuksei and C. Yilmaz. Design of s broadband elastic metamaterial via topologically optimized inertial amplification mechanisms. In M. Papadrakakis, M. Fragiadakis, and C. Papadimitriou, editors, *EURODYN 2020, XI International Conference on Structural Dynamics*, Athens, Greece, 23-26 November 2020 2020. <https://doi.org/10.47964/1120.9337.19454>.
- R. Zaccherini, A. Colombi, A. Palermo, V. K. Dertimanis, A. Marzani, H. R. Thomsen, B. Stojadinović, and E. N. Chatzi. Locally resonant metasurfaces for shear waves in granular media. *Phys. Rev. Applied*, 13:034055, Mar 2020. doi: 10.1103/PhysRevApplied.13.034055. URL <https://link.aps.org/doi/10.1103/PhysRevApplied.13.034055>.
- J. Zadeh. The role of fuzzy logic in the management of uncertainty in expert systems. *Fuzzy Sets and Systems*, 11:199–228, 1983.
- W. Zahlten, P. Demmert, and W. B. Kratzig. An Object-Oriented Approach to Physically Nonlinear Problems in Computational Mechanics. In *Computing in Civil and Building Engineering: Proceedings of the Sixth International Conference on Computing in Civil and Building Engineering*, Berlin, Germany, July 12-15 1995.
- G. W. Zeglinski, R. S. Han, and P. Aitchison. Object oriented matrix classes for use in a finite element code using C++. *International Journal for Numerical Methods in Engineering*, 37:3921–3937, 1994.
- A. Zerva. *Spatial variation of seismic ground motions: modeling and engineering applications*. CRC Press, 2009. ISBN ISBN-10: 0849399297; ISBN-13: 978-0849399299.

- A. Zerva and V. Zervas. Spatial variation of seismic ground motions: An overview. *ASME Applied Mechanics Revue*, 55(3):271–297, May 2002.
- L. Zhang and A. K. Chopra. Three-dimensional analysis of spatially varying ground motions around a uniform canyon in a homogeneous half-space. *Earthquake Engineering & Structural Dynamics*, 20 (10):911–926, 1991.
- L. Zhang, M. McVay, and P. Lai. Centrifuge testing of vertically loaded battered pile groups in sand. *Geotechnical Testing Journal*, 21(4):281–288, 1998. No paper yet.
- L. Zhang, M. McVay, and P. Lai. Numerical analysis of laterally loaded 3x3 to 7x3 pile groups in sands. *Journal of Geotechnical and Geoenvironmental Engineering*, 125(11):936–946, Nov. 1999.
- Y.-y. Zhang, K. A. Harries, and W.-c. Yuan. Experimental and numerical investigation of the seismic performance of hollow rectangular bridge piers constructed with and without steel fiber reinforced concrete. *Engineering Structures*, 48:255–265, 2013.
- J. Zhao, H. Li, M. Wu, and T. Li. Dynamic uniaxial compression tests on a granite. *International Journal of Rock Mechanics and Mining Sciences*, 36(2):273–277, February 1999.
- M. Zhou, G. Ravichandran, and A. Rosakis. Dynamically propagating shear bands in impact-loaded prenotched plates-ii. numerical simulations. *Journal of the Mechanics and Physics of Solids*, 44(6): 1007–1032, 1996.
- L. Zhu and L. A. Rivera. A note on the dynamic and static displacements from a point source in multilayered media. *Geophysical Journal International*, 148(3):619–627, 2002.
- Z. Zhu, I. Ahmad, and A. Mirmiran. Fiber element modeling for seismic performance of bridge columns made of concrete-filled frp tubes. *Engineering structures*, 28(14):2023–2035, 2006.
- H. Ziegler. Discussion of some objections to thermomechanical orthogonality. *Ingenieur-Archiv*, 50(3): 149–164, 1981.
- H. Ziegler and C. Wehrli. The derivation of constitutive relations from the free energy and the dissipation function. *Advances in Applied Mechanics*, 25:183–238, 1987.
- O. Zienkiewicz, A. Chan, M. Pastor, B. Schrefler, and T. Shiomi. *Computational Geomechanics—with Special Reference to Earthquake Engineering*. John Wiley and Sons Ltd., Baffins Lane, Chichester, West Sussex PO19 IUD, England, 1999a.

- O. C. Zienkiewicz. The Finite Element Method. McGraw - Hill Book Company, 3rd edition, 1977. ISBN 0-07-084072-5.
- O. C. Zienkiewicz and T. Shiomi. Dynamic behaviour of saturated porous media; the generalized Biot formulation and its numerical solution. International Journal for Numerical and Analytical Methods in Geomechanics, 8:71–96, 1984.
- O. C. Zienkiewicz and R. L. Taylor. The Finite Element Method, volume 1. McGraw - Hill Book Company, fourth edition, 1991a.
- O. C. Zienkiewicz and R. L. Taylor. The Finite Element Method, volume 2. McGraw - Hill Book Company, Fourth edition, 1991b.
- O. C. Zienkiewicz and R. L. Taylor. The Finite Element Method, Volume 1, The Basis, 5th Edition. Butterworth Heinemann, London, 2000.
- O. C. Zienkiewicz, A. H. C. Chan, M. Pastor, B. A. Schrefler, and T. Shiomi. Computational Geomechanics with Special Reference to Earthquake Engineering. John Wiley and Sons., 1999b. ISBN 0-471-98285-7.
- T. Zimmermann and D. Eyheramendy. Object-oriented finite elements I. principles of symbolic derivations and automatic programming. Computer Methods in Applied Mechanics and Engineering, 132:259–276, 1996.
- T. Zimmermann, Y. Dubois-Pèlerin, and P. Bomme. Object oriented finite element programming: I. governing principles. Computer Methods in Applied Mechanics and Engineering, 98:291–303, 1992a.
- T. Zimmermann, Y. Dubois-Pèlerin, and P. Bomme. Object Oriented Finite Element Programming: Theory and Smalltalk V Implementation for FEM_Objects PC 01. Elmepress International, P.O.Box 2 CH 1015 Lausanne 15, Switzerland, 1992b.

Part 700

Appendix

Appendix 701

Useful Formulae

(1985-1989-1993-2021-)

701.1 Chapter Summary and Highlights

701.2 Stress and Strain

This section reviews small deformation stress and strain measures used in this report.

701.2.1 Stress

In this work, the tensile stress is assumed positive, and in general we follow classical strength of materials (mechanics of materials) conventions for stress and strain. The stress tensor σ_{ij} is defined as

$$\sigma_{ij} = \lim_{A_i \rightarrow 0} \frac{F_j}{A_i} \quad (701.1)$$

where F_j is a traction (force) in the j direction and A_i is an infinitesimal surface area with normal in i direction. Cauchy stress tensor has a total of nine components, six of which are independent (symmetry $\sigma_{ij} = \sigma_{ji}$):

$$\boldsymbol{\sigma} = \begin{pmatrix} \sigma_{xx} & \sigma_{xy} & \sigma_{xz} \\ \sigma_{yx} & \sigma_{yy} & \sigma_{yz} \\ \sigma_{zx} & \sigma_{zy} & \sigma_{zz} \end{pmatrix} = \begin{pmatrix} \sigma_x & \sigma_{xy} & \sigma_{zx} \\ \sigma_{xy} & \sigma_y & \sigma_{yz} \\ \sigma_{zx} & \sigma_{yz} & \sigma_z \end{pmatrix} \quad (701.2)$$

In small deformation theory, this stress is symmetric, that is, $\sigma_{xy} = \sigma_{yx}$, $\sigma_{yz} = \sigma_{zy}$, and $\sigma_{zx} = \sigma_{xz}$. There are only six independent components and sometimes the stress can be expressed in the vector form

$$\boldsymbol{\sigma} = \{\sigma_{xx}, \sigma_{yy}, \sigma_{zz}, \sigma_{xy}, \sigma_{yz}, \sigma_{zx}\} \quad (701.3)$$

The principle stresses σ_1 , σ_2 , and σ_3 ($\sigma_1 \geq \sigma_2 \geq \sigma_3$) are the eigenvalues of the symmetric tensor σ_{ij} in Equation 701.2 and can be obtained by solving the equation

$$\begin{vmatrix} \sigma_{xx} - \sigma & \sigma_{xy} & \sigma_{xz} \\ \sigma_{yx} & \sigma_{yy} - \sigma & \sigma_{yz} \\ \sigma_{zx} & \sigma_{zy} & \sigma_{zz} - \sigma \end{vmatrix} = \mathbf{0} \quad (701.4)$$

or in alternative form

$$\sigma^3 - I_1\sigma^2 - I_2\sigma - I_3 = 0 \quad (701.5)$$

The three first-type stress invariants are then

$$\begin{aligned} I_1 &= \sigma_{ii} \\ &= \sigma_{xx} + \sigma_{yy} + \sigma_{zz} \\ &= \sigma_1 + \sigma_2 + \sigma_3 \end{aligned} \quad (701.6)$$

$$\begin{aligned}
I_2 &= \frac{1}{2}\sigma_{ij}\sigma_{ji} \\
&= -(\sigma_{xx}\sigma_{yy} + \sigma_{yy}\sigma_{zz} + \sigma_{zz}\sigma_{xx}) + (\sigma_{xy}^2 + \sigma_{yz}^2 + \sigma_{zx}^2) \\
&= -(\sigma_1\sigma_2 + \sigma_2\sigma_3 + \sigma_3\sigma_1)
\end{aligned} \tag{701.7}$$

$$\begin{aligned}
I_3 &= \frac{1}{3}\sigma_{ij}\sigma_{jk}\sigma_{ki} = \det(\sigma_{ij}) \\
&= \sigma_{xx}\sigma_{yy}\sigma_{zz} + 2\sigma_{xy}\sigma_{yz}\sigma_{zx} - (\sigma_{xx}\sigma_{yz}^2 + \sigma_{yz}\sigma_{zx}^2 + \sigma_{zz}\sigma_{xy}^2) \\
&= \sigma_1\sigma_2\sigma_3
\end{aligned} \tag{701.8}$$

The stress σ_{ij} can be decomposed into the hydrostatic stress $\sigma_m\delta_{ij}$ and deviatoric stress s_{ij} as $\sigma_{ij} = \sigma_m\delta_{ij} + s_{ij}$, with the definitions

$$\sigma_m = \frac{1}{3}I_1, \quad s_{ij} = \sigma_{ij} - \frac{1}{3}\sigma_{kk}\delta_{ij} \tag{701.9}$$

where δ_{ij} is the Kronecker operator such that $\delta_{ij} = 1$ for $i = j$ and $\delta_{ij} = 0$ for $i \neq j$.

Since both hydrostatic and deviatoric stresses are stress tensors, they have their own coordinate-independent stress invariants respectively. The three invariants of the hydrostatic stress are

$$I_1 = 3\sigma_m = I_1, \quad I_2 = -3\sigma_m^2 = -\frac{1}{3}I_1^2, \quad I_3 = \sigma_m^3 = \frac{1}{27}I_1^3 \tag{701.10}$$

Since I_1 , I_2 and I_3 are all simple functions of I_1 , the hydrostatic stress state can therefore be represented by only one variable I_1 .

The three eigenvalues of the deviatoric stresses s_{ij} are called principal deviatoric stresses, with the order $s_1 \geq s_2 \geq s_3$. The three invariants of the deviatoric stress are

$$J_1 = s_{ii} = 0 \tag{701.11}$$

$$\begin{aligned}
J_2 &= \frac{1}{2}s_{ij}s_{ji} \\
&= \frac{1}{3}I_1^2 + I_2 \\
&= \frac{1}{6}[(\sigma_1 - \sigma_2)^2 + (\sigma_2 - \sigma_3)^2 + (\sigma_3 - \sigma_1)^2] \\
&= -(s_{xx}s_{yy} + s_{yy}s_{zz} + s_{zz}s_{xx}) + (s_{xy}^2 + s_{yz}^2 + s_{zx}^2) \\
&= \frac{1}{2}(s_1^2 + s_2^2 + s_3^2) = -(s_1s_2 + s_2s_3 + s_3s_1)
\end{aligned} \tag{701.12}$$

$$\begin{aligned}
J_3 &= \frac{1}{3}s_{ij}s_{jk}s_{ki} = \det(s_{ij}) \\
&= I_3 + \frac{1}{3}I_1I_2 + \frac{2}{27}I_1^3 = I_3 - \frac{1}{3}I_1J_2 - \frac{1}{27}I_1^3 \\
&= \frac{1}{27}(2\sigma_1 - \sigma_2 - \sigma_3)(2\sigma_2 - \sigma_3 - \sigma_1)(2\sigma_3 - \sigma_1 - \sigma_2) \\
&= s_{xx}s_{yy}s_{zz} + 2s_{xy}s_{yz}s_{zx} - (s_{xx}s_{yz}^2 + s_{yy}s_{zx}^2 + s_{zz}s_{xy}^2) \\
&= s_1s_2s_3
\end{aligned} \tag{701.13}$$

The deviatoric stress state can therefore be represented by only two variables J_2 and J_3 .

Combining hydrostatic and deviatoric stress, we can conclude that the stress state can be represented by three variables I_1 , J_2 and J_3 . Using the three invariants (I_1, J_2, J_3) or its equivalents instead of the nine components of σ_{ij} is widely used in geomechanics.

The stress state may also be described in three dimensional space (p, q, θ_σ) , defined as

$$p = -\frac{1}{3}I_1 \quad (701.14)$$

$$q = \sqrt{3J_2} \quad (701.15)$$

$$\theta_\sigma = \frac{1}{3} \arccos \left(\frac{3\sqrt{3}}{2} \frac{J_3}{\sqrt{J_2^3}} \right) \quad (701.16)$$

where $\theta_{\sigma_{ij}}$ is the stress Lode's angle ($0 \leq \theta_{\sigma_{ij}} \leq \pi/3$). A stress state with $\theta_\sigma = 0$ corresponds to the meridian of conventional triaxial compression (CTC), while $\theta_\sigma = \pi/3$ to the meridian of conventional triaxial extension (CTE). The relationship between $(\sigma_1, \sigma_2, \sigma_3)$ and (p, q, θ_σ) is

$$\begin{pmatrix} \sigma_1 \\ \sigma_2 \\ \sigma_3 \end{pmatrix} = -p + \frac{2}{3}q \begin{pmatrix} \cos \theta_\sigma \\ \cos(\theta_\sigma - \frac{2}{3}\pi) \\ \cos(\theta_\sigma + \frac{2}{3}\pi) \end{pmatrix} \quad (701.17)$$

The line of the principal stress space diagonal is called hydrostatic axis. Any plane perpendicular to the hydrostatic axis is an deviatoric plane, or π plane. The Haigh-Westergaard three dimensional stress coordinate system $(\xi, \rho, \theta_\sigma)$ [Chen and Han \(1988a\)](#), is defined as

$$\xi = \frac{I_1}{\sqrt{3}} = -\sqrt{3}p \quad (701.18)$$

$$\rho = \sqrt{2J_2} = \sqrt{\frac{2}{3}}q \quad (701.19)$$

The Haigh-Westergaard invariants have physical meanings. ξ is the distance of the deviatoric plane to the origin of the Haigh-Westergaard coordinates, and ρ is the distance of a stress point to the hydrostatic line and represents the magnitude of the deviatoric stress. The projections of the axes σ_1 , σ_2 and σ_3 on the deviatoric plane are assumed σ'_1 , σ'_2 and σ'_3 respectively. (ρ, θ_σ) is the polar coordinate system in the deviatoric plane with the σ'_1 the polar axis and θ_σ the polar angle. The relationship between $(\sigma_1, \sigma_2, \sigma_3)$ and $(\xi, \rho, \theta_\sigma)$ is

$$\begin{pmatrix} \sigma_1 \\ \sigma_2 \\ \sigma_3 \end{pmatrix} = \frac{1}{\sqrt{3}}\xi + \sqrt{\frac{2}{3}}\rho \begin{pmatrix} \cos \theta_\sigma \\ \cos(\theta_\sigma - \frac{2}{3}\pi) \\ \cos(\theta_\sigma + \frac{2}{3}\pi) \end{pmatrix} \quad (701.20)$$

701.2.2 Strain

Point $P(x_i)$ and nearby point $Q(x_i + dx_i)$ displace due to applied loading to new positions $P(x_i + U_i)$ and $Q(u_i + (\partial u_i / \partial x_j) dx_j)$. We can define a displacement gradient tensor $u_{i,j}$ as

$$u_{i,j} = \frac{\partial u_i}{\partial x_j} \quad (701.21)$$

Matrix form of the displacement gradient can decomposed into the symmetric and antisymmetric parts

$$\begin{pmatrix} u_{1,1} & u_{1,2} & u_{1,3} \\ u_{2,1} & u_{2,2} & u_{2,3} \\ u_{3,1} & u_{3,2} & u_{3,3} \end{pmatrix} = \begin{pmatrix} u_{1,1} & \frac{1}{2}(u_{1,2} + u_{2,1}) & \frac{1}{2}(u_{1,3} + u_{3,1}) \\ \frac{1}{2}(u_{2,1} + u_{1,2}) & u_{2,2} & \frac{1}{2}(u_{2,3} + u_{3,2}) \\ \frac{1}{2}(u_{3,1} + u_{1,3}) & \frac{1}{2}(u_{3,2} + u_{2,3}) & u_{3,3} \end{pmatrix} + \begin{pmatrix} 0 & \frac{1}{2}(u_{1,2} - u_{2,1}) & \frac{1}{2}(u_{1,3} - u_{3,1}) \\ \frac{1}{2}(u_{2,1} - u_{1,2}) & 0 & \frac{1}{2}(u_{2,3} - u_{3,2}) \\ \frac{1}{2}(u_{3,1} - u_{1,3}) & \frac{1}{2}(u_{3,2} - u_{2,3}) & 0 \end{pmatrix} \quad (701.22)$$

or

$$u_{i,j} = \epsilon_{ij} + w_{ij} \quad (701.23)$$

where

$$\epsilon_{ij} = \frac{1}{2} (u_{i,j} + u_{j,i}) \quad (701.24)$$

$$w_{ij} = \frac{1}{2} (u_{i,j} - u_{j,i}) \quad (701.25)$$

The symmetric part of the deformation gradient tensor, ϵ_{ij} , is the small deformation strain tensor ¹, while the antisymmetric part of the deformation gradient tensor, w_{ij} , is the rotation motion tensor. The matrix form of the strain ϵ_{ij} is

$$\epsilon = \begin{pmatrix} \epsilon_{xx} & \epsilon_{xy} & \epsilon_{xz} \\ \epsilon_{yx} & \epsilon_{yy} & \epsilon_{yz} \\ \epsilon_{zx} & \epsilon_{zy} & \epsilon_{zz} \end{pmatrix} = \begin{pmatrix} \epsilon_x & \frac{1}{2}\gamma_{xy} & \frac{1}{2}\gamma_{xz} \\ \frac{1}{2}\gamma_{yx} & \epsilon_y & \frac{1}{2}\gamma_{yz} \\ \frac{1}{2}\gamma_{zx} & \frac{1}{2}\gamma_{zy} & \epsilon_z \end{pmatrix} \quad (701.26)$$

The engineering strain is usually expressed in the vector form

$$\boldsymbol{\epsilon} = \{\epsilon_x, \epsilon_y, \epsilon_z, \gamma_{xy}, \gamma_{yz}, \gamma_{zx}\}^T \quad (701.27)$$

Note that the engineering shear strain γ_{ij} is the double of the corresponding strain component ϵ_{ij} .

¹Here the second and higher order derivative terms are neglected due to the small deformation assumption.

Similar to the stress tensor, the strain tensor also has three principle strains $\epsilon_i (\epsilon_1 \geq \epsilon_2 \geq \epsilon_3)$, and three strain invariants I'_1 , I'_2 , and I'_3 , defined as

$$\begin{aligned} I'_1 &= \epsilon_{ii} \\ &= \epsilon_v \\ &= \epsilon_{xx} + \epsilon_{yy} + \epsilon_{zz} \\ &= \epsilon_1 + \epsilon_2 + \epsilon_3 \end{aligned} \tag{701.28}$$

$$\begin{aligned} I'_2 &= \frac{1}{2}\epsilon_{ij}\epsilon_{ji} \\ &= -(\epsilon_{xx}\epsilon_{yy} + \epsilon_{yy}\epsilon_{zz} + \epsilon_{zz}\epsilon_{xx}) + (\epsilon_{xy}^2 + \epsilon_{yz}^2 + \epsilon_{zx}^2) \\ &= -(\epsilon_1\epsilon_2 + \epsilon_2\epsilon_3 + \epsilon_3\epsilon_1) \end{aligned} \tag{701.29}$$

$$\begin{aligned} I'_3 &= \frac{1}{3}\epsilon_{ij}\epsilon_{jk}\epsilon_{ki} = \det(\epsilon_{ij}) \\ &= \epsilon_{xx}\epsilon_{yy}\epsilon_{zz} + 2\epsilon_{xy}\epsilon_{yz}\epsilon_{zx} - (\epsilon_{xx}\epsilon_{yz}^2 + \epsilon_{yz}\epsilon_{zx}^2 + \epsilon_{zx}\epsilon_{xy}^2) \\ &= \epsilon_1\epsilon_2\epsilon_3 \end{aligned} \tag{701.30}$$

The first strain invariant is also called the volumetric strain ϵ_v .

The strain ϵ_{ij} can be decomposed into the hydrostatic strain $\epsilon_m \delta_{ij}$ and deviatoric strain e_{ij} through $\epsilon_{ij} = \epsilon_m \delta_{ij} + e_{ij}$ where:

$$\epsilon_m = \frac{1}{3}I'_1, \quad e_{ij} = \epsilon_{ij} - \frac{1}{3}\epsilon_{kk}\delta_{ij} \tag{701.31}$$

Since both hydrostatic and deviatoric strains are strain tensors, they have their own strain invariants respectively. The three invariants of the hydrostatic strain are

$$I'_1 = 3\epsilon_m = I'_1, \quad I'_2 = -3\epsilon_m^2 = -\frac{1}{3}(I'_1)^2, \quad I'_3 = \epsilon_m^3 = \frac{1}{27}(I'_1)^3 \tag{701.32}$$

The hydrostatic strain state can therefore be represented by only one variable I'_1 .

The three eigenvalues of the deviatoric strains e_{ij} are called principal deviatoric strains, with the order $e_1 \geq e_2 \geq e_3$. The three invariants of the deviatoric strain are

$$J'_1 = e_{ii} = 0 \tag{701.33}$$

$$\begin{aligned} J'_2 &= \frac{1}{2}e_{ij}e_{ji} \\ &= \frac{1}{3}(I'_1)^2 + I'_2 \\ &= \frac{1}{6}[(\epsilon_1 - \epsilon_2)^2 + (\epsilon_2 - \epsilon_3)^2 + (\epsilon_3 - \epsilon_1)^2] \\ &= -(e_{xx}e_{yy} + e_{yy}e_{zz} + e_{zz}e_{xx}) + (e_{xy}^2 + e_{yz}^2 + e_{zx}^2) \\ &= \frac{1}{2}(e_1^2 + e_2^2 + e_3^2) = -(e_1e_2 + e_2e_3 + e_3e_1) \end{aligned} \tag{701.34}$$

$$\begin{aligned}
J'_3 &= \frac{1}{3}e_{ij}e_{jk}e_{ki} = \det(e_{ij}) \\
&= I'_3 + \frac{1}{3}I'_1I'_2 + \frac{2}{27}(I'_1)^3 = I_3 - \frac{1}{3}I'_1J'_2 - \frac{1}{27}(I'_1)^3 \\
&= \frac{1}{27}(2\epsilon_1 - \epsilon_2 - \epsilon_3)(2\epsilon_2 - \epsilon_3 - \epsilon_1)(2\epsilon_3 - \epsilon_1 - \epsilon_2) \\
&= e_{xx}e_{yy}e_{zz} + 2e_{xy}e_{yz}e_{zx} - (e_{xx}e_{yz}^2 + e_{yy}e_{zx}^2 + e_{zz}e_{xy}^2) \\
&= e_1e_2e_3
\end{aligned} \tag{701.35}$$

The deviatoric strain state can therefore be represented by only two variables J'_2 and J'_3 .

Combining the hydrostatic and deviatoric strain, we can conclude that the strain state can be represented by three variables I'_1 , J'_2 and J'_3 .

Strain state may also be represented with another three invariant $(\epsilon_p, \epsilon_q, \theta_\epsilon)$, defined as

$$\epsilon_p = -I'_1 = -\epsilon_v \tag{701.36}$$

$$\epsilon_q = 2\sqrt{\frac{J'_2}{3}} \tag{701.37}$$

$$\theta_\epsilon = \frac{1}{3}\arccos\left(\frac{3\sqrt{3}}{2}\frac{J'_3}{\sqrt{(J'_2)^3}}\right) \tag{701.38}$$

where θ_ϵ is the strain Lode's angle and $0 \leq \theta_\epsilon \leq \pi/3$. The relationship between $(\epsilon_1, \epsilon_2, \epsilon_3)$ and $(\epsilon_p, \epsilon_q, \theta_\epsilon)$ is

$$\begin{pmatrix} \epsilon_1 \\ \epsilon_2 \\ \epsilon_3 \end{pmatrix} = -\frac{1}{3}\epsilon_p + \sqrt{\frac{3}{2}}\epsilon_q \begin{pmatrix} \cos \theta_\epsilon \\ \cos(\theta_\epsilon - \frac{2}{3}\pi) \\ \cos(\theta_\epsilon + \frac{2}{3}\pi) \end{pmatrix} \tag{701.39}$$

701.3 Derivatives of Stress Invariants

In this part of the Appendix, we shall derive some useful formulae, that are rarely found² in texts treating elasto-plastic problems in mechanics of solid continua.

First derivative of I_1 with respect to stress tensor σ_{ij} :

$$\frac{\partial I_1}{\partial \sigma_{ij}} = \frac{\partial \sigma_{kk}}{\partial \sigma_{ij}} = \delta_{ij}$$

First derivative of J_{2D} with respect to stress tensor σ_{ij} :

²if found at all.

$$\begin{aligned}
\frac{\partial J_{2D}}{\partial \sigma_{ij}} &= \frac{\partial(\frac{1}{2}s_{mn}s_{nm})}{\partial \sigma_{ij}} = \frac{1}{2} \frac{\partial s_{mn}}{\partial \sigma_{ij}} s_{nm} + \frac{1}{2} \frac{\partial s_{nm}}{\partial \sigma_{ij}} s_{mn} = \\
&= \frac{\partial s_{nm}}{\partial \sigma_{ij}} s_{mn} = \frac{\partial(\sigma_{nm} - \frac{1}{3}\sigma_{kk}\delta_{nm})}{\partial \sigma_{ij}} s_{mn} = (\delta_{ni}\delta_{jm} - \frac{1}{3}\delta_{nm}\delta_{ki}\delta_{jk})s_{mn} = \\
&= (\delta_{ni}\delta_{jm} - \frac{1}{3}\delta_{nm}\delta_{ij})s_{mn} = \delta_{ni}\delta_{jm}s_{nm} - \frac{1}{3}\delta_{nm}\delta_{ij}s_{mn} = s_{ij}^{\dagger}
\end{aligned}$$

First derivative of J_{3D} with respect to stress tensor σ_{pq} :

$$\begin{aligned}
\frac{\partial J_{3D}}{\partial \sigma_{pq}} &= \frac{\partial(\frac{1}{3}s_{ij}s_{jk}s_{ki})}{\partial \sigma_{pq}} = \frac{1}{3} \frac{\partial s_{ij}}{\partial \sigma_{pq}} s_{jk}s_{ki} + \frac{1}{3} \frac{\partial s_{jk}}{\partial \sigma_{pq}} s_{ij}s_{ki} + \frac{1}{3} \frac{\partial s_{ki}}{\partial \sigma_{pq}} s_{ij}s_{jk} = \\
&= \frac{\partial s_{ij}}{\partial \sigma_{pq}} s_{jk}s_{ki} = \frac{\partial(\sigma_{ij} - \frac{1}{3}\sigma_{kk}\delta_{ij})}{\partial \sigma_{pq}} s_{jk}s_{ki} = (\delta_{ip}\delta_{qj} - \frac{1}{3}\delta_{ij}\delta_{kp}\delta_{qk})s_{jk}s_{ki} = \\
&= \delta_{ip}\delta_{qj}s_{jk}s_{ki} - \frac{1}{3}\delta_{ij}\delta_{kp}\delta_{qk}s_{jk}s_{ki} = s_{qk}s_{kp} - \frac{2}{3}\delta_{pq}J_{2D} = t_{pq}^{\ddagger}
\end{aligned}$$

First derivative of s_{pq} with respect to stress tensor σ_{mn} , or second derivative of J_{2D} with respect to stress tensors σ_{pq} and σ_{mn} :

$$\begin{aligned}
\frac{\partial s_{pq}}{\partial \sigma_{mn}} &= \frac{\partial \left(\sigma_{pq} - \frac{1}{3}\delta_{pq}\sigma_{kk} \right)}{\partial \sigma_{mn}} = \frac{\partial \left(\left(\delta_{mp}\delta_{nq} - \frac{1}{3}\delta_{pq}\delta_{mn} \right) \sigma_{mn} \right)}{\partial \sigma_{mn}} = \\
&= \left(\delta_{mp}\delta_{nq} - \frac{1}{3}\delta_{pq}\delta_{mn} \right) = p_{pqmn}
\end{aligned}$$

Second derivative of J_{3D} with respect to stress tensors σ_{pq} and σ_{mn} :

$$\begin{aligned}
\frac{\partial t_{pq}}{\partial \sigma_{mn}} &= \frac{\partial \left(s_{qk}s_{kp} - \frac{2}{3}\delta_{pq}J_{2D} \right)}{\partial \sigma_{mn}} = \frac{\partial (s_{qk}s_{kp})}{\partial \sigma_{mn}} - \frac{\partial \left(\frac{2}{3}\delta_{pq}J_{2D} \right)}{\partial \sigma_{mn}} = \\
&= \frac{\partial (s_{qk}s_{kp})}{\partial \sigma_{mn}} - \frac{2}{3}\delta_{pq}\frac{\partial J_{2D}}{\partial \sigma_{mn}} = \frac{\partial s_{qk}}{\partial \sigma_{mn}} s_{kp} + s_{qk} \frac{\partial s_{kp}}{\partial \sigma_{mn}} - \frac{2}{3}\delta_{pq}s_{mn} = \\
&= \left(\delta_{qm}\delta_{nk} - \frac{1}{3}\delta_{qk}\delta_{nm} \right) s_{kp} + s_{qk} \left(\delta_{km}\delta_{np} - \frac{1}{3}\delta_{kp}\delta_{nm} \right) - \frac{2}{3}\delta_{pq}s_{mn} = \\
&= \left(\delta_{qm}s_{np} - \frac{1}{3}s_{qp}\delta_{nm} \right) + \left(s_{qm}\delta_{np} - \frac{1}{3}s_{qp}\delta_{nm} \right) - \frac{2}{3}\delta_{pq}s_{mn} = \\
&= s_{np}\delta_{qm} + s_{qm}\delta_{np} - \frac{2}{3}s_{qp}\delta_{nm} - \frac{2}{3}\delta_{pq}s_{mn} = w_{pqmn}
\end{aligned}$$

Multiplying stiffness tensor E_{ijkl} with compliance tensor D_{klpq} :

[†]because $\delta_{nm}\delta_{ij}s_{mn} \equiv 0$

[‡]since $\frac{1}{3}\delta_{ij}\delta_{kp}\delta_{qk}s_{jk}s_{ki} = \frac{1}{3}\delta_{kp}\delta_{qk}s_{ik}s_{ki} = \frac{1}{3}\delta_{qp}s_{ik}s_{ki} = \frac{2}{3}\delta_{pq}J_{2D}$ see also Chen and Han (1988a) page 222

$$\begin{aligned}
& E_{ijkl} D_{klpq} = \\
& \frac{E}{2(1+\nu)} \frac{1+\nu}{2E} \left(\frac{2\nu}{1-2\nu} \delta_{ij} \delta_{kl} + \delta_{ik} \delta_{jl} + \delta_{il} \delta_{jk} \right) \left(\frac{-2\nu}{1+\nu} \delta_{kl} \delta_{pq} + \delta_{kp} \delta_{lq} + \delta_{kq} \delta_{lp} \right) = \\
& \quad \frac{1}{4} (\delta_{ik} \delta_{jl} \delta_{kp} \delta_{lq} + \delta_{il} \delta_{jk} \delta_{kp} \delta_{lq} + \delta_{ik} \delta_{jl} \delta_{kq} \delta_{lp} + \delta_{il} \delta_{jk} \delta_{kq} \delta_{lp}) + \\
& + \frac{\nu}{2(1-2\nu)} (\delta_{ij} \delta_{kl} \delta_{kp} \delta_{lq} + \delta_{ij} \delta_{kl} \delta_{kq} \delta_{lp}) - \frac{\nu}{2(1+\nu)} (\delta_{ik} \delta_{jl} \delta_{kl} \delta_{pq} + \delta_{il} \delta_{jk} \delta_{kl} \delta_{pq}) - \\
& \quad - \frac{\nu^2}{(1-2\nu)(1+\nu)} \delta_{ij} \delta_{kl} \delta_{kl} \delta_{pq} = \\
& \quad \frac{1}{2} (\delta_{ip} \delta_{jq} + \delta_{iq} \delta_{jp}) + \\
& + \frac{\nu}{2(1-2\nu)} (\delta_{ij} \delta_{kq} \delta_{kp} + \delta_{ij} \delta_{kp} \delta_{kq}) - \frac{\nu}{2(1+\nu)} (\delta_{il} \delta_{jl} \delta_{pq} + \delta_{il} \delta_{jl} \delta_{pq}) - \\
& \quad - \frac{3\nu^2}{(1-2\nu)(1+\nu)} \delta_{ij} \delta_{pq} = \\
& \quad \frac{1}{2} (\delta_{ip} \delta_{jq} + \delta_{iq} \delta_{jp}) + \\
& + \frac{\nu}{2(1-2\nu)} (\delta_{ij} \delta_{pq} + \delta_{ij} \delta_{pq}) - \frac{\nu}{2(1+\nu)} (\delta_{ij} \delta_{pq} + \delta_{ij} \delta_{pq}) - \\
& \quad - \frac{3\nu^2}{(1-2\nu)(1+\nu)} \delta_{ij} \delta_{pq} = \\
& \quad \frac{1}{2} (\delta_{ip} \delta_{jq} + \delta_{iq} \delta_{jp}) + \\
& + \frac{\nu}{(1-2\nu)} \delta_{ij} \delta_{pq} - \frac{\nu}{2(1+\nu)} \delta_{ij} \delta_{pq} - \\
& \quad - \frac{3\nu^2}{(1-2\nu)(1+\nu)} \delta_{ij} \delta_{pq} = \\
& \quad \frac{1}{2} (\delta_{ip} \delta_{jq} + \delta_{iq} \delta_{jp}) + \\
& + \frac{\nu(1+\nu) - \nu(1-2\nu) - 3\nu^2}{(1-2\nu)(1+\nu)} \delta_{ij} \delta_{pq} = \\
& \quad \frac{1}{2} (\delta_{ip} \delta_{jq} + \delta_{iq} \delta_{jp}) = I_{ijpq}^{\text{sym}}
\end{aligned}$$

Appendix 702

The nDarray Programming Tool

(1993-1995-1996-1999-)

702.1 Chapter Summary and Highlights

Material in this chapter is based on the following publications Jeremić (1993); Jeremić and Sture (1998).

This section describes a programming tool, nDarray, which is designed using an Object Oriented Paradigm (OOP) and implemented in the C++ programming language. Finite element equations, represented in terms of multidimensional tensors are easily manipulated and programmed. The usual matrix form of the finite element equations are traditionally coded in FORTRAN, which makes it difficult to build and maintain complex program systems. Multidimensional data systems and their implementation details are seldom transparent and thus not easily dealt with and usually avoided. On the other hand, OOP together with efficient programming in C++ allows building new concrete data types, namely tensors of any order, thus hiding the lower level implementation details. These concrete data types prove to be quite useful in implementing complicated tensorial formulae associated with the numerical solution of various elastic and elastoplastic problems in solid mechanics. They permit implementing complex nonlinear continuum mechanics theories in an orderly manner. Ease of use and the immediacy of the nDarray programming tool in constitutive driver programming and in building finite element classes will be shown.

702.2 Introduction

In implementing complex programming systems for finite element computations, the analyst is usually faced with the challenge of transforming complicated tensorial formulae to a matrix form. Considerable amount of time in solving problems by the finite element method is often devoted to the actual implementation process. If one decides to use FORTRAN, a number of finite element and numerical libraries are readily available. Although quick results can be produced in solving simpler problems, when implementing complex small deformation elastoplastic or large deformation elastic and elastoplastic algorithms, C++ provides clear benefits.

Some of the improvements C++ provides over C and FORTRAN are classes for encapsulating abstractions, the possibility of building user-defined concrete data types and operator overloading for expressing complex formulae in a natural way. In the following we shall show that the nDarray tool will allow analysts to be a step closer to the problem space and a step further away from the underlying machine.

As most analysts know, the intention (Stroustrup, 1994) behind C++ was not to replace C. Instead, C was extended with far more freedom given to the program designer and implementor. In C and FORTRAN, large applications become collections of programs and functions, order and the structure are left to the programmer. The C++ programming language embodies the OOP, which can be used to

simplify and organize complex programs. One can build a hierarchy of derived classes and nest classes inside other classes. A concern in C and FORTRAN programming languages is handling data type conflicts and data which are being operated on or passed. The C++ programming language extends the definition of type to include abstract data types. With abstract data types, data can be encapsulated with the methods that operate on it. The C++ programming language offers structure and mechanisms to handle larger, more complex programming systems. Object Oriented technology, with function and operator overloading, inheritance and other features, provides means of attacking a problem in a natural way. Once basic classes are implemented, one can concentrate on the physics of a problem. By building further abstract data types one can describe the physics of a problem rather than spend time on the lower level programming issues. One should keep in mind the adage, credited to the original designer and implementor of C++ programming language, Bjarne Stroustrup: "C makes it easy to shoot yourself in the foot, C++ makes it harder, but when you do, it blows away your whole leg".

Rather than attempting here to give a summary of Object Oriented technology we will suggest useful references for readers who wish to explore the subject in greater depth ([Booch, 1994](#)). The current language definition is given in the *Working Paper for Draft Proposed International Standard for Information Systems—Programming Language C++* ([ANS, 1995](#)). Detailed description of language evolution and main design decisions are given by [Stroustrup \(1994\)](#). Useful sets of techniques, explanations and directions for designing and implementing robust C++ code are given in books ([Coplien, 1992](#)) ([Eckel, 1989](#)) and journal articles ([Koenig, 1989 - 1993](#)) ([Various Authors, 1991-](#)).

Increased interest in using Object Oriented techniques for finite element programming has resulted in a number ([Donescu and Laursen, 1996](#)) ([Eyheramendy and Zimmermann, 1996](#)) ([Forde et al., 1990](#)) ([Miller, 1991](#)) ([Pidaparti and Hudli, 1993](#)) ([Scholz, 1992](#)) ([Zeglinski et al., 1994](#)) of experimental developments and implementations. Programming techniques used in some of the papers are influenced by the FORTRAN programming style. Examples provided in some of the above mentioned papers are readable by C++ experts only. It appears that none of the authors have used Object Oriented techniques for complex elastoplasticity computations.

702.3 nDarray Programming Tool

702.3.1 Introduction to the nDarray Programming Tool

The nDarray programming tool is a set of classes written in the C++ programming language. The main purpose of the package is to facilitate algebraic manipulations with matrices, vectors and tensors that are often found in computer codes for solving engineering problems. The package is designed and implemented using the Object Oriented philosophy. Great care has been given to the problem of

cross-platform and cross-compiler portability. Currently, the nDarray set of classes has been tested and running under the following C++ compilers:

- Sun CC on SunOS and Solaris platforms,
- IBM xlC on AIX RISC/6000 platforms,
- Borland C++ and Microsoft C++ on DOS/Windows platforms,
- CodeWarrior C++ on Power Macintosh platform,
- GNU g++ on SunOS, SOLARIS, LINUX, AIX, HPUX and AMIGA platforms.

702.3.2 Abstraction Levels

nDarray tool has the following simple class hierarchy:

```
nDarray_rep, nDarray
    matrix
        vector
        tensor
```

Indentation of class names implies the inheritance level. For example, class vector is derived from class matrix, which, in turn is derived from classes nDarray and nDarray_rep. The idea is to subdivide classes into levels of abstraction, and hide the implementation from end users. This means that the end user can use the nDarray tool on various levels.

- At the highest level of abstraction, one can use tensor, matrix and vector objects without knowing anything about the implementation and the inner workings. They are all designed and implemented as concrete data types. In spite of the very powerful code that can be built using Object Oriented technology, it would be unwise to expect proficiency in Object Oriented techniques and the C++ programming language from end users. It was our aim to provide power programming with multidimensional data types to users with basic knowledge of C.
- At a lower abstraction level, users can address the task of the actual implementation of operators and functions for vector, matrix and tensor classes. A number of improvements can be made, especially in optimizing some of the operators.
- The lowest level of abstraction is associated with nDarray and nDarray_rep classes. Arithmetic operators¹ are implemented at this level.

¹Like addition and subtraction.

Next, classes are described from the base and down the inheritance tree. Later we focus our attention on nDarray usage examples. Our goal is to provide a useful programming tool, rather than to teach OOP or to show C++ implementation. For readers interested in actual implementation details, source code, examples and makefiles are available at <http://sokocalo.engr.ucdavis.edu/~jeremic>.

702.3.2.1 nDarray_rep class

The nDarray_rep class is a data holder and represents an n dimensional array object. A simple memory manager, implemented with the *reference counting idiom* (Coplien, 1992) is used. The memory manager uses rather inefficient built-in C memory allocation functions. Performance can be improved if one designs and implements specially tailored allocation functions for fast heap manipulations. Another possible improvement is in using memory resources other than heap memory. Sophisticated memory management introduced by the reference counting is best explained by Coplien (1992). The nDarray_rep class is not intended for stand-alone use. It is closely associated with the nDarray class.

The data structure of nDarray_rep introduces a minimal amount of information about a multidimensional array object. The actual data are stored as a one-dimensional array of double numbers. Rank, total number of elements, and array of dimensions are all that is needed to represent an multidimensional object. The data structure is allocated dynamically from the heap, and memory is reclaimed by the system after the object has gone out of scope.

702.3.2.2 nDarray class

The nDarray class together with the nDarray_rep class represents the abstract base for derived multidimensional data types: matrices, vectors and tensors. Objects derived from the nDarray class are generated dynamically by constructor functions at the first appearance of an object and are destroyed at the end of the block in which the object is referenced. The reference counting idiom provides for the object's life continuation after the end of the block where it was defined. To extend an object's life, a standard C++ compiler would by default call constructor functions, thus making the entire process of returning large objects from functions quite inefficient. By using reference counting idiom, destructor and constructor functions manipulate reference counter which results in a simple copying of a pointer to nDarray_rep object. By using this technique, copying of large objects is made very efficient.

Objects can be created from an array of values, or from a single scalar value, as shown in Table 702.1. Some of the frequently used multidimensional arrays are predefined and can be constructed by sending the proper flag to the constructor function. For example by sending the "I" flag one creates Kronecker delta δ_{ij} and by sending "e" flag, one creates a rank 3 Levi-Civita permutation tensor e_{ijk} . Functions and operators common to multidimensional data types are defined in the nDarray

constructor function	description
nDarray(int rank_of_nD=1, double initval=0.0)	default
nDarray(int rank_of_nD, const int *pdim, double *val)	from array
nDarray(int rank_of_nD, const int *pdim, double initval)	from scalar value
nDarray(const char *flag, int rank_of_nD, const int *pdim)	unit nDarrays
nDarray(const nDarray & x)	copy-initializer
nDarray(int rank_of_nD, int rows, int cols, double *val)	special for matrix
nDarray(int rank_of_nD, int rows, int cols, double initval)	special for matrix

Table 702.1: nDarray constructor functions.

class, as described in Table 702.2. These common operators and functions are inherited by derived classes. Occasionally, some of the functions will be redefined, overloaded in derived classes. In tensor multiplications we need additional information about indices. For example $C_{il} = (A_{ijk} + B_{ijk}) * D_{jkl}$ coded $C=(A("ijk") + B("ijk")) * D("jkl")$, the temporary in brackets will receive ijk indices, to be used for multiplication with D_{jkl} . It is interesting to note (Koenig, 1989 - 1993) that operator $+=$ is defined as a member and $+$ is defined as an inline function in terms of $+=$ operator.

702.3.2.3 Matrix and Vector Classes

The matrix class is derived from the nDarray class through the public construct. It inherits common operators and functions from the base nDarray class, but it also adds its own set of functions and operators. Table (702.3) summarizes some of the more important additional functions and operators for the matrix class. The vector class defines vector objects and is derived and inherits most operators and data members from the matrix class. Some functions, like copy constructor, are overloaded in order to handle specifics of a vector object.

702.3.2.4 Tensor Class

The main goal of the tensor class development was to provide the implementing analyst with the ability to write the following equation directly into a computer program:

$$d\sigma_{mn} = -^{old}r_{ij}T_{ijmn}^{-1} - d\lambda E_{ijkl}^{n+1}m_{kl}T_{ijmn}^{-1}$$

as:

```
dsigma = -(r("ij")*Tinv("ijmn")) - dlambda*((E("ijkl")*dQods("kl"))*Tinv("ijmn"));
```

operator or function	left value	right value	description
=	nDarray	nDarray	nDarray assignment
+	nDarray	nDarray	nDarray addition
+=	nDarray	nDarray	nDarray addition
-		nDarray	unary minus
-	nDarray	nDarray	nDarray subtraction
--=	nDarray	nDarray	nDarray subtraction
*	double	nDarray	scalar multiplication (from left)
*	nDarray	double	scalar multiplication (from right)
==	nDarray	nDarray	nDarray comparison
val(...)	nDarray		reference to members of nDarray
cval(...)	nDarray		members of nDarray
trace()	nDarray		trace of square nDarray
eigenvalues()	nDarray		eigenvalues of rank 2 square nDarray
eigenvectors()	nDarray		eigenvectors of rank 2 square nDarray
General_norm()	nDarray		general p-th norm of nDarray
nDsqrt()	nDarray		square root of nDarray
print(...)	nDarray		generic print function

Table 702.2: Public functions and operators for nDarray class.

operator or function	left value	right value	description
=	matrix	matrix	matrix assignment
*	matrix	matrix	matrix multiplication
transpose()	matrix		matrix transposition
determinant()	matrix		determinant of a matrix
inverse()	matrix		matrix inversion

Table 702.3: Matrix class functions and operators (added on nDarray class definitions).

Instead of developing theory in terms of indicial notation, then converting everything to matrix notation and then implementing it, we were able to copy formulae directly from their indicial form to the C++ source code.

In addition to the definitions in the base nDarray class, the tensor class adds some specific functions and operators. Table 702.4 summarizes some of the main new functions and operators. The most

operator or function	left value	right value	description
+	tensor	tensor	tensor addition
-	tensor	tensor	tensor subtraction
*	tensor	tensor	tensor multiplication
transpose0110()	tensor		$A_{ijkl} \rightarrow A_{ikjl}$
transpose0101()	tensor		$A_{ijkl} \rightarrow A_{ilkj}$
transpose0111()	tensor		$A_{ijkl} \rightarrow A_{iljk}$
transpose1100()	tensor		$A_{ijkl} \rightarrow A_{jikl}$
transpose0011()	tensor		$A_{ijkl} \rightarrow A_{ijlk}$
transpose1001()	tensor		$A_{ijkl} \rightarrow A_{ljki}$
transpose11()	tensor		$a_{ij} \rightarrow a_{ji}$
symmetrize11()	tensor		symmetrize second order tensor
determinant()	tensor		determinant of 2nd order tensor
inverse()	tensor		tensor inversion (2nd, 4th order)

Table 702.4: Additional and overloaded functions and operators for tensor class.

significant addition is the tensor multiplication operator. With the help of a simple indicial parser, the multiplication operator contracts or expands indices and yields a resulting tensor of the correct rank. The resulting tensor receives proper indices, and can be used in further calculations on the same code statement.

702.4 Finite Element Classes

702.4.1 Stress, Strain and Elastoplastic State Classes

The next step in our development was to use the nDarray tool classes for constitutive level computations. The simple extension was design and implementation of infinitesimal stress and strain tensor classes, namely stresstensor and straintensor. Both classes are quite similar, they inherit all the functions from

the tensor class and we add some tools that are specific to them. Both stress and strain tensors are implemented as full second order 3×3 tensors. Symmetry of stress and strain tensor was not used to save storage space. Table 702.5 summarizes some of the main functions added on for the stresstensor class.

operator or function	description
IInvariant1()	first stress invariant I1
IInvariant2()	second stress invariant I2
IInvariant3()	third stress invariant I3
JInvariant2()	second deviatoric stress invariant J2
JInvariant3()	third deviatoric stress invariant J3
deviator()	stress deviator
principal()	principal stresses on diagonal
sigma_octahedral()	octahedral mean stress
tau_octahedral()	octahedral shear stress
xi()	Haigh–Westergard coordinate ξ
rho()	Haigh–Westergard coordinate ρ
p_hydrostatic()	hydrostatic stress invariant
q_deviatoric()	deviatoric stress invariant
theta()	θ stress invariant (Lode's angle)

Table 702.5: Additional methods for stress tensor class.

Further on, we defined an elastoplastic state, which according to incremental theory of elastoplasticity with internal variables, is completely defined with the stress tensor and a set of internal variables. This definition led us to define an elastoplastic state termed class `ep_state`. Objects of type `ep_state` contain a stress tensor and a set of scalar or tensorial internal variables².

702.4.2 Material Model Classes

With all the previous developments, the design and implementation of various elastoplastic material models was not a difficult task. A generic class `Material_Model` defines techniques that form a framework for small deformation elastoplastic computations. Table 702.6 summarizes some of the main methods defined for the `Material_Model` class in terms of yield (F) and potential (Q) functions.

²Internal variables can be characterized as tensors of even order, where, for example, zero tensor is a scalar internal variable associated with isotropic hardening and second order tensors can be associated with kinematic hardening.

operator or function	description
F	F Yield function value
dFods	$\partial F / \partial \sigma_{ij}$
dQods	$\partial Q / \partial \sigma_{ij}$
d2Qods2	$\partial^2 Q / \partial \sigma_{ij} \partial \sigma_{kl}$
dpoverds	$\partial p / \partial \sigma_{ij}$
dqoverds	$\partial q / \partial \sigma_{ij}$
dthetaoverds	$\partial \theta / \partial \sigma_{ij}$
d2poverds2	$\partial^2 p / \partial \sigma_{ij} \partial \sigma_{kl}$
d2qoverds2	$\partial^2 q / \partial \sigma_{ij} \partial \sigma_{kl}$
d2thetaoverds2	$\partial^2 \theta / \partial \sigma_{ij} \partial \sigma_{kl}$
ForwardPredictorEPState	Explicit predictor elastoplastic state
BackwardEulerEPState	Implicit return elastoplastic state
ForwardEulerEPState	Explicit return elastoplastic state
BackwardEulerCTensor	Algorithmic tangent stiffness tensor
ForwardEulerCTensor	Continuum tangent stiffness tensor

Table 702.6: Some of the methods in material model class.

It is important to note that all the material model dependent functions are defined as virtual functions. Integration algorithms are designed and implemented using template algorithms, and each implemented material model appends its own yield and potential functions and appropriate derivatives. Implementation of additional material models requires coding of yield and potential functions and respective derivative functions.

702.4.3 Stiffness Matrix Class

Starting from the incremental equilibrium of the stationary body, the principle of virtual displacements and with the finite element approximation of the displacement field $u \approx \hat{u}_a = H_I \bar{u}_{Ia}$, the weak form of equilibrium can be expressed as (Zienkiewicz and Taylor, 1991a)

$$\bigcup_m \int_{V^m} H_{I,b} E_{abcd} H_{J,d} dV^m \bar{u}_{Jc} = \bigcup_m \int_{V^m} f_a H_I dV^m \text{ or } (f_{Ia}(\bar{u}_{Jc}))_{int} = \lambda (f_{Ia})_{ext}$$

where E_{abcd} is the constitutive tangent stiffness tensor³. The element stiffness tensor is recognized as

$$k_{aIcJ}^e = \int_{V^m} H_{I,b} \tan E_{abcd} H_{J,d} dV^m$$

This generic form for the finite element stiffness tensor is easily programmed with the help of the nDarray tool. A simple implementation example is provided later. It should be noted that the element stiffness tensor in this case is a four-dimensional tensor. It is the task of the assembly function to collect proper terms for addition in a global stiffness matrix.

702.5 Examples

702.5.1 Tensor Examples

Some of the basic tensorial calculations with tensors are presented. Tensors have a default constructor that creates a first order tensor with one element initialized to 0.0:

```
tensor t1;
```

Tensors can be constructed and initialized from a given set of numbers:

```
static double t2values[] = { 1,2,3,
                            4,5,6,
                            7,8,9 };
tensor t2( 2, DefDim2, t2values ); // order 2; 3x3 tensor (like matrix)
```

Here, DefDim2, DefDim3 and DefDim4 are arrays of dimensions for the second, third and fourth order tensor⁴. A fourth order tensor with 0.0 value assignment and dimension 3 in each order ($3 \times 3 \times 3 \times 3$) is constructed in the following way:

```
tensor ZERO(4,DefDim4,0.0);
```

Tensors can be multiplied using indicial notation. The following example will do a tensorial multiplication of previously defined tensors t2 and t4 so that $tst1 = t2_{ij}t4_{ijkl}t4_{klpq}t2_{pq}$. Note that the memory is dynamically allocated to accept the proper tensor dimensions that will result from the multiplication⁵

```
tensor tst1 = t2("ij")*t4("ijkl")*t4("klpq")*t2("pq");
```

Inversion of tensors is possible. It is defined for 2 and 4 order tensors only. The fourth order tensor inversion is done by converting it to matrix, inverting that matrix and finally converting matrix back to tensor.

```
tensor t4inv_2 = t4.inverse();
```

³Which may be continuum or algorithmic (Jeremić and Sture, 1997) tangent stiffness tensor

⁴In this case dimensions are 3 in every order.

⁵In this case it will be zero dimensional tensor with one element.

There are two built-in tensor types, *Levi-Civita permutation tensor* ϵ_{ijk} and *Kronecker delta tensor* δ_{ij}

```
tensor e("e",3,DefDim3);      // Levi-Civita permutation tensor
tensor I2("I", 2, DefDim2);  // Kronecker delta tensor
```

Trace and determinant functions for tensors are used as follows

```
double deltatrace = I2.trace();
double deltadet = I2.determinant();
```

Tensors can be compared to within a square root of *machine epsilon*⁶ tolerance

```
tensor I2again = I2;
if ( I2again == I2 )
    printf("I2again == I2  TRUE (OK)");
else
    printf("I2again == I2  NOTTRUE");
```

702.5.2 Fourth Order Isotropic Tensors

Some of the fourth order tensors used in continuum mechanics are built quite readily. The most general representation of the fourth order isotropic tensor includes the following fourth order unit isotropic tensors⁷

```
tensor I_ijkl = I2("ij")*I2("kl");
```

The resulting tensor I_{ijkl} will have the correct indices, $I_{ijkl} = I_2{}_{ij}I_2{}_{kl}$. Note that I_{ijkl} is just a name for the tensor, and the $_ijkl$ part reminds the implementor what that tensor is representing.

The real indices, $*ijkl$ in this case, are stored in the tensor object, and can be used further or changed appropriately. The next tensor that is needed is a fourth order unit tensor obtained by transposing the previous one in the minor indices,

```
tensor I_ikjl = I_ijkl.transpose0110();
```

while the third tensor needed for representation of general isotropic tensor is constructed by using similar transpose function

```
tensor I_iljk = I_ijkl.transpose0111();
```

The inversion function can be checked for fourth order tensors:

⁶Machine epsilon (*macheps*) is defined as the smallest distinguishable positive number (in a given precision, i.e. float (32 bits), double (64 bits) or long double (80 bits), such that $1.0 + \text{macheps} > 1.0$ yields true on the given computer platform. For example, double precision arithmetics (64 bits), on the Intel 80x86 platform yields *macheps*=1.08E-19 while on the SUN SPARCstation and DEC platforms *macheps*=2.22E-16.

⁷Remember that I_2 was constructed as the Kronecker delta tensor δ_{ij} .

```

tensor I_ikjl_inv_2 = I_ikjl.inverse();
if ( I_ikjl == I_ikjl_inv_2 )
    printf(" I_ikjl == I_ikjl_inv_2 (OK) !");
else
    printf(" I_ikjl != I_ikjl_inv_2 !");

```

Creating a symmetric and skew symmetric unit fourth order tensors gets to be quite simple by using tensor addition and scalar multiplication

```

tensor I4s = (1./2.)*(I_ikjl+I_iljk);
tensor I4sk = (1./2.)*(I_ikjl-I_iljk);

```

Another interesting example is a numerical check of the $e - \delta$ identity ([Lubliner, 1990](#)) ($e_{ijm}e_{klm} = \delta_{ik}\delta_{jl} - \delta_{il}\delta_{jk}$)

```

tensor id = e("ijm")*e("klm") - (I_ikjl - I_iljk);
if ( id == ZERO )
    printf(" e-delta identity HOLDS !! ");

```

702.5.3 Elastic Isotropic Stiffness and Compliance Tensors

The linear isotropic elasticity tensor E_{ijkl} can be built from Young's modulus E and Poisson's ratio ν

```

double Ey = 20000; // Young's modulus of elasticity
double nu = 0.2; // Poisson's Ratio
tensor E = ((2.*Ey*nu)/(2.*(1.+nu)*(1-2.*nu)))*I_ijkl + (Ey/(1.+nu))*I4s;

```

Similarly, the compliance tensor is

```
tensor D = (-nu/Ey)*I_ijkl + ((1.0+nu)/Ey)*I4s;
```

One can multiply the two and check if the result is equal to the symmetric fourth order unit tensor

```

tensor test = E("ijkl")*D("klpq");
if ( test == I4s )
    printf(" test == I4s TRUE (OK up to sqrt(macheps)) ");
else
    printf(" test == I4s NOTTRUE ");

```

The linear isotropic elasticity and compliance tensors can be obtained in a different way, by using Lamé constants λ and μ

```

double lambda = nu * Ey / (1. + nu) / (1. - 2. * nu);
double mu = Ey / (2. * (1. + nu));
tensor E = lambda*I_ijkl + (2.*mu)*I4s; // stiffness tensor
tensor D = (-nu/Ey)*I_ijkl + (1. / (2.*mu))*I4s; // compliance tensor

```

702.5.4 Second Derivative of θ Stress Invariant

As an extended example of nDarray tool usage, the implementation for the second derivative of the stress invariant θ (Lode angle) is presented. The derivative is used for implicit constitutive integration schemes applied to three invariant material models. The original equation reads:

$$\begin{aligned} \frac{\partial^2 \theta}{\partial \sigma_{pq} \partial \sigma_{mn}} &= \\ &- \left(\frac{9}{2} \frac{\cos 3\theta}{q^4 \sin(3\theta)} + \frac{27}{4} \frac{\cos 3\theta}{q^4 \sin^3 3\theta} \right) s_{pq} s_{mn} + \frac{81}{4} \frac{1}{q^5 \sin^3 3\theta} s_{pq} t_{mn} + \\ &+ \left(\frac{81}{4} \frac{1}{q^5 \sin 3\theta} + \frac{81}{4} \frac{\cos^2 3\theta}{q^5 \sin^3 3\theta} \right) t_{pq} s_{mn} - \frac{243}{4} \frac{\cos 3\theta}{q^6 \sin^3 3\theta} t_{pq} t_{mn} + \\ &+ \frac{3}{2} \frac{\cos(3\theta)}{q^2 \sin(3\theta)} p_{pqmn} - \frac{9}{2} \frac{1}{q^3 \sin(3\theta)} w_{pqmn} \end{aligned}$$

where:

$$q = \sqrt{\frac{3}{2} s_{ij} s_{ij}} \quad ; \quad \cos 3\theta = \frac{3\sqrt{3}}{2} \frac{\frac{1}{3} s_{ij} s_{jk} s_{ki}}{\sqrt{(\frac{1}{2} s_{ij} s_{ij})^3}} \quad ; \quad s_{ij} = \sigma_{ij} - \frac{1}{3} \sigma_{kk} \delta_{ij}$$

$$w_{pqmn} = s_{np} \delta_{qm} + s_{qm} \delta_{np} - \frac{2}{3} s_{qp} \delta_{nm} - \frac{2}{3} \delta_{pq} s_{mn} \quad ; \quad p_{pqmn} = \delta_{mp} \delta_{nq} - \frac{1}{3} \delta_{pq} \delta_{mn}$$

and the implementation follows:

```
tensor Yield_Criteria::d2thetaoverds2(stresstensor & stress)
{
    tensor ret( 4, DefDim4, 0.0);
    tensor I2("I", 2, DefDim2);
    tensor I_pqmn = I2("pq")*I2("mn");
    tensor I_pmqn = I_pqmn.transpose0110();
    double J2D = stress.JInvariant2();
    tensor s = stress.deviator();
    tensor t = s("qk")*s("kp") - I2*(J2D*(2.0/3.0));
    double theta = stress.theta();
    double q_dev = stress.q_deviatoric();

    //setting up some constants
    double c3t      = cos(3*theta);
    double s3t      = sin(3*theta);
    double s3t3     = s3t*s3t*s3t;
    double q3       = q_dev * q_dev * q_dev;
    double q4       = q3 * q_dev;
    double q5       = q4 * q_dev;
```

```

double q6      = q5 * q_dev;
double tempss = -(9.0/2.0)*(c3t)/(q4*s3t)-(27.0/4.0)*(c3t/(s3t3*q4));
double tempst = +(81.0/4.0)*(1.0)/(s3t3*q5);
double tempts = +(81.0/4.0)*(1.0/(s3t*q5))+(81.0/4.0)*(c3t*c3t)/(s3t3*q5);
double temptt = -(243.0/4.0)*(c3t/(s3t3*q6));
double tempp  = +(3.0/2.0)*(c3t/(s3t*q_dev*q_dev));
double tempw  = -(9.0/2.0)*(1.0/(s3t*q3));
tensor s_pq_d_mn = s("pq")*I2("mn");
tensor s_pn_d_mq = s_pq_d_mn.transpose0101();
tensor d_pq_s_mn = I2("pq")*s("mn");
tensor d_pn_s_mq = d_pq_s_mn.transpose0101();
tensor p = I_pmqn - I_pqmn*(1.0/3.0);
tensor w = s_pn_d_mq+d_pn_s_mq - s_pq_d_mn*(2.0/3.0)-d_pq_s_mn*(2.0/3.0);
// finally
ret = (s("pq")*s("mn")*tempss + s("pq")*t("mn")*tempst +
       t("pq")*s("mn")*tempt + t("pq")*t("mn")*temptt +
       p*tempp + w*tempw );
return ret;
}

```

702.5.5 Application to Computations in Elastoplasticity

A useful application of the previously described classes is for elastoplastic computations. If the Newton iterative scheme is used at the global equilibrium level, then in order to preserve a quadratic rate, a consistent, algorithmic tangent stiffness (ATS) tensor should be used. For a general class of three-invariant, non-associated, hardening or softening material models, ATS is defined ([Jeremić and Sture, 1997](#)) as:

$$consE_{pqmn}^{ep} = R_{pqmn} - \frac{R_{pqkl}^{n+1} H_{kl}^{n+1} n_{ij} R_{ijmn}}{n+1 n_{ot} R_{otpq}^{n+1} H_{pq} + n+1 \xi_* h_*}$$

where

$$m_{kl} = \frac{\partial Q}{\partial \sigma_{kl}} \quad ; \quad n_{kl} = \frac{\partial F}{\partial \sigma_{kl}} \quad ; \quad \xi_* = \frac{\partial F}{\partial q_*} \quad ; \quad T_{ijmn} = \delta_{im} \delta_{nj} + \Delta \lambda E_{ijkl} \frac{\partial m_{kl}}{\partial \sigma_{mn}}$$

$$H_{kl} = {}^{n+1}m_{kl} + \Delta \lambda \frac{\partial m_{kl}}{\partial q_*} h_* \quad ; \quad R_{mnkl} = \left({}^{n+1}T_{ijmn} \right)^{-1} E_{ijkl}$$

A straightforward implementation of the above tensorial formula follows:

```

double Ey = Criterion.E();
double nu = Criterion.nu();
tensor Eel = StiffnessTensorE(Ey,nu);

```

```

tensor I2("I", 2, DefDim2);
tensor I_ijkl = I2("ij")*I2("kl");
tensor I_ikjl = I_ijkl.transpose0110();
tensor m = Criterion.dQods(final_stress);
tensor n = Criterion.dFods(final_stress);
double lambda = current_lambda_get();
tensor d2Qoverds2 = Criterion.d2Qods2(final_stress);
tensor T = I_ikjl + Eel("ijkl")*d2Qoverds2("klmn")*lambda;
tensor Tinv = T.inverse();
tensor R = Tinv("ijmn")*Eel("ijkl");
double h_ = h(final_stress);
double xi_ = xi(final_stress);
double hardMod_ = h_* xi_;
tensor d2Qodqast2 = d2Qoverdqast2(final_stress);
tensor H = m + d2Qodqast2 * lambda * h_;
//  

tensor upper = R("pqkl")*H("kl")*n("ij")*R("ijmn");
double lower = (n("ot")*R("otpq"))*H("pq")).trace();
lower = lower + hardMod_;
tensor Ep = upper*(1./lower);
tensor Eep = R - Ep; // elastoplastic ATS constitutive tensor

```

This ATS tensor can be used further in building finite element stiffness tensors, as will be shown in our next example.

702.5.6 Stiffness Matrix Example

By applying a numerical integration technique to the stiffness matrix equation

$$k_{aIcJ}^e = \int_{V^m} H_{I,b} E_{abcd} H_{J,d} dV^m$$

individual contributions are summed into the element stiffness tensor. This process can be implemented on a integration point level by using the nDarray tool as

$$K = K + H("Ib") * E("abcd") * H("Jd") * weight ;$$

It is interesting to note the lack of loops at this level of implementation. However, there exists a loop over integration points which contributes stiffness to the element tensor.

702.6 Performance Issues

In the course of developing the nDarray tool, execution speed was not a priority or issue that we tried to perfect. The benefit of being able to implement and test various numerical algorithms in a straightforward manner was the main concern. The efficiency of the nDarray tool when compared with FORTRAN or C was never assessed. In all honesty, some of the formulae implemented in C++ with the help of the nDarray tool would be difficult to implement in FORTRAN or C. The entire question of efficiency of the nDarray as compared to FORTRAN or C codes might thus remain unanswered for the time being.

The efficiency of C++ for numerical computations has been under consideration ([Robison, 1996](#)) for some time now. Poor efficiency and possible remedies for improving efficiency of C++ computations has been reported in literature ([Robison, 1996](#)) ([Veldhuizen, 1995b](#)) ([Veldhuizen, 1996](#)). Novel techniques, such as *Template Expressions* ([Veldhuizen, 1995b](#)) can be used to achieve and sometimes surpass the performance of hand-tuned FORTRAN or C codes.

702.7 Summary and Future Directions

A novel programming tool, named nDarray, has been presented which facilitates implementation of tensorial formulae. It was shown how OOP and efficient programming in C++ allows building of new concrete data types, in this case tensors of any order. In a number of examples these new data types were shown to be useful in implementing tensorial formulae associated with the numerical solution of various elastic and elastoplastic problems with the finite element method. The nDarray tool is been used in developing of the FEMtools tools library. The FEMtools tools library includes a set of finite elements, various solvers, solution procedures for non-linear finite element system of equations and other useful functions.

Appendix 703

Closed Form Gradients to the Plastic Potential Function

(1993-1994-)

703.1 Chapter Summary and Highlights

A complete derivation of gradients to the Potential and Yield function follows. The yield function F and potential function Q are functions of the stress tensor σ_{ij} and plastic internal variable tensor q_* . Only derivatives with respect to the stress tensor σ_{ij} are given here. It is assumed that any stress state can be represented with three stress invariants p , q and θ given in the following form:

$$p = -\frac{1}{3}I_1 \quad q = \sqrt{3J_{2D}} \quad \cos 3\theta = \frac{3\sqrt{3}}{2} \frac{J_{3D}}{\sqrt{(J_{2D})^3}} \quad (703.1)$$

$$I_1 = \sigma_{kk} \quad J_{2D} = \frac{1}{2}s_{ij}s_{ij} \quad J_{3D} = \frac{1}{3}s_{ij}s_{jk}s_{ki} \quad s_{ij} = \sigma_{ij} - \frac{1}{3}\sigma_{kk}\delta_{ij} \quad (703.2)$$

and stresses are chosen as positive in tension. One can write the Potential Function in the following form:

$$Q = Q(p, q, \theta) \quad (703.3)$$

and the derivation follows. Hopefully the pace of derivation is rather slow, thus little explanation will be given until the end of the derivation. Chain rule of differentiation yields:

$$\frac{\partial Q}{\partial \sigma_{ij}} = \frac{\partial Q}{\partial p} \frac{\partial p}{\partial \sigma_{ij}} + \frac{\partial Q}{\partial q} \frac{\partial q}{\partial \sigma_{ij}} + \frac{\partial Q}{\partial \theta} \frac{\partial \theta}{\partial \sigma_{ij}} \quad (703.4)$$

and the intermediate derivatives are:

$$\frac{\partial p}{\partial \sigma_{ij}} = \frac{\partial(-\frac{1}{3}\sigma_{kk})}{\partial \sigma_{ij}} = -\frac{1}{3} \delta_{ij} \quad (703.5)$$

$$\frac{\partial q}{\partial \sigma_{ij}} = \frac{\partial \sqrt{3J_{2D}}}{\partial \sigma_{ij}} = \frac{\sqrt{3}}{2} \frac{1}{\sqrt{J_{2D}}} \frac{\partial J_{2D}}{\partial \sigma_{ij}} = \frac{\sqrt{3}}{2} \frac{1}{\sqrt{J_{2D}}} s_{ij} = \frac{3}{2} \frac{1}{q} s_{ij} \quad (703.6)$$

$$\begin{aligned} & \frac{\partial \theta}{\partial \sigma_{ij}} = \\ &= \frac{1}{3} \frac{-1}{\sqrt{1 - (\frac{3\sqrt{3}}{2} \frac{J_{3D}}{J_{2D}^{3/2}})^2}} \frac{3\sqrt{3}}{2} \left(\frac{\partial J_{3D}}{\partial \sigma_{ij}} \frac{1}{\sqrt{(J_{2D})^3}} - \frac{3}{2} J_{3D} \frac{\partial J_{2D}}{\partial \sigma_{ij}} \frac{1}{\sqrt{(J_{2D})^5}} \right) = \\ &= \frac{1}{3\sqrt{1 - (\frac{3\sqrt{3}}{2} \frac{J_{3D}}{J_{2D}^{3/2}})^2}} \frac{3\sqrt{3}}{2} \left(-t_{ij} \frac{1}{\sqrt{(J_{2D})^3}} + \frac{3}{2} J_{3D} s_{ij} \frac{1}{\sqrt{(J_{2D})^5}} \right) = \\ &= \frac{1}{\sin 3\theta} \frac{\sqrt{3}}{2} \left(\frac{3}{2} J_{3D} \frac{1}{\sqrt{(J_{2D})^5}} s_{ij} - \frac{1}{\sqrt{(J_{2D})^3}} t_{ij} \right) = \\ &= \frac{\sqrt{3}}{2} \frac{1}{\sin(3\theta)} \left(\frac{\sqrt{3} \cos(3\theta)}{q^2} s_{ij} - \frac{3\sqrt{3}}{q^3} t_{ij} \right) = \\ &= \frac{3}{2} \frac{\cos(3\theta)}{q^2 \sin(3\theta)} s_{ij} - \frac{9}{2} \frac{1}{q^3 \sin(3\theta)} t_{ij} \end{aligned} \quad (703.7)$$

Second derivatives of the potential function Q using again the chain rule of differentiation are as follows:

$$\begin{aligned}
\frac{\partial^2 Q}{\partial \sigma_{pq} \partial \sigma_{mn}} &= \frac{\partial \left(\frac{\partial Q}{\partial \sigma_{pq}} \right)}{\partial \sigma_{mn}} = \\
&\frac{\partial \left(\frac{\partial Q}{\partial p} \frac{\partial p}{\partial \sigma_{pq}} + \frac{\partial Q}{\partial q} \frac{\partial q}{\partial \sigma_{pq}} + \frac{\partial Q}{\partial \theta} \frac{\partial \theta}{\partial \sigma_{pq}} \right)}{\partial \sigma_{mn}} = \\
&\frac{\partial \left(\frac{\partial Q}{\partial p} \right)}{\partial \sigma_{mn}} \frac{\partial p}{\partial \sigma_{pq}} + \frac{\partial Q}{\partial p} \frac{\partial^2 p}{\partial \sigma_{pq} \partial \sigma_{mn}} + \\
&+ \frac{\partial \left(\frac{\partial Q}{\partial q} \right)}{\partial \sigma_{mn}} \frac{\partial q}{\partial \sigma_{pq}} + \frac{\partial Q}{\partial q} \frac{\partial^2 q}{\partial \sigma_{pq} \partial \sigma_{mn}} + \\
&+ \frac{\partial \left(\frac{\partial Q}{\partial \theta} \right)}{\partial \sigma_{mn}} \frac{\partial \theta}{\partial \sigma_{pq}} + \frac{\partial Q}{\partial \theta} \frac{\partial^2 \theta}{\partial \sigma_{pq} \partial \sigma_{mn}} = \\
&\left(\frac{\partial^2 Q}{\partial p^2} \frac{\partial p}{\partial \sigma_{mn}} + \frac{\partial^2 Q}{\partial p \partial q} \frac{\partial q}{\partial \sigma_{mn}} + \frac{\partial^2 Q}{\partial p \partial \theta} \frac{\partial \theta}{\partial \sigma_{mn}} \right) \frac{\partial p}{\partial \sigma_{pq}} + \frac{\partial Q}{\partial p} \frac{\partial^2 p}{\partial \sigma_{pq} \partial \sigma_{mn}} + \\
&+ \left(\frac{\partial^2 Q}{\partial q \partial p} \frac{\partial p}{\partial \sigma_{mn}} + \frac{\partial^2 Q}{\partial q^2} \frac{\partial q}{\partial \sigma_{mn}} + \frac{\partial^2 Q}{\partial q \partial \theta} \frac{\partial \theta}{\partial \sigma_{mn}} \right) \frac{\partial q}{\partial \sigma_{pq}} + \frac{\partial Q}{\partial q} \frac{\partial^2 q}{\partial \sigma_{pq} \partial \sigma_{mn}} + \\
&+ \left(\frac{\partial^2 Q}{\partial \theta \partial p} \frac{\partial p}{\partial \sigma_{mn}} + \frac{\partial^2 Q}{\partial \theta \partial q} \frac{\partial q}{\partial \sigma_{mn}} + \frac{\partial^2 Q}{\partial \theta^2} \frac{\partial \theta}{\partial \sigma_{mn}} \right) \frac{\partial \theta}{\partial \sigma_{pq}} + \frac{\partial Q}{\partial \theta} \frac{\partial^2 \theta}{\partial \sigma_{pq} \partial \sigma_{mn}}
\end{aligned}$$

and the intermediate derivatives are as follows:

$$\frac{\partial^2 p}{\partial \sigma_{pq} \partial \sigma_{mn}} = \frac{\partial^2 \left(-\frac{1}{3} \sigma_{kk} \right)}{\partial \sigma_{pq} \partial \sigma_{mn}} = \frac{\partial \left(-\frac{1}{3} \delta_{kp} \delta_{qk} \right)}{\partial \sigma_{mn}} = \emptyset$$

$$\begin{aligned}
\frac{\partial^2 q}{\partial \sigma_{pq} \partial \sigma_{mn}} &= \frac{\partial \left(\frac{\partial q}{\partial \sigma_{pq}} \right)}{\partial \sigma_{mn}} = \\
&\frac{\partial \left(\frac{\sqrt{3}}{2} \frac{1}{\sqrt{J_{2D}}} s_{pq} \right)}{\partial \sigma_{mn}} = \frac{\sqrt{3}}{2} \frac{1}{\sqrt{J_{2D}}} \frac{\partial s_{pq}}{\partial \sigma_{mn}} + \frac{\sqrt{3}}{2} \frac{\partial}{\partial \sigma_{mn}} \frac{1}{\sqrt{J_{2D}}} s_{pq} = \\
&\frac{\sqrt{3}}{2} \frac{1}{\sqrt{J_{2D}}} \left(\delta_{pm} \delta_{nq} - \frac{1}{3} \delta_{pq} \delta_{km} \delta_{nk} \right) + \frac{\sqrt{3}}{2} \left(\frac{-1}{2} \left(\frac{1}{(\sqrt{J_{2D}})^3} \right) s_{mn} \right) s_{pq} = \\
&\frac{\sqrt{3}}{2} \frac{1}{\sqrt{J_{2D}}} \left(\delta_{pm} \delta_{nq} - \frac{1}{3} \delta_{pq} \delta_{nm} \right) - \frac{\sqrt{3}}{4} \left(\frac{1}{\sqrt{J_{2D}}} \right)^3 s_{mn} s_{pq} = \\
&\frac{3}{2} \frac{1}{q} \left(\delta_{pm} \delta_{nq} - \frac{1}{3} \delta_{pq} \delta_{nm} \right) - \frac{9}{4} \frac{1}{q^3} s_{mn} s_{pq}
\end{aligned}$$

Let us introduce a slightly different form for the equation $\frac{\partial^2 \theta}{\partial \sigma_{pq} \partial \sigma_{mn}}$ in order to simplify writing:

$$\frac{\partial \theta}{\partial \sigma_{pq}} = \frac{3}{2} \frac{\cos(3\theta)}{q^2 \sin(3\theta)} s_{pq} - \frac{9}{2} \frac{1}{q^3 \sin(3\theta)} t_{pq} =$$

$$= AS s_{pq} + AT t_{pq}$$

where:

$$AS = \frac{3}{2} \frac{\cos(3\theta)}{q^2 \sin(3\theta)}$$

$$AT = -\frac{9}{2} \frac{1}{q^3 \sin(3\theta)}$$

Now the problem will be separated in two smaller problems, namely:

$$\begin{aligned} \frac{\partial^2 \theta}{\partial \sigma_{pq} \partial \sigma_{mn}} &= \frac{\partial \frac{\partial \theta}{\partial \sigma_{pq}}}{\partial \sigma_{mn}} = \\ \frac{\partial \left(\frac{3}{2} \frac{\cos(3\theta)}{q^2 \sin(3\theta)} s_{pq} - \frac{9}{2} \frac{1}{q^3 \sin(3\theta)} t_{pq} \right)}{\partial \sigma_{mn}} &= \\ \frac{\partial (AS s_{pq} + AT t_{pq})}{\partial \sigma_{mn}} &= \\ \frac{\partial (AS s_{pq})}{\partial \sigma_{mn}} + \frac{\partial (AT t_{pq})}{\partial \sigma_{mn}} & \end{aligned}$$

Now let us take a look at $\frac{\partial(AS s_{pq})}{\partial \sigma_{mn}}$. Since:

$$\begin{aligned}
& \frac{\partial (AS \ s_{pq})}{\partial \sigma_{mn}} = \\
& \frac{\partial AS}{\partial \sigma_{mn}} \ s_{pq} + AS \ \frac{\partial s_{pq}}{\partial \sigma_{mn}} = \\
& \left(\frac{\partial AS}{\partial q} \frac{\partial q}{\partial \sigma_{mn}} + \frac{\partial AS}{\partial \theta} \frac{\partial \theta}{\partial \sigma_{mn}} \right) s_{pq} + AS \ \frac{\partial s_{pq}}{\partial \sigma_{mn}} = \\
& \left(\frac{-3 \cdot \cot(3\theta)}{q^3} \frac{3}{2} \frac{1}{q} s_{mn} + \right. \\
& \left. + \frac{-4.5 \csc(3\theta)^2}{q^2} \left(\frac{3}{2} \frac{\cos(3\theta)}{q^2 \sin(3\theta)} s_{mn} - \frac{9}{2} \frac{1}{q^3 \sin(3\theta)} t_{mn} \right) \right) s_{pq} + \\
& \frac{3}{2} \frac{\cos(3\theta)}{q^2 \sin(3\theta)} p_{pqmn} = \\
& -\frac{9}{2} \frac{\cos 3\theta}{q^4 \sin(3\theta)} s_{pq} s_{mn} - \frac{27}{4} \frac{\cos 3\theta}{q^4 \sin^3 3\theta} s_{pq} s_{mn} + \frac{81}{4} \frac{1}{q^5 \sin^3 3\theta} s_{pq} t_{mn} + \\
& \frac{3}{2} \frac{\cos(3\theta)}{q^2 \sin(3\theta)} p_{pqmn} = \\
& -\left(\frac{9}{2} \frac{\cos 3\theta}{q^4 \sin(3\theta)} + \frac{27}{4} \frac{\cos 3\theta}{q^4 \sin^3 3\theta} \right) s_{pq} s_{mn} + \frac{81}{4} \frac{1}{q^5 \sin^3 3\theta} s_{pq} t_{mn} + \\
& \frac{3}{2} \frac{\cos(3\theta)}{q^2 \sin(3\theta)} p_{pqmn}
\end{aligned}$$

where:

$$p_{pqmn} = \frac{\partial s_{pq}}{\partial \sigma_{mn}} = \left(\delta_{mp} \delta_{nq} - \frac{1}{3} \delta_{pq} \delta_{mn} \right)$$

is the projection tensor and:

$$\frac{\partial AS}{\partial q} = \frac{-3 \cdot \cot(3\theta)}{q^3}$$

$$\frac{\partial AS}{\partial \theta} = \frac{-4.5 \csc(3\theta)^2}{q^2}$$

The second member is $\frac{\partial (AT \ t_{pq})}{\partial \sigma_{mn}}$:

$$\begin{aligned}
& \frac{\partial (AT \ t_{pq})}{\partial \sigma_{mn}} = \\
& \frac{\partial AT}{\partial \sigma_{mn}} \ t_{pq} + AT \ \frac{\partial t_{pq}}{\partial \sigma_{mn}} = \\
& \left(\frac{\partial AT}{\partial q} \frac{\partial q}{\partial \sigma_{mn}} + \frac{\partial AT}{\partial \theta} \frac{\partial \theta}{\partial \sigma_{mn}} \right) \ t_{pq} + AT \ \frac{\partial t_{pq}}{\partial \sigma_{mn}} = \\
& \left(\frac{13.5 \csc(3\theta)}{q^4} \frac{3}{2} \frac{1}{q} s_{mn} + \right. \\
& \left. + \frac{13.5 \cot(3\theta) \csc(3\theta)}{q^3} \left(\frac{3}{2} \frac{\cos(3\theta)}{q^2 \sin(3\theta)} s_{mn} - \frac{9}{2} \frac{1}{q^3 \sin(3\theta)} t_{mn} \right) \right) \ t_{pq} + \\
& + - \frac{9}{2} \frac{1}{q^3 \sin(3\theta)} w_{pqmn} = \\
& \frac{81}{4} \frac{1}{q^5 \sin 3\theta} \ t_{pq} \ s_{mn} + \frac{81}{4} \frac{\cos^2 3\theta}{q^5 \sin^3 3\theta} \ t_{pq} \ s_{mn} - \frac{243}{4} \frac{\cos 3\theta}{q^6 \sin^3 3\theta} \ t_{pq} \ t_{mn} - \\
& - \frac{9}{2} \frac{1}{q^3 \sin(3\theta)} w_{pqmn} = \\
& \left(\frac{81}{4} \frac{1}{q^5 \sin 3\theta} + \frac{81}{4} \frac{\cos^2 3\theta}{q^5 \sin^3 3\theta} \right) \ t_{pq} \ s_{mn} - \frac{243}{4} \frac{\cos 3\theta}{q^6 \sin^3 3\theta} \ t_{pq} \ t_{mn} - \\
& - \frac{9}{2} \frac{1}{q^3 \sin(3\theta)} w_{pqmn}
\end{aligned}$$

where:

$$w_{pqmn} = \frac{\partial t_{pq}}{\partial \sigma_{mn}} = s_{np}\delta_{qm} + s_{qm}\delta_{np} - \frac{2}{3}s_{qp}\delta_{nm} - \frac{2}{3}\delta_{pq}s_{mn}$$

$$\frac{\partial AT}{\partial q} = \frac{13.5 \csc(3\theta)}{q^4}$$

$$\frac{\partial AT}{\partial \theta} = \frac{13.5 \cot(3\theta) \csc(3\theta)}{q^3}$$

Then finally by collecting terms back again we have:

$$\begin{aligned} & \frac{\partial^2 \theta}{\partial \sigma_{pq} \partial \sigma_{mn}} = \\ & \frac{\partial (AS \ s_{pq})}{\partial \sigma_{mn}} + \frac{\partial (AT \ t_{pq})}{\partial \sigma_{mn}} = \\ & - \left(\frac{9}{2} \frac{\cos 3\theta}{q^4 \sin(3\theta)} + \frac{27}{4} \frac{\cos 3\theta}{q^4 \sin^3 3\theta} \right) s_{pq} s_{mn} + \frac{81}{4} \frac{1}{q^5 \sin^3 3\theta} s_{pq} t_{mn} + \\ & + \left(\frac{81}{4} \frac{1}{q^5 \sin 3\theta} + \frac{81}{4} \frac{\cos^2 3\theta}{q^5 \sin^3 3\theta} \right) t_{pq} s_{mn} - \frac{243}{4} \frac{\cos 3\theta}{q^6 \sin^3 3\theta} t_{pq} t_{mn} + \\ & + \frac{3}{2} \frac{\cos(3\theta)}{q^2 \sin(3\theta)} p_{pqmn} - \frac{9}{2} \frac{1}{q^3 \sin(3\theta)} w_{pqmn} \end{aligned}$$

Appendix 704

Hyperelasticity, Detailed Derivations

(1995-1996-)

704.1 Chapter Summary and Highlights

704.2 Simo–Serrin's Formula

In order to derive the analytical gradient of the fourth order tensor

$$\mathcal{M}_{IJKL} = \frac{\partial M_{II}}{\partial C_{KL}} \quad (704.1)$$

we shall proceed by using the third equation in (106.86).

$$\begin{aligned} \frac{\partial M_{II}}{\partial C_{KL}} &= \frac{1}{D_{(A)}} \left(I_{IKJL} - \frac{\partial I_1}{\partial C_{KL}} \delta_{IJ} + 2\lambda_{(A)} \frac{\partial \lambda_{(A)}}{\partial C_{KL}} \delta_{IJ} + \right. \\ &\quad + \frac{\partial I_3}{\partial C_{KL}} \lambda_{(A)}^{-2} (C^{-1})_{IJ} - 2\lambda_{(A)}^{-3} \frac{\partial \lambda_{(A)}}{\partial C_{KL}} I_3 (C^{-1})_{IJ} + \frac{\partial (C^{-1})_{IJ}}{\partial C_{KL}} \lambda_{(A)}^{-2} I_3 \Big) - \\ &\quad - \frac{1}{D_{(A)}^2} \frac{\partial D_{(A)}}{\partial C_{KL}} \left(C_{IJ} - \left(I_1 - \lambda_{(A)}^2 \right) \delta_{IJ} + I_3 \lambda_{(A)}^{-2} (C^{-1})_{IJ} \right) \end{aligned} \quad (704.2)$$

where it was used that

$$\frac{\partial C_{IJ}}{\partial C_{KL}} = I_{IKJL} \quad (704.3)$$

Derivatives $\partial \lambda_{(A)} / \partial C_{KL}$ can be found by starting from equation for C_{IJ} (106.63) and differentiating it

$$dC_{IJ} = 2\lambda_A d\lambda_{(A)} \left(N_I^{(A)} N_J^{(A)} \right)_A + \lambda_A^2 \left(dN_I^{(A)} N_J^{(A)} \right)_A + \lambda_A^2 \left(N_I^{(A)} dN_J^{(A)} \right)_A \quad (704.4)$$

By premultiplying previous equation with $N_J^{(A)}$ and post-multiplying with $N_I^{(A)}$, and by noting that

$$N_I^{(A)} dN_I^{(A)} \equiv 0 \quad ; \quad \|N_I^{(A)}\| \equiv 1 \quad (704.5)$$

we get

$$N_J^{(A)} dC_{IJ} N_I^{(A)} = 2\lambda_A d\lambda_{(A)} \quad (704.6)$$

or

$$dC_{IJ} N_I^{(A)} N_J^{(A)} = dC_{IJ} \lambda_{(A)} M_{IJ}^{(A)} = 2\lambda_A d\lambda_{(A)} \Rightarrow \frac{\partial \lambda_A}{\partial C_{KL}} = \frac{1}{2} \lambda_{(A)} (M_{KL}^{(A)})_A \quad (704.7)$$

It can be proved¹ that

$$\frac{\partial I_1}{\partial C_{KL}} = \delta_{IJ} \quad ; \quad \frac{\partial I_2}{\partial C_{KL}} = I_1 \delta_{KL} - C_{KL} \quad ; \quad \frac{\partial I_3}{\partial C_{KL}} = I_3 (C^{-1})_{KL} \quad (704.8)$$

and since $I_3 = J^2$

$$\frac{\partial J}{\partial C_{KL}} = \frac{1}{2} J (C^{-1})_{KL} \quad (704.9)$$

¹See Marsden and Hughes (1983)

With this in mind, equation (704.2) can be rewritten as:

$$\begin{aligned} \frac{\partial M_{IJ}}{\partial C_{KL}} &= \frac{1}{D_{(A)}} \left(I_{IKJL} - \delta_{KL} \delta_{IJ} + 2\lambda_{(A)}^2 \frac{1}{2} M_{KL}^{(A)} \delta_{IJ} + \right. \\ &\quad + I_3 \lambda_{(A)}^{-2} (C^{-1})_{IJ} (C^{-1})_{KL} - \lambda_{(A)}^{-2} I_3 (C^{-1})_{IJ} M_{KL}^{(A)} + \\ &\quad + \frac{1}{2} \left((C^{-1})_{IK} (C^{-1})_{JL} + (C^{-1})_{IL} (C^{-1})_{JK} \right) \lambda_{(A)}^{-2} I_3 \Big) - \\ &\quad - \frac{1}{D_{(A)}} \frac{\partial D_{(A)}}{\partial C_{KL}} M_{IJ} \end{aligned} \quad (704.10)$$

where the definition of M_{IJ} from equation (106.86) was used and also:

$$\frac{\partial (C^{-1})_{IJ}}{\partial C_{KL}} = -\frac{1}{2} \left((C^{-1})_{IK} (C^{-1})_{JL} + (C^{-1})_{IL} (C^{-1})_{JK} \right) = I_{IJKL}^{(C^{-1})} \quad (704.11)$$

Relation (704.11) can be obtained if one starts from the identity:

$$C_{IJ} (C^{-1})_{JK} = \delta_{IK} \quad (704.12)$$

which after differentiation reads:

$$\begin{aligned} dC_{IJ} (C^{-1})_{JK} + C_{IJ} d(C^{-1})_{JK} &= 0 \Rightarrow \\ \Rightarrow d(C^{-1})_{JK} &= -(C^{-1})_{JM} dC_{MN} (C^{-1})_{NK} = \\ &= -\frac{1}{2} \left((C^{-1})_{JM} (C^{-1})_{KN} + (C^{-1})_{JN} (C^{-1})_{KM} \right) dC_{MN} \Rightarrow \\ \Rightarrow \frac{\partial (C^{-1})_{JK}}{\partial C_{MN}} &= -\frac{1}{2} \left((C^{-1})_{JM} (C^{-1})_{KN} + (C^{-1})_{JN} (C^{-1})_{KM} \right) \end{aligned} \quad (704.13)$$

The derivative of $D_{(A)}$, that was defined in equation (106.77) as

$$D_{(A)} = 2\lambda_{(A)}^4 - I_1 \lambda_{(A)}^2 + I_3 \lambda_{(A)}^{-2} \quad (704.14)$$

is given by:

$$\begin{aligned}
\frac{\partial D_{(A)}}{\partial C_{KL}} &= 8\lambda_{(A)}^3 \frac{\partial \lambda_{(A)}}{\partial C_{KL}} - \frac{\partial I_1}{\partial C_{KL}} \lambda_{(A)}^2 - 2\lambda_{(A)} I_1 \frac{\partial \lambda_{(A)}}{\partial C_{KL}} + \frac{\partial I_3}{\partial C_{KL}} \lambda_{(A)}^{-2} - 2\lambda_{(A)}^{-3} I_3 \frac{\partial \lambda_{(A)}}{\partial C_{KL}} \\
&= 4\lambda_{(A)}^4 M_{KL}^{(A)} - \delta_{KL} \lambda_{(A)}^2 - \lambda_{(A)}^2 I_1 M_{KL}^{(A)} + I_3 (C^{-1})_{KL} \lambda_{(A)}^{-2} - \lambda_{(A)}^{-2} I_3 M_{KL}^{(A)} \\
&= \left(4\lambda_{(A)}^4 - \lambda_{(A)}^2 I_1 - \lambda_{(A)}^{-2} I_3 \right) M_{KL}^{(A)} - \delta_{KL} \lambda_{(A)}^2 + I_3 (C^{-1})_{KL} \lambda_{(A)}^{-2} \\
&= D'_{(A)} M_{KL}^{(A)} - \delta_{KL} \lambda_{(A)}^2 + I_3 (C^{-1})_{KL} \lambda_{(A)}^{-2}
\end{aligned} \tag{704.15}$$

where $D'_{(A)} = 4\lambda_{(A)}^4 - \lambda_{(A)}^2 I_1 - \lambda_{(A)}^{-2} I_3$. With the previous derivations, equation (704.10) can be written in expanded form as:

$$\begin{aligned}
\frac{\partial M_{IJ}}{\partial C_{KL}} &= \frac{1}{D_{(A)}} \left(I_{IKJL} - \delta_{KL} \delta_{IJ} + 2\lambda_{(A)}^2 \frac{1}{2} M_{KL}^{(A)} \delta_{IJ} + \right. \\
&\quad + I_3 \lambda_{(A)}^{-2} (C^{-1})_{IJ} (C^{-1})_{KL} - \lambda_{(A)}^{-2} I_3 (C^{-1})_{IJ} M_{KL}^{(A)} + \\
&\quad + \frac{1}{2} \left((C^{-1})_{IK} (C^{-1})_{JL} + (C^{-1})_{IL} (C^{-1})_{JK} \right) \lambda_{(A)}^{-2} I_3 - \\
&\quad \left. - \left(D'_{(A)} M_{KL}^{(A)} - \delta_{KL} \lambda_{(A)}^2 + I_3 (C^{-1})_{KL} \lambda_{(A)}^{-2} \right) M_{IJ} \right)
\end{aligned} \tag{704.16}$$

If one collects similar terms, equation (704.16), also known as *Simo–Serrin's formula* can be written in the final form as:

$$\begin{aligned}
\frac{\partial M_{IJ}}{\partial C_{KL}} &= \mathcal{M}_{IJKL} = \\
&= \frac{1}{D_{(A)}} \left(I_{IKJL} - \delta_{KL} \delta_{IJ} + \lambda_{(A)}^2 \left(\delta_{IJ} M_{KL}^{(A)} + M_{IJ}^{(A)} \delta_{KL} \right) + \right. \\
&\quad + I_3 \lambda_{(A)}^{-2} \left((C^{-1})_{IJ} (C^{-1})_{KL} + \frac{1}{2} \left((C^{-1})_{IK} (C^{-1})_{JL} + (C^{-1})_{IL} (C^{-1})_{JK} \right) \right) - \\
&\quad \left. - \lambda_{(A)}^{-2} I_3 \left((C^{-1})_{IJ} M_{KL}^{(A)} + M_{IJ}^{(A)} (C^{-1})_{KL} \right) - D'_{(A)} M_{IJ}^{(A)} M_{KL}^{(A)} \right)
\end{aligned} \tag{704.17}$$

704.3 Derivation of $\partial^2 \text{vol}W / (\partial C_{IJ} \partial C_{KL})$

The volumetric part $\partial^2 \text{vol}W / (\partial C_{IJ} \partial C_{KL})$ can be derived by starting from the equation (106.96):

$$\begin{aligned}
& \frac{\partial^2{}^{vol}W}{\partial C_{IJ} \partial C_{KL}} = \\
& \frac{\partial \left(\frac{1}{2} \frac{\partial {}^{vol}W}{\partial J} J (C^{-1})_{IJ} \right)}{\partial C_{KL}} = \\
& \frac{1}{2} \frac{\partial \left(\frac{\partial {}^{vol}W}{\partial J} \right)}{\partial C_{KL}} J (C^{-1})_{IJ} + \frac{1}{2} \frac{\partial {}^{vol}W}{\partial J} \frac{\partial (J)}{\partial C_{KL}} (C^{-1})_{IJ} + \frac{1}{2} \frac{\partial {}^{vol}W}{\partial J} J \frac{\partial ((C^{-1})_{IJ})}{\partial C_{KL}} = \\
& \frac{1}{2} \frac{\partial^2 ({}^{vol}W)}{\partial J \partial J} \frac{\partial J}{\partial C_{KL}} J (C^{-1})_{IJ} + \frac{1}{2} \frac{\partial {}^{vol}W}{\partial J} \frac{1}{2} J (C^{-1})_{KL} (C^{-1})_{IJ} + \frac{1}{2} \frac{\partial {}^{vol}W}{\partial J} J I_{IJKL}^{(C^{-1})} = \\
& \frac{1}{4} J^2 \frac{\partial^2 {}^{vol}W}{\partial J \partial J} (C^{-1})_{KL} (C^{-1})_{IJ} + \frac{1}{4} J \frac{\partial {}^{vol}W}{\partial J} (C^{-1})_{KL} (C^{-1})_{IJ} + \frac{1}{2} J \frac{\partial {}^{vol}W}{\partial J} I_{IJKL}^{(C^{-1})} = \\
& \frac{1}{4} \left(J^2 \frac{\partial^2 {}^{vol}W}{\partial J \partial J} + J \frac{\partial {}^{vol}W}{\partial J} \right) (C^{-1})_{KL} (C^{-1})_{IJ} + \frac{1}{2} J \frac{\partial {}^{vol}W}{\partial J} I_{IJKL}^{(C^{-1})} \tag{704.18}
\end{aligned}$$

where equations (704.11) and (704.9) were used.

704.4 Derivation of $\partial^2{}^{iso}W/(\partial C_{IJ} \partial C_{KL})$

The isochoric part $\partial^2{}^{iso}W/(\partial C_{IJ} \partial C_{KL})$ can be derived by starting from equation (106.97)

$$\begin{aligned}
& \frac{\partial^2 isoW(\lambda_{(A)})}{\partial C_{IJ} \partial C_{KL}} = \\
& \frac{1}{2} \frac{\partial \left(w_A (M_{IJ}^{(A)})_A \right)}{\partial C_{KL}} = \\
& \frac{1}{2} \frac{\partial w_A}{\partial C_{KL}} (M_{IJ}^{(A)})_A + \frac{1}{2} w_A \frac{\partial (M_{IJ}^{(A)})_A}{\partial C_{KL}} = \\
& \frac{1}{2} \frac{\partial w_A}{\partial \lambda_B} \frac{1}{2} \lambda_{(B)} (M_{KL}^{(B)})_B (M_{IJ}^{(A)})_A + \frac{1}{2} w_A (\mathcal{M}_{IJKL}^{(A)})_A = \\
& \frac{1}{4} Y_{AB} (M_{KL}^{(B)})_B (M_{IJ}^{(A)})_A + \frac{1}{2} w_A (\mathcal{M}_{IJKL}^{(A)})_A
\end{aligned} \tag{704.19}$$

where equation (704.7) was used and tensor Y_{AB} is defined as:

$$Y_{AB} = \frac{\partial w_A}{\partial \lambda_B} \lambda_{(B)} \tag{704.20}$$

704.5 Derivation of w_A

$$w_A = \frac{\partial isoW}{\partial \lambda_{(A)}} \lambda_A = \frac{\partial isoW}{\partial \tilde{\lambda}_B} \frac{\partial \tilde{\lambda}_B}{\partial \lambda_{(A)}} \lambda_A \tag{704.21}$$

where $\tilde{\lambda}_B$ is the isochoric part of the stretch defined as

$$\tilde{\lambda}_B = J^{-\frac{1}{3}} \lambda_B \tag{704.22}$$

From the definition of $\tilde{\lambda}_B$ in equation (704.22) it follows

$$\frac{\partial \tilde{\lambda}_B}{\partial \lambda_{(A)}} = \frac{\partial J^{-\frac{1}{3}}}{\partial \lambda_{(A)}} \lambda_B + J^{-\frac{1}{3}} \frac{\partial \lambda_B}{\partial \lambda_{(A)}} = -\frac{1}{3} J^{-\frac{1}{3}} \lambda_{(A)}^{-1} \lambda_B + J^{-\frac{1}{3}} \delta_{B(A)} \tag{704.23}$$

since

$$\frac{\partial J^{-\frac{1}{3}}}{\partial \lambda_{(A)}} = -\frac{1}{3} J^{-\frac{4}{3}} \frac{\partial \lambda_1 \lambda_2 \lambda_3}{\partial \lambda_{(A)}} = -\frac{1}{3} J^{-\frac{4}{3}} J \lambda_{(A)}^{-1} = -\frac{1}{3} J^{-\frac{1}{3}} \lambda_{(A)}^{-1} \tag{704.24}$$

then

$$\begin{aligned}
w_A &= -\frac{1}{3} J^{-\frac{1}{3}} \frac{\partial isoW}{\partial \tilde{\lambda}_B} \lambda_{(A)}^{-1} \lambda_B \lambda_{(A)} + J^{-\frac{1}{3}} \frac{\partial isoW}{\partial \tilde{\lambda}_B} \delta_{B(A)} \lambda_{(A)} \\
&= -\frac{1}{3} \frac{\partial isoW}{\partial \tilde{\lambda}_B} \tilde{\lambda}_B + \frac{\partial isoW}{\partial \tilde{\lambda}_{(A)}} \tilde{\lambda}_{(A)}
\end{aligned} \tag{704.25}$$

704.6 Derivation of Y_{AB}

By starting from equation 704.20

$$Y_{AB} = \frac{\partial w_A}{\partial \lambda_B} \lambda_{(B)} \quad (704.26)$$

and by using equation 704.25

$$w_A = -\frac{1}{3} \frac{\partial^{iso}W}{\partial \tilde{\lambda}_C} \tilde{\lambda}_C + \frac{\partial^{iso}W}{\partial \tilde{\lambda}_{(A)}} \tilde{\lambda}_{(A)} \quad (704.27)$$

we can write:

$$Y_{AB} = \frac{\partial w_A}{\partial \tilde{\lambda}_D} \frac{\partial \tilde{\lambda}_D}{\partial \lambda_B} \lambda_{(B)} \quad (704.28)$$

By first considering $\partial w_A / \partial \tilde{\lambda}_D$ we get:

$$\begin{aligned} \frac{\partial w_A}{\partial \tilde{\lambda}_D} &= \frac{\partial \left(-\frac{1}{3} \frac{\partial^{iso}W}{\partial \tilde{\lambda}_C} \tilde{\lambda}_C + \frac{\partial^{iso}W}{\partial \tilde{\lambda}_{(A)}} \tilde{\lambda}_{(A)} \right)}{\partial \tilde{\lambda}_D} \\ &= -\frac{1}{3} \frac{\partial^2 isoW}{\partial \tilde{\lambda}_C \partial \tilde{\lambda}_D} \tilde{\lambda}_C - \frac{1}{3} \frac{\partial^{iso}W}{\partial \tilde{\lambda}_C} \frac{\partial \tilde{\lambda}_C}{\partial \tilde{\lambda}_D} + \frac{\partial^2 isoW}{\partial \tilde{\lambda}_{(A)} \partial \tilde{\lambda}_D} \tilde{\lambda}_{(A)} + \frac{\partial^{iso}W}{\partial \tilde{\lambda}_{(A)}} \frac{\partial \tilde{\lambda}_{(A)}}{\partial \tilde{\lambda}_D} \\ &= -\frac{1}{3} \frac{\partial^2 isoW}{\partial \tilde{\lambda}_C \partial \tilde{\lambda}_D} \tilde{\lambda}_C - \frac{1}{3} \frac{\partial^{iso}W}{\partial \tilde{\lambda}_C} \delta_{CD} + \frac{\partial^2 isoW}{\partial \tilde{\lambda}_{(A)} \partial \tilde{\lambda}_D} \tilde{\lambda}_{(A)} + \frac{\partial^{iso}W}{\partial \tilde{\lambda}_{(A)}} \delta_{(A)D} \\ &= -\frac{1}{3} \frac{\partial^2 isoW}{\partial \tilde{\lambda}_C \partial \tilde{\lambda}_D} \tilde{\lambda}_C - \frac{1}{3} \frac{\partial^{iso}W}{\partial \tilde{\lambda}_D} + \frac{\partial^2 isoW}{\partial \tilde{\lambda}_{(A)} \partial \tilde{\lambda}_D} \tilde{\lambda}_{(A)} + \frac{\partial^{iso}W}{\partial \tilde{\lambda}_{(A)}} \delta_{(A)D} \end{aligned} \quad (704.29)$$

Next, from equation 704.23, we have that

$$\frac{\partial \tilde{\lambda}_D}{\partial \lambda_{(B)}} = -\frac{1}{3} J^{-\frac{1}{3}} \lambda_{(B)}^{-1} \lambda_D + J^{-\frac{1}{3}} \delta_{D(B)} \quad (704.30)$$

and by multiplying the result for $\partial w_A / \partial \tilde{\lambda}_D$ from equation 704.29 and the result for $\partial \tilde{\lambda}_D / \partial \lambda_{(B)}$ from equation 704.30 we obtain:

$$\begin{aligned} \frac{\partial w_A}{\partial \tilde{\lambda}_D} \frac{\partial \tilde{\lambda}_D}{\partial \lambda_{(B)}} &= + \frac{1}{9} \frac{\partial^{2iso}W}{\partial \tilde{\lambda}_C \partial \tilde{\lambda}_D} \tilde{\lambda}_C J^{-\frac{1}{3}} \lambda_{(B)}^{-1} \lambda_D - \frac{1}{3} \frac{\partial^{2iso}W}{\partial \tilde{\lambda}_C \partial \tilde{\lambda}_D} \tilde{\lambda}_C J^{-\frac{1}{3}} \delta_{D(B)} \\ &\quad + \frac{1}{9} \frac{\partial^{iso}W}{\partial \tilde{\lambda}_D} J^{-\frac{1}{3}} \lambda_{(B)}^{-1} \lambda_D - \frac{1}{3} \frac{\partial^{iso}W}{\partial \tilde{\lambda}_D} J^{-\frac{1}{3}} \delta_{D(B)} \\ &\quad - \frac{1}{3} \frac{\partial^{2iso}W}{\partial \tilde{\lambda}_{(A)} \partial \tilde{\lambda}_D} \tilde{\lambda}_{(A)} J^{-\frac{1}{3}} \lambda_{(B)}^{-1} \lambda_D + \frac{\partial^{2iso}W}{\partial \tilde{\lambda}_{(A)} \partial \tilde{\lambda}_D} \tilde{\lambda}_{(A)} J^{-\frac{1}{3}} \delta_{D(B)} \\ &\quad - \frac{1}{3} \frac{\partial^{iso}W}{\partial \tilde{\lambda}_{(A)}} \delta_{(A)D} J^{-\frac{1}{3}} \lambda_{(B)}^{-1} \lambda_D + \frac{\partial^{iso}W}{\partial \tilde{\lambda}_{(A)}} \delta_{(A)D} J^{-\frac{1}{3}} \delta_{D(B)} \\ &= + \frac{1}{9} \frac{\partial^{2iso}W}{\partial \tilde{\lambda}_C \partial \tilde{\lambda}_D} \tilde{\lambda}_C \lambda_{(B)}^{-1} \tilde{\lambda}_D - \frac{1}{3} \frac{\partial^{2iso}W}{\partial \tilde{\lambda}_C \partial \tilde{\lambda}_{(B)}} \tilde{\lambda}_C J^{-\frac{1}{3}} \\ &\quad + \frac{1}{9} \frac{\partial^{iso}W}{\partial \tilde{\lambda}_D} \lambda_{(B)}^{-1} \tilde{\lambda}_D - \frac{1}{3} \frac{\partial^{iso}W}{\partial \tilde{\lambda}_{(B)}} J^{-\frac{1}{3}} \\ &\quad - \frac{1}{3} \frac{\partial^{2iso}W}{\partial \tilde{\lambda}_{(A)} \partial \tilde{\lambda}_D} \tilde{\lambda}_{(A)} \lambda_{(B)}^{-1} \tilde{\lambda}_D + \frac{\partial^{2iso}W}{\partial \tilde{\lambda}_{(A)} \partial \tilde{\lambda}_{(B)}} \tilde{\lambda}_{(A)} J^{-\frac{1}{3}} \\ &\quad - \frac{1}{3} \frac{\partial^{iso}W}{\partial \tilde{\lambda}_{(A)}} \lambda_{(B)}^{-1} \tilde{\lambda}_{(A)} + \frac{\partial^{iso}W}{\partial \tilde{\lambda}_{(A)}} \delta_{(A)(B)} J^{-\frac{1}{3}} \end{aligned} \quad (704.31)$$

where equation 704.22 was used. The final form for Y_{AB} is obtained by multiplying equation 704.31 with $\tilde{\lambda}_{(B)}$ to obtain:

$$\begin{aligned}
 Y_{AB} = & \frac{\partial w_A}{\partial \tilde{\lambda}_D} \frac{\partial \tilde{\lambda}_D}{\partial \lambda_B} \lambda_{(B)} = \\
 & + \frac{1}{9} \frac{\partial^2 isoW}{\partial \tilde{\lambda}_C \partial \tilde{\lambda}_D} \tilde{\lambda}_C \lambda_{(B)}^{-1} \tilde{\lambda}_D \lambda_{(B)} - \frac{1}{3} \frac{\partial^2 isoW}{\partial \tilde{\lambda}_C \partial \tilde{\lambda}_{(B)}} \tilde{\lambda}_C \tilde{\lambda}_{(B)} \\
 & + \frac{1}{9} \frac{\partial^2 isoW}{\partial \tilde{\lambda}_D} \lambda_{(B)}^{-1} \tilde{\lambda}_D \lambda_{(B)} - \frac{1}{3} \frac{\partial^2 isoW}{\partial \tilde{\lambda}_{(B)}} \tilde{\lambda}_{(B)} \\
 & - \frac{1}{3} \frac{\partial^2 isoW}{\partial \tilde{\lambda}_{(A)} \partial \tilde{\lambda}_D} \tilde{\lambda}_{(A)} \lambda_{(B)}^{-1} \tilde{\lambda}_D \lambda_{(B)} + \frac{\partial^2 isoW}{\partial \tilde{\lambda}_{(A)} \partial \tilde{\lambda}_{(B)}} \tilde{\lambda}_{(A)} \tilde{\lambda}_{(B)} \\
 & - \frac{1}{3} \frac{\partial^2 isoW}{\partial \tilde{\lambda}_{(A)} \partial \tilde{\lambda}_{(B)}} \lambda_{(B)}^{-1} \tilde{\lambda}_{(A)} \lambda_{(B)} + \frac{\partial^2 isoW}{\partial \tilde{\lambda}_{(A)}} \delta_{(A)(B)} \tilde{\lambda}_{(B)}
 \end{aligned} \tag{704.32}$$

By recognizing that $\lambda_{(B)}^{-1} \lambda_{(B)} \equiv 1$ and after rearranging elements, we can finally write the equation for Y_{AB} as:

$$\begin{aligned}
 Y_{AB} = & \frac{\partial^2 isoW}{\partial \tilde{\lambda}_{(A)} \partial \tilde{\lambda}_{(B)}} \delta_{(A)(B)} \tilde{\lambda}_{(B)} + \frac{\partial^2 isoW}{\partial \tilde{\lambda}_{(A)} \partial \tilde{\lambda}_{(B)}} \tilde{\lambda}_{(A)} \tilde{\lambda}_{(B)} \\
 & - \frac{1}{3} \left(\frac{\partial^2 isoW}{\partial \tilde{\lambda}_C \partial \tilde{\lambda}_{(B)}} \tilde{\lambda}_C \tilde{\lambda}_{(B)} + \frac{\partial^2 isoW}{\partial \tilde{\lambda}_{(B)} \partial \tilde{\lambda}_D} \tilde{\lambda}_{(B)} + \frac{\partial^2 isoW}{\partial \tilde{\lambda}_{(A)} \partial \tilde{\lambda}_D} \tilde{\lambda}_{(A)} \tilde{\lambda}_D + \frac{\partial^2 isoW}{\partial \tilde{\lambda}_{(A)} \partial \tilde{\lambda}_{(B)}} \tilde{\lambda}_{(A)} \right) \\
 & + \frac{1}{9} \left(\frac{\partial^2 isoW}{\partial \tilde{\lambda}_C \partial \tilde{\lambda}_D} \tilde{\lambda}_C \tilde{\lambda}_D + \frac{\partial^2 isoW}{\partial \tilde{\lambda}_D} \tilde{\lambda}_D \right)
 \end{aligned} \tag{704.33}$$

Appendix 705

Body and Surface Wave Analytic Solutions

(2005-2001-2010-2011-2018-2019-2021-)

(In collaboration with Dr. Nima Tafazzoli, Mr. Chang-Gyun Jeong, and Dr. Hexiang Wang)

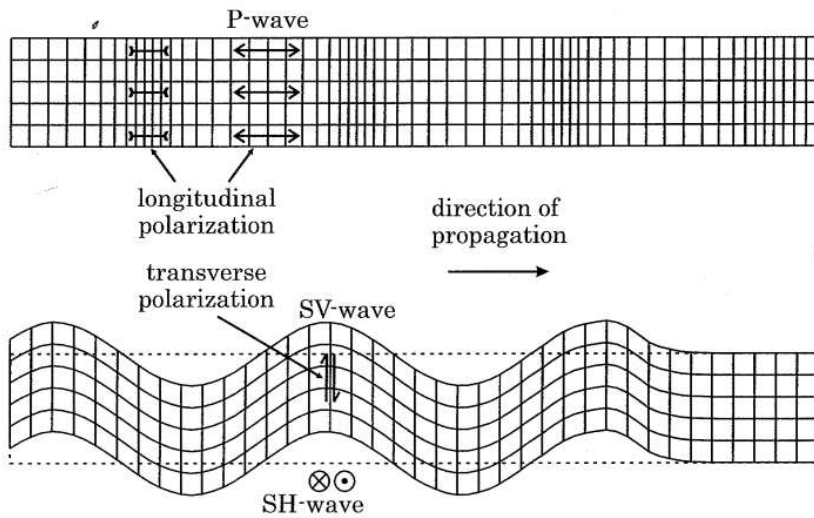


Figure 705.1: Motion due to plane pressure waves (P-wave) and shear waves (S-wave) ([Semblat and Pecker, 2009](#))

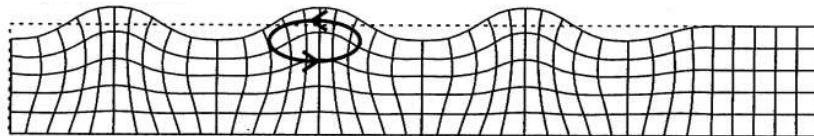


Figure 705.2: Particle movement due to surface Rayleigh waves near free surface ([Semblat and Pecker, 2009](#))

705.1 3D Seismic Wave Field: Analytic Solution

In this chapter, wave field generation methods using analytic solution, and frequency wavenumber integration method are introduced. Theoretical background and examples are presented for each method.

705.1.1 Analytic solution

Seismic waves can be categorized as body waves and surface waves. The seismic body waves are traveling through the interior of the earth whereas the surface waves are traveling through the surface of the earth.

There are two different body waves, such as the pressure wave (also called as P wave, Figure 705.1 top) and the shear waves (also called as S wave, Figure 705.1 bottom). The shear waves which have the same velocity V_S can be polarized along its plane location to the direction of propagation (vertical plane - SV and horizontal plane - SH, Figure 705.1 bottom).

Surface waves are mainly categorized as Rayliegh waves ([Rayleigh, 1885](#)) and Love waves ([Love,](#)

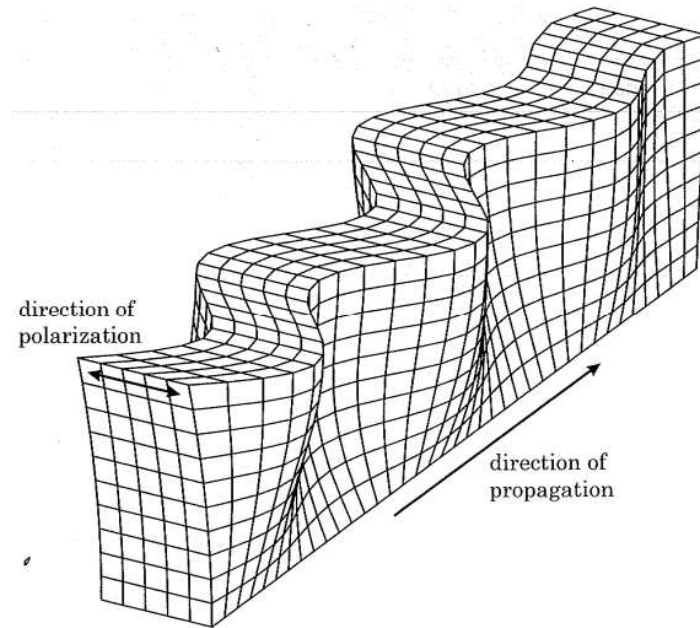


Figure 705.3: Displacements due to surface Love waves (Semblat and Pecker, 2009)

1911). The Rayleigh waves induce elliptical ground movement near the surface (Figure 705.2) whereas the Love waves induce shearing movement (Figure 705.3).

Following sections introduce full three dimensional exact-solution and its examples for plane body and surface waves in homogeneous media. The chapter does not include full derivation of equations since it's beyond the scope. Instead, final equations for body and surface waves are presented.

The original works for those problems are done by Green (1848), Knott (1899), and Wiechert and Zoeppritz (1907). The notations and equations hereafter are mainly based on Semblat and Pecker (2009) and Aki and Richard's work (Aki and Richards, 2002).

705.1.1.1 Wave equations for body waves

Hereafter, the reflection and refraction coefficients are indicated by using its wave component symbols. An acute and grave accents are adapted to explain the direction of propagation. The acute accent indicates an upcoming wave, and the grave accent indicates a down-going wave (e.g. \acute{P} , \grave{P}). For example, if the upcoming incident wave type is P and down-going reflected wave type is S, then reflected wave will be indicated as $\acute{P}\grave{S}$.

Reflected and transmitted waves arising from incident SH wave In the case of SH incident wave on the interface between two half-spaces, reflected wave is SH wave (Figure 705.4). The vector displacements

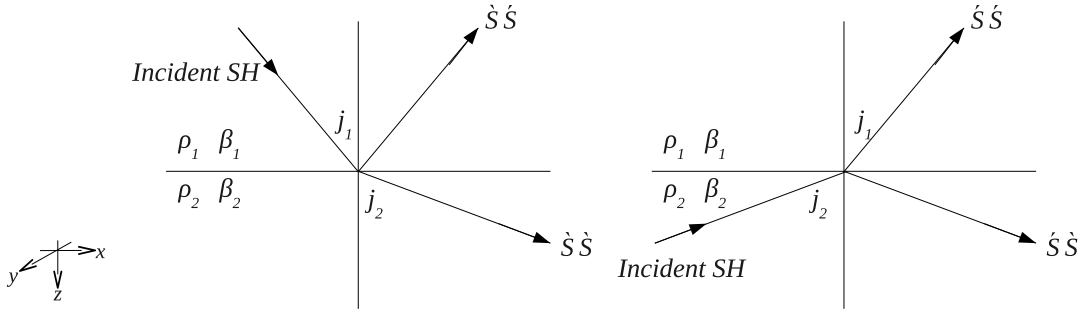


Figure 705.4: Schematic cartoon to show all possible coefficients of reflection and transmission with SH incident wave

for the downgoing and upgoing incident SH waves can be calculated as below equation (705.1) and (705.2), respectively (Aki and Richards, 2002).

$$\begin{aligned}
 (\text{Downgoing SH}) &= S(0, S, 0) \exp \left[i\omega \left(px + \frac{\cos j_1}{\beta_1} z - t \right) \right] \\
 (\text{Upgoing SH}) &= S(0, S, 0) \dot{S} \dot{S} \exp \left[i\omega \left(px - \frac{\cos j_1}{\beta_1} z - t \right) \right] \\
 (\text{Downgoing SH}) &= S(0, S, 0) \dot{S} \dot{S} \exp \left[i\omega \left(px + \frac{\cos j_2}{\beta_2} z - t \right) \right]
 \end{aligned} \tag{705.1}$$

$$\begin{aligned}
 (\text{Upgoing SH}) &= S(0, S, 0) \exp \left[i\omega \left(px - \frac{\cos j_2}{\beta_2} z - t \right) \right] \\
 (\text{Upgoing SH}) &= S(0, S, 0) \dot{S} \dot{S} \exp \left[i\omega \left(px - \frac{\cos j_1}{\beta_1} z - t \right) \right] \\
 (\text{downgoing SH}) &= S(0, S, 0) \dot{S} \dot{S} \exp \left[i\omega \left(px + \frac{\cos j_2}{\beta_2} z - t \right) \right]
 \end{aligned} \tag{705.2}$$

where,

$$\begin{aligned}
 \dot{S} \dot{S} &= \frac{\rho_1 \beta_1 \cos j_1 - \rho_2 \beta_2 \cos j_2}{\Delta} \\
 \dot{S} \dot{S} &= \frac{2\rho_2 \beta_2 \cos j_2}{\Delta} \\
 \dot{S} \dot{S} &= \frac{2\rho_1 \beta_1 \cos j_1}{\Delta} \\
 \dot{S} \dot{S} &= -\dot{S} \dot{S} \\
 \Delta &= \rho_1 \beta_1 \cos j_1 + \rho_2 \beta_2 \cos j_2
 \end{aligned} \tag{705.3}$$

where α is the P wave velocity, β is the S wave velocity, ρ is the density, $p = (\sin i)/\alpha = (\sin j)/\beta$ is the ray parameter, and S is the amplitude of the incident wave.

Figure 705.4 shows all possible reflection and transmission coefficients with incident SH waves. Equation (705.4) is a ‘scattering matrix’ which includes every possible reflection and transmission coefficients

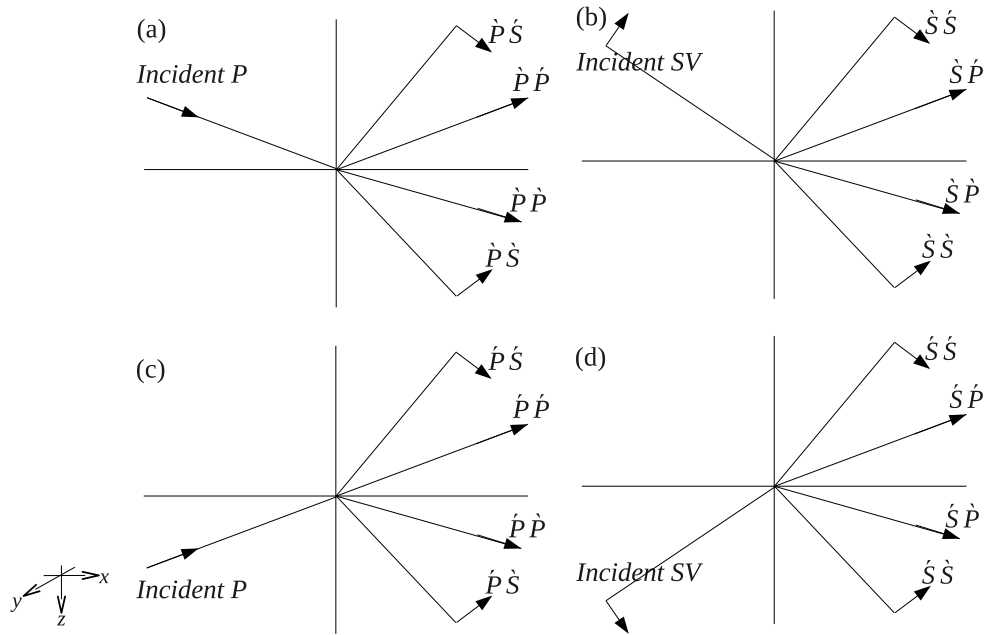


Figure 705.5: Schematic cartoon to show all possible coefficients of reflection and transmission with P/SV incident wave

for the problem. The matrix components have one to one relation with Figure 705.4.

$$\begin{pmatrix} \dot{S}\dot{S} & \dot{S}\dot{S} \\ \dot{S}\dot{S} & \dot{S}\dot{S} \end{pmatrix} \quad (705.4)$$

Reflected and transmitted waves arising from incident P/SV wave The displacements generated by the downgoing incident P/SV and upgoing incident P/SV waves can be calculated as below equation (705.5), (705.6), (705.7), and (705.8), respectively (Figure 705.5) (Aki and Richards, 2002).

$$\begin{aligned}
 (\text{Downgoing P}) &= S(\sin i_1, 0, \cos i_1) \exp \left[i\omega \left(px + \frac{\cos i_1}{\alpha_1} z - t \right) \right] \\
 (\text{Upgoing P}) &= S(\sin i_1, 0, -\cos i_1) \dot{P}\dot{P} \exp \left[i\omega \left(px - \frac{\cos i_1}{\alpha_1} z - t \right) \right] \\
 (\text{Upgoing SV}) &= S(\cos j_1, 0, \sin j_1) \dot{P}\dot{S} \exp \left[i\omega \left(px - \frac{\cos j_1}{\beta_1} z - t \right) \right] \\
 (\text{Downgoing P}) &= S(\sin i_2, 0, \cos i_2) \dot{P}\dot{P} \exp \left[i\omega \left(px + \frac{\cos i_2}{\alpha_2} z - t \right) \right] \\
 (\text{Downgoing SV}) &= S(\cos j_2, 0, -\sin j_2) \dot{P}\dot{S} \exp \left[i\omega \left(px + \frac{\cos j_2}{\beta_2} z - t \right) \right]
 \end{aligned} \quad (705.5)$$

$$\begin{aligned}
 & (\text{Downgoing SV}) = S(\cos j_1, 0, -\sin j_1) \exp \left[i\omega \left(px + \frac{\cos j_1}{\beta_1} z - t \right) \right] \\
 & (\text{Upgoing P}) = S(\sin i_1, 0, -\cos i_1) \dot{S} \dot{P} \exp \left[i\omega \left(px - \frac{\cos i_1}{\alpha_1} z - t \right) \right] \\
 & (\text{Upgoing SV}) = S(\cos j_1, 0, \sin j_1) \dot{S} \dot{S} \exp \left[i\omega \left(px - \frac{\cos j_1}{\beta_1} z - t \right) \right] \\
 & (\text{Downgoing P}) = S(\sin i_2, 0, \cos i_2) \dot{S} \dot{P} \exp \left[i\omega \left(px + \frac{\cos i_2}{\alpha_2} z - t \right) \right] \\
 & (\text{Downgoing SV}) = S(\cos j_2, 0, -\sin j_2) \dot{S} \dot{S} \exp \left[i\omega \left(px + \frac{\cos j_2}{\beta_2} z - t \right) \right]
 \end{aligned} \tag{705.6}$$

$$\begin{aligned}
 & (\text{Upgoing P}) = S(\sin i_2, 0, -\cos i_2) \exp \left[i\omega \left(px - \frac{\cos i_2}{\alpha_2} z - t \right) \right] \\
 & (\text{Upgoing P}) = S(\sin i_1, 0, -\cos i_1) \dot{P} \dot{P} \exp \left[i\omega \left(px - \frac{\cos i_1}{\alpha_1} z - t \right) \right] \\
 & (\text{Upgoing SV}) = S(\cos j_1, 0, \sin j_1) \dot{P} \dot{S} \exp \left[i\omega \left(px - \frac{\cos j_1}{\beta_1} z - t \right) \right] \\
 & (\text{Downgoing P}) = S(\sin i_2, 0, \cos i_2) \dot{P} \dot{P} \exp \left[i\omega \left(px + \frac{\cos i_2}{\alpha_2} z - t \right) \right] \\
 & (\text{Downgoing SV}) = S(\cos j_2, 0, -\sin j_2) \dot{P} \dot{S} \exp \left[i\omega \left(px + \frac{\cos j_2}{\beta_2} z - t \right) \right]
 \end{aligned} \tag{705.7}$$

$$\begin{aligned}
 & (\text{Upgoing SV}) = S(\cos j_2, 0, \sin j_2) \exp \left[i\omega \left(px - \frac{\cos j_2}{\beta_2} z - t \right) \right] \\
 & (\text{Upgoing P}) = S(\sin i_1, 0, -\cos i_1) \dot{S} \dot{P} \exp \left[i\omega \left(px - \frac{\cos i_1}{\alpha_1} z - t \right) \right] \\
 & (\text{Upgoing SV}) = S(\cos j_1, 0, \sin j_1) \dot{S} \dot{S} \exp \left[i\omega \left(px - \frac{\cos j_1}{\beta_1} z - t \right) \right] \\
 & (\text{Downgoing P}) = S(\sin i_2, 0, \cos i_2) \dot{S} \dot{P} \exp \left[i\omega \left(px + \frac{\cos i_2}{\alpha_2} z - t \right) \right] \\
 & (\text{Downgoing SV}) = S(\cos j_2, 0, -\sin j_2) \dot{S} \dot{S} \exp \left[i\omega \left(px + \frac{\cos j_2}{\beta_2} z - t \right) \right]
 \end{aligned} \tag{705.8}$$

where,

$$\begin{aligned}
 \dot{P}\dot{P} &= \left[\left(b \frac{\cos i_1}{\alpha_1} - c \frac{\cos i_2}{\alpha_2} \right) F - \left(a + d \frac{\cos i_1 \cos j_2}{\alpha_1 \beta_2} \right) H p^2 \right] / \mathbf{D} \\
 \dot{P}\dot{S} &= -2 \frac{\cos i_1}{\alpha_1} \left(ab + cd \frac{\cos i_2 \cos j_2}{\alpha_2 \beta_2} \right) p \alpha_1 / (\beta_1 \mathbf{D}) \\
 \dot{P}\dot{P} &= 2 \rho_1 \frac{\cos i_1}{\alpha_1} F \alpha_1 / (\alpha_2 \mathbf{D}) \\
 \dot{P}\dot{S} &= 2 \rho_1 \frac{\cos i_1}{\alpha_1} H p \alpha_1 / (\beta_2 \mathbf{D}) \\
 \dot{S}\dot{P} &= -2 \frac{\cos j_1}{\beta_1} \left(ab + cd \frac{\cos i_2 \cos j_2}{\alpha_2 \beta_2} \right) p \beta_1 / (\alpha_1 \mathbf{D}) \\
 \dot{S}\dot{S} &= - \left[\left(b \frac{\cos j_1}{\beta_1} - c \frac{\cos j_2}{\beta_2} \right) E - \left(a + d \frac{\cos i_2 \cos j_1}{\alpha_2 \beta_1} \right) G p^2 \right] / \mathbf{D} \\
 \dot{S}\dot{P} &= -2 \rho_1 \frac{\cos j_1}{\beta_1} G p \beta_1 / (\alpha_2 \mathbf{D}) \\
 \dot{S}\dot{S} &= 2 \rho_1 \frac{\cos j_1}{\beta_1} E \beta_1 / (\beta_2 \mathbf{D}) \\
 \dot{P}\dot{P} &= 2 \rho_2 \frac{\cos i_2}{\alpha_2} F \alpha_2 / (\alpha_1 \mathbf{D}) \\
 \dot{P}\dot{S} &= -2 \rho_2 \frac{\cos i_2}{\alpha_2} G p \alpha_2 / (\alpha_2 \mathbf{D}) \\
 \dot{P}\dot{P} &= - \left[\left(b \frac{\cos i_1}{\alpha_1} - c \frac{\cos i_2}{\alpha_2} \right) F + \left(a + d \frac{\cos i_2 \cos j_1}{\alpha_2 \beta_1} \right) G p^2 \right] / \mathbf{D} \\
 \dot{P}\dot{S} &= 2 \frac{\cos i_2}{\alpha_2} \left(ac + bd \frac{\cos i_1 \cos j_1}{\alpha_1 \beta_1} \right) p \alpha_2 / (\beta_2 \mathbf{D}) \\
 \dot{S}\dot{P} &= 2 \rho_2 \frac{\cos j_2}{\beta_2} H p \beta_2 / (\alpha_1 \mathbf{D}) \\
 \dot{S}\dot{S} &= 2 \rho_2 \frac{\cos j_2}{\beta_2} E \beta_2 / (\beta_1 \mathbf{D}) \\
 \dot{S}\dot{P} &= 2 \frac{\cos j_2}{\beta_2} \left(ac + bd \frac{\cos i_1 \cos j_1}{\alpha_1 \beta_1} \right) p \beta_2 / (\alpha_2 \mathbf{D}) \\
 \dot{S}\dot{S} &= \left[\left(b \frac{\cos j_1}{\beta_1} - c \frac{\cos j_2}{\beta_2} \right) E + \left(a + d \frac{\cos i_1 \cos j_2}{\alpha_1 \beta_2} \right) H p^2 \right] / \mathbf{D}
 \end{aligned} \tag{705.9}$$

$$\begin{aligned}
 a &= \rho_2 (1 - 2 \beta_2^2 p^2) - \rho_1 (1 - 2 \beta_1^2 p^2) \\
 b &= \rho_2 (1 - 2 \beta_2^2 p^2) + 2 \rho_1 \beta_1^2 p^2 \\
 c &= \rho_1 (1 - 2 \beta_1^2 p^2) + 2 \rho - 2 \beta_2^2 p^2 \\
 d &= 2(\rho_2 \beta_2^2 - \rho_1 \beta_1^2)
 \end{aligned} \tag{705.10}$$

$$\begin{aligned}
 E &= b \frac{\cos i_1}{\alpha_1} + c \frac{\cos i_2}{\alpha_2} \\
 F &= b \frac{\cos j_1}{\beta_1} + c \frac{\cos j_2}{\beta_2} \\
 G &= a - d \frac{\cos i_1}{\alpha_1} \frac{\cos j_2}{\beta_2} \\
 H &= a - d \frac{\cos i_2}{\alpha_2} \frac{\cos j_1}{\beta_1} \\
 \mathbf{D} &= EF + GH p^2 = (\det \mathbf{M}) / (\alpha_1 \alpha_2 \beta_1 \beta_2)
 \end{aligned} \tag{705.11}$$

$$\mathbf{M} = \begin{pmatrix} -\alpha_1 p & -\cos j_1 & \alpha_2 p & \cos j_2 \\ \cos i_1 & -\beta_1 p & \cos i_2 & -\beta_2 p \\ 2\rho_1 \beta_1^2 p \cos i_1 & \rho_1 \beta_1 (1 - 2\beta_1^2 p^2) & 2\rho_2 \beta_2^2 p \cos i_2 & \rho_2 \beta_2 (1 - 2\beta_2^2 p^2) \\ -\rho_1 \alpha_1 (1 - 2\beta_1^2 p^2) & 2\rho_1 \beta_1^2 p \cos j_1 & \rho_2 \alpha_2 (1 - 2\beta_2^2 p^2) & -2\rho_2 \beta_2^2 p \cos j_2 \end{pmatrix} \tag{705.12}$$

where α is the P wave velocity, β is the S wave velocity, ρ is the mass density, $p = (\sin i)/\alpha = (\sin j)/\beta$ is the ray parameter, and S is the amplitude of the incident wave.

Similar as the incident SH wave case, Figure 705.5 shows all possible reflection and transmission coefficients. Below equation (705.13) is a ‘scattering matrix’ which includes every possible reflection and transmission coefficients for the problem. The matrix components have one to one relation with Figure 705.5.

$$\begin{pmatrix} \dot{P}\dot{P} & \dot{S}\dot{P} & \dot{P}\dot{P} & \dot{S}\dot{P} \\ \dot{P}\dot{S} & \dot{S}\dot{S} & \dot{P}\dot{S} & \dot{S}\dot{S} \\ \dot{P}\dot{P} & \dot{S}\dot{P} & \dot{P}\dot{P} & \dot{S}\dot{P} \\ \dot{P}\dot{S} & \dot{S}\dot{S} & \dot{P}\dot{S} & \dot{S}\dot{S} \end{pmatrix} \tag{705.13}$$

705.1.1.2 Wave equations for surface waves

Surface wave with incident SH wave – Love wave The displacements of surface wave due to the incident SH wave can be obtained by solving wave equations under free-surface condition (zero traction on surface). Below equation (705.14) shows the time history displacement with incident SH wave

(Semblat and Pecker, 2009).

$$\begin{aligned} u_y^i &= A_{SH} \exp \left[\frac{i\omega}{V_S} \left(x \sin \theta_i^{SH} + z \cos \theta_i^{SH} - V_S t \right) \right] \\ u_y^R &= R_{SH} \exp \left[\frac{i\omega}{V_S} \left(x \sin \theta_R^{SH} - z \cos \theta_R^{SH} - V_S t \right) \right] \\ u_y &= u_y^i + u_y^R = 2A_{SH} \cos \left(\frac{\omega z \cos \theta_i^{SH}}{V_S} \right) \exp \left[\frac{i\omega}{V_S} (x \sin \theta_i - V_S t) \right] \end{aligned} \quad (705.14)$$

As shown in equation (705.14) displacements of waves induced by incident SH waves can be calculated by summing incident and reflected waves on the ground surface. The particle movement of a Love wave is a perpendicular to the propagation plane.

Surface wave with incident P/SV wave – Rayleigh wave. Equation (705.15) shows the displacements of surface wave due to the incident P/SV waves (Semblat and Pecker, 2009).

$$\begin{aligned} u_x &= \frac{i\omega}{V_R} A \left(e^{az} - \frac{2ab}{b^2 + \omega^2/V_R^2} e^{bz} \right) \exp \left[\frac{i\omega}{V_R} (x - V_R t) \right] \\ u_z &= aA \left(e^{az} - \frac{2\omega^2/V_R^2}{b^2 + \omega^2/V_R^2} e^{bz} \right) \exp \left[\frac{i\omega}{V_R} (x - V_R t) \right] \end{aligned} \quad (705.15)$$

where, $a^2 = \frac{\omega^2}{V_R^2} - \frac{\omega^2}{V_P^2}$, and $b^2 = \frac{\omega^2}{V_R^2} - \frac{\omega^2}{V_S^2}$.

Imaginary term on u_x shows that the components has a 90° phase shift from u_z . The particle movement of the wave is ellipses in x, z plane.

705.2 Matlab code – body wave solution

Listing 705.1: Example MATLAB code for surface waves

```

1 % =====
2 % body.m: inclined wave propagation closed-form solution for layered ground
3 %
4 % ref. Waves and Vibrations in Soils (Semblat and Pecker)
5 %
6 % Chang-Gyun Jeong
7 % Last update: 05/24/2011
8 % =====
9
10 clear all; clc;
11
12 %% initial condition
13 % wave type 'P' / 'SV' / 'SH'
14 wave = 'P';
15
16 % time

```

```

17 t_low = 0; t_up = 1;
18 dt = 0.01;
19 t_no = (t_up - t_low) / dt;
20
21 % x and z
22 min_x = 0; max_x = 100;
23 min_z = 0; max_z = 100;
24 delta_x = 2; delta_z = 2;
25
26 x = min_x : delta_x : max_x; x = x';
27 z = min_z : delta_z : max_z; z = z';
28
29 % frequency
30 freq = 10;
31 omega = freq * 2 * pi;
32
33
34 % incident angle and amplitude
35 th_P_i = 20; A_P = 1;
36 th_SV_i = 20; A_SV = 1;
37 th_SH_i = 20; A_SH = 1;
38
39 % velocity and shear modulus
40 V_S1 = 1000; V_S2 = 300;
41
42 nu = 0.3;
43 gamma = 20000; % (N/m^3)
44
45 V_P1 = V_S1 * sqrt((2 - 2 * nu) / (1 - 2 * nu));
46 V_P2 = V_S2 * sqrt((2 - 2 * nu) / (1 - 2 * nu));
47
48 G_1 = gamma * V_S1^2; G_2 = gamma * V_S2^2;
49
50 X_S = V_S2 / V_S1;
51 X_1 = V_P1 / V_S1;
52 X_2 = V_P2 / V_S2;
53
54 %% calculation
55 switch upper(wave)
56 case {'P'}
57     % angle and amplitude
58     th_P_P_r = th_P_i;
59     th_P_P_t = asind(sind(th_P_i) * V_P2 / V_P1);
60     th_SV_P_r = asind(sind(th_P_i) * V_S1 / V_P1);
61     th_SV_P_t = asind(sind(th_P_i) * V_S2 / V_P1);
62
63     temp_left = [-sind(th_P_i), -cosd(th_SV_P_r), sind(th_P_P_t), -cos(th_SV_P_t);...
64         cosd(th_P_i), -sind(th_SV_P_r), cosd(th_P_P_t), sind(th_SV_P_t);...
65         sind(2 * th_P_i), X_1 * cosd(2 * th_SV_P_r), X_1 / X_2 * X_S...
66         * sind(2 * th_P_P_t), -X_1 * X_S * cosd(2 * th_SV_P_t);...
67         -X_1 * cosd(2 * th_SV_P_r), sind(2 * th_SV_P_r), X_2 * X_S...
68         * cosd(2 * th_SV_P_t), X_S * sind(2 * th_SV_P_t)];
69
70     temp_right = A_P * [sind(th_P_i); cosd(th_P_i); sind(2 * th_P_i); X_1 *...
71         cosd(2 * th_SV_P_r)];
72
73     temp = temp_left \ temp_right;
74
75     R_SV_P = temp(1, 1);
76     R_P_P = temp(2, 1);
77     T_SV_P = temp(3, 1);
78     T_P_P = temp(4, 1);
79
80     % initialize matrix

```

```

81 ux_P_i = zeros(max(size(z)), max(size(x)));
82 uz_P_i = zeros(max(size(z)), max(size(x)));
83 ux_P_P_r = zeros(max(size(z)), max(size(x)));
84 uz_P_P_r = zeros(max(size(z)), max(size(x)));
85 ux_SV_P_r = zeros(max(size(z)), max(size(x)));
86 uz_SV_P_r = zeros(max(size(z)), max(size(x)));
87 ux_P_P_t = zeros(max(size(z)), max(size(x)));
88 uz_P_P_t = zeros(max(size(z)), max(size(x)));
89 ux_SV_P_t = zeros(max(size(z)), max(size(x)));
90 uz_SV_P_t = zeros(max(size(z)), max(size(x)));
91
92 % calculate incident, reflected, and transmitted wave
93 for t = t_low : dt : t_up
94     for i = 1 : max(size(x))
95         for j = 1 : max(size(z))
96             % incident P
97             ux_P_i(i, j) = real(A_P * sind(th_P_i) * (exp((1i * omega / V_P1) ...
98                 * (x(i, 1) * sind(th_P_i) + z(j, 1) * cosd(th_P_i) - V_P1 * t))));;
99             uz_P_i(i, j) = real(A_P * cosd(th_P_i) * (exp((1i * omega / V_P1) ...
100                 * (x(i, 1) * sind(th_P_i) + z(j, 1) * cosd(th_P_i) - V_P1 * t))));;
101             % reflected P
102             ux_P_P_r(i, j) = real(R_P_P * sind(th_P_P_r) * (exp((1i * omega / V_P1) ...
103                 * (x(i, 1) * sind(th_P_P_r) - z(j, 1) * cosd(th_P_P_r) - V_P1 * t))));;
104             uz_P_P_r(i, j) = real(-R_P_P * cosd(th_P_P_r) * (exp((1i * omega / V_P1) ...
105                 * (x(i, 1) * sind(th_P_P_r) - z(j, 1) * cosd(th_P_P_r) - V_P1 * t))));;
106             % reflected SV
107             ux_SV_P_r(i, j) = real(R_SV_P * cosd(th_SV_P_r) * (exp((1i * omega / V_S1) ...
108                 * (x(i, 1) * sind(th_SV_P_r) - z(j, 1) * cosd(th_SV_P_r) - V_S1 * t))));;
109             uz_SV_P_r(i, j) = real(R_SV_P * sind(th_SV_P_r) * (exp((1i * omega / V_S1) ...
110                 * (x(i, 1) * sind(th_SV_P_r) - z(j, 1) * cosd(th_SV_P_r) - V_S1 * t))));;
111             % transmitted P
112             ux_P_P_t(i, j) = real(T_P_P * sind(th_P_P_t) * (exp((1i * omega / V_P2) ...
113                 * (x(i, 1) * sind(th_P_P_t) + z(j, 1) * cosd(th_P_P_t) - V_P2 * t))));;
114             uz_P_P_t(i, j) = real(T_P_P * cosd(th_P_P_t) * (exp((1i * omega / V_P2) ...
115                 * (x(i, 1) * sind(th_P_P_t) + z(j, 1) * cosd(th_P_P_t) - V_P2 * t))));;
116             % transmitted SV
117             ux_SV_P_t(i, j) = real(-T_SV_P * cosd(th_SV_P_t) * (exp((1i * omega / V_S2) ...
118                 * (x(i, 1) * sind(th_SV_P_t) + z(j, 1) * cosd(th_SV_P_t) - V_S2 * t))));;
119             uz_SV_P_t(i, j) = real(T_SV_P * sind(th_SV_P_t) * (exp((1i * omega / V_S2) ...
120                 * (x(i, 1) * sind(th_SV_P_t) + z(j, 1) * cosd(th_SV_P_t) - V_S2 * t))));;
121         end
122     end
123
124     % plot
125     subplot(3,4,1)
126     surf(x, z, ux_P_i,'EdgeColor','none'); axis([0 100 0 100 -4 4])
127     xlabel('x direction'); ylabel('z direction'); view(3)
128     title('Incident P x comp.')
129     subplot(3,4,2)
130     surf(x, z, uz_P_i,'EdgeColor','none'); axis([0 100 0 100 -4 4])
131     xlabel('x direction'); ylabel('z direction'); view(3)
132     title('Incident P z comp.')
133
134     subplot(3,4,5)
135     surf(x, z, ux_P_P_r,'EdgeColor','none'); axis([0 100 0 100 -4 4])
136     xlabel('x direction'); ylabel('z direction'); view(3)
137     title('Reflected P x comp.')
138     subplot(3,4,6)
139     surf(x, z, uz_P_P_r,'EdgeColor','none'); axis([0 100 0 100 -4 4])
140     xlabel('x direction'); ylabel('z direction'); view(3)
141     title('Reflected P z comp.')
142     subplot(3,4,7)
143     surf(x, z, ux_SV_P_r,'EdgeColor','none'); axis([0 100 0 100 -4 4])
144     xlabel('x direction'); ylabel('z direction'); view(3)

```

```

145 title('Reflected SV x comp.')
146 subplot(3,4,8)
147 surf(x, z, uz_SV_P_r,'EdgeColor','none'); axis([0 100 0 100 -4 4])
148 xlabel('x direction'); ylabel('z direction'); view(3)
149 title('Reflected SV z comp.')
150
151 subplot(3,4,9)
152 surf(x, z, ux_P_P_t,'EdgeColor','none'); axis([0 100 0 100 -4 4])
153 xlabel('x direction'); ylabel('z direction'); view(3)
154 title('Refracted P x comp.')
155 subplot(3,4,10)
156 surf(x, z, uz_P_P_t,'EdgeColor','none'); axis([0 100 0 100 -4 4])
157 xlabel('x direction'); ylabel('z direction'); view(3)
158 title('Refracted P z comp.')
159 subplot(3,4,11)
160 surf(x, z, ux_SV_P_t,'EdgeColor','none'); axis([0 100 0 100 -4 4])
161 title('Refracted SV x comp.')
162 subplot(3,4,12)
163 surf(x, z, uz_SV_P_t,'EdgeColor','none'); axis([0 100 0 100 -4 4])
164 title('Refracted SV z comp.')
165
166 drawnow
167 end
168
169 case {'SV'}
170 % angle and amplitude
171 th_P_SV_r = asind(sind(th_SV_i) * V_P1 / V_S1);
172 th_P_SV_t = asind(sind(th_SV_i) * V_P2 / V_S1);
173 th_SV_SV_r = th_SV_i;
174 th_SV_SV_t = asind(sind(th_SV_i) * V_S2 / V_S1);
175
176 temp_left = [cosd(th_SV_i), sind(th_P_SV_r), cosd(th_SV_SV_t), sin(th_P_SV_t);...
177   sind(th_SV_i), -cosd(th_P_SV_r), -sind(th_SV_SV_t), cosd(th_P_SV_t);...
178   -cosd(2 * th_SV_i), (-1 / X_1) * sind(2 * th_P_SV_r), X_S...];
179 * cosd(2 * th_SV_SV_t), (-X_S * X_2) * sind(2 * th_P_SV_t);...
180 -sind(2 * th_SV_i), X_1 * cosd(2 * th_SV_SV_r), -X_S...;
181 * sind(2 * th_SV_SV_t), -X_2 * X_S * cosd(2 * th_SV_SV_t);];
182
183 temp_right = A_SV * [cosd(th_SV_i); -sind(th_SV_i); cosd(2 * th_SV_i); ...
184   -sind(2 * th_SV_i)];
185
186 temp = temp_left \ temp_right;
187
188 R_P_SV = temp(1, 1);
189 R_SV_SV = temp(2, 1);
190 T_P_SV = temp(3, 1);
191 T_SV_SV = temp(4, 1);
192
193 % initialize matrix
194 ux_SV_i = zeros(max(size(z)), max(size(x)));
195 uz_SV_i = zeros(max(size(z)), max(size(x)));
196 ux_P_SV_r = zeros(max(size(z)), max(size(x)));
197 uz_P_SV_r = zeros(max(size(z)), max(size(x)));
198 ux_SV_SV_r = zeros(max(size(z)), max(size(x)));
199 uz_SV_SV_r = zeros(max(size(z)), max(size(x)));
200 ux_P_SV_t = zeros(max(size(z)), max(size(x)));
201 uz_P_SV_t = zeros(max(size(z)), max(size(x)));
202 ux_SV_SV_t = zeros(max(size(z)), max(size(x)));
203 uz_SV_SV_t = zeros(max(size(z)), max(size(x)));
204
205 % calculate incident, reflected, and transmitted wave
206 for t = t_low : dt : t_up
207 for i = 1 : max(size(x))
208 for j = 1 : max(size(z))

```

```

209 % incident SV
210 ux_SV_i(i, j) = real(A_SV * cosd(th_SV_i) * (exp((1i * omega / V_S1) ...
211     * (x(i, 1) * sind(th_SV_i) + z(j, 1) * cosd(th_SV_i) - V_S1 * t))));;
212 uz_SV_i(i, j) = real(-A_SV * sind(th_SV_i) * (exp((1i * omega / V_S1) ...
213     * (x(i, 1) * sind(th_SV_i) + z(j, 1) * cosd(th_SV_i) - V_S1 * t))));;
214 % reflected P
215 ux_P_SV_r(i, j) = real(R_P_SV * cosd(th_P_SV_r) * (exp((1i * omega / V_P1) ...
216     * (x(i, 1) * sind(th_P_SV_r) - z(j, 1) * cosd(th_P_SV_r) - V_P1 * t))));;
217 uz_P_SV_r(i, j) = real(R_P_SV * sind(th_P_SV_r) * (exp((1i * omega / V_P1) ...
218     * (x(i, 1) * sind(th_P_SV_r) - z(j, 1) * cosd(th_P_SV_r) - V_P1 * t))));;
219 % reflected SV
220 ux_SV_SV_r(i, j) = real(-R_SV_SV * sind(th_SV_SV_r) * (exp((1i * omega / V_S1) ...
221     * (x(i, 1) * sind(th_SV_SV_r) - z(j, 1) * cosd(th_SV_SV_r) - V_S1 * t))));;
222 uz_SV_SV_r(i, j) = real(R_SV_SV * cosd(th_SV_SV_r) * (exp((1i * omega / V_S1) ...
223     * (x(i, 1) * sind(th_SV_SV_r) - z(j, 1) * cosd(th_SV_SV_r) - V_S1 * t))));;
224 % transmitted P
225 ux_P_SV_t(i, j) = real(T_P_SV * cosd(th_P_SV_t) * (exp((1i * omega / V_P2) ...
226     * (x(i, 1) * sind(th_P_SV_t) + z(j, 1) * cosd(th_P_SV_t) - V_P2 * t))));;
227 uz_P_SV_t(i, j) = real(-T_P_SV * sind(th_P_SV_t) * (exp((1i * omega / V_P2) ...
228     * (x(i, 1) * sind(th_P_SV_t) + z(j, 1) * cosd(th_P_SV_t) - V_P2 * t))));;
229 % transmitted SV
230 ux_SV_SV_t(i, j) = real(T_SV_SV * sind(th_SV_SV_t) * (exp((1i * omega / V_S2) ...
231     * (x(i, 1) * sind(th_SV_SV_t) + z(j, 1) * cosd(th_SV_SV_t) - V_S2 * t))));;
232 uz_SV_SV_t(i, j) = real(-T_SV_SV * cosd(th_SV_SV_t) * (exp((1i * omega / V_S2) ...
233     * (x(i, 1) * sind(th_SV_SV_t) + z(j, 1) * cosd(th_SV_SV_t) - V_S2 * t))));;
234 end
235 end
236
237 % plot
238 subplot(3,4,1)
239 surf(x, z, ux_SV_i,'EdgeColor','none'); axis([0 100 0 100 -4 4])
240 xlabel('x direction'); ylabel('z direction'); view(3)
241 title('Incident SV x comp.')
242
243 subplot(3,4,2)
244 surf(x, z, uz_SV_i,'EdgeColor','none'); axis([0 100 0 100 -4 4])
245 xlabel('x direction'); ylabel('z direction'); view(3)
246 title('Incident SV z comp.')
247
248 subplot(3,4,5)
249 surf(x, z, ux_P_SV_r,'EdgeColor','none'); axis([0 100 0 100 -4 4])
250 xlabel('x direction'); ylabel('z direction'); view(3)
251 title('Reflected P x comp.')
252
253 subplot(3,4,6)
254 surf(x, z, uz_P_SV_r,'EdgeColor','none'); axis([0 100 0 100 -4 4])
255 xlabel('x direction'); ylabel('z direction'); view(3)
256 title('Reflected P z comp.')
257
258 subplot(3,4,7)
259 surf(x, z, ux_SV_SV_r,'EdgeColor','none'); axis([0 100 0 100 -4 4])
260 xlabel('x direction'); ylabel('z direction'); view(3)
261 title('Reflected SV x comp.')
262
263 subplot(3,4,8)
264 surf(x, z, uz_SV_SV_r,'EdgeColor','none'); axis([0 100 0 100 -4 4])
265 xlabel('x direction'); ylabel('z direction'); view(3)
266 title('Reflected SV z comp.')
267
268 subplot(3,4,9)
269 surf(x, z, ux_P_SV_t,'EdgeColor','none'); axis([0 100 0 100 -4 4])
270 xlabel('x direction'); ylabel('z direction'); view(3)
271 title('Refracted P x comp.')
272

```

```

273 subplot(3,4,10)
274 surf(x, z, uz_P_SV_t,'EdgeColor','none'); axis([0 100 0 100 -4 4])
275 xlabel('x direction'); ylabel('z direction'); view(3)
276 title('Refracted P z comp.')
277
278 subplot(3,4,11)
279 surf(x, z, ux_SV_SV_t,'EdgeColor','none'); axis([0 100 0 100 -4 4])
280 xlabel('x direction'); ylabel('z direction'); view(3)
281 title('Refracted SV x comp.')
282
283 subplot(3,4,12)
284 surf(x, z, uz_SV_SV_t,'EdgeColor','none'); axis([0 100 0 100 -4 4])
285 xlabel('x direction'); ylabel('z direction'); view(3)
286 title('Refracted SV z comp.')
287
288 drawnow
289 end
290
291 case {'SH'}
292 % angle and amplitude
293 th_SH_r = th_SH_i;
294 th_SH_t = asind(sind(th_SH_i) * V_S2 / V_S1);
295
296 R_SH = A_SH * (G_1 * V_S2 * cosd(th_SH_i) - G_2 * V_S1 * cosd(th_SH_t))...
297 / (G_1 * V_S2 * cosd(th_SH_i) + G_2 * V_S1 * cosd(th_SH_t));
298 T_SH = A_SH * (2 * G_1 * V_S2 * cosd(th_SH_i) / (G_1 * V_S2 * cosd(th_SH_i)...
299 + G_2 * V_S1 * cosd(th_SH_t)));
300
301 % initialize matrix
302 uy_SH_i = zeros(max(size(z)), max(size(x)));
303 uy_SH_r = zeros(max(size(z)), max(size(x)));
304 uy_SH_t = zeros(max(size(z)), max(size(x)));
305
306 % calculate incident, reflected, and transmitted wave
307 for t = t_low : dt : t_up
308     for i = 1 : max(size(x))
309         for j = 1 : max(size(z))
310             % incident SH
311             uy_SH_i(i, j) = real(A_SH * (exp((1i * omega / V_S1) * (x(i, 1) ...
312                 * sind(th_SH_i) + z(j, 1) * cosd(th_SH_i) - V_S1 * t))));;
313             % reflected SH
314             uy_SH_r(i, j) = real(R_SH * (exp((1i * omega / V_S1) * (x(i, 1) ...
315                 * sind(th_SH_r) - z(j, 1) * cosd(th_SH_r) - V_S1 * t))));;
316             % refracted SH
317             uy_SH_t(i, j) = real(T_SH * (exp((1i * omega / V_S2) * (x(i, 1) ...
318                 * sind(th_SH_t) + z(j, 1) * cosd(th_SH_t) - V_S2 * t))));;
319             % adding incident and reflected SH
320             adding_SH(i,j) = (uy_SH_i(i, j) - uy_SH_r(i, j)) / 2;
321
322         end
323     end
324
325 subplot(3,1,1)
326 surf(x, z, uy_SH_i,'EdgeColor','none'); axis([0 100 0 100 -4 4])
327 xlabel('x direction'); ylabel('z direction'); view(3)
328 title('Incident')
329 subplot(3,1,2)
330 surf(x, z, uy_SH_r,'EdgeColor','none'); axis([0 100 0 100 -4 4])
331 xlabel('x direction'); ylabel('z direction'); view(3)
332 title('Reflected')
333 subplot(3,1,3)
334 surf(x, z, uy_SH_t,'EdgeColor','none'); axis([0 100 0 100 -4 4])
335 xlabel('x direction'); ylabel('z direction'); view(3)
336 title('Refracted')

```

```
337 % surf(x, z, adding_SH,'EdgeColor','none'); xlabel('x direction'); ylabel('z direction'); view(3)
338
339     drawnow
340
341 end
```

705.3 Matlab code – surface wave solution

Listing 705.2: Example MATLAB code for surface waves

```

1 % =====
2 % surf.m: inclined wave propagation closed-form exact solution for surface waves
3 %
4 % ref. Waves and Vibrations in Soils (Semblat and Pecker, 2009)
5 %
6 % Chang-Gyun Jeong
7 % Last update: 03/27/2011
8 %
9 % =====
10 clear all; clc;
11 %
12 % coordinates to see waves
13 x_cord = 0; z_cord = 0;
14 %
15 % time limit for time history
16 t_low = 0; t_up = 10; dt = 0.01;
17 %
18 % wave frequency and initial time for phase
19 freq = 10; % natural frequency of wave
20 t = 0.0; % initial time for phase
21 omega = freq * 2 * pi; % omega
22 %
23 % incident angle and amplitude
24 A_P = 1; % incident amp. (P wave)
25 A_SH = 1; % incident amp. (SH wave)
26 th_SH_i = 20; % incident angle. (SH wave)
27 %
28 % velocity and shear modulus (r is assumed to 20 kN/m^3)
29 v = 0.3; % Poisson's ratio
30 V_S1 = 50; % Vs for layer 1
31 %
32 V_R = V_S1 * (0.862 + 1.14 * v) / (1 + v); % Rayleigh wave velocity
33 V_P1 = V_S1 * sqrt((2 - 2 * v) / (1 - 2 * v)); % Vp for layer 1
34 %
35 % calculate Rayleigh waves
36 a = -1*abs(sqrt(omega^2 / V_R^2 - omega^2 / V_P1^2));
37 b = -1*abs(sqrt(omega^2 / V_R^2 - omega^2 / V_S1^2));
38 %
39 fq_u_x_R = A_P * 1i * omega / V_R * ...
40   (exp(a * z_cord) - ((2 * a * b / (b^2 + omega^2 / V_R^2)) * exp(b * z_cord))) ...
41   * exp((1i * omega / V_R) * (x_cord - V_R * t));
42 fq_u_z_R = A_P * a * ...
43   (exp(a * z_cord) - ((2 * omega^2 / V_R^2) / (b^2 + omega^2 / V_R^2) * exp(b * z_cord))) ...
44   * exp((1i * omega / V_R) * (x_cord - V_R * t));
45 %
46 % calculate Love waves
47 fq_u_y_L = 2 * A_SH * cosd(omega * z_cord * cosd(th_SH_i) / V_S1) ...
48   * (exp((1i * omega / V_S1) * (x_cord * sind(th_SH_i) - V_S1 * t)));
49 %
50 % calculate phase angle and amplitude of harmonic motion
51 time_ang_x=angle(fq_u_x_R); % phase angle (R wave, x)
52 time_abs_x=abs(fq_u_x_R); % amplitude (R wave, x)
53 time_ang_z=angle(fq_u_z_R); % phase angle (R wave, z)
54 time_abs_z=abs(fq_u_z_R); % amplitude (R wave, z)
55 time_ang_y=angle(fq_u_y_L); % phase angle (L wave, y)
56 time_abs_y=abs(fq_u_y_L); % amplitude angle (L wave, y)
57 %
58 % calculate time history Rayleigh wave
59

```

```
60 time = t_low : dt : t_up;
61
62 u_x_R = time_abs_x * cos(2*freq*pi*time+time_ang_x) ;
63 u_z_R = time_abs_z * cos(2*freq*pi*time+time_ang_z) ;
64
65 % calculate time history Love wave
66 u_y_L = time_abs_y * cos(2*freq*pi*time+time_ang_y) ;
67
68 % plot
69 subplot(1,4,1)
70 plot(u_x_R, u_z_R)
71 xlabel('x'); ylabel('z');
72 axis([-4 4 -4 4])
73
74 subplot(1,4,2)
75 plot(u_y_L, u_z_R)
76 xlabel('y'); ylabel('z');
77 axis([-4 4 -4 4])
78
79 subplot(1,4,3)
80 plot(u_x_R, u_y_L)
81 xlabel('x'); ylabel('y');
82 axis([-4 4 -4 4])
83
84 subplot(1,4,4)
85 plot3(u_x_R, u_y_L, u_z_R)
86 axis([-4 4 -4 4 -4 4])
87 xlabel('x'); ylabel('y'); zlabel('z');
```

705.4 Matlab code – Ricker wavelet as an input motion

Listing 705.3: Example MATLAB code for Ricker wavelet as an input motion

```

1 % =====
2 % Ricker.m: Ricker wavelet propagation on 3D space closed-form exact solution
3 %
4 % ref. Waves and Vibrations in Soils (Semblat and Pecker, 2009)
5 %
6 % Chang-Gyun Jeong
7 % Last update: 01. 05. 2012.
8 % =====
9
10 clf; clc; clear all;
11
12 %% Initial condition
13 % max frequency, amplitude, and input angle of ricker wavelet
14 f_max = 1;
15 amplitude = 0.005;
16 th = 40;
17
18 % amplitude ratio
19 % ar_PP = 1;
20 % arR = 1;
21
22 % coordinate for extracting waves
23 xxx = 0;
24 zzz = 900;
25
26 dx = 100;
27 x_min = 0;
28 x_max = xxx;
29
30 dz = 100;
31 z_min = 0;
32 z_max = zzz;
33
34 nx = x_max / dx + 1;
35 nz = z_max / dz + 1;
36
37 % Poisson's ratio and wave velocity of ground
38 v = 0.1;
39 Vs = 700;
40 Vp = Vs * sqrt((2 - 2 * v) / (1 - 2 * v));
41 Vr = Vs * (0.862 + 1.14 * v) / (1 + v);
42
43 % time step, peak time, max and min time
44 dt = 0.01;
45 t_min = 0;
46 t_max = 20;
47 t_peak = 4;
48
49 % parameters for plotting
50 t_min_pl = 0;
51 t_max_pl = 10;
52 d_min_pl = -0.02;
53 d_max_pl = 0.02;
54
55 f_min_pl = 0;
56 f_max_pl = 5;
57 f_amp_min_pl = 0;
58 f_amp_max_pl = 0.0006;
59

```

```

60 % amplitude and angle calculation for reducing computation time
61 thrp = asind(sind(th) * Vp / Vs);
62 thrs = asind(sind(th) * Vs / Vp);
63
64 ss = sind(th) / Vs;
65 cc = cosd(th) / Vs;
66 ssrp = sind(thrp) / Vp;
67 ccrp = cosd(thrp) / Vp;
68 ssp = sind(th) / Vp;
69 ccp = cosd(th) / Vp;
70 ssrs = sind(thrs) / Vs;
71 ccrs = cosd(thrs) / Vs;
72
73 as = amplitude * sind(th);
74 ac = amplitude * cosd(th);
75
76 %% Ricker wavelet
77 k = 1;
78 for t = t_min:dt:t_max
79     j = 1;
80     for z = z_min:dz:z_max
81         i = 1;
82         for x = x_min:dx:x_max
83             SV_i_x(i, j) = ac * ...
84                 ((1 - 2 * pi^2 * f_max^2 * (t - t_peak + x * ss + z * cc)^2) * ...
85                 exp(-pi^2 * f_max^2 * ...
86                     (t - t_peak + x * ss + z * cc)^2));
87             SV_i_z(i, j) = as * ...
88                 ((1 - 2 * pi^2 * f_max^2 * (t - t_peak + x * ss + z * cc)^2) * ...
89                 exp(-pi^2 * f_max^2 * ...
90                     (t - t_peak + x * ss + z * cc)^2));
91
92             SVP_r_x(i, j) = as * sind(thrp) * ...
93                 ((1 - 2 * pi^2 * f_max^2 * (t - t_peak + x * ssrp - z * ccrp)^2) * ...
94                 exp(-pi^2 * f_max^2 * ...
95                     (t - t_peak + x * ssrp - z * ccrp)^2));
96             SVP_r_z(i, j) = as * cos(thrp) * ...
97                 ((1 - 2 * pi^2 * f_max^2 * (t - t_peak + x * ssrp + z * ccrp)^2) * ...
98                 exp(-pi^2 * f_max^2 * ...
99                     (t - t_peak + x * ssrp + z * ccrp)^2));
100
101             SVSV_r_x(i, j) = ac * cosd(th) * ...
102                 ((1 - 2 * pi^2 * f_max^2 * (t - t_peak + x * ss - z * cc)^2) * ...
103                 exp(-pi^2 * f_max^2 * ...
104                     (t - t_peak + x * ss - z * cc)^2));
105             SVSV_r_z(i, j) = as * sind(th) * ...
106                 ((1 - 2 * pi^2 * f_max^2 * (t - t_peak + x * ss - z * cc)^2) * ...
107                 exp(-pi^2 * f_max^2 * ...
108                     (t - t_peak + x * ss - z * cc)^2));
109
110             P_i_x(i, j) = ac * ...
111                 ((1 - 2 * pi^2 * f_max^2 * (t + 1.35 - t_peak + x * ssp + z * ccp)^2) * ...
112                 exp(-pi^2 * f_max^2 * ...
113                     (t + 1.35 - t_peak + x * ssp + z * ccp)^2));
114             P_i_z(i, j) = as * ...
115                 ((1 - 2 * pi^2 * f_max^2 * (t + 1.35 - t_peak + x * ssp + z * ccp)^2) * ...
116                 exp(-pi^2 * f_max^2 * ...
117                     (t + 1.35 - t_peak + x * ssp + z * ccp)^2));
118
119             PP_r_x(i, j) = as * sind(th) * ...
120                 ((1 - 2 * pi^2 * f_max^2 * (t + 1.35 - t_peak + x * ssp - z * ccp)^2) * ...
121                 exp(-pi^2 * f_max^2 * ...
122                     (t + 1.35 - t_peak + x * ssp - z * ccp)^2));
123             PP_r_z(i, j) = as * cos(th) * ...

```

```

124    ((1 - 2 * pi^2 * f_max^2 * (t + 1.35 - t_peak + x * ssp + z * ccp)^2) * ...
125    exp(-pi^2 * f_max^2 * ...
126    (t + 1.35 - t_peak + x * ssp + z * ccp)^2));
127
128    PSV_r_x(i, j) = ac * cosd(thrs) * ...
129    ((1 - 2 * pi^2 * f_max^2 * (t + 1.35 - t_peak + x * ssrs - z * ccrs)^2) * ...
130    exp(-pi^2 * f_max^2 * ...
131    (t + 1.35 - t_peak + x * ssrs - z * ccrs)^2));
132    PSV_r_z(i, j) = as * sind(thrs) * ...
133    ((1 - 2 * pi^2 * f_max^2 * (t + 1.35 - t_peak + x * ssrs - z * ccrs)^2) * ...
134    exp(-pi^2 * f_max^2 * ...
135    (t + 1.35 - t_peak + x * ssrs - z * ccrs)^2));
136
137
138    total_x(i, j) = SV_i_x(i, j) + SVP_r_x(i, j) + SVSV_r_x(i, j) + ...
139    P_i_x(i, j) + PP_r_x(i, j) + PSV_r_x(i, j);
140    total_z(i, j) = SV_i_z(i, j) + SVP_r_z(i, j) + SVSV_r_z(i, j) + ...
141    P_i_z(i, j) + PP_r_z(i, j) + PSV_r_z(i, j);
142
143    i = i + 1;
144  end
145  j = j + 1;
146 end
147
148 disp_1(k) = SV_i_x(nx, nz) + P_i_x(nx, nz);
149 disp_2(k) = SV_i_z(nx, nz) + P_i_z(nx, nz);
150 disp_3(k) = SVP_r_x(nx, nz) + PP_r_x(nx, nz);
151 disp_4(k) = SVP_r_z(nx, nz) + PP_r_z(nx, nz);
152 disp_5(k) = SVSV_r_x(nx, nz) + PSV_r_x(nx, nz);
153 disp_6(k) = SVSV_r_z(nx, nz) + PSV_r_z(nx, nz);
154
155 time_hist(k) = t;
156
157 k = k + 1;
158 end
159
160 % Fourier transform
161 Fs = 1 / dt;
162 NFFT = 2^nextpow2(((t_max - t_min) / dt));
163 F_1 = fft(disp_1, NFFT) / ((t_max - t_min) / dt);
164 F_2 = fft(disp_2, NFFT) / ((t_max - t_min) / dt);
165 F_3 = fft(disp_3, NFFT) / ((t_max - t_min) / dt);
166 F_4 = fft(disp_4, NFFT) / ((t_max - t_min) / dt);
167 F_5 = fft(disp_5, NFFT) / ((t_max - t_min) / dt);
168 F_6 = fft(disp_6, NFFT) / ((t_max - t_min) / dt);
169 F_7 = fft(disp_1 + disp_3 + disp_5, NFFT) / ((t_max - t_min) / dt);
170 F_8 = fft(disp_2 + disp_4 + disp_6, NFFT) / ((t_max - t_min) / dt);
171 fq = (Fs / 2) * linspace(0, 1, NFFT / 2 + 1);
172
173 %% Rayleigh wave
174 z = 0;
175 x = 0;
176 t = 0;
177
178 omega = fq * 2 * pi();
179 Ax=2 * abs(F_1(1:NFFT/2+1));
180 Az=2 * abs(F_2(1:NFFT/2+1));
181
182 omega(1) = 0.000001;
183
184 for i = 1 : max(size(fq))
185   a = 1*abs(sqrt(omega(i)^2 / Vr^2 - omega(i)^2 / Vp^2));
186   b = 1*abs(sqrt(omega(i)^2 / Vr^2 - omega(i)^2 / Vs^2));
187

```

```

188 surf_x(i) = (1i * omega(i) * Ax(i) / Vr) * (exp(a * z) - (2 * a * b * exp(b * z)) / ...
189     (b^2 + omega(i)^2 / Vr^2)) * exp(1i * omega(i) * (x - Vr * t) / Vr);
190 surf_z(i) = a * Az(i) * (exp(a * z) - (2 * omega(i)^2 * exp(b * z) / Vr^2) / ...
191     (b^2 + omega(i)^2 / Vr^2)) * exp(1i * omega(i) * (x - Vr * t) / Vr);
192 end
193
194 % calculate phase angle and amplitude of R wave
195 time_ang_x=angle(surf_x);
196 time_abs_x=abs(surf_x);
197 time_ang_z=angle(surf_z);
198 time_abs_z=abs(surf_z);
199
200 for i = 1:max(size(fq))
201     j = 1;
202     for time = t_min:dt:t_max;
203         u_x_R(i, j) = time_abs_x(i) * cos(omega(i) * (time - t_peak) - time_ang_x(i));
204         u_z_R(i, j) = time_abs_z(i) * cos(omega(i) * (time - t_peak) - time_ang_z(i));
205         j = j + 1;
206     end
207     i = i + 1;
208 end
209
210 u_x = sum(u_x_R);
211 u_z = sum(u_z_R);
212
213 % get max amplitude of R wave to scale it
214 max_R_x = max(u_x);
215 max_R_z = max(u_z);
216
217 % R wave will be recalculated on the point of interest
218 z = xxx;
219 x = zzz;
220
221 for i = 1 : max(size(fq))
222     a = 1*abs(sqrt(omega(i)^2 / Vr^2 - omega(i)^2 / Vp^2));
223     b = 1*abs(sqrt(omega(i)^2 / Vr^2 - omega(i)^2 / Vs^2));
224
225     surf_x(i) = (1i * omega(i) * Ax(i) / Vr) * (exp(a * z) - (2 * a * b * exp(b * z)) / ...
226         (b^2 + omega(i)^2 / Vr^2)) * exp(1i * omega(i) * (x - Vr * t) / Vr);
227     surf_z(i) = a * Az(i) * (exp(a * z) - (2 * omega(i)^2 * exp(b * z) / Vr^2) / ...
228         (b^2 + omega(i)^2 / Vr^2)) * exp(1i * omega(i) * (x - Vr * t) / Vr);
229 end
230
231 % calculate phase angle and amplitude of R wave
232 time_ang_x=angle(surf_x);
233 time_abs_x=abs(surf_x);
234 time_ang_z=angle(surf_z);
235 time_abs_z=abs(surf_z);
236
237 for i = 1:max(size(fq))
238     j = 1;
239     for time = t_min:dt:t_max;
240         u_x_R(i, j) = time_abs_x(i) * cos(omega(i) * (time - t_peak) - time_ang_x(i));
241         u_z_R(i, j) = time_abs_z(i) * cos(omega(i) * (time - t_peak) - time_ang_z(i));
242         j = j + 1;
243     end
244     i = i + 1;
245 end
246
247 u_x = sum(u_x_R);
248 u_z = sum(u_z_R);
249
250 % scale R wave
251 u_x = u_x * amplitude / max_R_x;

```

```

252 u_z = u_z * amplitude / max_R_x;
253
254 % set amplitude of R wave as zero
255 % u_x = 0;
256 % u_z = 0;
257
258 % add all displacement (R + input + reflect)
259 u_xx = u_x + disp_1 + disp_3 + disp_5;
260 u_zz = u_z + disp_2 + disp_4 + disp_6;
261
262 % Fourier transform
263 F_9 = fft(u_x, NFFT) / ((t_max - t_min) / dt);
264 F_10 = fft(u_z, NFFT) / ((t_max - t_min) / dt);
265 F_11 = fft(u_xx, NFFT) / ((t_max - t_min) / dt);
266 F_12 = fft(u_zz, NFFT) / ((t_max - t_min) / dt);
267
268 % make final output matrix
269 disp_out(:, 1) = time_hist';
270 disp_out(:, 2) = u_xx';
271 disp_out(:, 4) = u_zz';
272
273 %% plot
274
275 % figure 1: all components
276 figure(1)
277 subplot(6, 2, 1)
278 plot(time_hist, disp_1, time_hist, disp_2)
279 ylim([d_min_pl d_max_pl])
280 xlim([t_min_pl t_max_pl])
281 xlabel('Time (s)')
282 ylabel('Displacement (m)')
283 title('Input SV + P')
284
285 subplot(6, 2, 3)
286 plot(time_hist, disp_3, time_hist, disp_4)
287 ylim([d_min_pl d_max_pl])
288 xlim([t_min_pl t_max_pl])
289 xlabel('Time (s)')
290 ylabel('Displacement (m)')
291 title('Reflected P')
292
293 subplot(6, 2, 5)
294 plot(time_hist, disp_5, time_hist, disp_6)
295 ylim([d_min_pl d_max_pl])
296 xlim([t_min_pl t_max_pl])
297 xlabel('Time (s)')
298 ylabel('Displacement (m)')
299 title('Reflected SV')
300
301 subplot(6, 2, 7)
302 plot(time_hist, disp_1 + disp_3 + disp_5, time_hist, disp_2 + disp_4 + disp_6)
303 ylim([d_min_pl d_max_pl])
304 xlim([t_min_pl t_max_pl])
305 xlabel('Time (s)')
306 ylabel('Displacement (m)')
307 title('Body total')
308
309 subplot(6,2,9)
310 plot(time_hist, u_x, time_hist, u_z)
311 ylim([d_min_pl d_max_pl])
312 xlim([t_min_pl t_max_pl])
313 xlabel('Time (s)')
314 ylabel('Displacement (m)')
315 title('Surf. Rayleigh')

```

```

316 subplot(6,2,11)
317 plot(time_hist, u_xx, time_hist, u_zz)
318 ylim([d_min_pl d_max_pl])
319 xlim([t_min_pl t_max_pl])
320 xlabel('Time (s)')
321 ylabel('Displacement (m)')
322 title('Body and Surface Total')
323
324 subplot(6,2,2)
325 plot(fq, 2 * abs(F_1(1:NFFT/2+1)), fq, 2 * abs(F_2(1:NFFT/2+1)))
326 ylim([f_amp_min_pl f_amp_max_pl])
327 xlim([f_min_pl f_max_pl])
328 xlabel('Frequency (Hz)')
329 ylabel('Fourier Amplitude')
330 title('Input SV + P')
331
332 subplot(6,2,4)
333 plot(fq, 2 * abs(F_3(1:NFFT/2+1)), fq, 2 * abs(F_4(1:NFFT/2+1)))
334 ylim([f_amp_min_pl f_amp_max_pl])
335 xlim([f_min_pl f_max_pl])
336 xlabel('Frequency (Hz)')
337 ylabel('Fourier Amplitude')
338 title('Reflected P')
339
340 subplot(6,2,6)
341 plot(fq, 2 * abs(F_5(1:NFFT/2+1)), fq, 2 * abs(F_6(1:NFFT/2+1)))
342 ylim([f_amp_min_pl f_amp_max_pl])
343 xlim([f_min_pl f_max_pl])
344 xlabel('Frequency (Hz)')
345 ylabel('Fourier Amplitude')
346 title('Reflected SV')
347
348 subplot(6,2,8)
349 plot(fq, 2 * abs(F_7(1:NFFT/2+1)), fq, 2 * abs(F_8(1:NFFT/2+1)))
350 ylim([f_amp_min_pl f_amp_max_pl])
351 xlim([f_min_pl f_max_pl])
352 xlabel('Frequency (Hz)')
353 ylabel('Fourier Amplitude')
354 title('Body Total')
355
356 subplot(6,2,10)
357 plot(fq, 2 * abs(F_9(1:NFFT/2+1)), fq, 2 * abs(F_10(1:NFFT/2+1)))
358 ylim([f_amp_min_pl f_amp_max_pl])
359 xlim([f_min_pl f_max_pl])
360 xlabel('Frequency (Hz)')
361 ylabel('Fourier Amplitude')
362 title('Surf. Rayleigh')
363
364 subplot(6,2,12)
365 plot(fq, 2 * abs(F_11(1:NFFT/2+1)), fq, 2 * abs(F_12(1:NFFT/2+1)))
366 ylim([f_amp_min_pl f_amp_max_pl])
367 xlim([f_min_pl f_max_pl])
368 xlabel('Frequency (Hz)')
369 ylabel('Fourier Amplitude')
370 title('Body and Surface Total')
371

```

705.5 Wave Potential Formulation – Domain Reduction Method

Methodology presented here is from [Wang et al. \(2021\)](#).

Presented is a methodology developed to investigate influence of inclined body and surface seismic wave on linear or nonlinear earthquake soil structure interaction (ESSI) behavior of soil-structure systems. Methodology is based on Wave Potential Formulation (WPF) ([Thomson, 1950](#); [Haskell, 1953](#)) as well as Domain Reduction Method (DRM) ([Bielak et al., 2003a](#)).

Presented WPF-DRM methodology consists of three main steps:

1. Analytic development of free field ground motions for a layered half space, excited by an incident, inclined plane wave. Development of this seismic wave field is relying on wave potential formulation in frequency-wave number domain. Time domain spatially varying ground motions are then synthesized through inverse Fourier transformation.
2. Development of the Effective Earthquake Forces, from DRM formulation, is then performed using free field seismic motions developed in the previous step.
3. Earthquake Soil Structure Interaction (ESSI) analysis of the soil-structure system is then performed using effective earthquake forces that are applied to a single layer of finite elements surrounding soil-structure system, so called DRM layer. The only waves that are radiated from the soil-structure system and exit the DRM layer are due to oscillations of the structure. These outgoing waves are absorbed by damping layers.

Sections ?? and ?? below provide details of Wave Potential Formulation and Domain Reduction Method, respectively.

Appendix 706

Body and Surface Wave Numerical Modeling

(2010-2012-2018-2019-2021-)

(In collaboration with Dr. Nima Tafazzoli, Mr. Chang-Gyun Jeong and Dr. Hexiang Wang)

706.1 Integral equations

Second method to generate wave fields is frequency-wavenumber integration method. The fk package is a frequency-wavenumber integration ([Haskell, 1964](#); [Wang and Herrmann, 1980](#)) code developed by [Zhu and Rivera \(2002\)](#). The fk code package can be downloaded from <http://www.eas.slu.edu/People/LZhu>. In this section, using fk code package, wave propagation is simulated. The main modules of the fk code package and its function are shown as followings.

1. fk – compute Green's functions
2. syn – compute synthetic seismogram
3. fk.pl – PERL script to simplify the use of fk

First of all, Green's function is computed by fk with ground model properties (model layer dimension, shear and P wave velocity, density, Q and so on) and source, station (receiver) properties (source depth, epicentral distance, wave propagation direction, and receiver depth and so on). Then, Using syn with calculated Green's function, seismograph is synthesized with given variables such as magnitude, fault strike/dip/rake, and station azimuth. Synthesized seismograph (by syn) are stored as binary / Seismic Analysis Code (SAC) form ([Goldstein and Snoke, 2005](#)). Thus, in addition to fk package, Python code to run fk package iteratively, convert results from binary to ASCII text, and make plot is developed (plot.py). All necessary variables to run fk and syn can be adjusted in plot.py. Variables are explained in next sections and can also be found in source codes (fk.f, syn.c, fk.pl, and plot.py)

706.1.1 fk3.0 package

In this section, fk3.0 package is briefly introduced. All source code can be downloaded from <http://www.eas.slu.edu/People/LZhu>.

706.1.1.1 fk and 'sample_input'

Program fk can be run by using input text file or using PERL wrapper fk.pl as shown in next section. Example input file 'sample_input' is used to run fk. 'sample_input' is included in fk package. Total layer number, source layer number, source type, and receiver layer number are defined in the first row of input file. Layer properties are defined from second to fourth row (layer thickness / Vp / Vs / density / Qp / Qs values are defined from the first column to sixth column, respectively). Then, sigma, number of

sampling points, sampling interval, tapering factor, high / low pass filter frequencies, slowness limit, epicentral distances are defined. In example, variables can be set as following.

Line1: 3 2 2 1 0

3 – total number of layers

2 – source is located at the top of 2nd layer

2 – double coupled source (0: explosion, 1: single coupled)

1 – receiver is located at the top of 1st layer

0 – consider both up and down going wave (1: down going wave, -1: up going wave)

Line2: 10.0000 6.3000 3.5000 2.7860 1000.00 500.00

10.0 – depth (km)

6.3 – Vp (km/s)

3.5 – Vs (km/s)

2.7860 – density (g/cm³)

1000 – Qp

500 – Qs

Line3: 25.0000 6.3000 3.5000 2.7860 1000.00 500.00

ref. Line2

Line4: 0.0000 8.1000 4.7000 3.3620 1600.00 800.00

ref. Line2

Line5: 2 512 0.2 0.5 25 2 1 1

2 – sigma in 1/trace length, the small imaginary frequency (2 – 3)

512 – number of points in the time domain

0.2 – time step (sec, dt)

0.5 – tapering factor to suppress high frequencies

25 – number of points to be saved before t0

2 – smooth factor to increase the sampling rate

1 1 – high pass filter (wc1, wc2)

Line6: 0. 1 0.3 15

0. 1 – minimum and maximum slowness, to sepcify the window for the wavenumber integration
(pmin, pmax)

0.3 – wavenumber sampling interval
15 – the maximum wavenumber at zero frequency

Line7: 1

1 – number of distance ranges

Line8: 200.00 20.00 200.grn.

200.00 – distance (km)

20.00 – t0

200.grn. – output file name

706.1.1.2 fk.pl

fk also can be run by PERL wrapper. Using the PERL wrapper fk.pl is strongly recommended by Zhu (README file of fk package). Since most of variables those are introduced on prior section are set to default values and also can be adjusted on the command line, it is much easier to use fk.pl than run fk.

706.1.1.3 syn

Using syn with calculated Green's function, seismogram is computed. Direction of fault (strike / dip / rake) and recording station (azimuth), magnitude have to be defined to run syn.

706.1.1.4 plot.py

As mentioned above, output seismogram is in SAC form (binary). PERL script plot.py is coded to convert binary to ASCII, run fk / syn repetitively, perform Fourier transform, and plot figures. Necessary options to run fk and syn can be adjusted in plot.py.

706.1.2 3D seismic wave field generation using integral equation

Using fk package, 3D seismic wave field is generated. Analysis for the most common fault mechanism (strike-slip, dip-slip, and normal fault) are presented. A real earthquake example (Northridge) is also given toward the end of the section.

706.1.2.1 Case 1: strike-slip fault / single layer ground

The first example is strike slip fault case. Model is as shown in Figure 706.1. Ground, fault, and wave properties are shown as below.

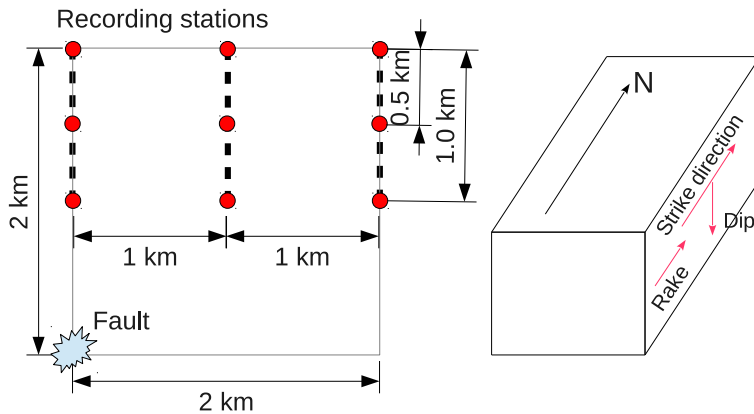


Figure 706.1: Ground and fault model used for analysis, results are captured on circles

- Ground properties

- $V_S = 1 \text{ km/s}$
- $V_P/V_S = 1.73$
- Poisson's ratio = 0.25
- Density = 1.32 g/cm^3
- Shear modulus = 1.32 GPa
- Elastic modulus = 3.31 GPa

- Fault properties

- Moment magnitude = 3.5
- Strike = 0°
- Dip = 90°
- Rake = 0°
- Double - coupled source
- Triangular source time function

- Wave properties

- $\Delta t = 0.1 \text{ s}$ (Max available freq. = 5 Hz, Nyquist freq.)

As indicated above, single layer ground ($V_s = 1 \text{ km/s}$) is modeled. Fault is located at 2 km depth, 2 km away from the recording points (stations). Double coupled fault source is assumed and triangular

source time function is used (Aki and Richards, 2002). Nine recording points are set as recording stations (Figure 706.1). Direction of the fault is aligned parallel to the north (strike = 0°) and recording station azimuth is set to 0° , 45° , and 90° .

Figure 706.2 – 706.10 show analyses results for the example. Legends on figures mean ‘component (epicentral distance, receiver depth)’. EW, NS, and UD components mean East - West, North - South, and Up - Down, respectively (those terms are used for all seismograms, hereafter).

Only EW components are predicted on the stations at 0° azimuth (Figure 706.2 – 706.4) and NS components are showed up on the station at 90° azimuth (Figure 706.8 – 706.10). On the station at 45° azimuth, all components (EW, NS, and UD) are observed.

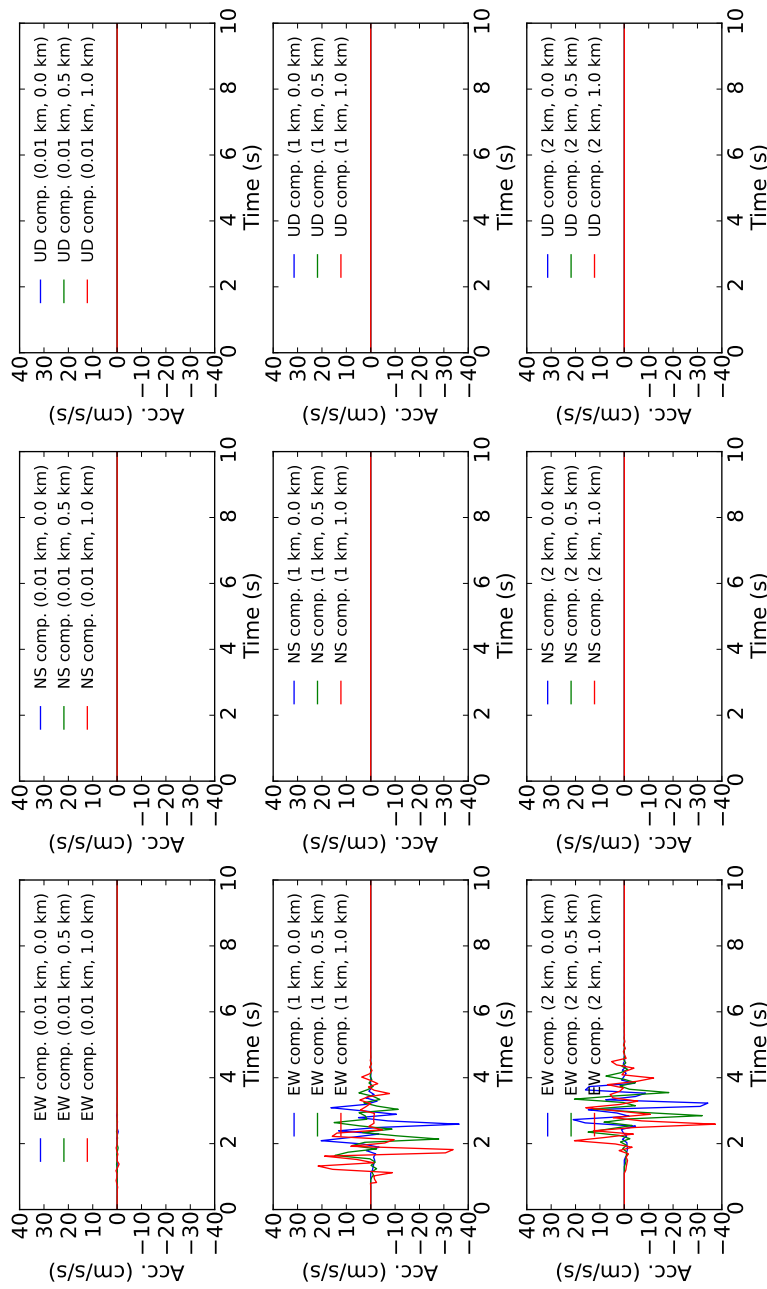


Figure 706.2: Calculated time history acceleration, station azimuth = 0°

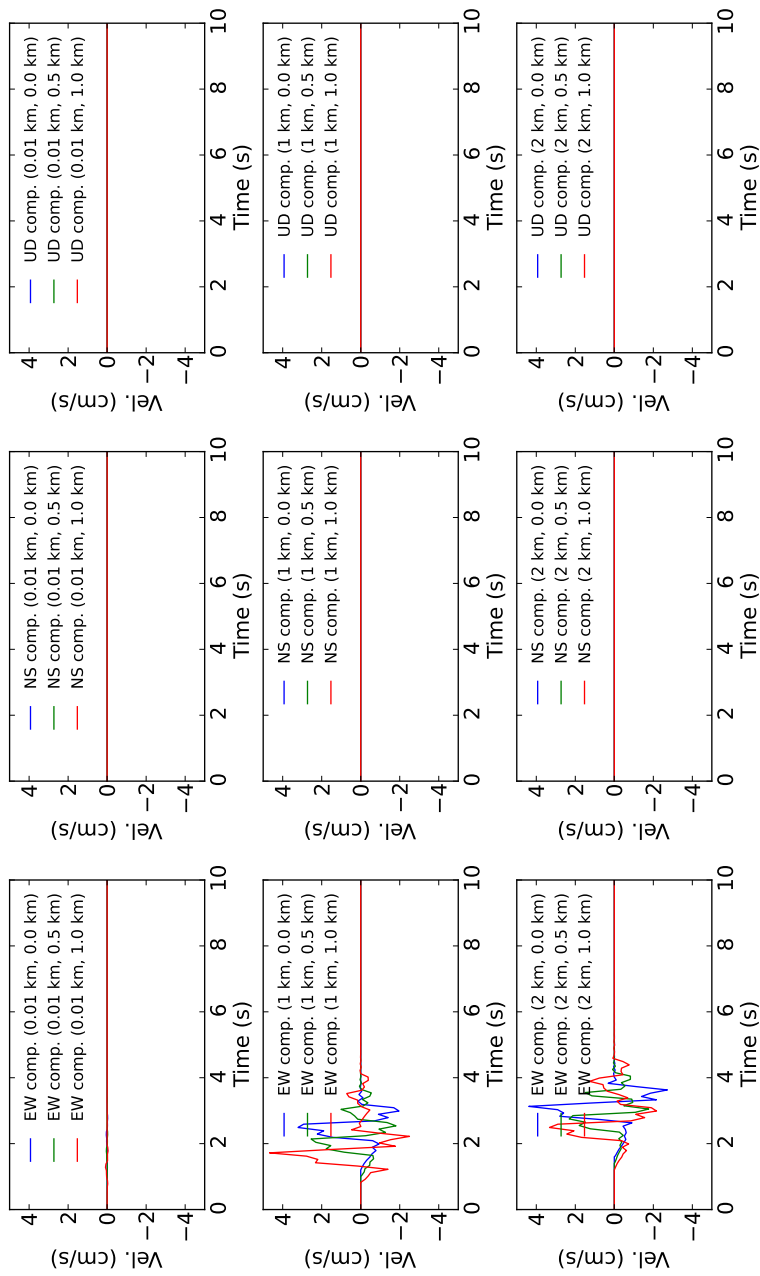


Figure 706.3: Calculated time history velocity, station azimuth = 0°

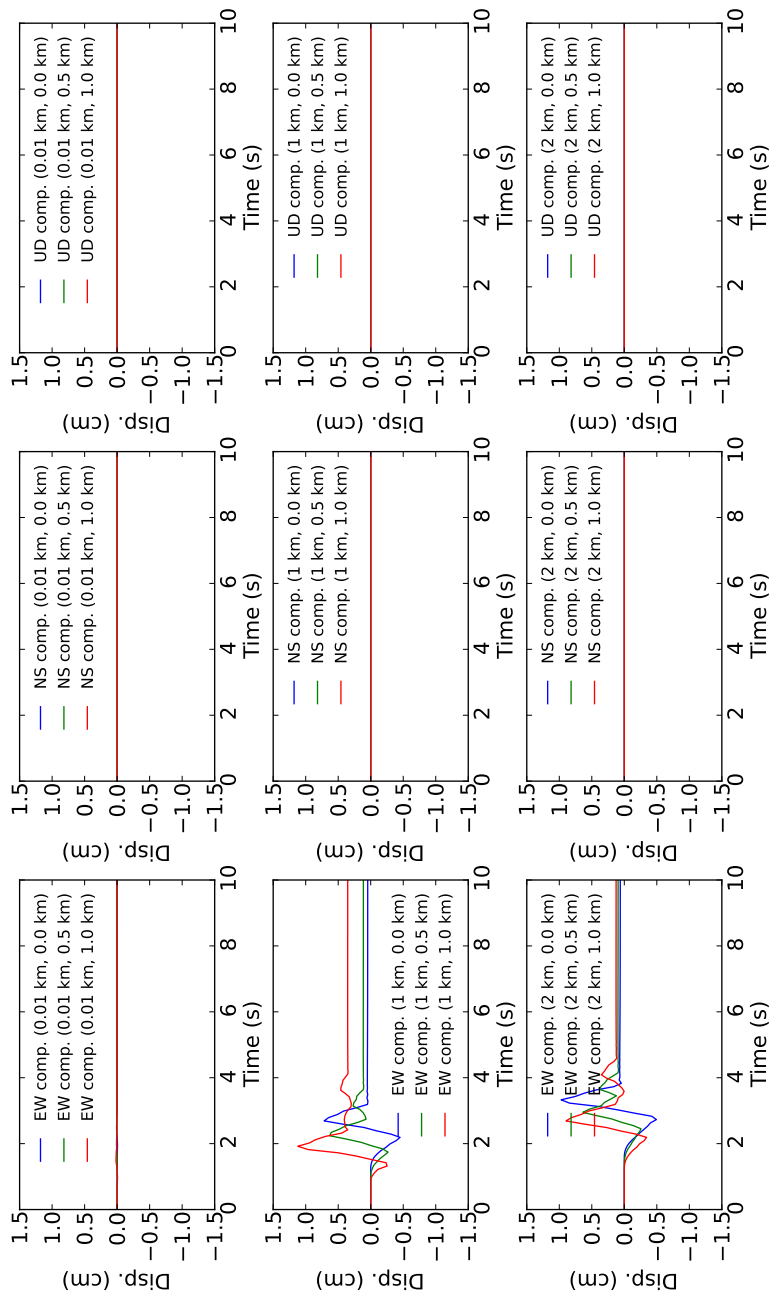
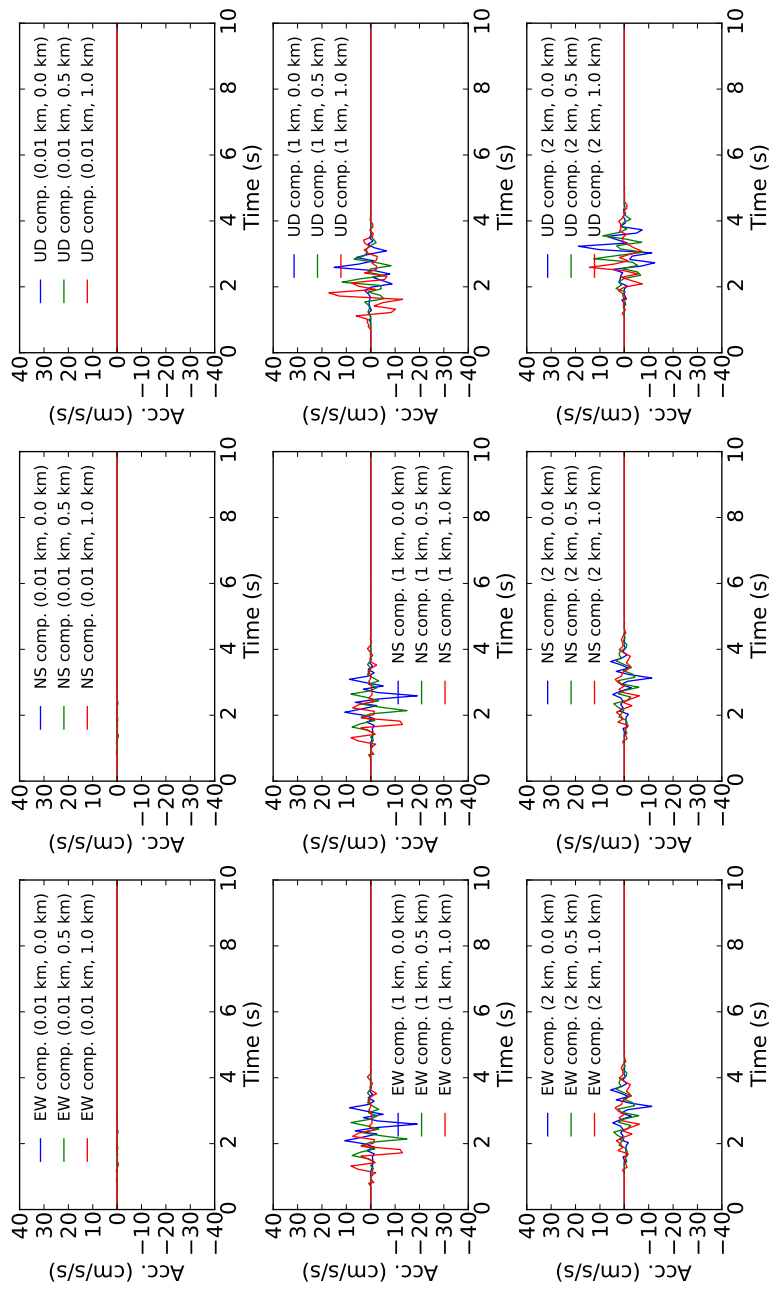


Figure 706.4: Calculated time history displacement, station azimuth = 0°

Figure 706.5: Calculated time history acceleration, station azimuth = 45°

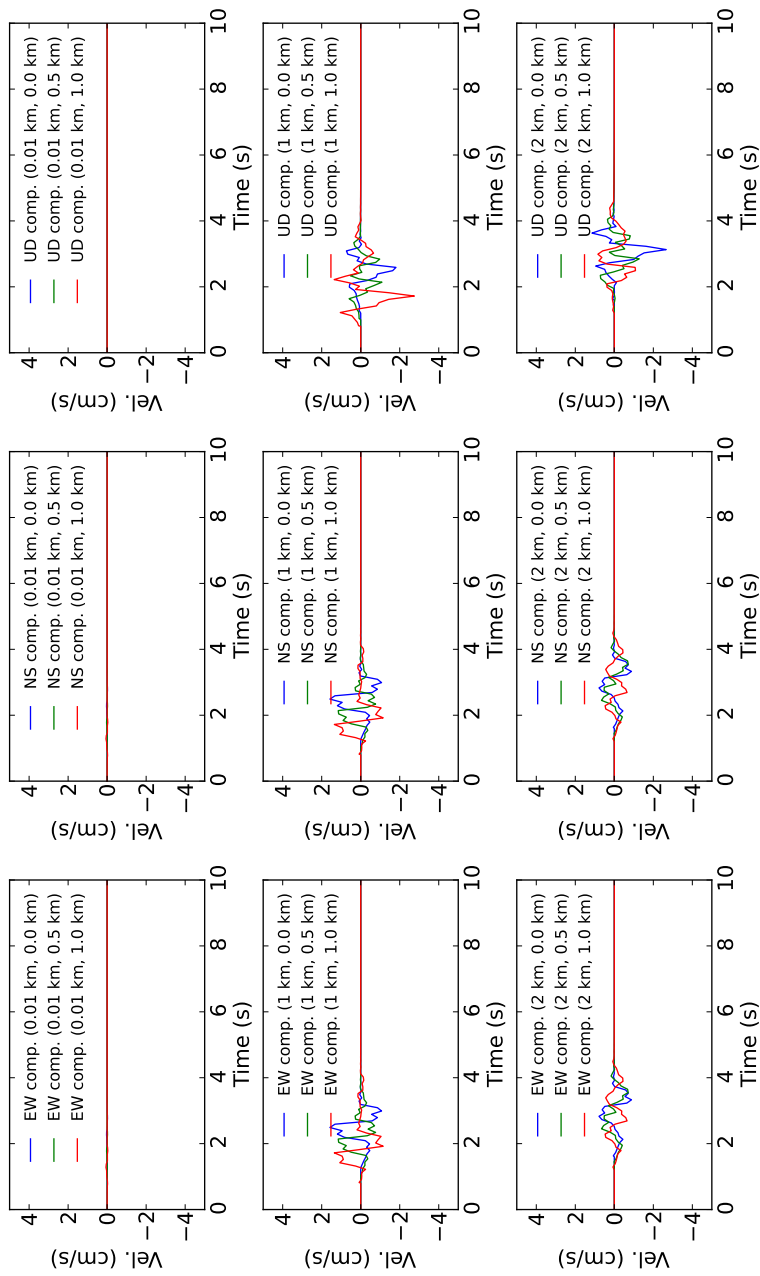
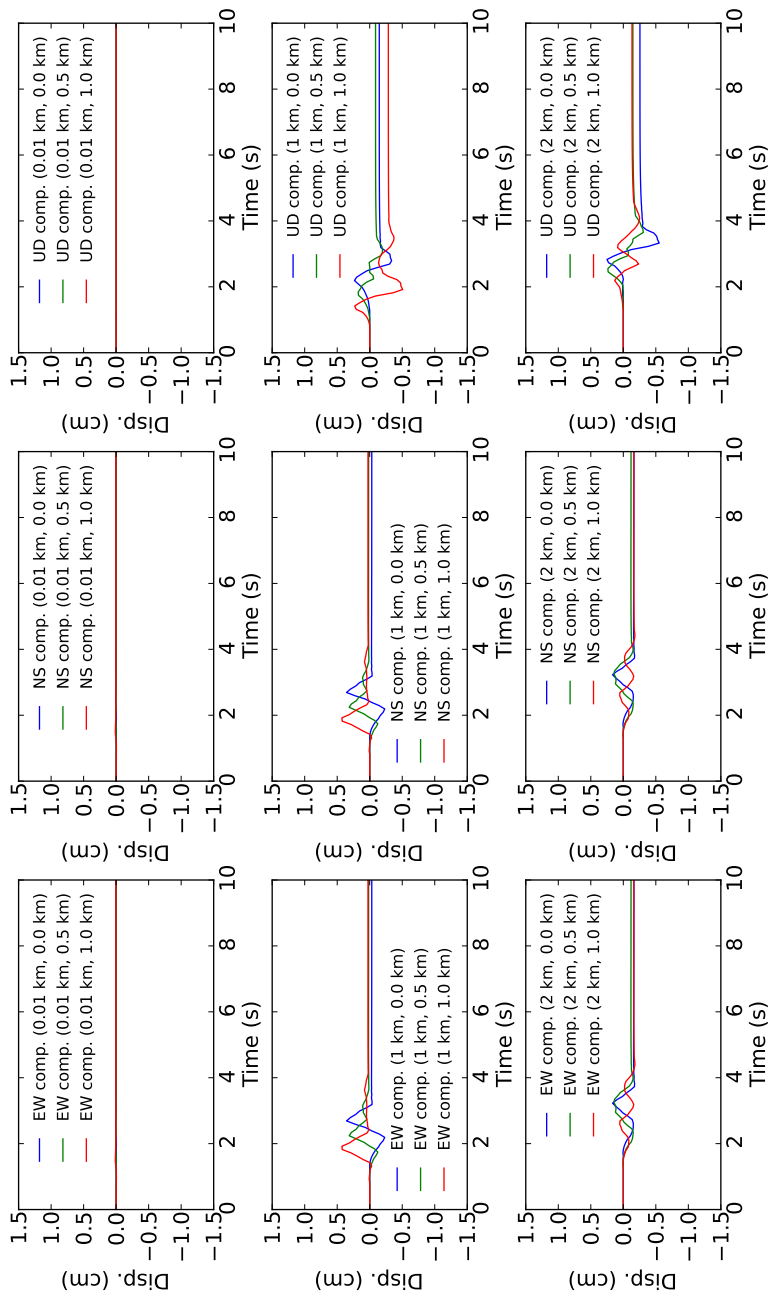


Figure 706.6: Calculated time history velocity, station azimuth = 45°

Figure 706.7: Calculated time history displacement, station azimuth = 45°

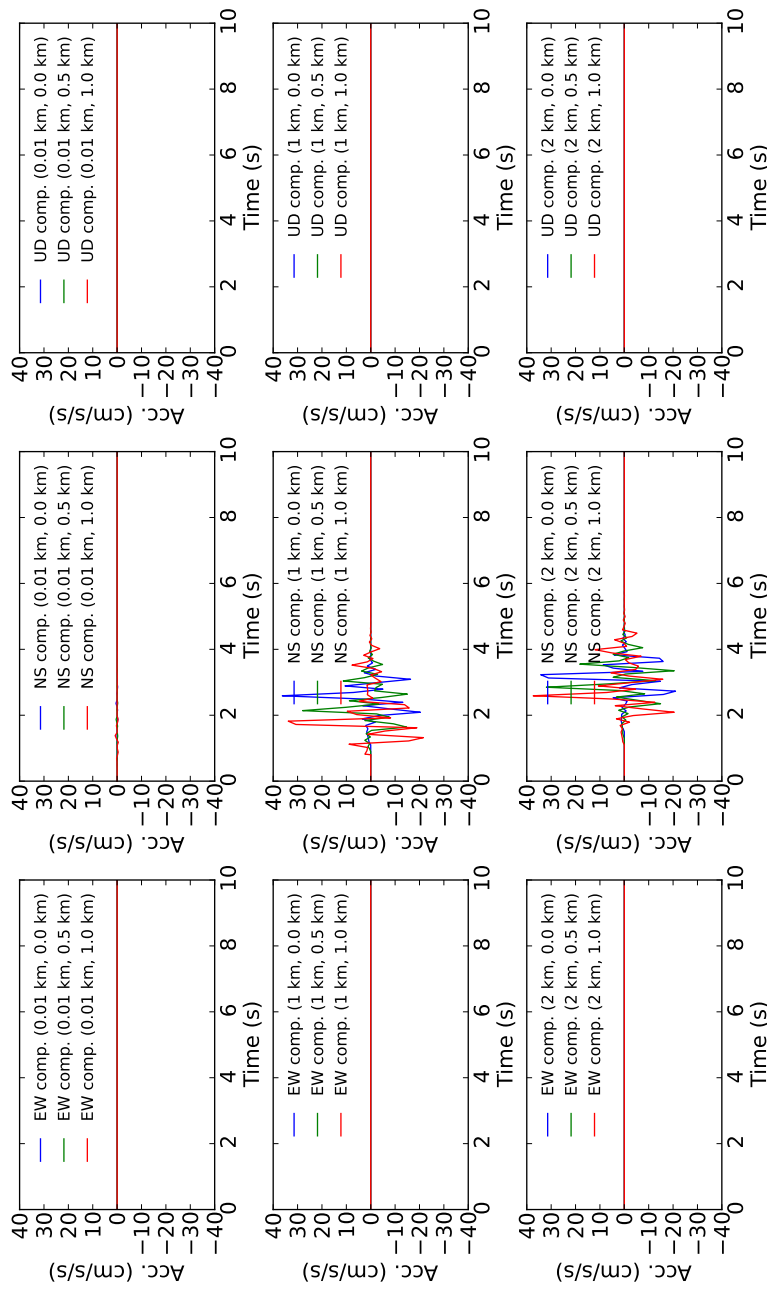


Figure 706.8: Calculated time history acceleration, station azimuth = 90°

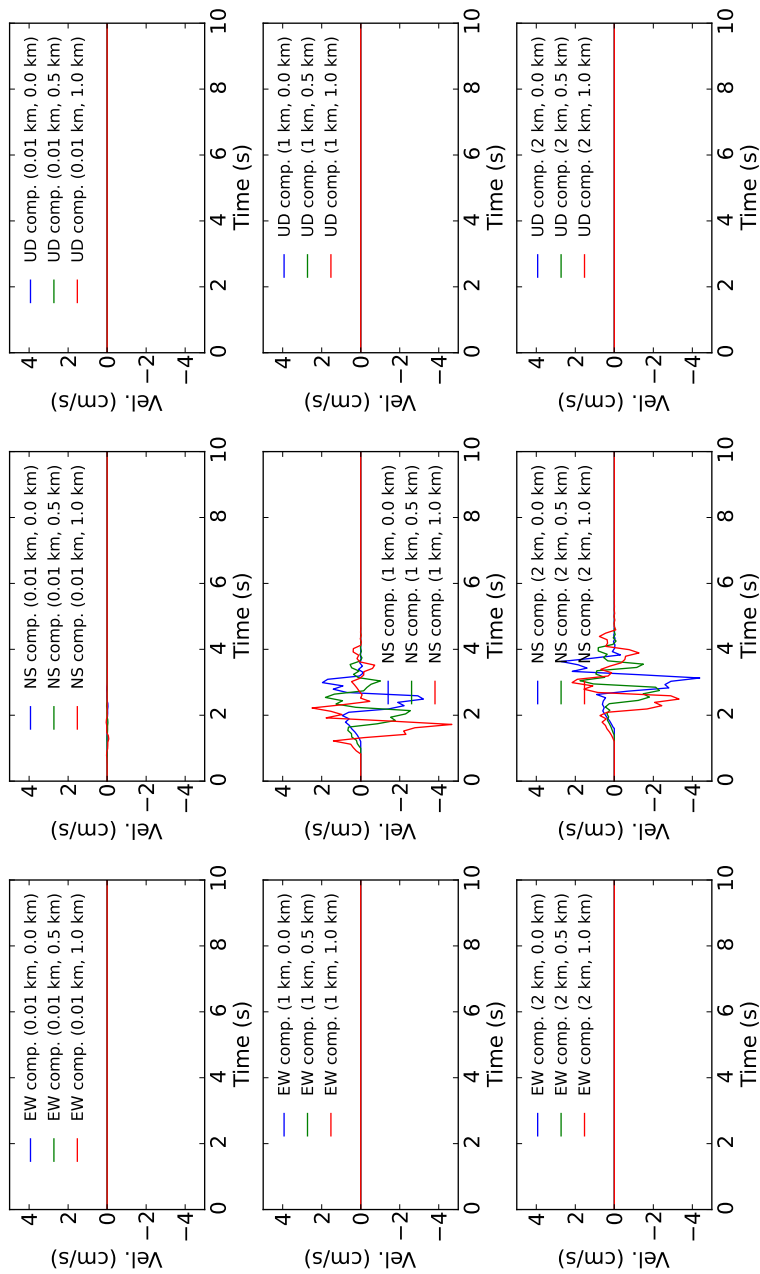


Figure 706.9: Calculated time history velocity, station azimuth = 90°

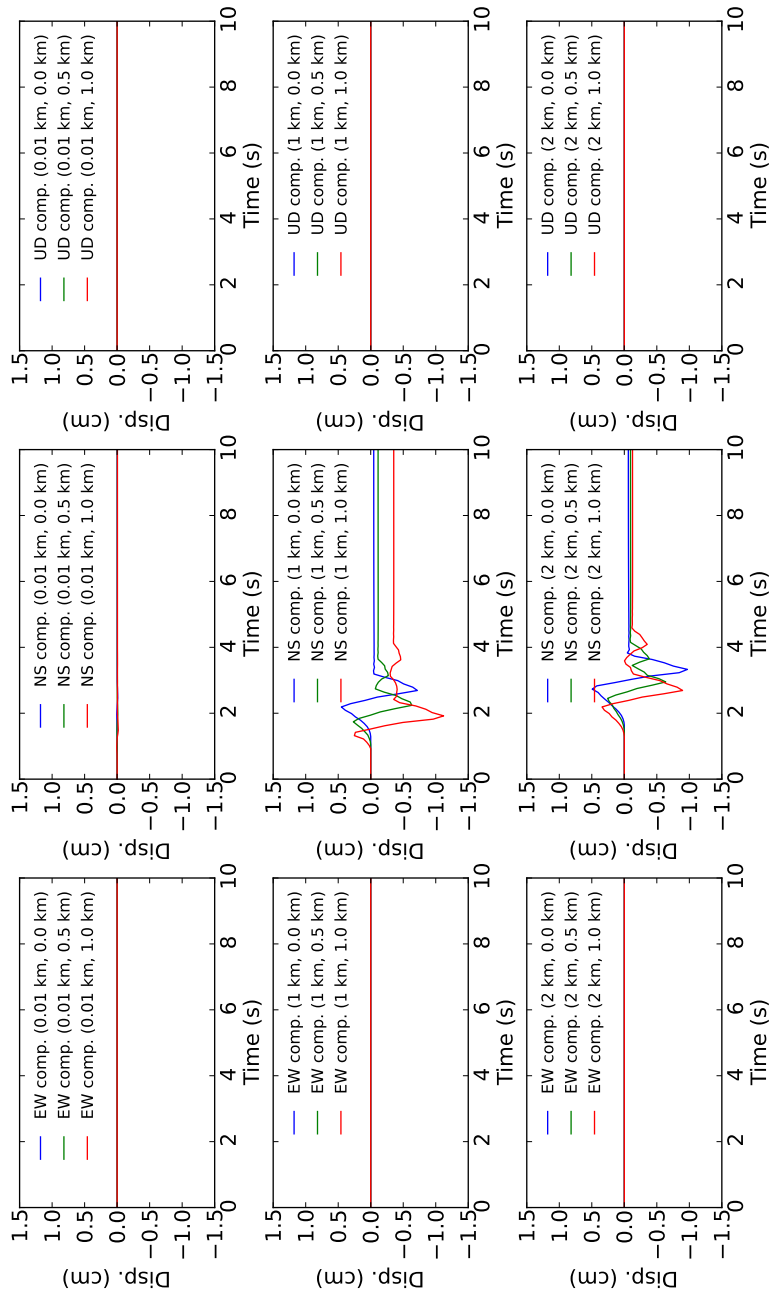


Figure 706.10: Calculated time history displacement, station azimuth = 90°

706.1.2.2 Case 2: dip-slip fault / single layer ground

Similar fault is tested for vertical (dip) slip (rake = 90°) fault case. Figure 706.11 shows model used for the analysis. Ground, fault, and wave properties are shown as below.

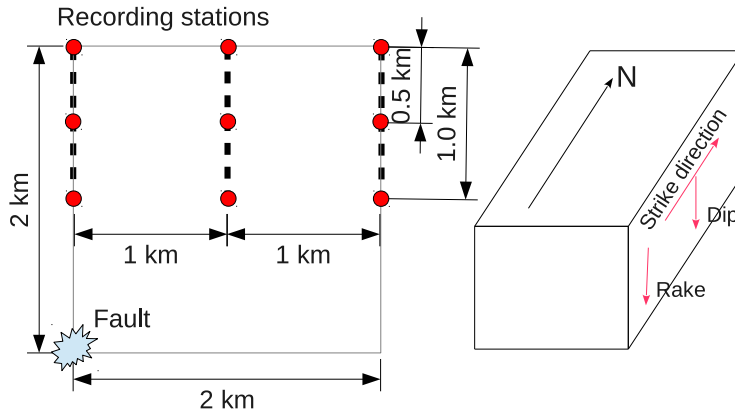


Figure 706.11: Ground and fault model used for analysis, results are captured on circles

- Ground properties

- $V_S = 1 \text{ km/s}$
- $V_P/V_S = 1.73$
- Poisson's ratio = 0.25
- Density = 1.32 g/cm^3
- Shear modulus = 1.32 GPa
- Elastic modulus = 3.31 GPa

- Fault properties

- Moment magnitude = 3.5
- Strike = 0°
- Dip = 90°
- Rake = 90°
- Double - coupled source
- Triangular source time function

- Wave properties

- $dt = 0.1$ s (Max available freq. = 5 Hz, Nyquist freq.)

Similar to the strike slip example, single layer ground ($V_s = 1$ km/s) is modeled. Fault is located at 2 km depth, 2 km away from the recording stations. Double coupled fault source is assumed and triangular source time function is used (Aki and Richards, 2002). Nine recording points are set as recording stations (Figure 706.11). Direction of the fault is aligned parallel to the north (strike = 0°) and rake is 90° . Station azimuth is set to 0° , 45° , and 90° .

Figure 706.12 – 706.20 show analyses results for this example. Since it's dip slip case, permanent deformation on UD components are observed (Figure 706.17 and 706.20).

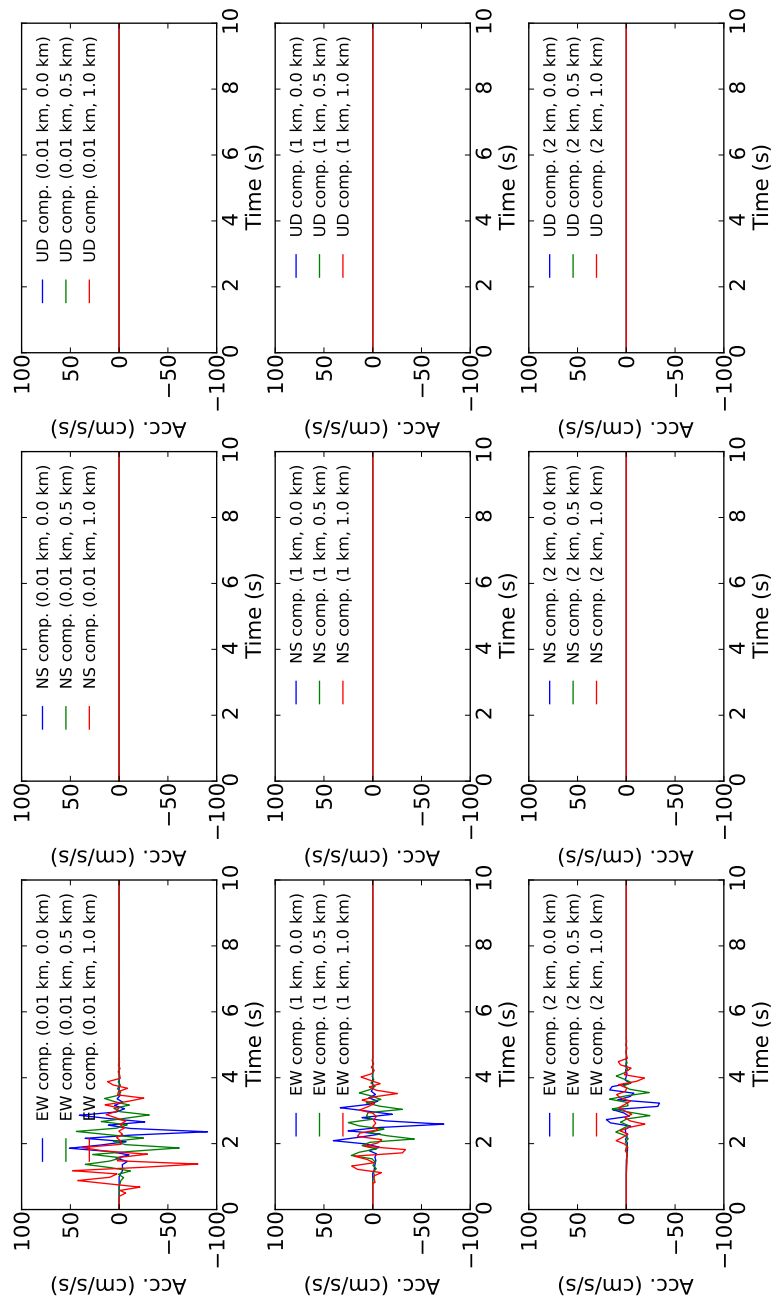


Figure 706.12: Calculated time history acceleration, station azimuth = 0°

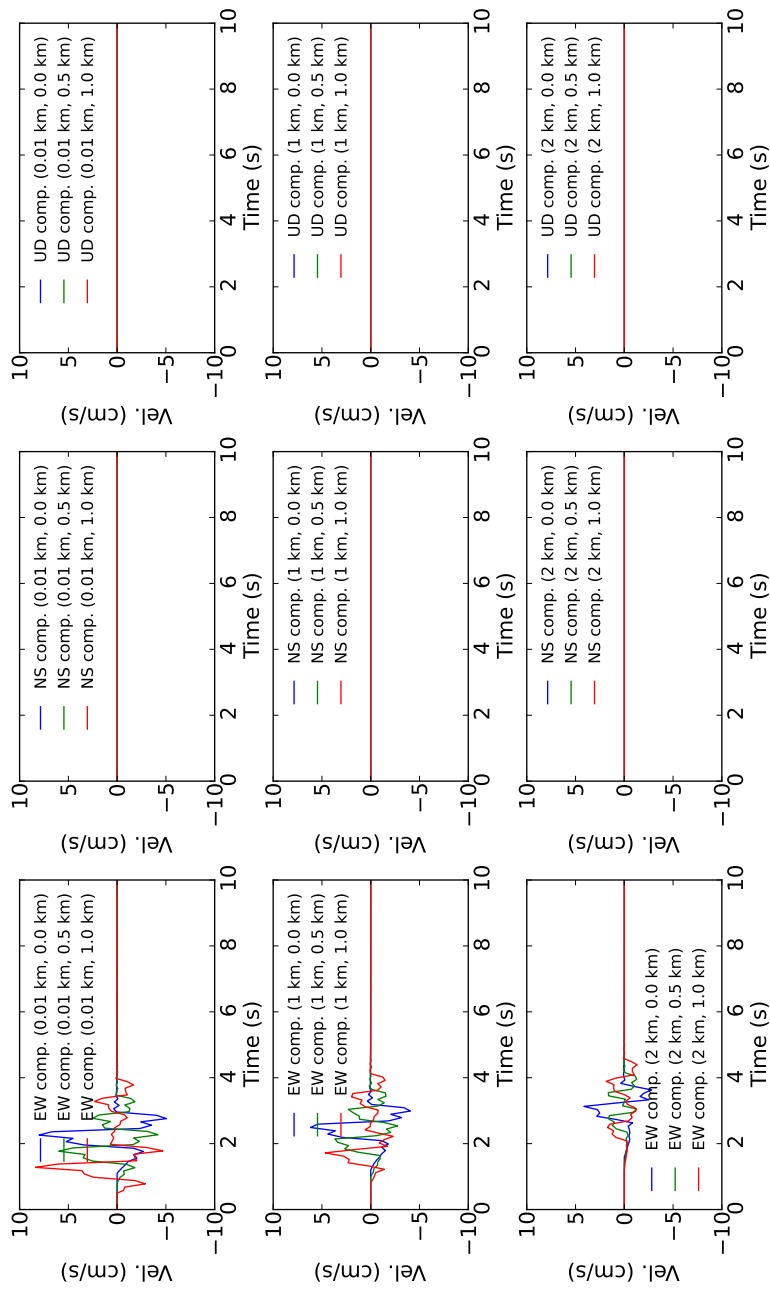


Figure 706.13: Calculated time history velocity, station azimuth = 0°

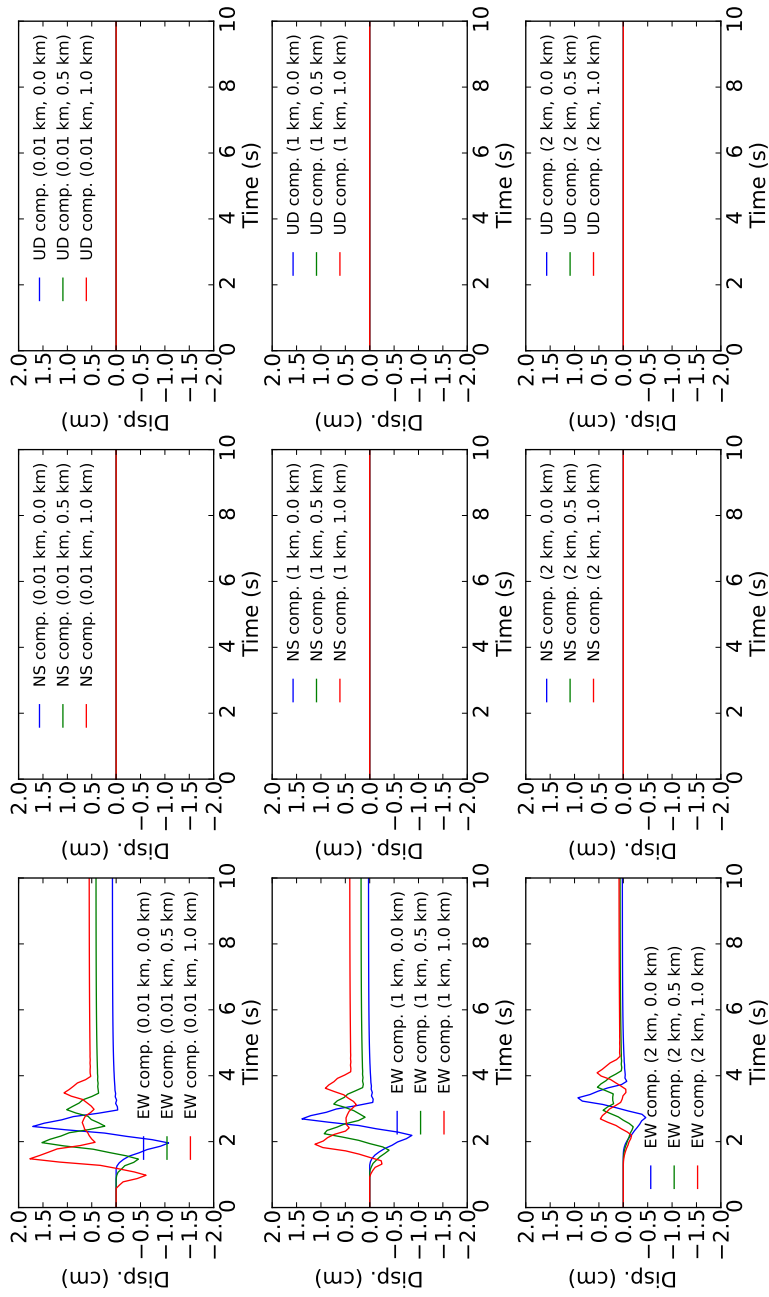


Figure 706.14: Calculated time history displacement, station azimuth = 0°

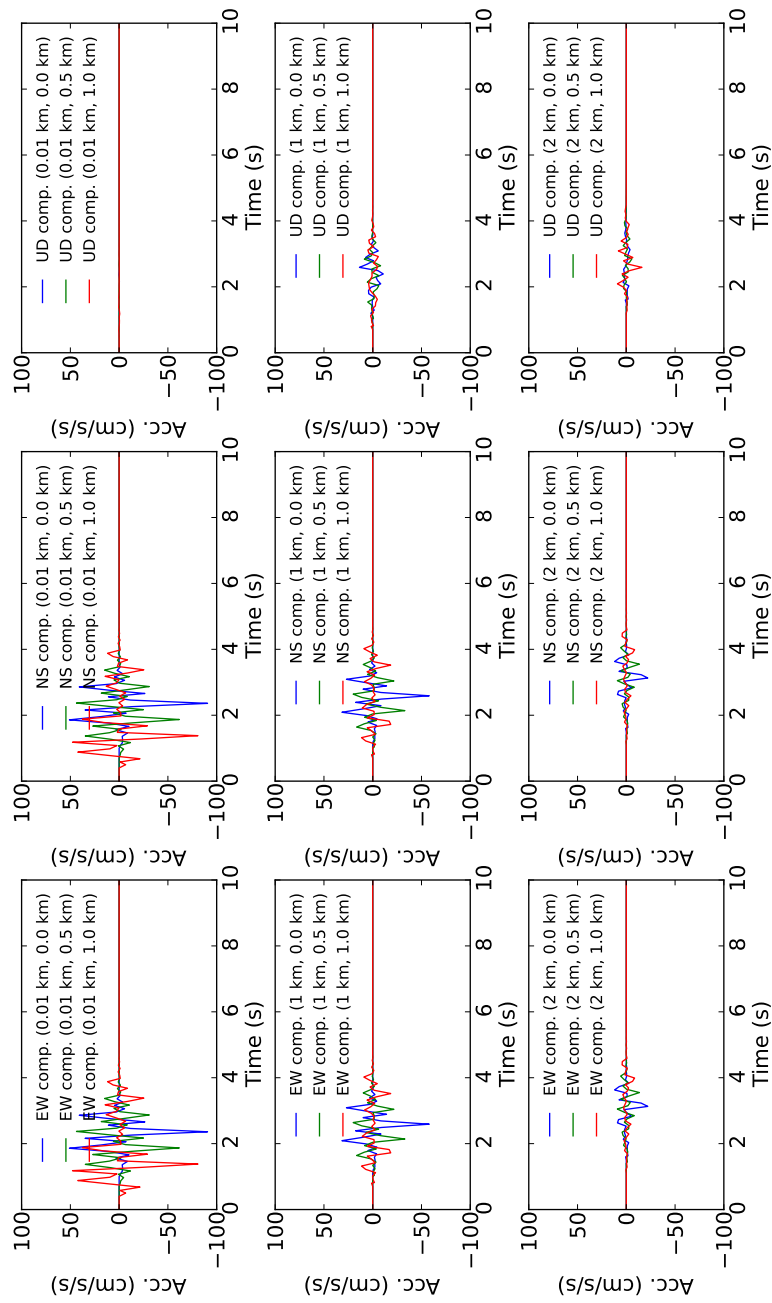
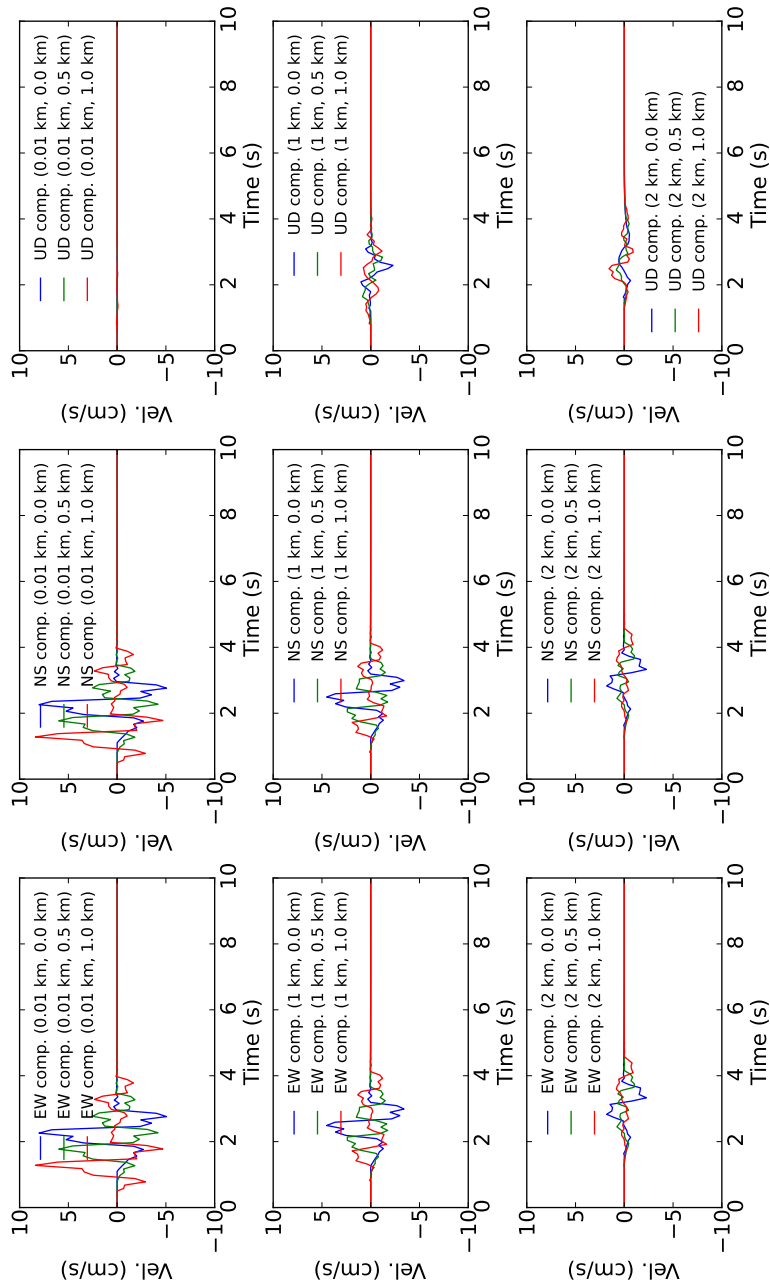


Figure 706.15: Calculated time history acceleration, station azimuth = 45°

Figure 706.16: Calculated time history velocity, station azimuth = 45°

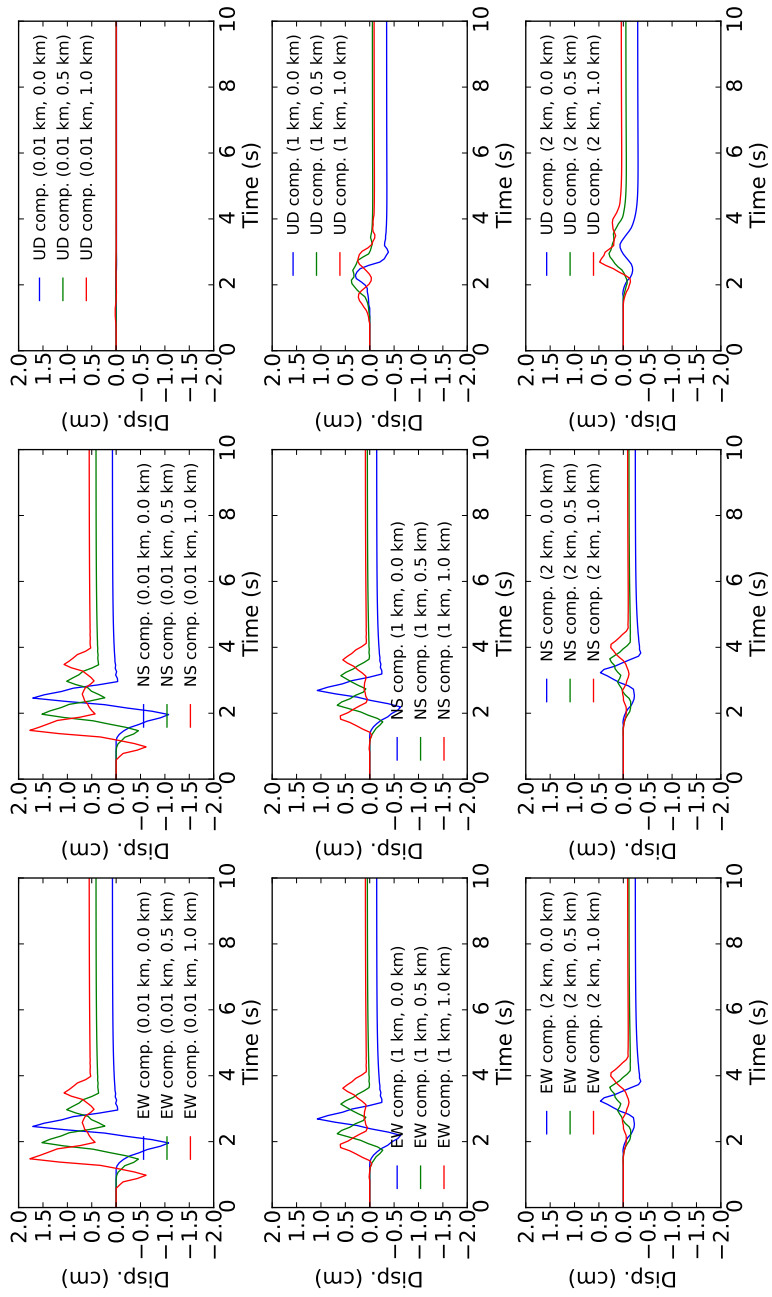
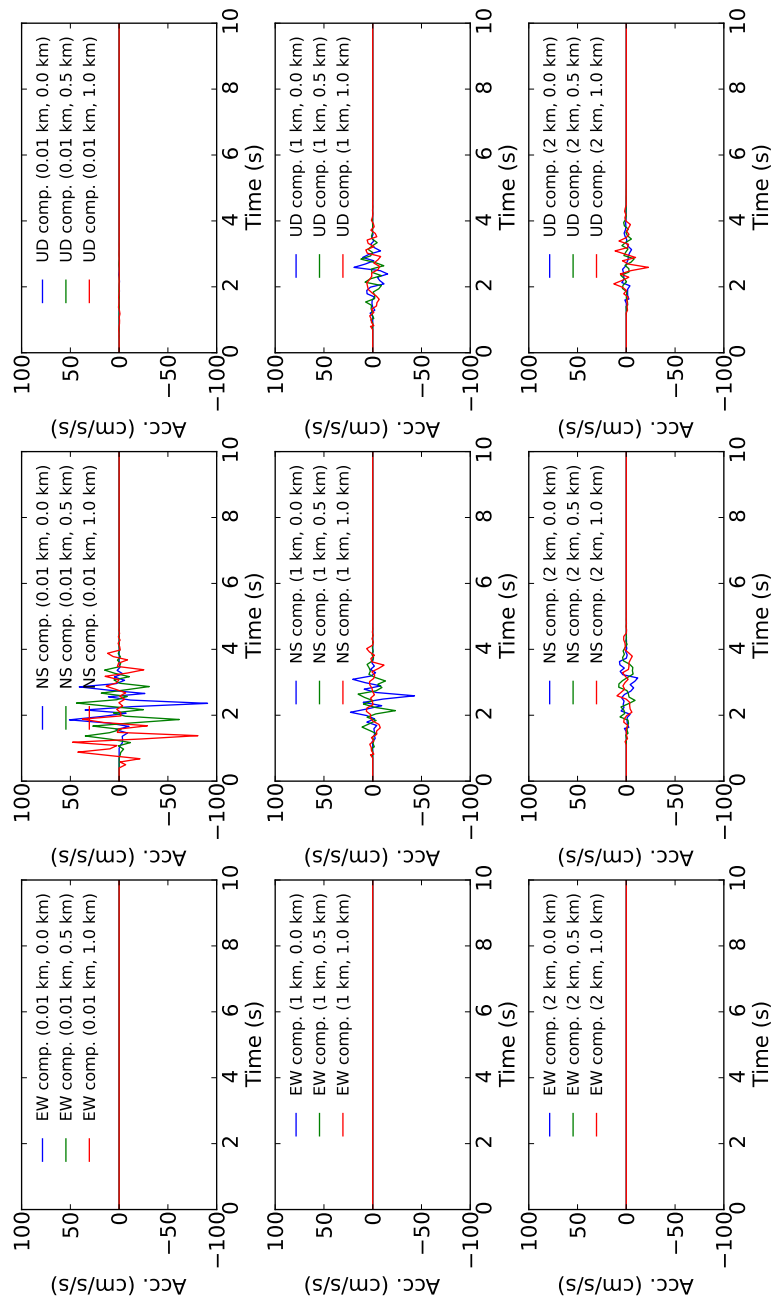


Figure 706.17: Calculated time history displacement, station azimuth = 45°

Figure 706.18: Calculated time history acceleration, station azimuth = 90°

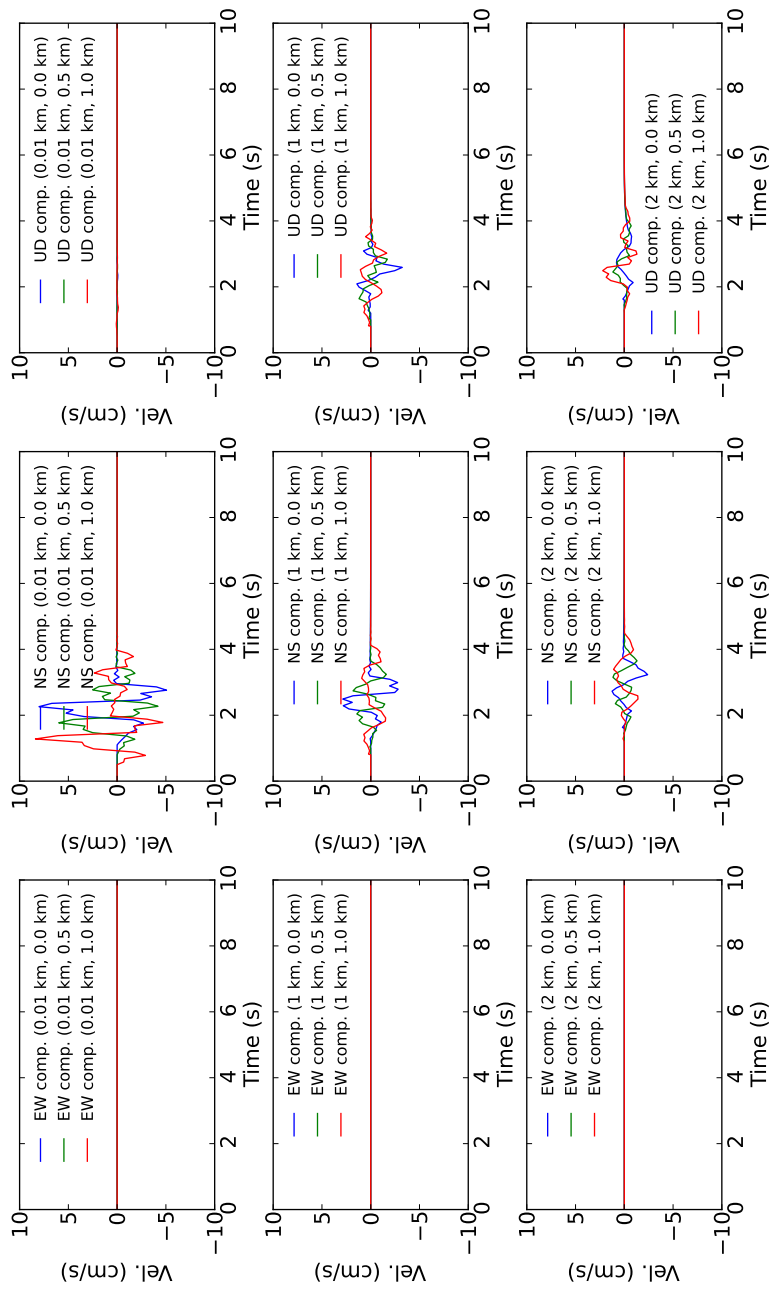


Figure 706.19: Calculated time history velocity, station azimuth = 90°

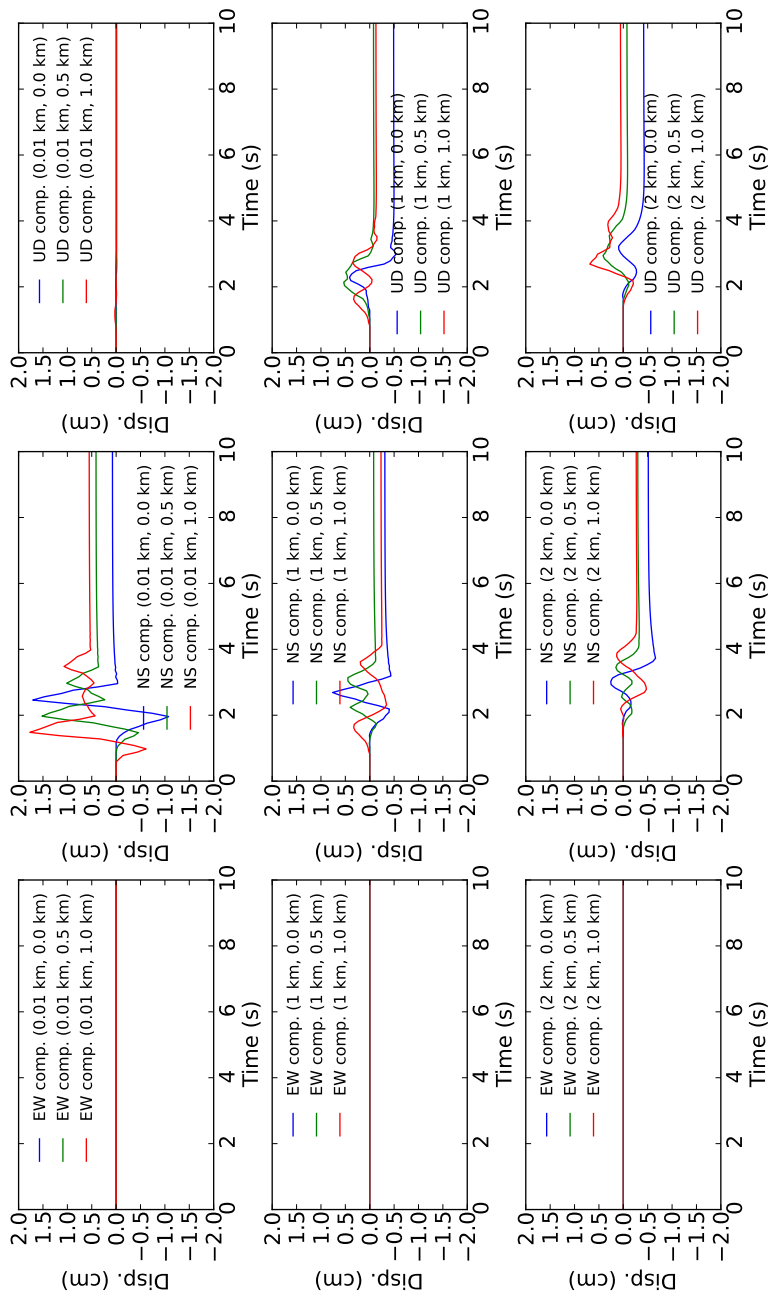


Figure 706.20: Calculated time history displacement, station azimuth = 90°

706.1.2.3 Case 3: normal fault / single layer ground

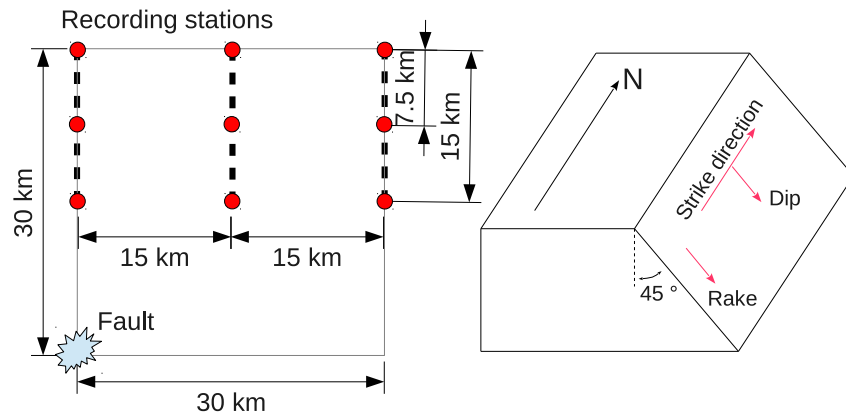


Figure 706.21: Ground and fault model used for analysis, results are captured on circles

Normal fault is tested. Figure 706.21 shows model used for the analysis. Wave is propagated through the single layer ground ($V_s = 1 \text{ km/s}$). Properties are shown as below.

- Ground properties

- $V_s = 1 \text{ km/s}$
- $V_p/V_s = 1.73$
- Poisson's ratio = 0.25
- Density = 1.32 g/cm^3
- Shear modulus = 1.32 GPa
- Elastic modulus = 3.31 GPa

- Fault properties

- Moment magnitude = 5.0
- Strike = 0°
- Dip = 45°
- Rake = 90°
- Double - coupled source
- Triangular source time function

- Wave properties

- $dt = 0.1$ s (Max available freq. = 5 Hz, Nyquist freq.)

In this example, the distance between the fault and the station is increased and magnitude is changed also ($M_w = 5.0$). Fault is located at 30 km depth, 30 km away from the recording stations (Figure 706.21). Double coupled fault source is assumed and triangular source time function is used (Aki and Richards, 2002). Recording points are similar as prior examples (total 9 stations). Azimuth of recording station is set to 0° , 45° , and 90° .

Figure 706.22 – 706.30 show analyses results. Since the distance between fault and station is increased to 30 km and waves are propagated through the ground with relatively low shear wave velocity, arrival of propagating and reflecting waves can be observed easily (the first arrival of P wave followed by S wave). Permanent displacements by the fault movement are observed as desired at all stations (0° , 45° , and 90°).

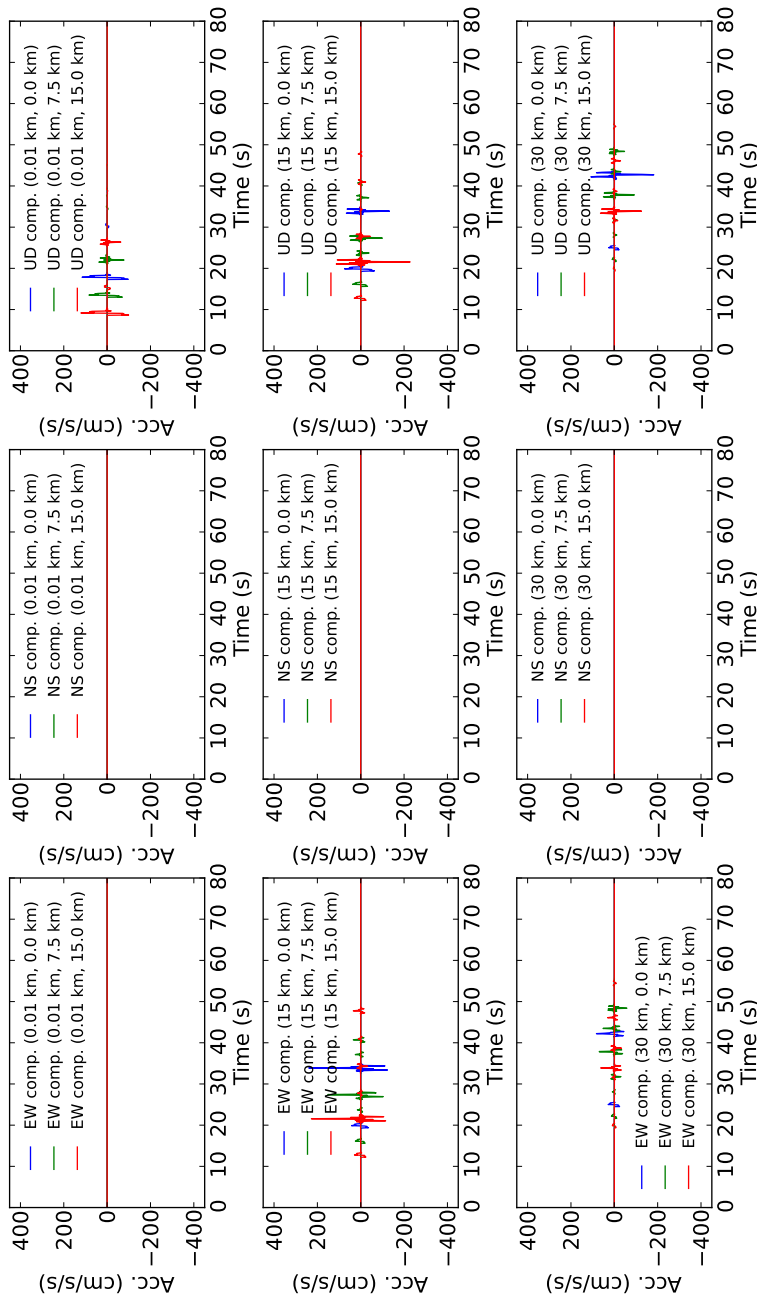


Figure 706.22: Calculated time history acceleration, station azimuth = 0°

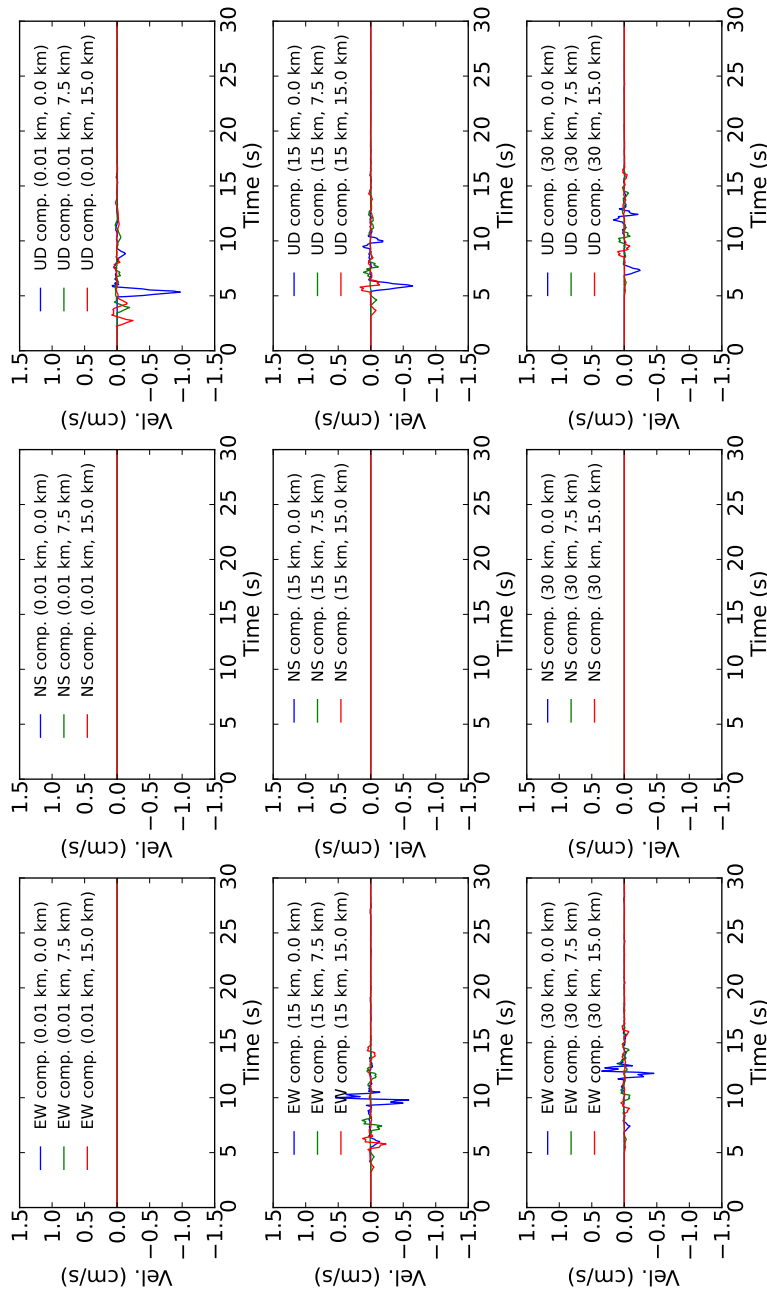
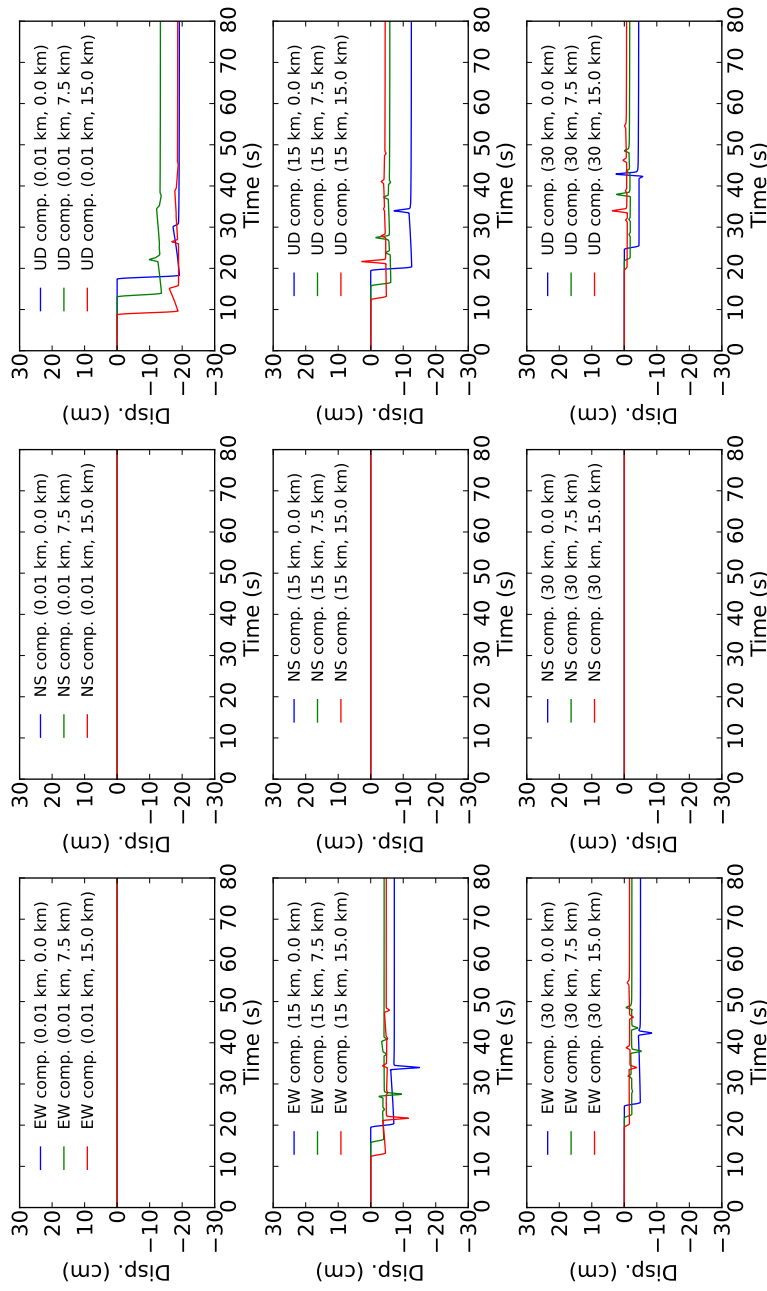


Figure 706.23: Calculated time history velocity, station azimuth = 0°

Figure 706.24: Calculated time history displacement, station azimuth = 0°

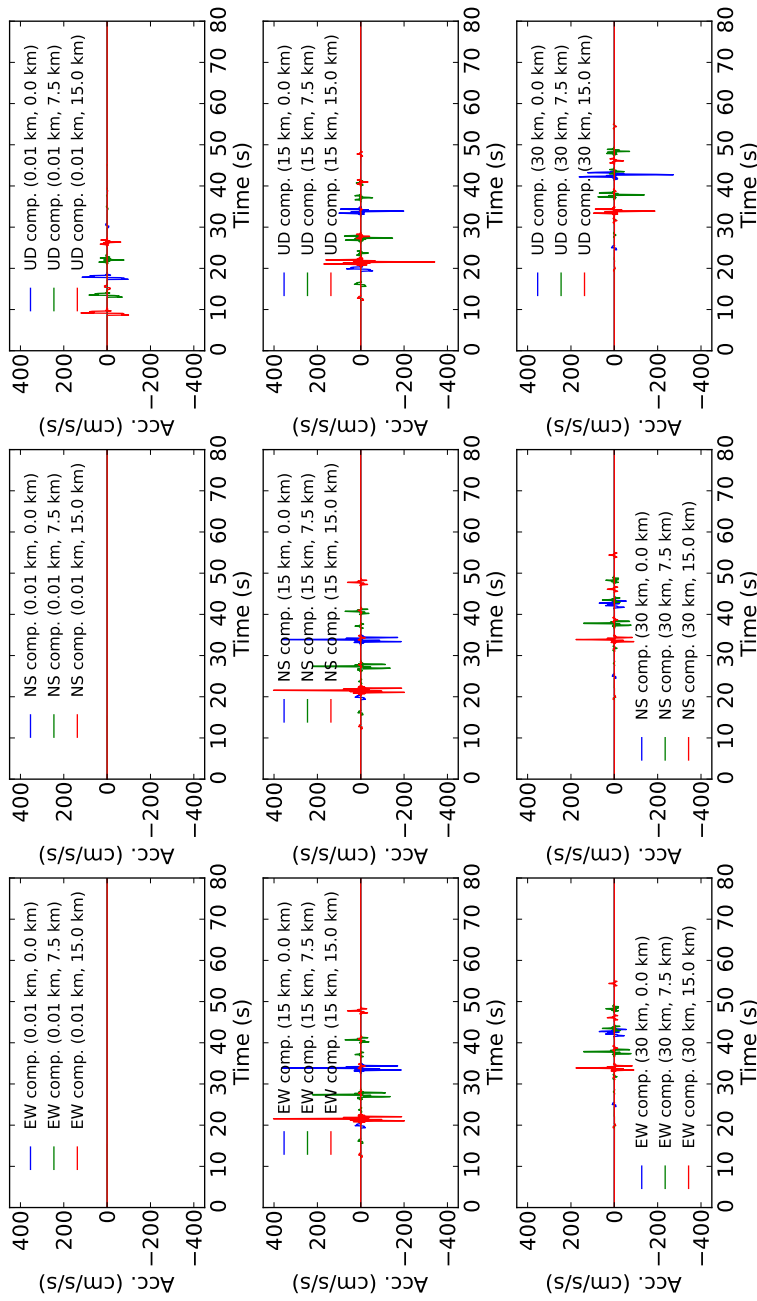


Figure 706.25: Calculated time history acceleration, station azimuth = 45°

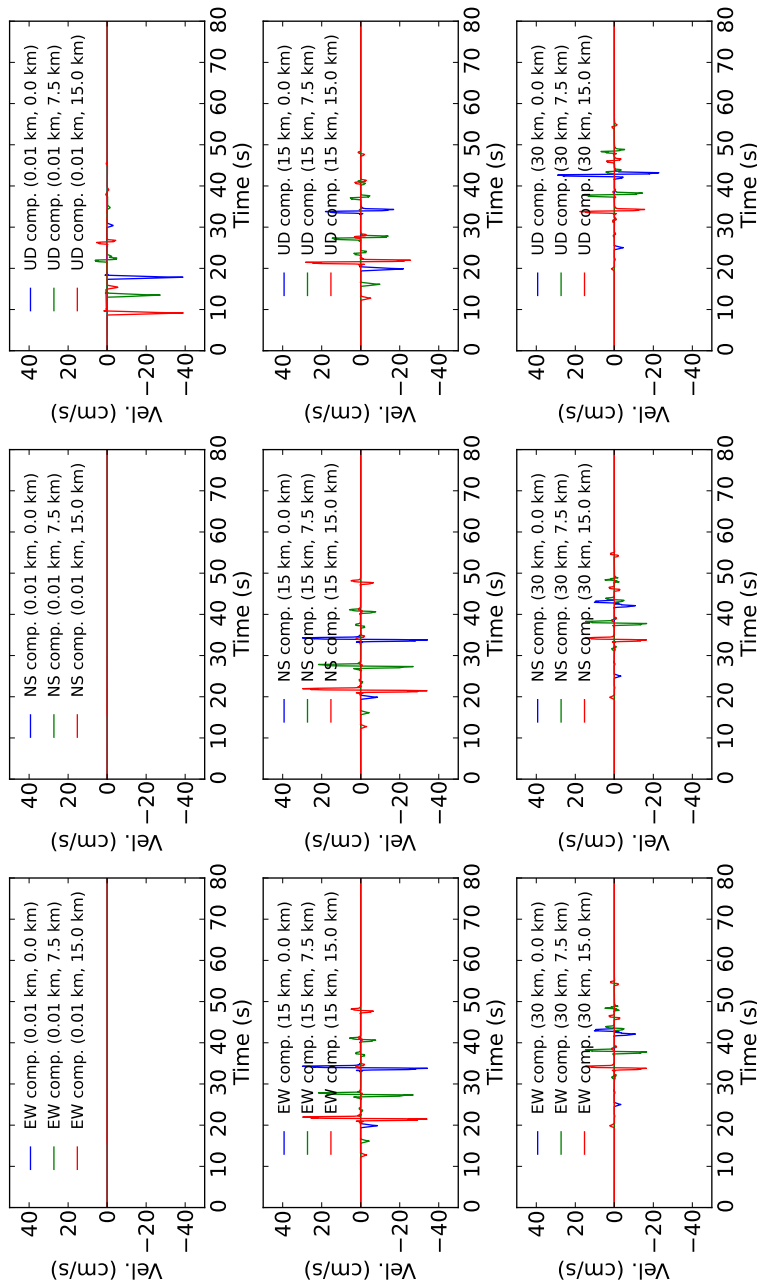


Figure 706.26: Calculated time history velocity, station azimuth = 45°

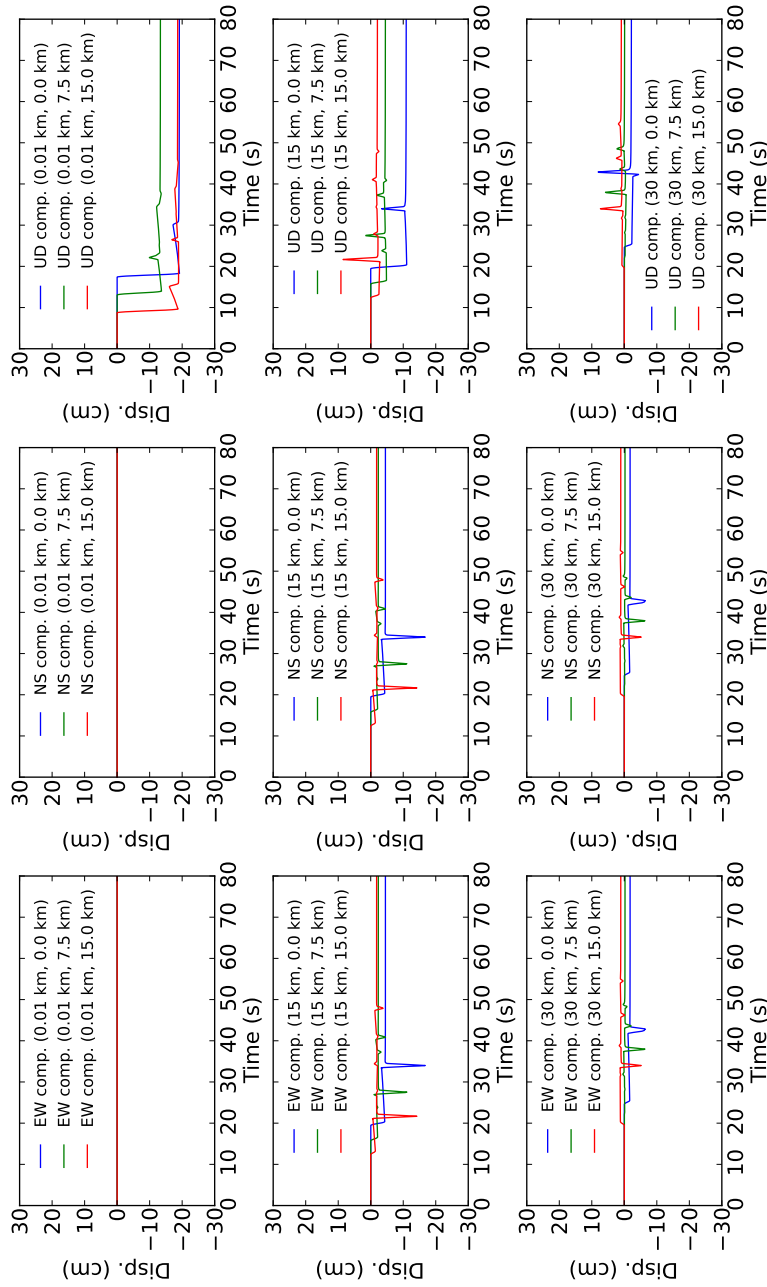


Figure 706.27: Calculated time history displacement, station azimuth = 45°

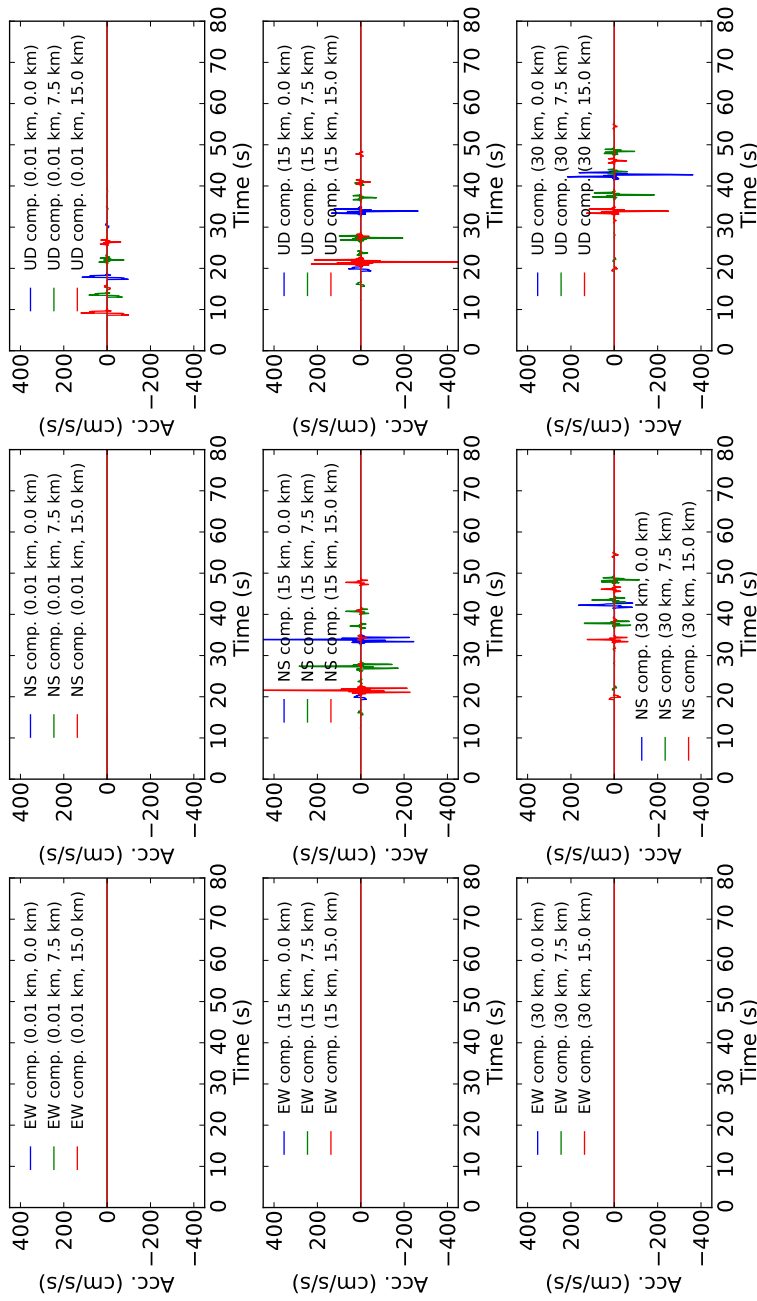


Figure 706.28: Calculated time history acceleration, station azimuth = 90°

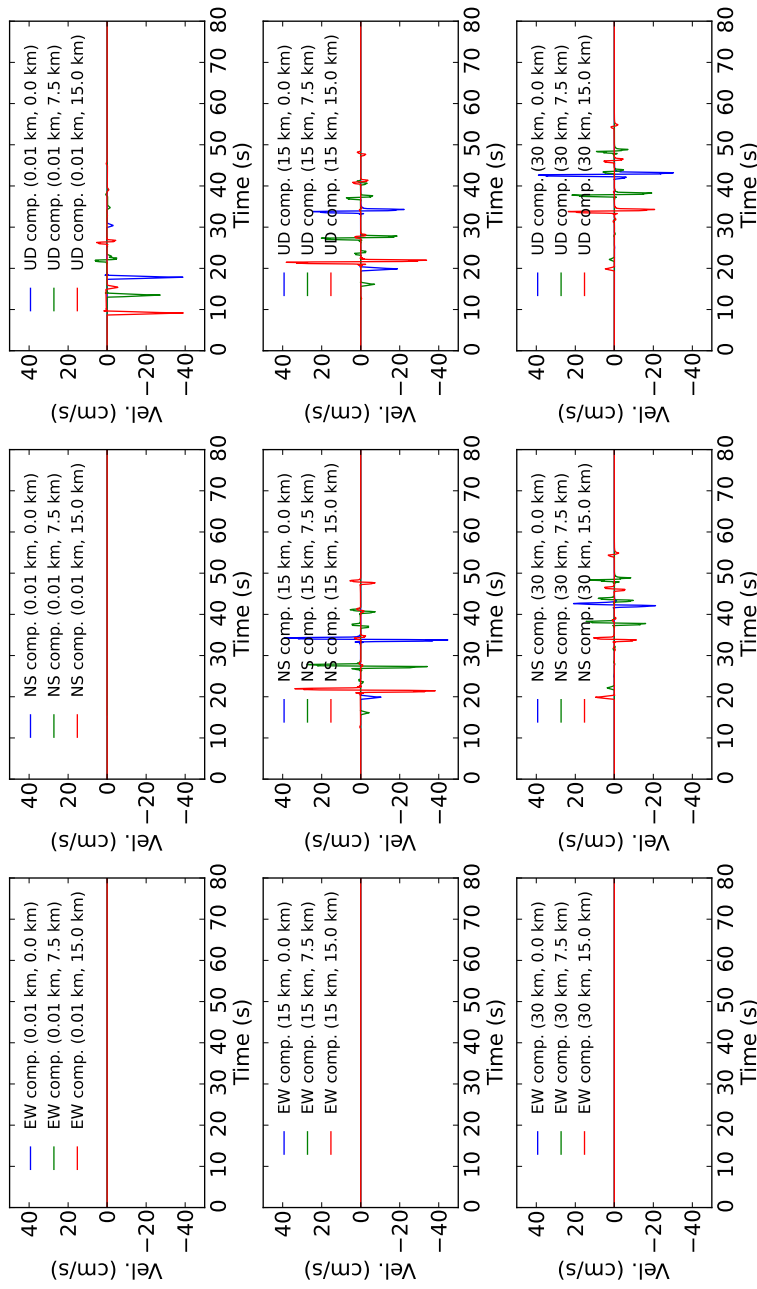


Figure 706.29: Calculated time history velocity, station azimuth = 90°

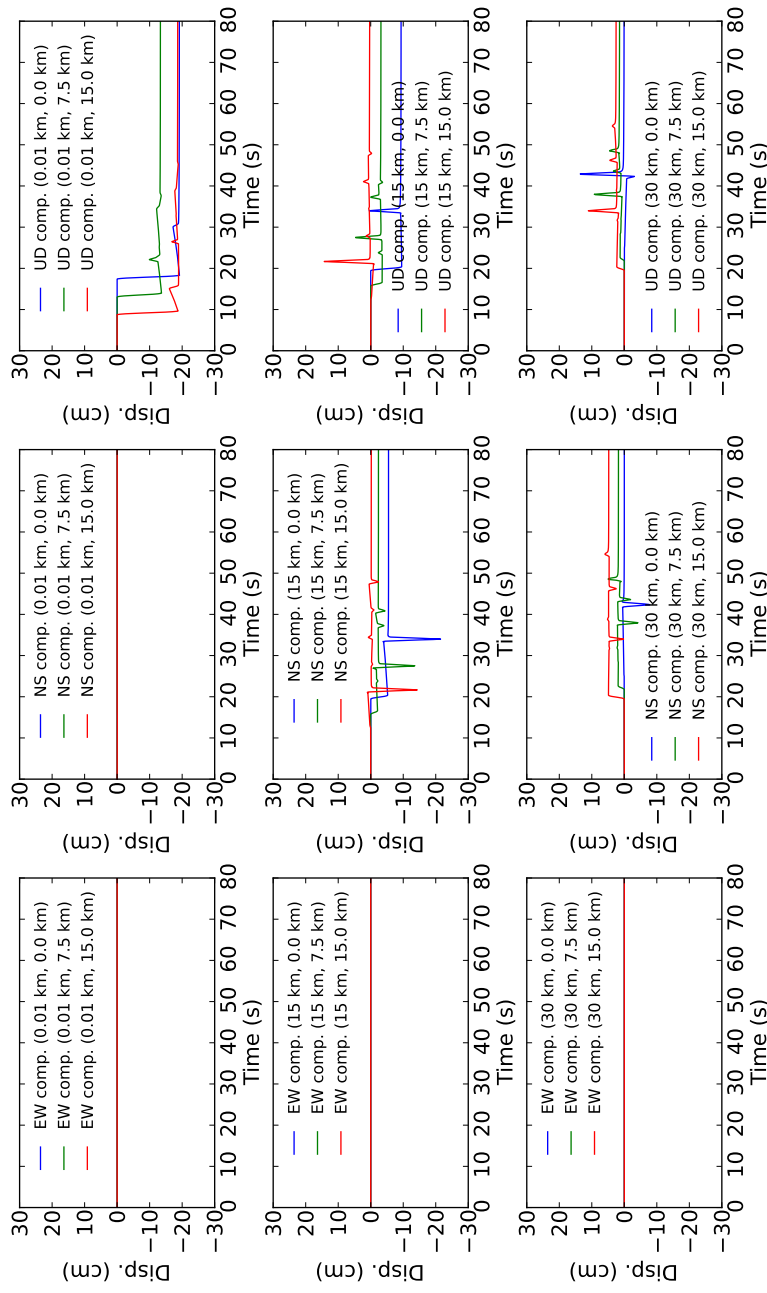


Figure 706.30: Calculated time history displacement, station azimuth = 90°

706.1.2.4 Case 4: normal fault / layered ground

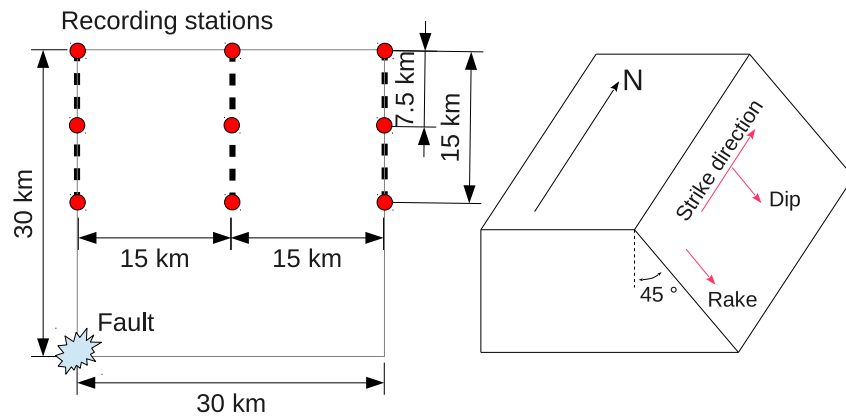


Figure 706.31: Ground and fault model used for analysis, results are captured on circles

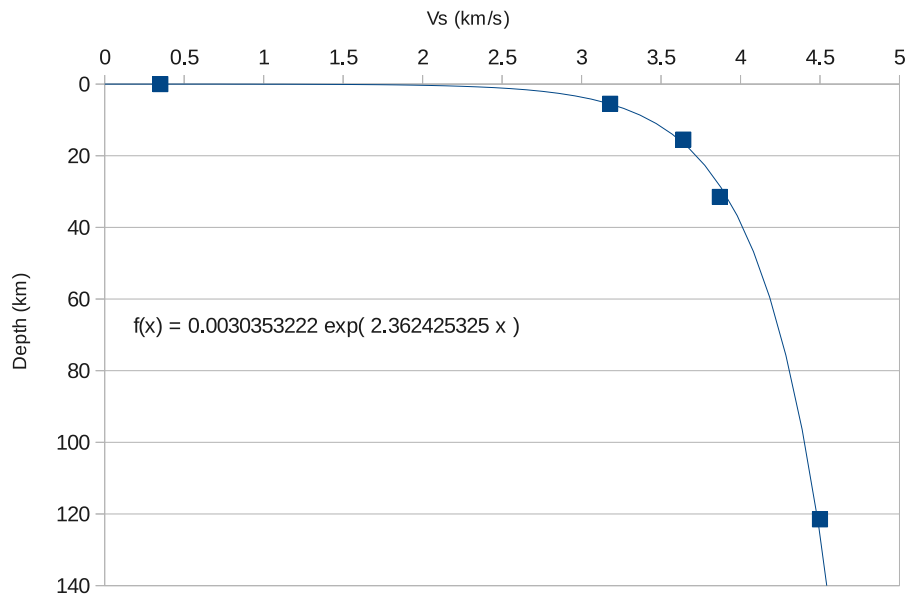


Figure 706.32: Vs profile, square points are hk model; blue line is trend line based on hk model

Normal fault within layered ground is modeled. Model is as shown Figure 706.31 and 706.32. Properties are shown below.

- Ground properties: see Figure 706.32 and Table 706.1
- Fault properties

- Moment magnitude = 5.0
- Strike = 0°
- Dip = 45°
- Rake = 90°
- Double - coupled source
- Triangular source time function
- Wave properties
 - $dt = 0.1$ s (Max available freq. = 5 Hz, Nyquist freq.)

Fault is located at depth of 30 km, 30 km away from the recording point (station) at surface. Double coupled fault source is assumed and triangular source time function is used ([Aki and Richards, 2002](#)). Recording points are similar as prior examples (total 9 stations). The 1D standard southern California model ([Hadley and Kanamori \(1977\)](#), hk model hereafter) is used for ground layering. As shown in Figure 706.32, hk model is interpolated and divided to define ground layer (Table 706.1).

Results are shown on Figure 706.33 – 706.35. Since wave is propagated through the layered ground, compared to prior examples, more realistic waves are observed.

Table 706.1: Ground properties for the example

Depth (km)	Thickness (km)	VS (km/s)	VP/Vs	QB (km/s)	VP (km/s)	Poisson's R	Density (g/cm ³)	G (GPa)	E (GPa)
0.01	0.01	0.50	1.730	500	0.87	0.25	1.05	0.27	0.67
0.02	0.01	0.80	1.730	500	1.38	0.25	1.21	0.77	1.93
0.03	0.01	0.97	1.730	500	1.68	0.25	1.31	1.23	3.07
0.04	0.01	1.09	1.730	500	1.89	0.25	1.37	1.64	4.09
0.05	0.01	1.19	1.730	500	2.05	0.25	1.43	2.01	5.01
0.06	0.01	1.26	1.730	500	2.19	0.25	1.47	2.34	5.86
0.07	0.01	1.33	1.730	500	2.30	0.25	1.51	2.66	6.64
0.08	0.01	1.38	1.730	500	2.40	0.25	1.54	2.95	7.36
0.09	0.01	1.43	1.730	500	2.48	0.25	1.56	3.22	8.04
0.1	0.01	1.48	1.730	500	2.56	0.25	1.59	3.48	8.69
0.2	0.10	1.77	1.730	500	3.07	0.25	1.75	5.50	13.75
0.3	0.10	1.94	1.730	500	3.36	0.25	1.85	6.98	17.44
0.4	0.10	2.07	1.730	500	3.57	0.25	1.91	8.17	20.41
0.5	0.10	2.16	1.730	500	3.74	0.25	1.97	9.18	22.93
0.6	0.10	2.24	1.730	500	3.87	0.25	2.01	10.06	25.13
0.7	0.10	2.30	1.730	500	3.98	0.25	2.04	10.85	27.10
0.8	0.10	2.36	1.730	500	4.08	0.25	2.08	11.56	28.88
0.9	0.10	2.41	1.730	500	4.17	0.25	2.10	12.21	30.51
1	0.10	2.45	1.730	500	4.25	0.25	2.13	12.82	32.02
1.5	0.50	2.63	1.730	500	4.54	0.25	2.22	15.33	38.30
2.5	1.00	2.84	1.730	500	4.92	0.25	2.34	18.92	47.28
3.5	1.00	2.98	1.730	500	5.16	0.25	2.42	21.57	53.89
4.5	1.00	3.09	1.730	500	5.35	0.25	2.48	23.70	59.21
5.5	1.00	3.18	1.730	600	5.50	0.25	2.53	25.59	63.93
16	10.50	3.64	1.731	600	6.30	0.25	2.70	36.02	92.26

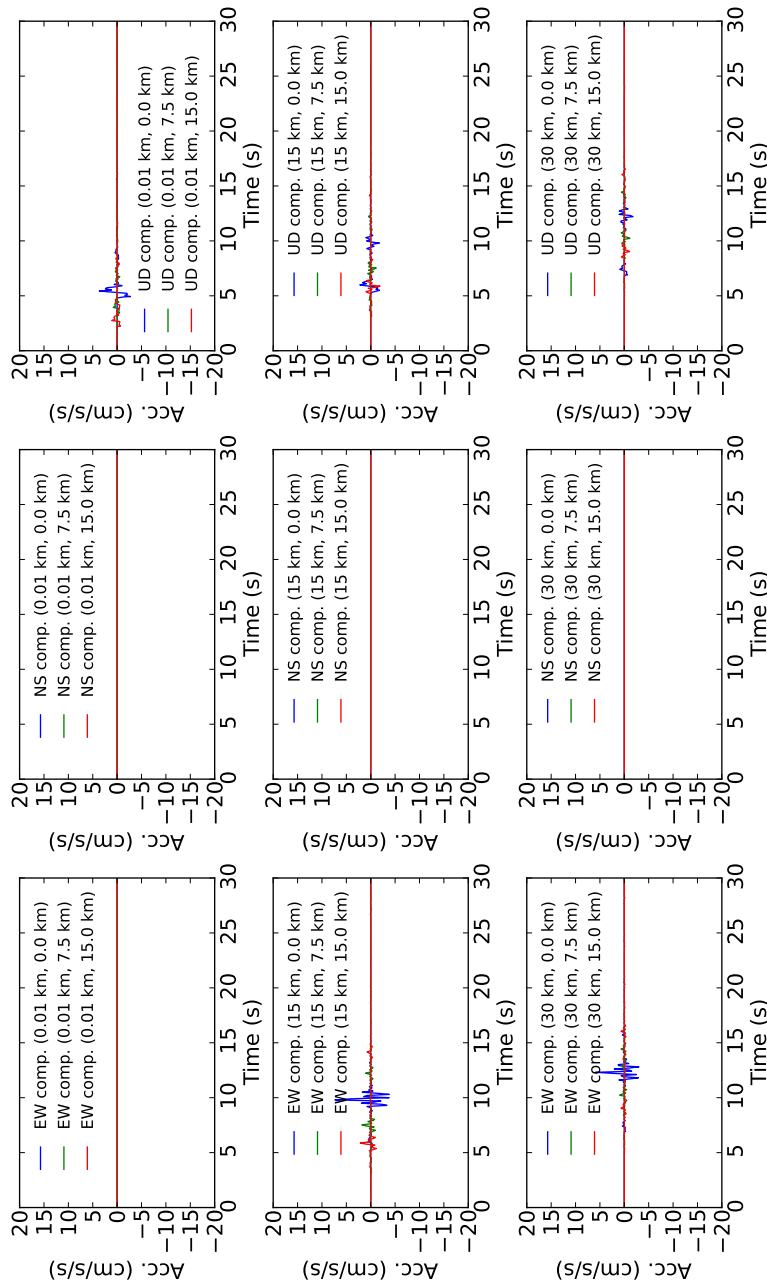


Figure 706.33: Calculated time history acceleration, station azimuth = 0°

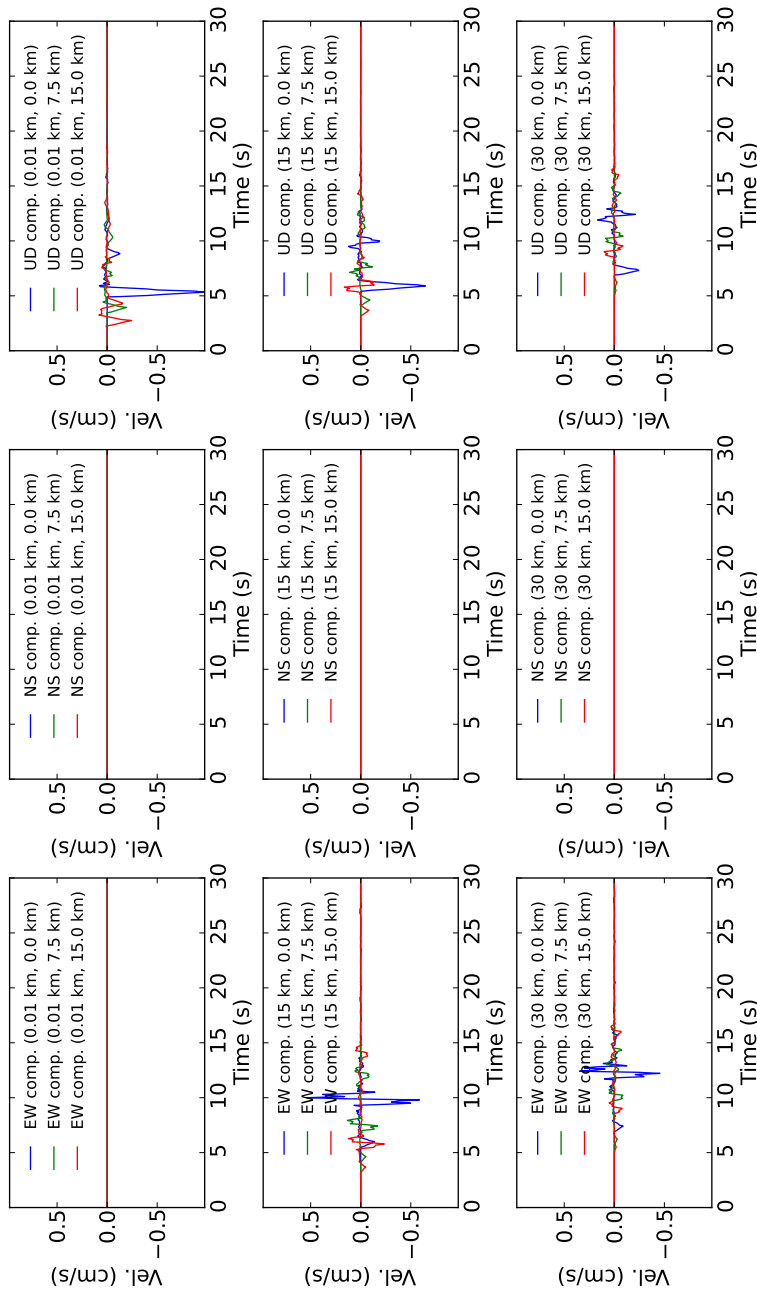


Figure 706.34: Calculated time history velocity, station azimuth = 0°

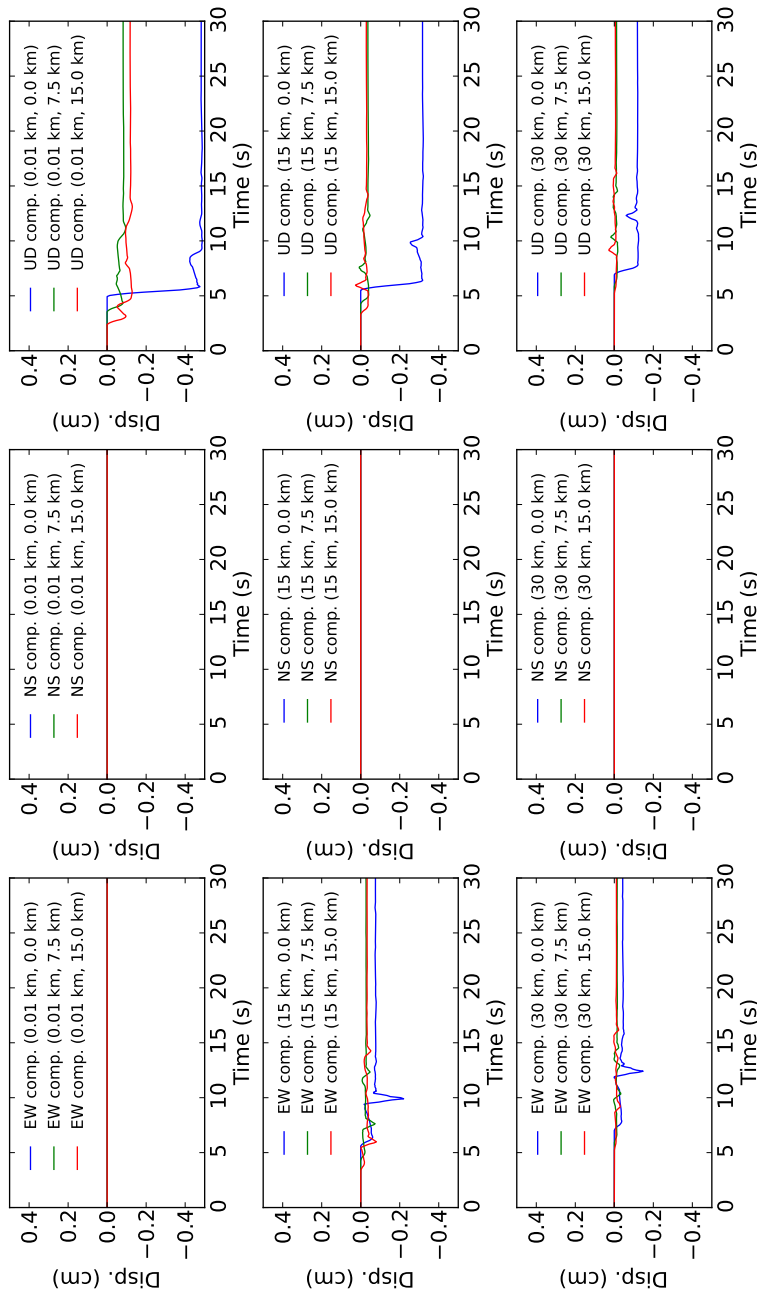


Figure 706.35: Calculated time history displacement, station azimuth = 0°

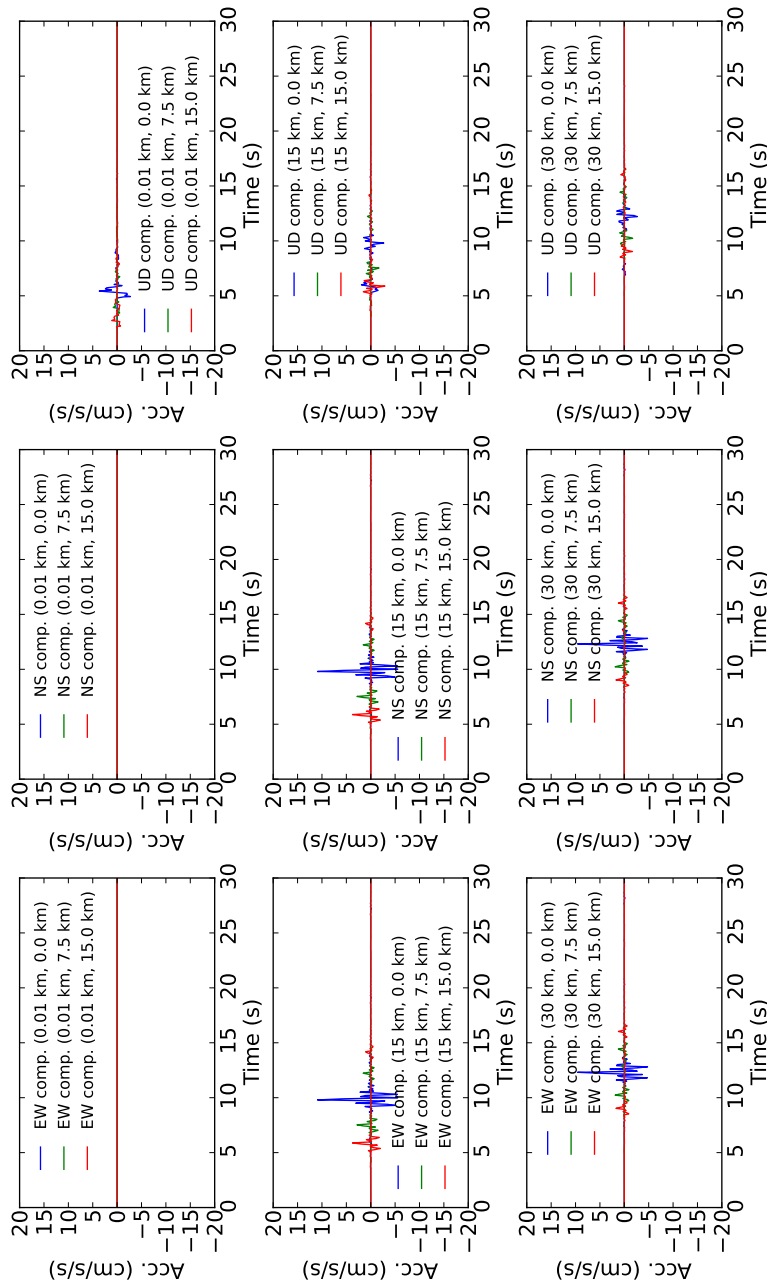


Figure 706.36: Calculated time history acceleration, station azimuth = 45°

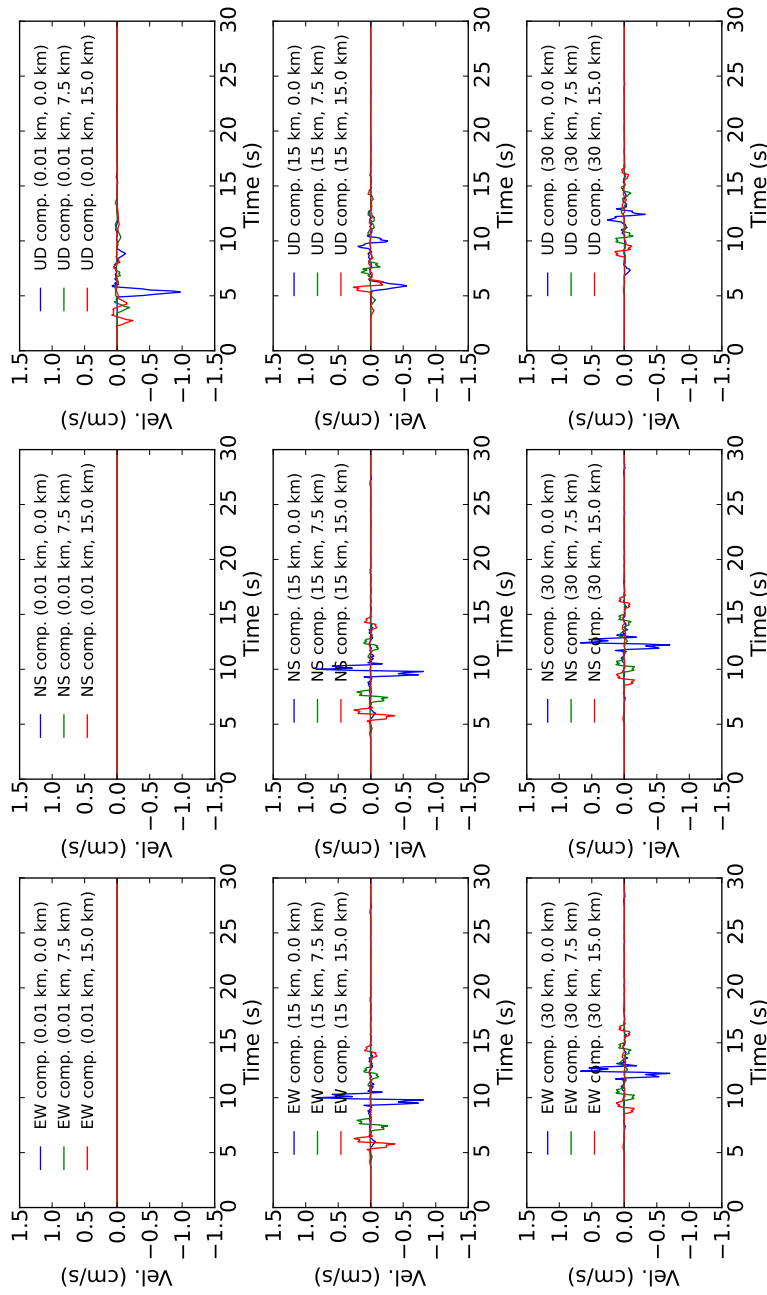


Figure 706.37: Calculated time history velocity, station azimuth = 45°

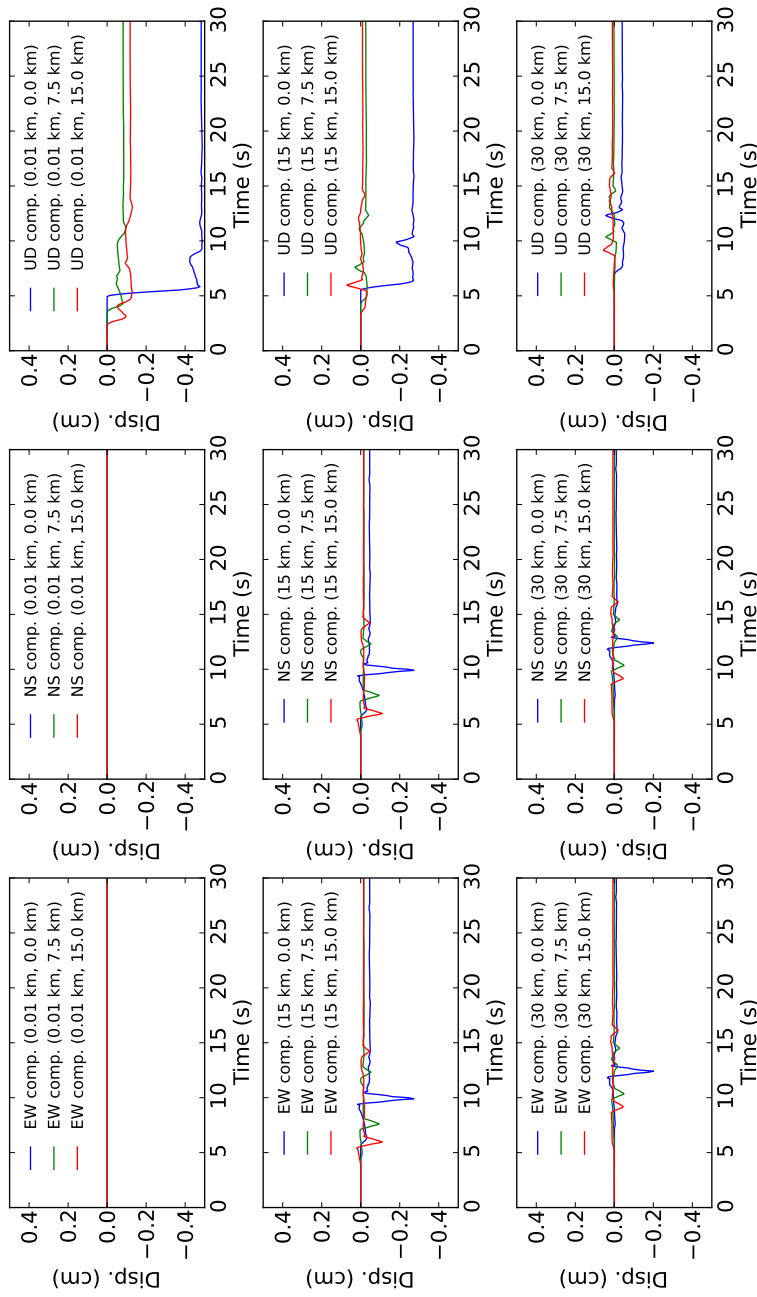


Figure 706.38: Calculated time history displacement, station azimuth = 45°

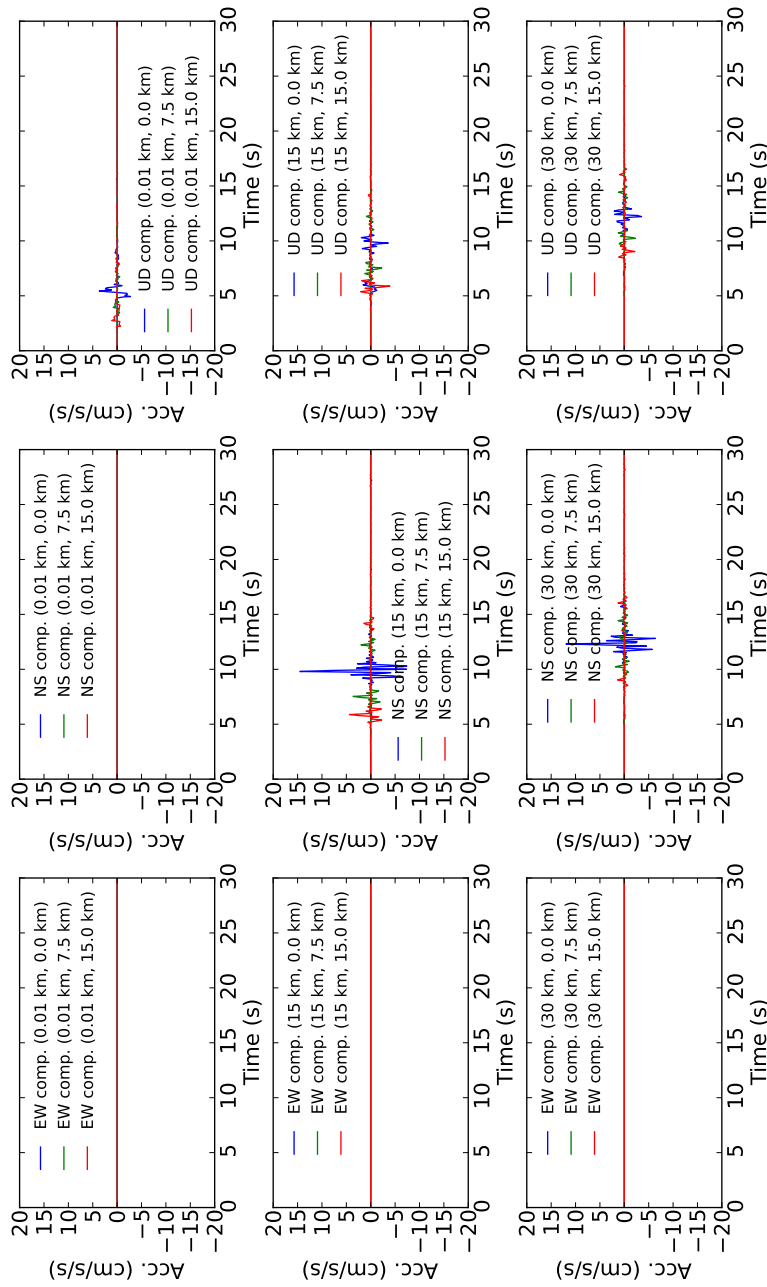


Figure 706.39: Calculated time history acceleration, station azimuth = 90°

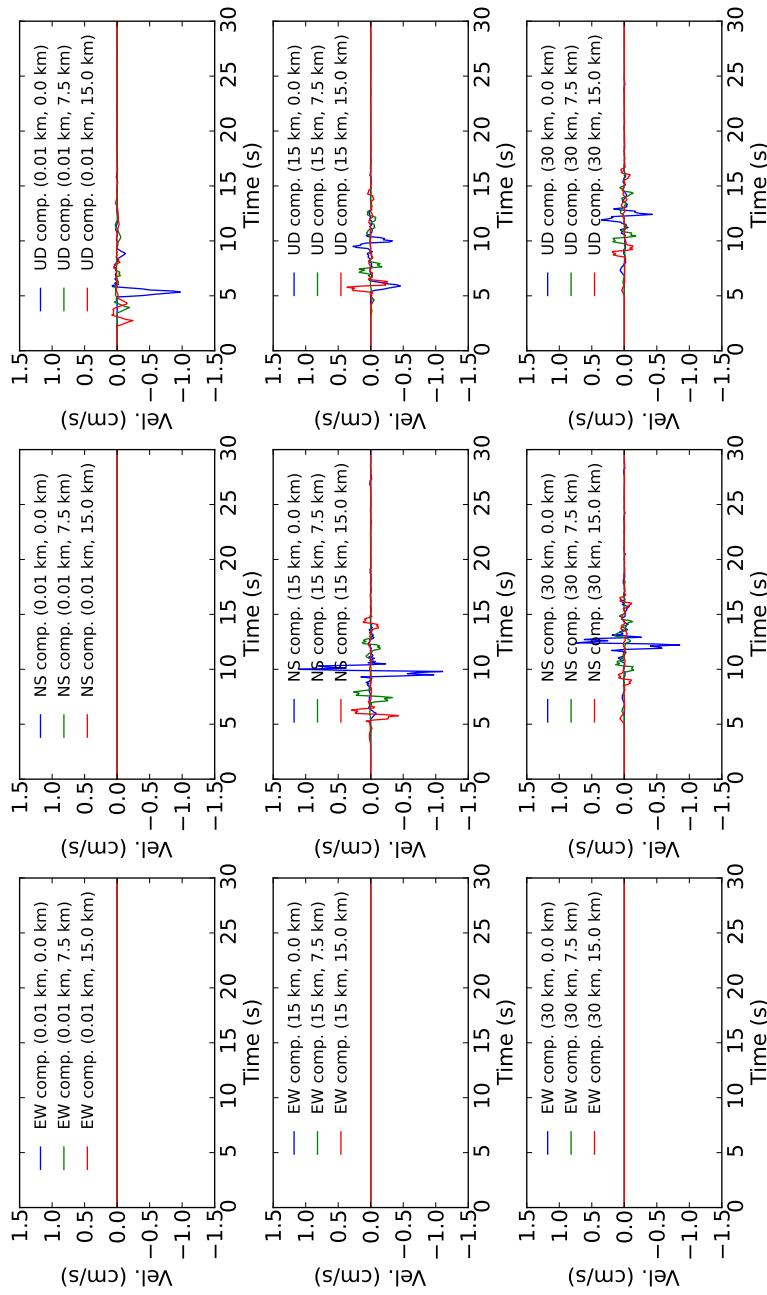


Figure 706.40: Calculated time history velocity, station azimuth = 90°

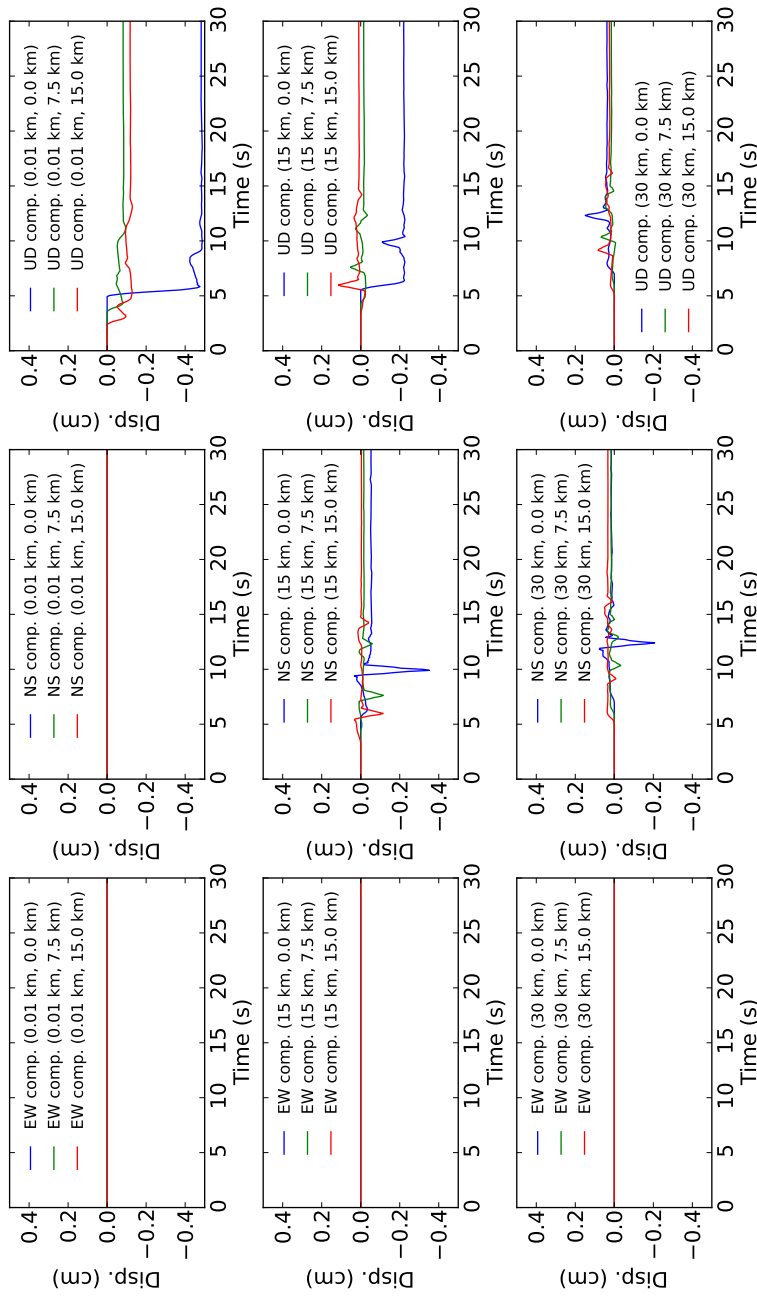


Figure 706.41: Calculated time history displacement, station azimuth = 90°

706.1.2.5 Case 5: Northridge earthquake / layered ground

In this example, Northridge earthquakes are simulated. Northridge earthquake has occurred on January, 1994 with a moment magnitude of 6.7. Properties are shown as below and partly adapted from Hisada (2008) and Wald et al. (1996).

- Ground properties: see Table 706.2
- Fault properties
 - Moment magnitude = 6.7
 - Strike = 122°
 - Dip = 40°
 - Rake = 140°
 - Double - coupled source
 - Triangular source time function
- Wave properties
 - $dt = 0.05 \text{ s}$ (Max available freq. = 10 Hz, Nyquist freq.)

Source depth is set as 25 km and epicentral distance from the fault to the station is set as 30 km.

Station is located on the ground surface. As shown in Table 706.2, ground is divided into 9 layers (Hisada, 2008).

Figure 706.42 shows analyses results. Computed results are compared with measured one. Measured records are obtained from cosmos virtual data center <http://db.cosmos-eq.org/>. As shown in Figure 706.42, predicted seismogram agrees well with measured ones considering the fk package assumes a single point source and simplified ground.pdf.

Table 706.2: Ground properties for the example

Depth (km)	Thickness (km)	VS (km/s)	VP/Vs (km/s)	QB (km/s)	VP (km/s)	Poisson's R (g/cm3)	Density (GPa)	G (GPa)	E (GPa)
0.05	0.05	0.30	1.730	600	0.52	0.25	0.94	0.08	0.21
0.1	0.05	0.40	1.730	600	0.69	0.25	0.99	0.16	0.40
0.2	0.10	0.50	1.730	600	0.87	0.25	1.05	0.26	0.65
0.3	0.10	0.75	1.730	600	1.30	0.25	1.19	0.67	1.67
0.5	0.20	1.00	1.730	600	1.73	0.25	1.32	1.32	3.31
1.5	1.00	2.00	1.730	600	3.46	0.25	1.88	7.51	18.76
4	2.50	3.20	1.730	600	5.54	0.25	2.54	26.03	65.02
27	23.00	3.60	1.730	600	6.23	0.25	2.76	35.81	89.46
40	13.00	3.90	1.730	900	6.75	0.25	2.93	44.55	111.30

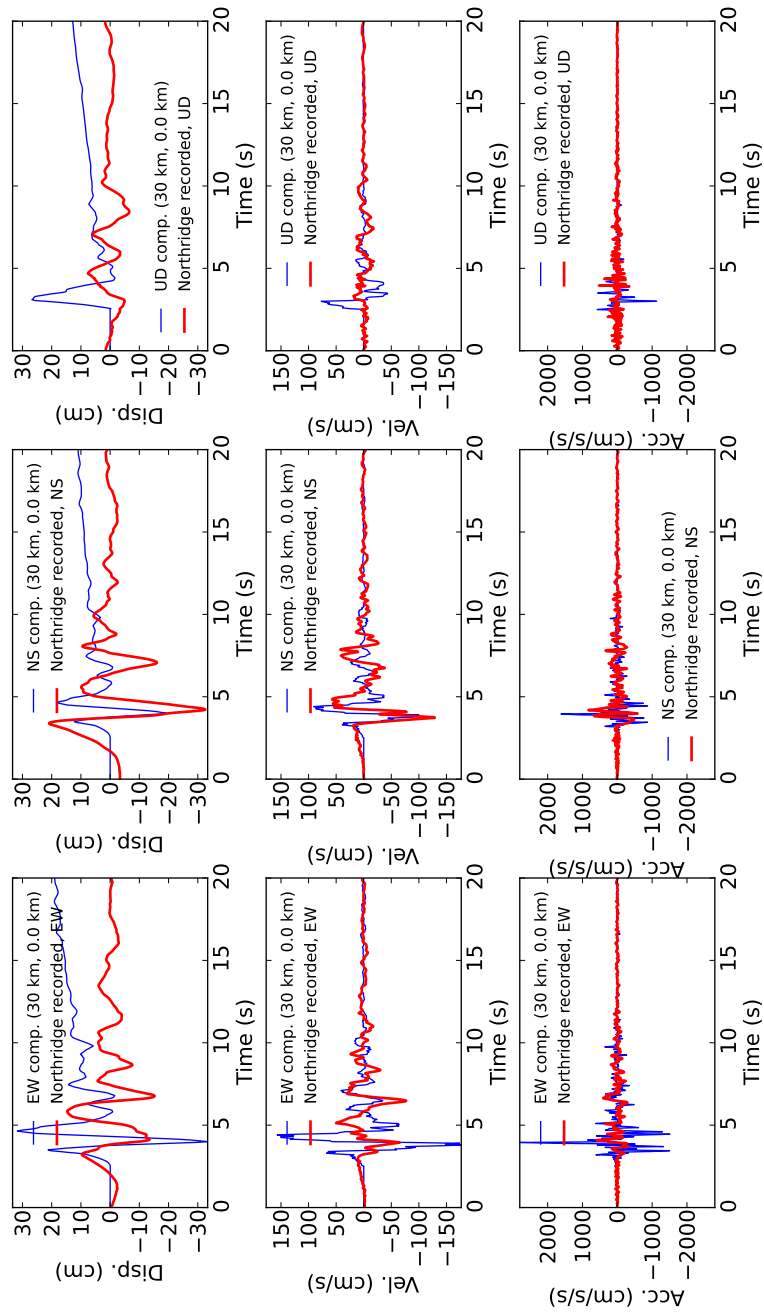


Figure 706.42: Analysis result, thick line is observed (SYL station, <http://db.cosmos-eq.org/>); results presented by the thin line are calculated using fk/syn

Appendix 707

Real-ESSI Illustrative Examples

(2015-2016-2017-2018-2019-2021-)

(In collaboration with Dr. Yuan Feng, Prof. José Abell, Prof. Sumeet Kumar Sinha, Prof. Han Yang and Dr. Hexiang Wang)

This chapter presents a number of illustrative examples. The main aim is simple: present Real-ESSI Simulator features (available elements, algorithms, domain specific language (DSL), &c.) through a number of simple examples. It is noted that all presented elements and algorithms work in sequential and parallel mode. However, presented examples are very small, and parallel mode will not bring any benefits.

707.1 Elastic Beam Element Under Static Loading

This is a simple beam example under static loading in three directions. The diagram below shows the loading in one bending direction.

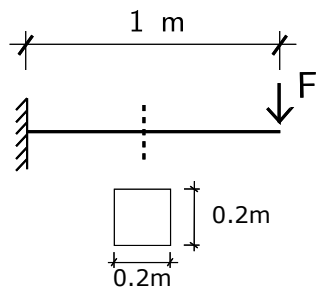


Figure 707.1: The cantilever model

ESSI model fei/DSL file:

```

1 model name "beam_1element" ;
2 // define the node coordinates
3 add node # 1 at ( 0.0*m , 0.0*m, 0.0*m) with 6 dofs;
4 add node # 2 at ( 1.0*m , 0.0*m, 0.0*m) with 6 dofs;
5 // Geometry: width and height. Help the beam definition.
6 b=0.2*m;
7 h=0.2*m;
8 I=b*h^3/12.0;
9 // define the beam element
10 add element # 1 type beam_elastic with nodes (1,2)
11   cross_section = b*h
12   elastic_modulus = 1e9*N/m^2
13   shear_modulus = 5e8*N/m^2
14   torsion_Jx = 0.33*b*h^3
15   bending_Iy = I
16   bending_Iz = I
17   mass_density = 0*kg/m^3
18   xz_plane_vector = ( 1, 0, 1 )
19   joint_1_offset = (0*m, 0*m, 0*m)
20   joint_2_offset = (0*m, 0*m, 0*m);
21 // add boundary condition
22 fix node # 1 dofs all;
23 // axial loading
24 new loading stage "axial";
25 add load # 1 to node # 2 type linear Fx = 1*N;
26 define load factor increment 1;
27 define algorithm With_no_convergence_check ;
28 define solver ProfileSPD;
29 simulate 1 steps using static algorithm;
```

```
30 // bending in one direction
31 new loading stage "bending1";
32 remove load # 1;
33 add load # 2 to node # 2 type linear Fy = 1*N;
34 define load factor increment 1;
35 define algorithm With_no_convergence_check ;
36 define solver ProfileSPD;
37 simulate 1 steps using static algorithm;
38 // bending in the other direction
39 new loading stage "bending2";
40 remove load # 2;
41 add load # 3 to node # 2 type linear Fz = 1*N;
42 define load factor increment 1;
43 define algorithm With_no_convergence_check ;
44 define solver ProfileSPD;
45 simulate 1 steps using static algorithm;
46
47 bye;
```

The ESSI model fei/DSL files for this example can be downloaded [here](#).

707.2 Elastic Beam Element under Dynamic Loading

Problem description:

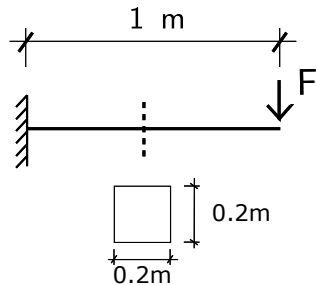


Figure 707.2: The cantilever model.

ESSI model fei/DSL file:

```

1 model name "beam_1element" ;
2
3 // add node
4 add node # 1 at ( 0.0*m , 0.0*m, 0.0*m) with 6 dofs;
5 add node # 2 at ( 1.0*m , 0.0*m, 0.0*m) with 6 dofs;
6   // Geometry: width and height
7 b=0.2*m;
8 h=0.2*m;
9 // Materials: properties
10 natural_period = 1*s;
11 natural_frequency = 2*pi/natural_period;
12 elastic_constant = 1e9*N/m^2;
13 I=b*h^3/12.0;
14 A=b*h;
15 L=1*m;
16 rho = (1.8751)^4*elastic_constant*I/(natural_frequency^2*L^4*A);
17 possion_ratio=0.3;
18 // add elements
19 add element # 1 type beam_elastic with nodes (1,2)
20   cross_section = b*h
21   elastic_modulus = elastic_constant
22   shear_modulus = elastic_constant/2/(1+possion_ratio)
23   torsion_Jx = 0.33*b*h^3
24   bending_Iy = b*h^3/12
25   bending_Iz = b*h^3/12
26   mass_density = rho
27   xz_plane_vector = ( 1, 0, 1)
28   joint_1_offset = (0*m, 0*m, 0*m)
```

```
29     joint_2_offset = (0*m, 0*m, 0*m);
30
31 // add boundary condition
32 fix node # 1 dofs all;
33
34 // // -----
35 // // --slowLoading-----
36 // // add load in 180 seconds. (Slow)
37 // // -----
38 // new loading stage "slowLoading";
39 // add load # 1 to node # 2 type path_time_series
40 // Fz = 1.*N
41 // series_file = "slowLoading.txt" ;
42 // define dynamic integrator Newmark with gamma = 0.5 beta = 0.25;
43 // define algorithm With_no_convergence_check ;
44 // define solver ProfileSPD;
45 // simulate 2000 steps using transient algorithm
46 // time_step = 0.1*s;
47
48 // // -----
49 // // --fastLoading-----
50 // // add load in 0.6 seconds (Fast)
51 // // -----
52 // remove load # 1;
53 // new loading stage "fastLoading";
54 // add load # 2 to node # 2 type path_time_series
55 // Fz = 1.*N
56 // series_file = "fastLoading.txt" ;
57 // define dynamic integrator Newmark with gamma = 0.5 beta = 0.25;
58 // define algorithm With_no_convergence_check ;
59 // define solver ProfileSPD;
60 // simulate 1000 steps using transient algorithm
61 // time_step = 0.01*s;
62
63 // // -----
64 // // --freeVibration-----
65 // // add a load and then release to free vibration
66 // // -----
67 // remove load # 2;
68 new loading stage "freeVibration";
69 add load # 3 to node # 2 type path_time_series
70   Fz = 1.*N
71   series_file = "freeVibration.txt" ;
72 define dynamic integrator Newmark with gamma = 0.5 beta = 0.25;
73 define algorithm With_no_convergence_check ;
74 define solver ProfileSPD;
75 simulate 2000 steps using transient algorithm
76   time_step = 0.01*s;
77
78 bye;
```

Displacement Results

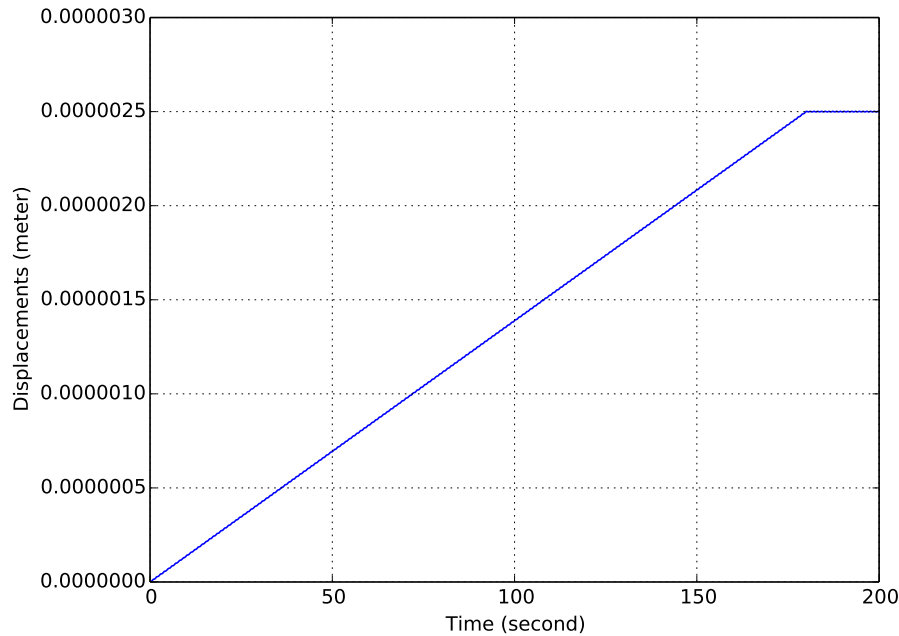


Figure 707.3: Slow loading condition, vertical displacements or the cantilever tip.

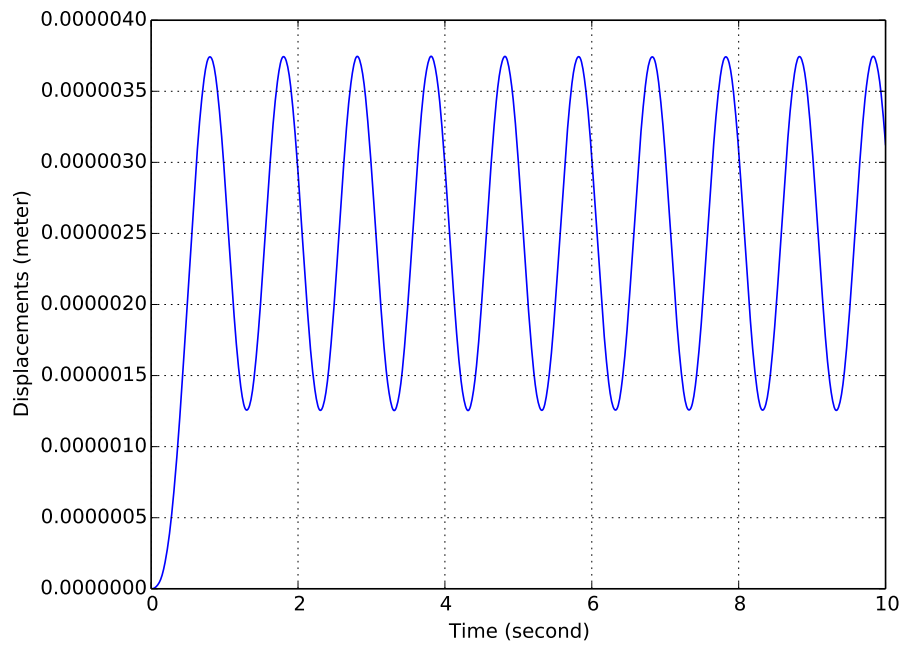


Figure 707.4: Fast loading condition, vertical displacements of the cantilever tip.

The ESSI model fei/DSL files for this example can be downloaded [here](#).

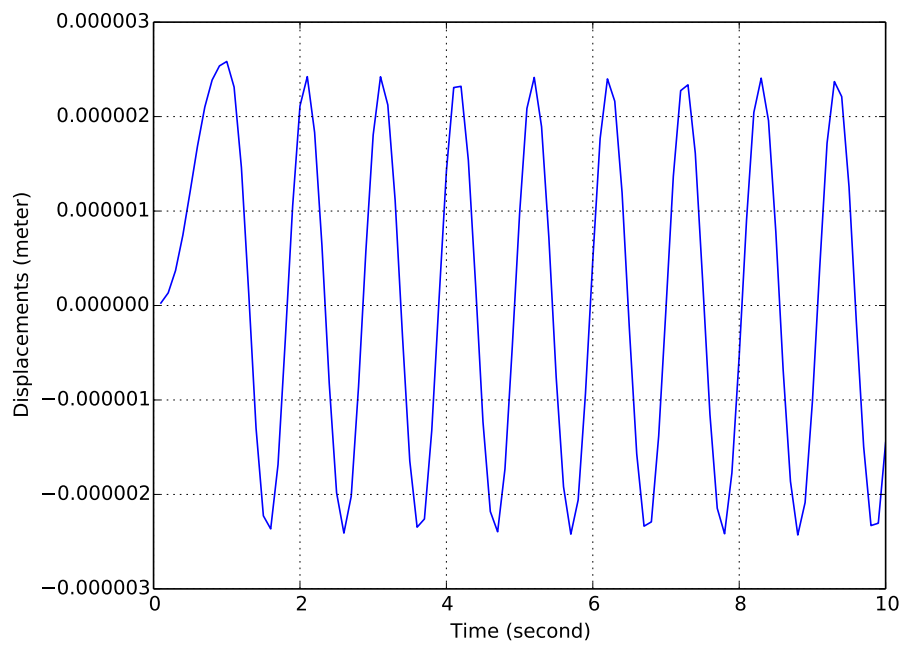


Figure 707.5: Free vibration, vertical displacements of the cantilever tip.

707.3 Cantilever, 5 Elastic Beam Elements

Problem description:

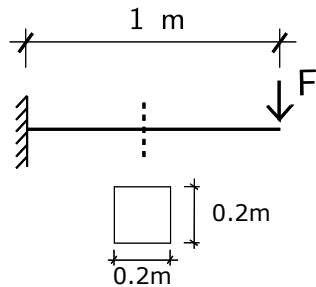


Figure 707.6: The cantilever model.

ESSI model fei/DSL file:

```

1 model name "beam_5element" ;
2
3 // add node
4 add node # 1 at ( 0.0*m , 0.0*m, 0.0*m) with 6 dofs;
5 add node # 2 at ( 0.2*m , 0.0*m, 0.0*m) with 6 dofs;
6 add node # 3 at ( 0.4*m , 0.0*m, 0.0*m) with 6 dofs;
7 add node # 4 at ( 0.6*m , 0.0*m, 0.0*m) with 6 dofs;
8 add node # 5 at ( 0.8*m , 0.0*m, 0.0*m) with 6 dofs;
9 add node # 6 at ( 1.0*m , 0.0*m, 0.0*m) with 6 dofs;
10
11 // Geometry: width and height
12 b=0.2*m;
13 h=0.2*m;
14
15 // Materials: properties
16 natural_period = 1*s;
17 natural_frequency = 2*pi/natural_period;
18 elastic_constant = 1e9*N/m^2;
19 I=b*h^3/12.0;
20 A=b*h;
21 L=1*m;
22 rho = (1.8751)^4*elastic_constant*I/(natural_frequency^2*L^4*A);
23 possion_ratio=0.3;
24
25 // Cross section geometry: width and height
26 b=0.2*m;
27 h=0.2*m;
28
29 // add elements
30 ii=1;
31 while (ii<6) {

```

```
32 add element # ii type beam_elastic with nodes (ii,ii+1)
33   cross_section = b*h
34   elastic_modulus = elastic_constant
35   shear_modulus = elastic_constant/2/(1+possession_ratio)
36   torsion_Jx = 0.33*b*h^3
37   bending_Iy = b*h^3/12
38   bending_Iz = b*h^3/12
39   mass_density = rho
40   xz_plane_vector = ( 1, 0, 1)
41   joint_1_offset = (0*m, 0*m, 0*m)
42   joint_2_offset = (0*m, 0*m, 0*m);
43   ii+=1;
44 }
45
46 // add boundary condition
47 fix node # 1 dofs all;
48
49 // // -----
50 // // --slowLoading-----
51 // // add load in 180 seconds.
52 // // -----
53 // new loading stage "slowLoading";
54 // add load # 1 to node # 6 type path_time_series
55 // Fz = 1.*N
56 // series_file = "slowLoading.txt" ;
57 // define dynamic integrator Newmark with gamma = 0.5 beta = 0.25;
58 // define algorithm With_no_convergence_check ;
59 // define solver ProfileSPD;
60 // simulate 2000 steps using transient algorithm
61 // time_step = 0.1*s;
62
63 // // -----
64 // // --fastLoading-----
65 // // add load in 0.6 seconds.
66 // // -----
67 // remove load # 1;
68 // new loading stage "fastLoading";
69 // add load # 2 to node # 6 type path_time_series
70 // Fz = 1.*N
71 // series_file = "fastLoading.txt" ;
72 // define dynamic integrator Newmark with gamma = 0.5 beta = 0.25;
73 // define algorithm With_no_convergence_check ;
74 // define solver ProfileSPD;
75 // simulate 1000 steps using transient algorithm
76 // time_step = 0.01*s;
77
78 // // -----
79 // // --freeVibration-----
80 // // add a load and then release for free vibration
81 // // -----
82 // remove load # 2;
```

```
83 new loading stage "freeVibration";
84 add load # 3 to node # 6 type path_time_series
85   Fz = 1.*N
86   series_file = "freeVibration.txt" ;
87 define dynamic integrator Newmark with gamma = 0.5 beta = 0.25;
88 define algorithm With_no_convergence_check ;
89 define solver ProfileSPD;
90 simulate 100 steps using transient algorithm
91   time_step = 0.1*s;
92
93 bye;
```

Displacement results

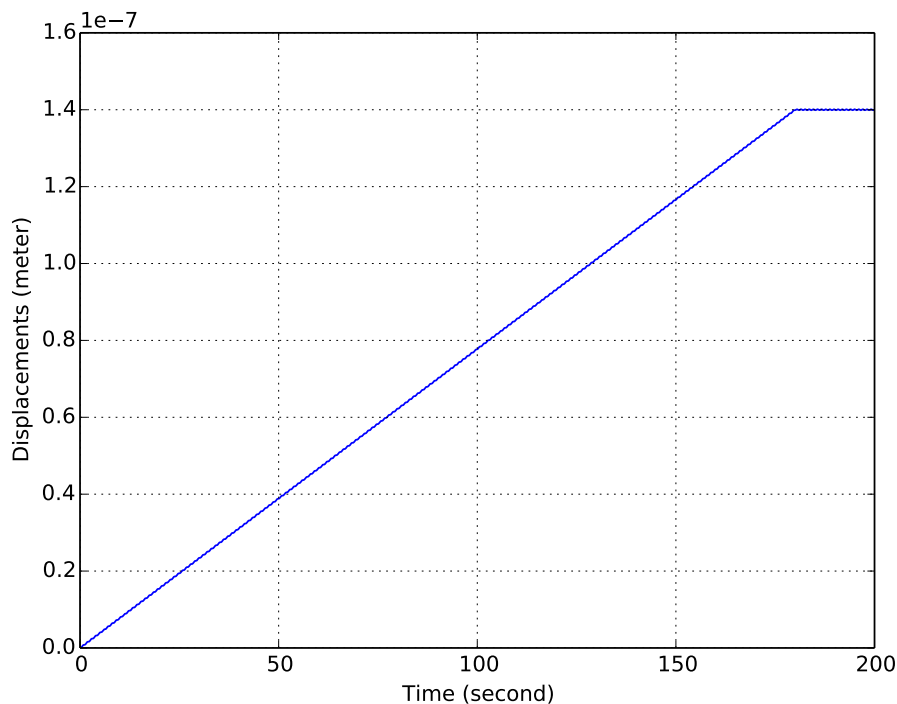


Figure 707.7: Slow loading condition, vertical displacements of the cantilever tip.

The ESSI model fei/DSL files for this example can be downloaded [here](#).

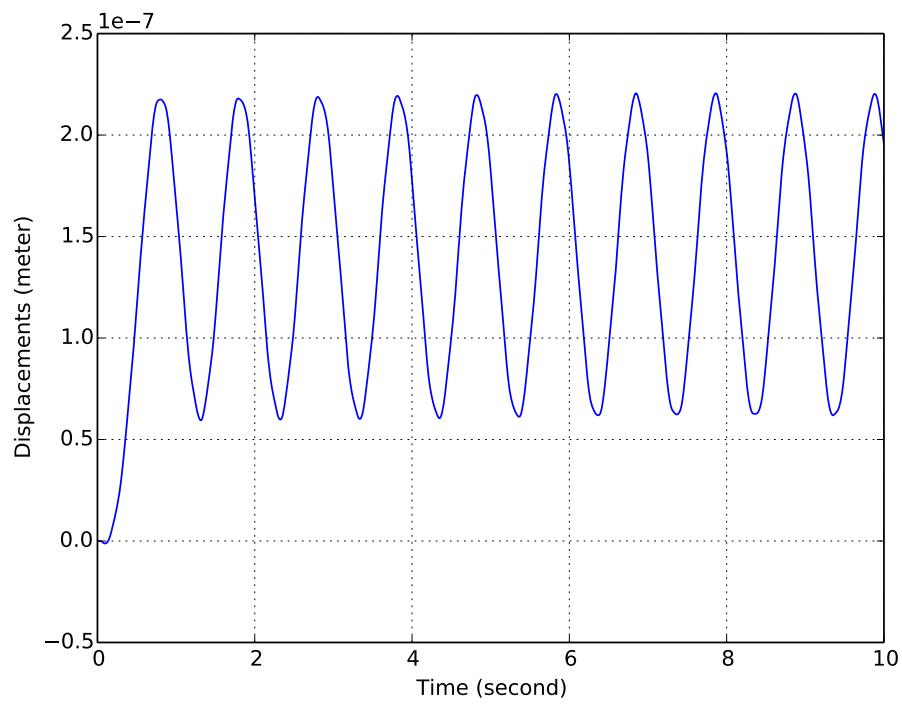


Figure 707.8: Fast loading condition, vertical displacements of the cantilever tip.

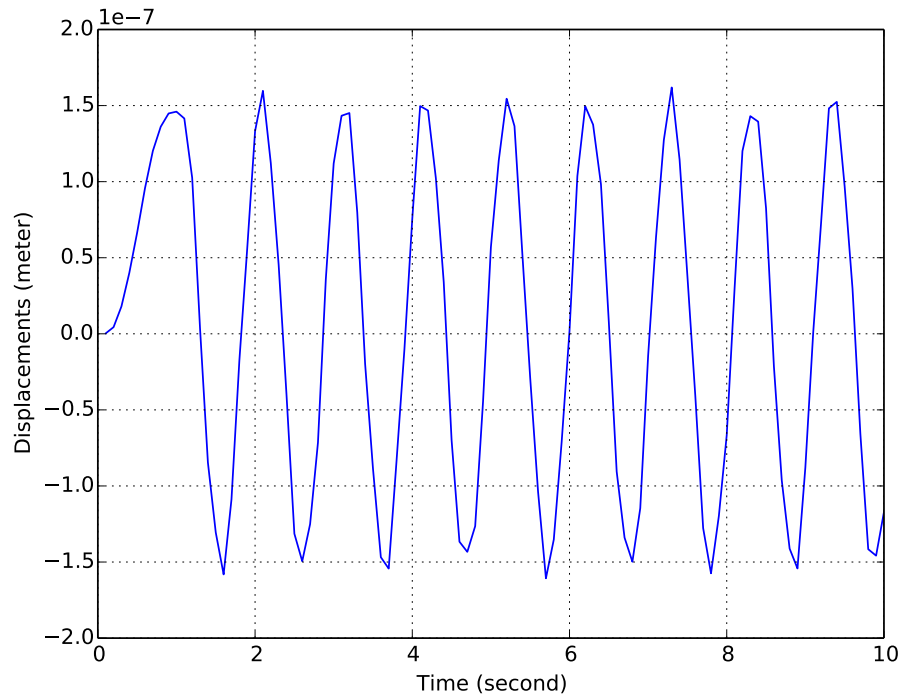


Figure 707.9: Free vibration condition, vertical displacements of the cantilever tip.

707.4 Cantilever, One 27 Node Brick Element, Dynamic Loading

Problem description:

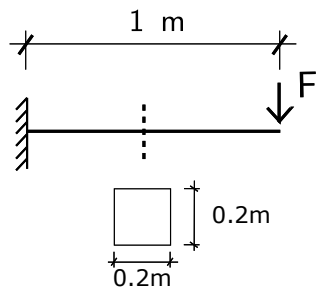


Figure 707.10: The cantilever model.

ESSI model fei/DSL file:

```

1 model name "brick_1element" ;
2
3 // Geometry: width and height
4 b=0.2*m;
5 h=0.2*m;
6
7 // Materials: properties
8 natural_period = 1*s;
9 natural_frequency = 2*pi/natural_period;
10 elastic_constant = 1e9*N/m^2;
11 I=b*h^3/12.0;
12 A=b*h;
13 L=1*m;
14 rho = (1.8751)^4*elastic_constant*I/(natural_frequency^2*L^4*A);
15 possion_ratio=0.3;
16
17
18 add material # 1 type linear_elastic_isotropic_3d_LT
19   mass_density = rho
20   elastic_modulus = elastic_constant
21   poisson_ratio = possion_ratio;
22
23 add node # 1 at ( 0.0000 *m, 0.2000 *m, 0.0000 *m) with 3 dofs;
24 add node # 2 at ( 0.0000 *m, 0.0000 *m, 0.0000 *m) with 3 dofs;
25 add node # 3 at ( 1.0000 *m, 0.2000 *m, 0.0000 *m) with 3 dofs;
26 add node # 4 at ( 1.0000 *m, 0.0000 *m, 0.0000 *m) with 3 dofs;
27 add node # 5 at ( 0.0000 *m, 0.0000 *m, 0.2000 *m) with 3 dofs;
28 add node # 6 at ( 1.0000 *m, 0.0000 *m, 0.2000 *m) with 3 dofs;
29 add node # 7 at ( 1.0000 *m, 0.2000 *m, 0.2000 *m) with 3 dofs;
30 add node # 8 at ( 0.0000 *m, 0.2000 *m, 0.2000 *m) with 3 dofs;
31 add node # 9 at ( 0.0000 *m, 0.1000 *m, 0.0000 *m) with 3 dofs;
```

```

32 add node # 10 at ( 0.5000 *m, 0.2000 *m, 0.0000 *m) with 3 dofs;
33 add node # 11 at ( 1.0000 *m, 0.1000 *m, 0.0000 *m) with 3 dofs;
34 add node # 12 at ( 0.5000 *m, 0.0000 *m, 0.0000 *m) with 3 dofs;
35 add node # 13 at ( 0.0000 *m, 0.1000 *m, 0.2000 *m) with 3 dofs;
36 add node # 14 at ( 0.5000 *m, 0.2000 *m, 0.2000 *m) with 3 dofs;
37 add node # 15 at ( 1.0000 *m, 0.1000 *m, 0.2000 *m) with 3 dofs;
38 add node # 16 at ( 0.5000 *m, 0.0000 *m, 0.2000 *m) with 3 dofs;
39 add node # 17 at ( 0.0000 *m, 0.0000 *m, 0.1000 *m) with 3 dofs;
40 add node # 18 at ( 0.0000 *m, 0.2000 *m, 0.1000 *m) with 3 dofs;
41 add node # 19 at ( 1.0000 *m, 0.2000 *m, 0.1000 *m) with 3 dofs;
42 add node # 20 at ( 1.0000 *m, 0.0000 *m, 0.1000 *m) with 3 dofs;
43 add node # 21 at ( 0.5000 *m, 0.1000 *m, 0.1000 *m) with 3 dofs;
44 add node # 22 at ( 0.0000 *m, 0.1000 *m, 0.1000 *m) with 3 dofs;
45 add node # 23 at ( 0.5000 *m, 0.2000 *m, 0.1000 *m) with 3 dofs;
46 add node # 24 at ( 1.0000 *m, 0.1000 *m, 0.1000 *m) with 3 dofs;
47 add node # 25 at ( 0.5000 *m, 0.0000 *m, 0.1000 *m) with 3 dofs;
48 add node # 26 at ( 0.5000 *m, 0.1000 *m, 0.0000 *m) with 3 dofs;
49 add node # 27 at ( 0.5000 *m, 0.1000 *m, 0.2000 *m) with 3 dofs;
50
51 add element # 1 type 27NodeBrickLT with nodes( 2, 1, 3, 4, 5, 8, 7, 6, 9, 10, ←
      11, 12, 13, 14, 15, 16, 17, 18, 19, 20, 21, 22, 23, 24, 25, 26, 27) use ←
      material # 1;
52
53 fix node # 1 dofs all;
54 fix node # 2 dofs all;
55 fix node # 5 dofs all;
56 fix node # 8 dofs all;
57 fix node # 9 dofs all;
58 fix node # 13 dofs all;
59 fix node # 17 dofs all;
60 fix node # 18 dofs all;
61 fix node # 22 dofs all;
62
63
64 // // -----
65 // // --slowLoading-----
66 // // -----
67 // new loading stage "slowLoading";
68 // add load # 1 to node # 4 type path_time_series Fz=1/36.0*N series_file = ←
      "slowLoading.txt" ;
69 // add load # 2 to node # 6 type path_time_series Fz=1/36.0*N series_file = ←
      "slowLoading.txt" ;
70 // add load # 3 to node # 3 type path_time_series Fz=1/36.0*N series_file = ←
      "slowLoading.txt" ;
71 // add load # 4 to node # 7 type path_time_series Fz=1/36.0*N series_file = ←
      "slowLoading.txt" ;
72 // add load # 5 to node # 20 type path_time_series Fz=1/9.0*N series_file = ←
      "slowLoading.txt" ;
73 // add load # 6 to node # 11 type path_time_series Fz=1/9.0*N series_file = ←
      "slowLoading.txt" ;
74 // add load # 7 to node # 15 type path_time_series Fz=1/9.0*N series_file = ←

```

```
    "slowLoading.txt" ;
75 // add load # 8 to node # 19 type path_time_series Fz=1/9.0*N series_file = ←
    "slowLoading.txt" ;
76 // add load # 9 to node # 24 type path_time_series Fz=4/9.0*N series_file = ←
    "slowLoading.txt" ;
77 // // add algorithm and solver
78 // define dynamic integrator Newmark with gamma = 0.5 beta = 0.25;
79 // define algorithm With_no_convergence_check ;
80 // define solver ProfileSPD;
81 // simulate 2000 steps using transient algorithm
82 // time_step = 0.1*s;
83
84 // // -----
85 // // --fastLoading-----
86 // // -----
87 // new loading stage "fastLoading";
88 // add load # 101 to node # 4 type path_time_series Fz=1/36.0*N series_file = ←
    "fastLoading.txt" ;
89 // add load # 102 to node # 6 type path_time_series Fz=1/36.0*N series_file = ←
    "fastLoading.txt" ;
90 // add load # 103 to node # 3 type path_time_series Fz=1/36.0*N series_file = ←
    "fastLoading.txt" ;
91 // add load # 104 to node # 7 type path_time_series Fz=1/36.0*N series_file = ←
    "fastLoading.txt" ;
92 // add load # 105 to node # 20 type path_time_series Fz=1/9.0*N series_file = ←
    "fastLoading.txt" ;
93 // add load # 106 to node # 11 type path_time_series Fz=1/9.0*N series_file = ←
    "fastLoading.txt" ;
94 // add load # 107 to node # 15 type path_time_series Fz=1/9.0*N series_file = ←
    "fastLoading.txt" ;
95 // add load # 108 to node # 19 type path_time_series Fz=1/9.0*N series_file = ←
    "fastLoading.txt" ;
96 // add load # 109 to node # 24 type path_time_series Fz=4/9.0*N series_file = ←
    "fastLoading.txt" ;
97 // // add algorithm and solver
98 // define dynamic integrator Newmark with gamma = 0.5 beta = 0.25;
99 // define algorithm With_no_convergence_check ;
100 // define solver ProfileSPD;
101 // simulate 1000 steps using transient algorithm
102 // time_step = 0.01*s;
103
104 // // -----
105 // // ←
106 // // -----
107 new loading stage "freeVibration";
108 add load # 201 to node # 4 type path_time_series Fz=1/36.0*N series_file = ←
    "freeVibration.txt" ;
109 add load # 202 to node # 6 type path_time_series Fz=1/36.0*N series_file = ←
    "freeVibration.txt" ;
110 add load # 203 to node # 3 type path_time_series Fz=1/36.0*N series_file = ←
```

```

111 "freeVibration.txt" ;
112 add load # 204 to node # 7 type path_time_series Fz=1/36.0*N series_file = <-
113 "freeVibration.txt" ;
114 add load # 205 to node # 20 type path_time_series Fz=1/9.0*N series_file = <-
115 "freeVibration.txt" ;
116 add load # 206 to node # 11 type path_time_series Fz=1/9.0*N series_file = <-
117 "freeVibration.txt" ;
118 add load # 207 to node # 15 type path_time_series Fz=1/9.0*N series_file = <-
119 "freeVibration.txt" ;
120 add load # 208 to node # 19 type path_time_series Fz=1/9.0*N series_file = <-
121 "freeVibration.txt" ;
122 add load # 209 to node # 24 type path_time_series Fz=4/9.0*N series_file = <-
123 "freeVibration.txt" ;
124 // add algorithm and solver
125 define dynamic integrator Newmark with gamma = 0.5 beta = 0.25;
define algorithm With_no_convergence_check ;
define solver ProfileSPD;
simulate 10000 steps using transient algorithm
  time_step = 0.001*s;
// end
bye;

```

Displacement results against time series

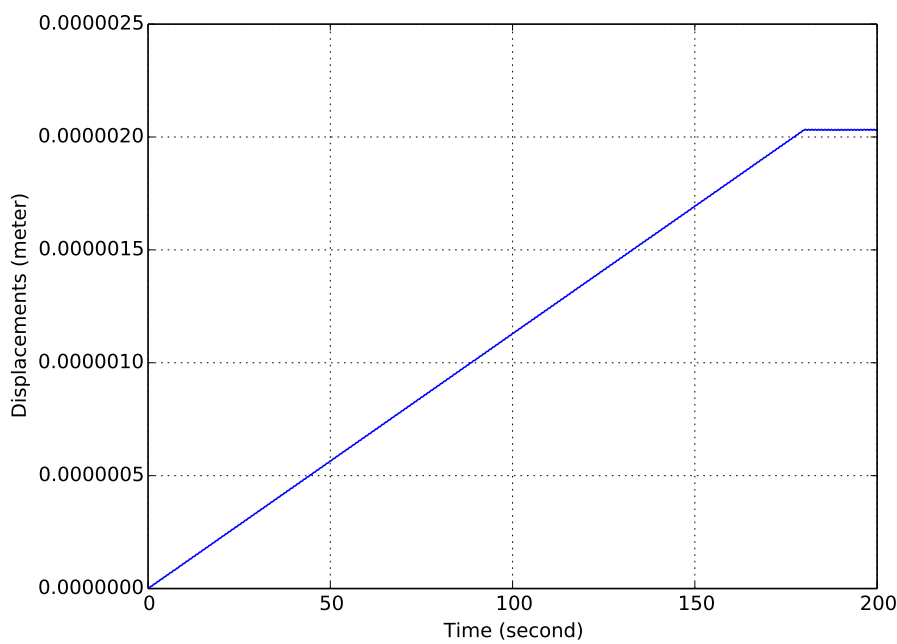


Figure 707.11: Slow loading condition, vertical displacements of the cantilever tip.

The ESSI model fei/DSL files for this example can be downloaded [here](#).

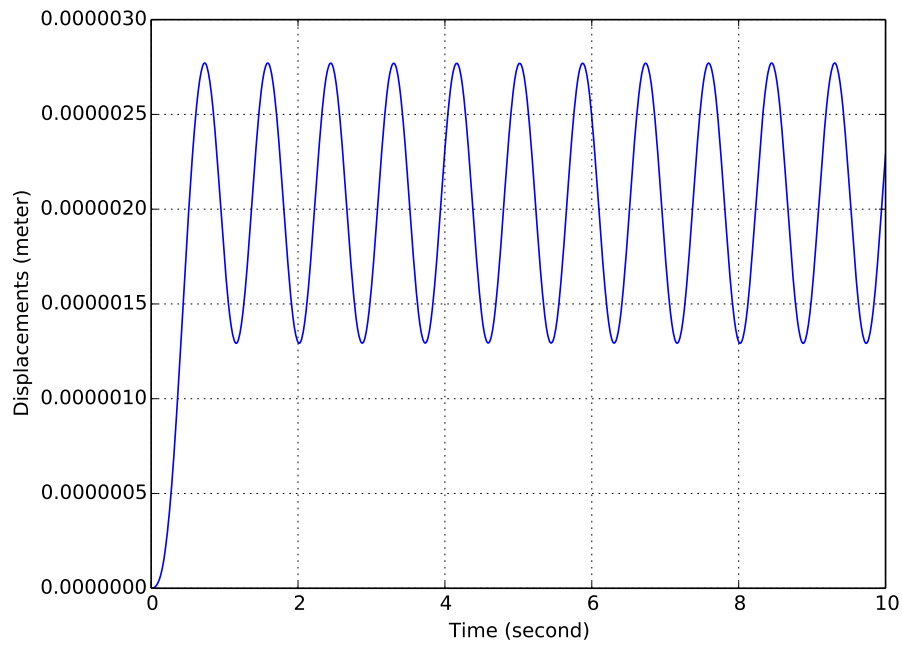


Figure 707.12: Fast loading condition, vertical displacements of the cantilever tip.

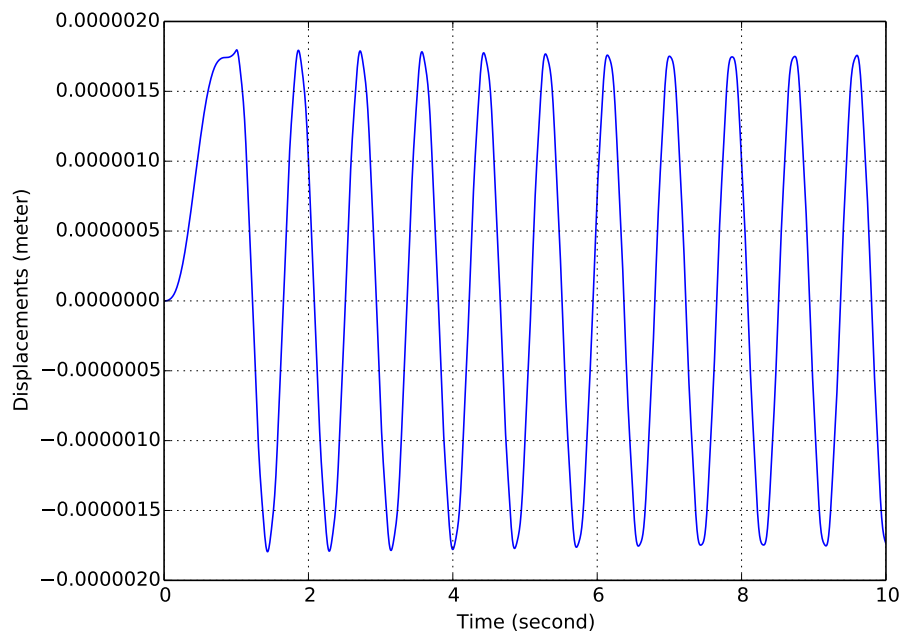


Figure 707.13: Free vibration condition, vertical displacements of the cantilever tip.

707.5 Simulate Cantilever Using Five 27 Node Brick Elements

Problem description:

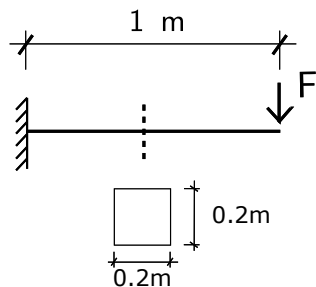


Figure 707.14: The cantilever model.

ESSI model fei/DSL file:

```

1 model name "brick_5element" ;
2
3 // Geometry: width and height
4 b=0.2*m;
5 h=0.2*m;
6
7 // Materials: properties
8 natural_period = 1*s;
9 natural_frequency = 2*pi/natural_period;
10 elastic_constant = 1e9*N/m^2;
11 I=b*h^3/12.0;
12 A=b*h;
13 L=1*m;
14 rho = (1.8751)^4*elastic_constant*I/(natural_frequency^2*L^4*A);
15 possion_ratio=0.3;
16
17
18 add material # 1 type linear_elastic_isotropic_3d_LT
19   mass_density = rho
20   elastic_modulus = elastic_constant
21   poisson_ratio = possion_ratio;
22
23 add node # 1 at (0.0*m, 0.0*m , 0.0*m) with 3 dofs;
24 add node # 2 at (0.1*m, 0.0*m , 0.0*m) with 3 dofs;
25 add node # 3 at (0.2*m, 0.0*m , 0.0*m) with 3 dofs;
26 add node # 4 at (0.0*m, 0.1*m , 0.0*m) with 3 dofs;
27 add node # 5 at (0.1*m, 0.1*m , 0.0*m) with 3 dofs;
28 add node # 6 at (0.2*m, 0.1*m , 0.0*m) with 3 dofs;
29 add node # 7 at (0.0*m, 0.2*m , 0.0*m) with 3 dofs;
30 add node # 8 at (0.1*m, 0.2*m , 0.0*m) with 3 dofs;
31 add node # 9 at (0.2*m, 0.2*m , 0.0*m) with 3 dofs;
```

```
32 fix node No 1 dofs ux uy uz;
33 fix node No 2 dofs ux uy uz;
34 fix node No 3 dofs ux uy uz;
35 fix node No 4 dofs ux uy uz;
36 fix node No 5 dofs ux uy uz;
37 fix node No 6 dofs ux uy uz;
38 fix node No 7 dofs ux uy uz;
39 fix node No 8 dofs ux uy uz;
40 fix node No 9 dofs ux uy uz;
41 fix node No 9 dofs ux uy uz;
42 e = 0;
43 hh = 0*m;
44 NBricks=5;
45 dz = 0.2*m;
46 while ( e < NBricks)
47 {
48     hh += dz;
49     add node # 10+18*e at (0.0*m, 0.0*m , hh - 0.5*dz) with 3 dofs;
50     add node # 11+18*e at (0.1*m, 0.0*m , hh - 0.5*dz) with 3 dofs;
51     add node # 12+18*e at (0.2*m, 0.0*m , hh - 0.5*dz) with 3 dofs;
52     add node # 13+18*e at (0.0*m, 0.1*m , hh - 0.5*dz) with 3 dofs;
53     add node # 14+18*e at (0.1*m, 0.1*m , hh - 0.5*dz) with 3 dofs;
54     add node # 15+18*e at (0.2*m, 0.1*m , hh - 0.5*dz) with 3 dofs;
55     add node # 16+18*e at (0.0*m, 0.2*m , hh - 0.5*dz) with 3 dofs;
56     add node # 17+18*e at (0.1*m, 0.2*m , hh - 0.5*dz) with 3 dofs;
57     add node # 18+18*e at (0.2*m, 0.2*m , hh - 0.5*dz) with 3 dofs;
58
59     add node # 19+18*e at (0.0*m, 0.0*m , hh) with 3 dofs;
60     add node # 20+18*e at (0.1*m, 0.0*m , hh) with 3 dofs;
61     add node # 21+18*e at (0.2*m, 0.0*m , hh) with 3 dofs;
62     add node # 22+18*e at (0.0*m, 0.1*m , hh) with 3 dofs;
63     add node # 23+18*e at (0.1*m, 0.1*m , hh) with 3 dofs;
64     add node # 24+18*e at (0.2*m, 0.1*m , hh) with 3 dofs;
65     add node # 25+18*e at (0.0*m, 0.2*m , hh) with 3 dofs;
66     add node # 26+18*e at (0.1*m, 0.2*m , hh) with 3 dofs;
67     add node # 27+18*e at (0.2*m, 0.2*m , hh) with 3 dofs;
68
69     add element # e+1 type 27NodeBrickLT with nodes
70     (
71         21+18*e,
72         27+18*e,
73         25+18*e,
74         19+18*e,
75
76         3+18*e,
77         9+18*e,
78         7+18*e,
79         1+18*e,
80
81         24+18*e,
82         26+18*e,
```

```
83     22+18*e,
84     20+18*e,
85
86     6+18*e,
87     8+18*e,
88     4+18*e,
89     2+18*e,
90
91     12+18*e,
92     18+18*e,
93     16+18*e,
94     10+18*e,
95
96     14+18*e,
97     15+18*e,
98     17+18*e,
99     13+18*e,
100    11+18*e,
101    23+18*e,
102    5+18*e
103 )
104 use material # 1;
105
106 e += 1;
107 };
108
109
110 e = e -1;
111
112
113 // // -----
114 // // --slowLoading
115 // // add the 1 Newton load in 180 seconds.
116 // //
117 // new loading stage "slowLoading";
118 // add load # 1 to node # (19+18*e) type path_time_series Fx=1/36.0*N ←
119 //   series_file = "slowLoading.txt";
120 // add load # 2 to node # (20+18*e) type path_time_series Fx=1/9.0*N ←
121 //   series_file = "slowLoading.txt";
122 // add load # 3 to node # (21+18*e) type path_time_series Fx=1/36.0*N ←
123 //   series_file = "slowLoading.txt";
124 // add load # 4 to node # (22+18*e) type path_time_series Fx=1/9.0*N ←
125 //   series_file = "slowLoading.txt";
```

```

126 // add load # 9 to node # (27+18*e) type path_time_series Fx=1/36.0*N ←
    series_file = "slowLoading.txt";
127 // // add algorithm and solver
128 // define dynamic integrator Newmark with gamma = 0.5 beta = 0.25;
129 // define algorithm With_no_convergence_check ;
130 // define solver ProfileSPD;
131 // simulate 2000 steps using transient algorithm
132 // time_step = 0.1*s;
133
134 // // -----
135 // // --fastLoading-
136 // // add the 1 Newton load in 0.6 seconds.
137 // //
138 // new loading stage "fastLoading";
139 // add load # 101 to node # (19+18*e) type path_time_series Fx=1/36.0*N ←
    series_file = "fastLoading.txt" ;
140 // add load # 102 to node # (20+18*e) type path_time_series Fx=1/9.0*N ←
    series_file = "fastLoading.txt" ;
141 // add load # 103 to node # (21+18*e) type path_time_series Fx=1/36.0*N ←
    series_file = "fastLoading.txt" ;
142 // add load # 104 to node # (22+18*e) type path_time_series Fx=1/9.0*N ←
    series_file = "fastLoading.txt" ;
143 // add load # 105 to node # (23+18*e) type path_time_series Fx=4/9.0*N ←
    series_file = "fastLoading.txt" ;
144 // add load # 106 to node # (24+18*e) type path_time_series Fx=1/9.0*N ←
    series_file = "fastLoading.txt" ;
145 // add load # 107 to node # (25+18*e) type path_time_series Fx=1/36.0*N ←
    series_file = "fastLoading.txt" ;
146 // add load # 108 to node # (26+18*e) type path_time_series Fx=1/9.0*N ←
    series_file = "fastLoading.txt" ;
147 // add load # 109 to node # (27+18*e) type path_time_series Fx=1/36.0*N ←
    series_file = "fastLoading.txt" ;
148 // // add algorithm and solver
149 // define dynamic integrator Newmark with gamma = 0.5 beta = 0.25;
150 // define algorithm With_no_convergence_check ;
151 // define solver ProfileSPD;
152 // simulate 1000 steps using transient algorithm
153 // time_step = 0.01*s;
154
155 // // -----
156 // // ←
157 // // --freeVibration-
158 // // add a load and then release to free vibration
159 new loading stage "freeVibration";
160 add load # 201 to node # (19+18*e) type path_time_series Fx=1/36.0*N ←
    series_file = "freeVibration.txt" ;
161 add load # 202 to node # (20+18*e) type path_time_series Fx=1/9.0*N series_file ←
    = "freeVibration.txt" ;
162 add load # 203 to node # (21+18*e) type path_time_series Fx=1/36.0*N ←
    series_file = "freeVibration.txt" ;

```

```

163 add load # 204 to node # (22+18*e) type path_time_series Fx=1/9.0*N series_file ←
164   = "freeVibration.txt" ;
165 add load # 205 to node # (23+18*e) type path_time_series Fx=4/9.0*N series_file ←
166   = "freeVibration.txt" ;
167 add load # 206 to node # (24+18*e) type path_time_series Fx=1/9.0*N series_file ←
168   = "freeVibration.txt" ;
169 add load # 207 to node # (25+18*e) type path_time_series Fx=1/36.0*N ←
170   series_file = "freeVibration.txt" ;
171 add load # 208 to node # (26+18*e) type path_time_series Fx=1/9.0*N series_file ←
172   = "freeVibration.txt" ;
173 // add algorithm and solver
174 define dynamic integrator Newmark with gamma = 0.5 beta = 0.25;
175 define algorithm With_no_convergence_check ;
176 define solver ProfileSPD;
177 simulate 100 steps using transient algorithm
    time_step = 0.1*s;
178
179 // end
180 bye;

```

Displacement Results.

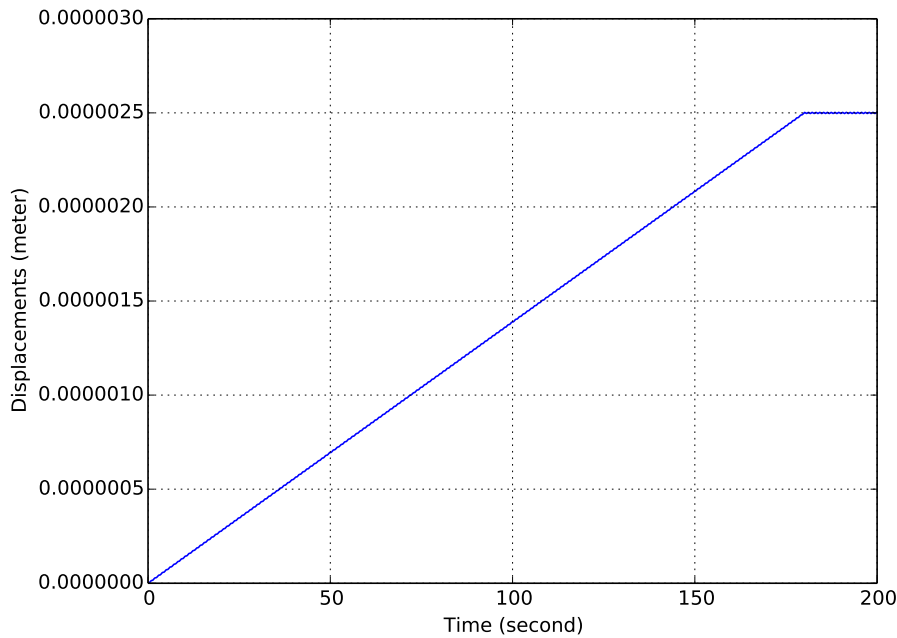


Figure 707.15: Slow loading condition, vertical displacements of the cantilever tip.

The ESSI model fei/DSL files for this example can be downloaded [here](#).

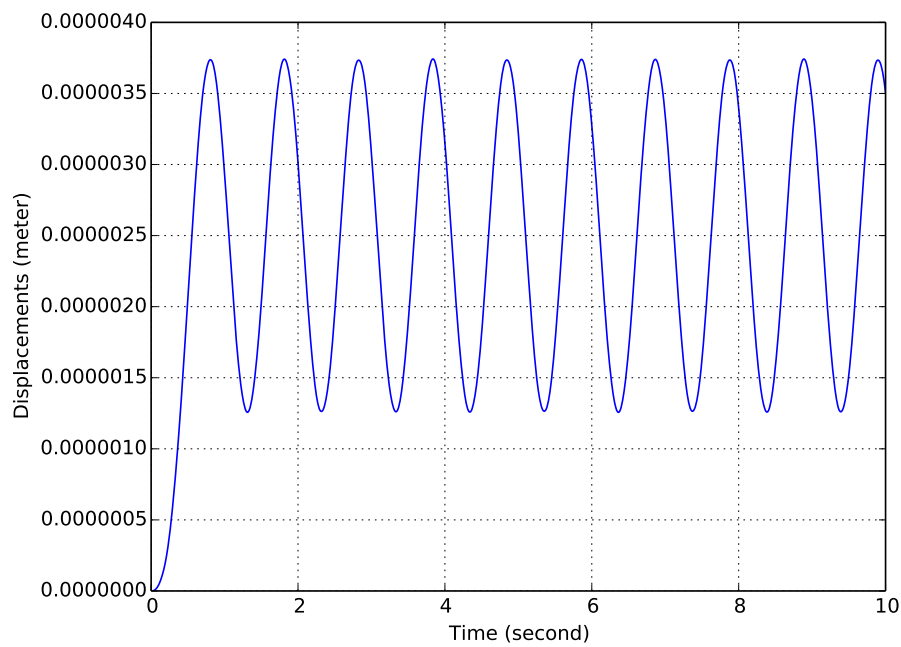


Figure 707.16: Fast loading condition, vertical displacements of the cantilever tip.

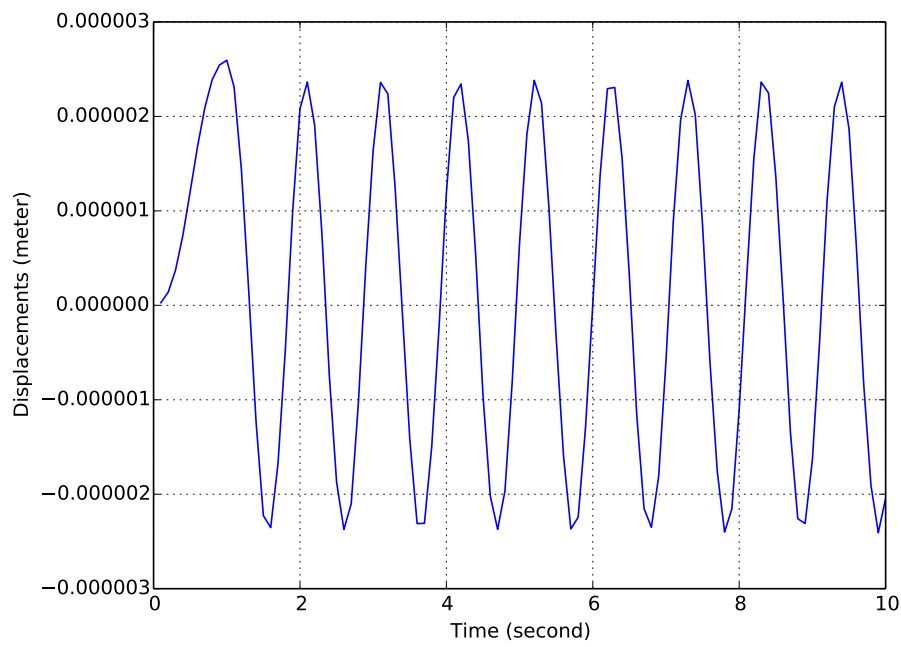


Figure 707.17: Free vibration condition, vertical displacements of the cantilever tip.

707.6 Elastic Beam Element under Dynamic Loading with concentrated mass

Problem description:

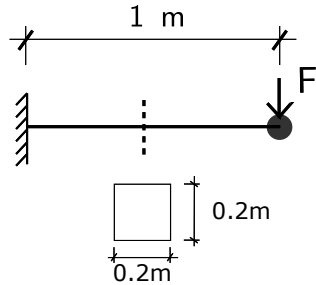


Figure 707.18: The cantilever-mass model.

ESSI model fei/DSL file:

```

1 model name "beam-mass_1element" ;
2
3 // add node
4 add node # 1 at ( 0.0*m , 0.0*m, 0.0*m) with 6 dofs;
5 add node # 2 at ( 1.0*m , 0.0*m, 0.0*m) with 6 dofs;
6
7 // Geometry: width and height
8 b=0.2*m;
9 h=0.2*m;
10
11 // Materials: properties
12 natural_period = 1*s;
13 natural_frequency = 2*pi/natural_period;
14 elastic_constant = 1e9*N/m^2;
15 I=b*h^3/12.0;
16 A=b*h;
17 L=1*m;
18 rho = (1.8751)^4*elastic_constant*I/(natural_frequency^2*L^4*A);
19 possion_ratio=0.3;
20
21 // add elements
22 add element # 1 type beam_elastic with nodes (1,2)
23   cross_section = b*h
24   elastic_modulus = elastic_constant
25   shear_modulus = elastic_constant/2/(1+possion_ratio)
26   torsion_Jx = 0.33*b*h^3
27   bending_Iy = b*h^3/12
28   bending_Iz = b*h^3/12

```